7816144

NACHMIAS, SOLOMON
A LEARNING CONTROL SYSTEM WITH APPLICATION TO FLIGHT SYSTEMS.

CITY UNIVERSITY OF NEW YORK, PH.D., 1978

A LEARNING CONTROL SYSTEM WITH APPLICATION TO FLIGHT SYSTEMS

by

Solomon Nachmias

A dissertation submitted to the Graduate
Faculty in Engineering in partial fulfillment of
the requirements for the degree of Doctor of Philosophy
The City University of New York

1978

This manuscript has been read and accepted for the Graduate Faculty in Engineering in satisfaction of the dissertation requirement for the degree of Doctor of Philosophy.

4/18/1978
date

Ralph Mekel
Chairman of Examining Committee

4/18/78
date

Executive Officer

Professor Ralph Mekel (Chairman)

Professor Se Jeung Oh

Professor Frederick Thau

Professor Louis Weinberg
Supervisory Committee

The City University of New York

Abstract

A LEARNING CONTROL SYSTEM WITH APPLICATION

TO FLIGHT SYSTEMS

by

Solomon Nachmias

Advisor: Professor Ralph Mekel

This dissertation presents the formulation of a learning control system and investigates its utilization as a flight control system for NASA's F-8 Digital Fly-By-Wire (DFBW) research aircraft. The study takes the best features of two methods, i.e. the gain scheduling and the adaptive control method, and attempts to eliminate the undesirable features of each. One of the characteristics of this learning control system is its ability to adjust a gain schedule in a prescribed manner to account for changing plant characteristics. Another important feature of this learning system is that it can improve its performance and the plant's performance in the course of its own operation.

The adaptive learning control system consists of three subsystems: 1) The Information Acquisition Subsystem which identifies the plant's parameters at a given operating condition. The mathematical technique is based upon a model-reference system configuration where the adaptive algorithm used to update the model's parameters are derived using both Liapunov's direct method and the Newton-Raphson method. 2) The Learning Algorithm Subsystem which relates the identified parameters to predetermined

analytical expressions describing the bahavior of the parameters over a range of operating conditions. The mathematical technique is based upon a sequential coefficient estimation derived using the least-square algorithm. 3) The Memory and Control Process Subsystem which consists of the collection of updated coefficients (memory) and the control laws derived by imposing desired plant performance characterictics.

An artificial plant is presented in order to illustrate the performance of the learning control system and to compare two different designs based upon two different information acquisition subsystems: 1) Liapunov's method and 2) Newton-Raphson method. For this case the models involved consisted of the uncoupled, linear time-invariant open-loop longitudinal and lateral dynamics of the F-8 aircraft associated with equilibrium flight.

In applying the learning control system to the piloted six-degree-of-freedom simulation of the F-8 aircraft, reduced order discrete models were used for the information acquisition subsystem to conform with the real-time constraint. Simulation experiments indicate that the learning control system was effective in compensating for parameter variations caused by changes in flight conditions over the entire flight envelope.

Acknowledgments

I wish to express my extreme gratitude to my dissertation supervisor, Professor Ralph Mekel, for the confidence, encouragement and guidance he extended to me during the course of this research. The many hours of technical discussions and his many valuable criticisms and suggestions are most appreciated.

I would like to thank all the members of my Doctoral guidance and examining committee, Dr. Raymond C. Montgomery (NASA Langley Research Center), Professors Fred E. Thau, Donald L. Schilling, Se Jeung Oh and Louis Weinberg for the time and effort each has taken to read and constructively criticize this dissertation.

I would especially like to express my thanks to Dr. Raymond C. Montgomery, for his continuous interest, encouragement and helpful suggestions throughout the preparation of this dissertation. The many hours of informative discussions about aircraft dynamics and flight control systems are greatly appreciated. I am also indebted to him and Mr. William H. Phillips for allowing me the use of NASA's real-time simulator. I would like to thank Mr. Martin T. Moul, Mr. Jarrell R. Elliott and Dr. John D. Bird (NASA personnel) for their many technical recommendations.

Thanks are also due to Professors Fred Thau and Donald Schilling for their suggested corrections of this manuscript.

The excellent typing of this dissertation was performed by Mrs. Jean Mekel whose efforts are deeply appreciated.

Finally, I would like to acknowledge the partial support given to me by the National Aeronautics and Space Administration to carry out this research under Grant No. NSG-1169.

TABLE OF CONTENTS

LIST OF FIGURES

LIST OF TABLES

GLOSSARY OF SYMBOLS

y - Plant state vector

σ_e - Plant input

p - Plant parameter vector

$A_p(p)$ - Plant system matrix

$B_p(p)$ - Plant input matrix

K - Feedback matrix

G - Feedforward matrix

σ_s - Control input

$A'_p(p)$ - Closed loop plant system matrix

$B'_p(p)$ - Closed loop plant input matrix

z - Model state vector (Liapunov's IAS)

$\hat{p}$ - Estimate of vector p

$A_m(\hat{p})$ - Model system matrix

$B_m(\hat{p})$ - Model input matrix

F - Model stable matrix

e - Model plant state error vector

b_i, d_i - Constant vectors

P, N_i, Q_i, Q - Constant matrices

η - Convergence index (Liapunov's IAS)

η_{min} - Minimum value of η

V_1, V_2, V_3 - Parts of Liapunov's function

V - Liapunov's function

u_i, w_i - Parameter misalignments vectors

V_{1max} - Maximum value of V_1

T_m - Time at which V_1 reaches V_{1max}

x - Model state vector (Newton-Raphson IAS)

$J(\hat{p})$ - Negative log-likelihood function

B_i - Inverse of the plant's state covariance matrix

$\hat{p}_j$ - The j-th iterate of vector $\hat{p}$

f_j - The gradient of $J(\hat{p})$

S_j - An approximation to $(\partial^2 J/\partial \hat{p}^2)^{-1}$

ρ_j - Scalar step size parameter

μ_{max} - Maximum eigenvalue of $S_j(\partial^2 J/\partial \hat{p}^2)$

μ_{min} - Minimum eigenvalue of $S_j(\partial^2 J/\partial \hat{p}^2)$

$\partial x/\partial \hat{p}$ - Sensitivity matrix

$\hat{p}_o$ - Initial estimate of vector p

ϵ_1 - Minimum value of $J(\hat{p})$

ϵ_2 - Minimum distance between two estimates of vector p

λ - Uncertainty vector of $\hat{p}$

R - Covariance matrix of λ

H(h) - Operating condition matrix

C - Coefficient vector

ϕ_k - Quadratic criterion

C_k - Least squares estimate of vector C

P_k - Covariance matrix of vector C_k

C_o - Initial estimate of vector C

$\tilde{C}_k$ - Error in estimating vector C

ξ_1 - minimum value of ϕ_k/k

ξ_2 - Minimum distance between two estimates of vector C

P_o - Initial covariance matrix of vector C

n - Order of system

N - Size of data base

q - Pitch rate

v - Forward velocity

α - Angle of attack

θ - Pitch angle

M - Mach number

L - Altitude

ΔK - Correction to matrix K

ΔG - Correction to matrix G

p - Roll rate

r - Yaw rate

β - Sideslip angle

ϕ - Roll angle

a_f - Trimmed angle of attack

δ_a - Aileron displacement

δ_r - Rudder displacement

γ - Flight path angle

T - Time increment for the real-time IAS

$\bar{\alpha}$ - Sensor measurement of α

$\bar{q}$ - Sensor measurement of q

b_{11} - The first diagonal element of matrix B_i

b_{22} - The second diagonal element of matrix B_i

$\bar{p}$ - Sensor measurement of p

$\bar{\beta}$ - Sensor measurement of β

$\bar{r}$ - Sensor measurement of r

ζ - Damping ratio

τ - Time constant

I - Information matrix

CHAPTER 1

INTRODUCTION

1.1 Statement of Problem

This dissertation presents the formulation of a learning control system. The problem that motivated the development of this learning control system was the desire to maintain uniform handling qualities of an aircraft over the entire flight envelope despite wide variations of dynamic pressure and other less predictable changes.

A Learning Control System (LCS) has been developed to accomplish this objective by adjusting, in a prescribed manner, the feedforward and feedback gains of the aircraft control system. The problem of designing the LCS was divided into the design problem of three basic subsystems that constitute the LCS. 1. The Information Acquisition Subsystem (IAS), 2. The Learning Algorithm Subsystem (LAS) and 3. The Memory and Control Process Subsystem (MCPS). Two techniques are developed for designing the IAS. The first technique makes use of Liapunov's direct method and the second technique is based on Newton-Raphson method. Each IAS may be combined with the LAS and MCPS to form a LCS. The LAS is designed using a sequential coefficient estimator technique which is based on iterative least-square algorithms. The MCPS consists of the collection of updated coefficients which are used to compute the feedforward and feedback gains via a set of control laws.

The next section describes a brief summary of prior work in this area. A more extensive description of prior work in adaptive and/or learning control systems is given in Chapter 2.

1.2 Summary of Prior Work

Over the years the need for adaptive control on aircraft has been debated. The alternative of scheduling autopilot gains according to sensed pressure, altitude and Mach number appears to work well for most aircraft and is relatively simple to implement. This gain scheduling has the advantage of allowing rapid changes in gains and feedback paths as a function of flight condition and vehicle configuration but suffers from the rather precise knowledge of the system dynamics required to establish a workable gain schedule. This is one of the reasons for the surge of interest in systems that automatically adjust feedback gains as a function of aircraft stability and control characteristics evaluated on-line in flight. These adaptive systems have not gained wide acceptance. The X-15 aircraft, to our knowledge, was the only previous aircraft that had an adaptive control system. Although it worked reasonably well, there were difficulties.[93] In designing adaptive control systems most important is the problem of guaranteeing stability of the adaptive and control loops of the system under operation[42,59]. Still another practical problem is the frequent need for a dithering signal to excite the system during periods of control inactivity. The signal must be subliminal to the pilot and crew. The need to limit the amplitude of this signal usually requires that the adaptive loops operate with a most unfavorable signal-to-noise ratio. The problems of the existing adaptive techniques indicate that the system should allow gain adjustments to be made only when the adaptive system passed certain tests. This restriction, however, may preclude rapid gain adjustments and if such adjustments are required, only a gain

scheduling system would be able to handle the problem. Seemingly, the next advance in flight control systems should take the best of the two worlds of gain scheduling and adaptive control and eliminate the undesirable features of each.

A suitable approach to design the information acquisition subsystem is the parameter adaptive model-reference system. This scheme consists of a system, a model, and an adaptive algorithm for adjusting the model parameters, such that the model will converge asymptotically to an equivalent input-output representation of the unknown system. This approach was first considered by Whitaker et al[89] in their application to controlling the behavior of an aircraft. A more extensive summary of prior work on parameter adaptive model-reference systems is presented in section 2.2.

The learning algorithm subsystem introduces memory capabilities to the overall system thus, resulting in a self-organizing or learning control system. The learning system has the capability of changing its basic structure (including the adaptive logic and the performance index) as a function of its experience and/or its environment. Such a system is usually expected to learn the solution to a control problem on-line, a process required because of, and despite, incomplete a priori knowledge of the plant and its environment. A more detailed description of prior work in the field of learning systems is presented in section 2.3.

1.3 Summary of Results Obtained

Chapters 4 and 5 present the results obtained by the application of the learning control system to control the longitudinal and lateral

dynamics of the F-8 DFBW aircraft.

In Chapter 4, the learning control system simulation is not concerned with real-time while the aircraft is in flight. For the modeling of the longitudinal and lateral dynamics of the plant, fourth order linearized representations are used associated with equilibrium flight. A comparison of two different learning control systems based upon two different information acquisition subsystems: 1) Liapunov method and 2) Newton-Raphson method is also discussed in this chapter. The comparison reveals that the Newton-Raphson information acquisition subsystem results in an overall superior performing learning control system.

Our learning control system developed in Chapter 3 is applied in Chapter 5 to the piloted six-degree-of-freedom simulation of the F-8 DFBW aircraft. Due to the real-time constraint, the information acquisition subsystem is implemented using reduced order models. More specifically, the longitudinal model describes only the short period longitudinal mode without considering the longitudinal phugoid mode because its time constant is normally large, and its definition is not a major element in adjusting the feedback gains of the primary control loops.

For the same reason, only the lateral predominant modes are characterized by our model namely, the lateral roll mode and the lateral Dutch roll mode. The reduced order models generate a modeling error noise. Due to the introduced modeling error noise and to assure proper learning of the system parameters, we develop convergence and confidence criteria.

As shown in the results of the piloted six-degree-of-freedom simulation of the F-8 DFBW aircraft, the handling qualities of the aircraft remain the same despite wide variation of flight conditions. This

in turn, implies that the learning control system may be applied to control plants whose parameters are functions of several variables. To do so, the same approach as presented in this dissertation may be followed with slight modifications depending upon the structure of the plant.

The main difference between the learning system developed here and parameter adaptive systems of the type studied in reference [80] is that the learning system recognizes patterns of the parameter estimates over the state space and parameterizes these estimates over that space for later use. For aircraft this implies that, for example, the parameter estimate M_{α} , partial derivative of the pitching moment with respect to angle of attack, be recognized as strongly dependent upon altitude and mach number (L,M) and that the explicit functional representation be determined for future use. Thus, if an aircraft has been flown previously at one (L,M) condition where a successful identification of M_{α} was made, a learning system as described here, would recall the previously learned value, whereas a parameter adaptive system would require another identification of M_{α}. For the latter case auxiliary inputs must disturb the vehicle on a regular basis to facilitate continual parameter identification. Alternatively, the learning system creates relationships among parameter estimates versus flight conditions and assembles these relationships into maps (memory) as information becomes available during normal flight without requiring auxiliary disturbance inputs.

The learning control system is an improvement over conventional gain scheduling techniques because it introduces a significant saving in storage and also makes practical the real time computation of the

parameters and the gains by a table look-up. As compared with conventional adaptive systems, the learning control system introduces an improvement because it does not require a dither signal to excite the system during periods of control inactivity. The learning control system may also be viewed as a parameter estimation system. In this case, it is a global estimator over the entire flight envelope, thus providing information about parameters that are functions of several other variables. To emphasize this aspect, we present in Chapter 5 three dimensional curves which describe the variation of the parameters with respect to altitude and mach number (L,M) as obtained from the learning control system.

1.4 Mathematical Formulation

The mathematical formulation and functional organization of the learning control system is presented in Chapter 3. Mathematical techniques used to design each subsystem are also developed in this chapter. Both Liapunov's direct method and Newton-Raphson method are used to design the adaptive algorithm of the information acquisition subsystem. These parameter adaptive approaches are found in sections 3.2 and 3.3 respectively where we also develop two convergence criteria, one for each individual information acquisition subsystem, as an aid in determining how much adaptation has taken place over the identification interval. This criterion may also be used as an aid in choosing the parameters of the adaptive algorithm based on the Liapunov's direct method. The development of the learning algorithm subsystem presented in section 3.4 is based on an iterative least-square algorithm. In section 3.5 we describe the memory and control process subsystem which

consists of the collection of updated coefficients that are used to compute the feedforward and feedback gains via a set of control laws.

The next chapter presents a review of adaptive and/or learning systems and flight control systems.

CHAPTER 2

HISTORICAL BACKGROUND

2.1. Introduction

This chapter presents a brief summary of the state of the art of adaptive and/or learning control systems as applied to flight control systems.

In general, adaptive and learning control systems represent an effort to extend the operating range of conventional control systems exposed to extraordinarily broad variations of environment or parameter values. If these variations are severe, it becomes necessary to alter certain system parameters to produce a satisfactory response over the entire range of operation. Furthermore, an adaptive and/or learning system also provides a means of continuously monitoring its own performance in relation to a given figure of merit (criterion) and thereby modify its own parameters by some action so as to approach the best performance.

The advancements of flight control systems and the theory required to permit increased performance of future aircraft will be discussed in sections 2.4 and 2.5 respectively.

Section 2.2 will discuss adaptive systems, in particular, Parameter Adaptive Model Reference Systems (PAMRS). PAMRS happen to be the very popular adaptive systems because they are useful in various applications which require rapid adaptation, for example, autopilots and the modeling of various systems such as socioeconomic or physiological systems.

Section 2.3 will examine the theoretical state of the art of Learning Control Systems (LCS) and the reasons for limited application of these

systems as apposed to adaptive control systems.

The evolution of analog to digital flight control systems which has spread through avionics so that it now reaches the central core of the automatic flight control systems and the reasons that are attributed to this occurrence are examined in section 2.4.

Finally, section 2.5 gives particular reference to the NASA F-8 Digital Fly-By-Wire (DFBW) program.

2.2. Parameter Adaptive Model Reference Systems (PAMRS)

One of the conceptually simplest and most flexible methods for system identification is the model reference system approach[8,9,22]. A known input is simultaneously fed to the process and to a model with adjustable parameters. The adjustable parameters are changed by an adjustment mechanism which receives the process output and the model output as inputs. If the algorithm for adjusting the parameters is designed properly, then the model-reference system output error will eventually vanish and the model will converge asymptotically to an equivalent input-output representation of the unknown system. Such schemes consisting of a system, a model, and an adaptive algorithm are usually referred to as parameter adaptive model-reference systems (PAMRS). PAMRS are well suited for on-line identification. A basic feature of PAMRS is that they can also be used in adaptive control where the roles of the system and the model are reversed[67,91].

The PAMRS formulation of the on-line identification problem was first considered by Whitaker et al[89] in their application to controlling the behavior of an aircraft. In their report, they derived the adaptive

algorithm based on the gradient of an even function of the error between model and reference system outputs. The error function chosen was very critical and convergence was not guaranteed.

Osburn et al[66] designed the PAMRS using a performance index minimization method which has since been referred as the MIT design rule. The performance index is the integral squared of the response error. This rule has been very popular due to its simplicity in practical implementation.

The requirement that the closed loop is stable is a necessary design criterion. Since the system consisting of the adjustable model, the process, and the adaptive algorithm is nonlinear the stability problem is not trivial. In order to guarantee system stability for all inputs one may use Liapunov's direct method to design the adaptive algorithm of PAMRS by selecting the design equations which satisfy conditions derived from Liapunov's second method. Other methods are also available*. Butchart and Shackcloth[9] first suggested the use of a quadratic Liapunov function, which was employed later by Parks[67] to redesign systems formerly designed by the MIT rule. However, Parks chooses the derivative of the Liapunov function negative semidefinite so that if the error goes to zero, the parameters stop changing and consequently the design equations become input dependent. In a paper by Shahein et al[75] this shortcoming is emphasized and an attempt is made to choose the derivative of the Liapunov function negative definite in error and parameter misalignment. However, the obtained parameter adjusting equations are dependent on the derivatives of the input and unknown parameters.

---

* See References (42, 43)

Practical applicability of the Liapunov designs of PAMRS is limited because disturbances and incomplete adaptation[46] have a destabilizing effect on the system stability. A serious limitation occurs when the plant output measurements are corrupted with noise, leading to biasing in the adaptive loop, and to erroneous parameter compensation. A related problem is created when the state variables required in the Liapunov identification method have to be generated from noisy measurements. This last problem can be partly circumvented by reducing the order of the required state variable generator (SVG)[60] by using the Kalman lemma[36] of a positive real transfer function, or by using reduced state feedback[67]. Another disadvantage is that the Liapunov design rule for adaptive control may not be applicable to cases where the plant parameters cannot be directly adjusted. Such a case was mentioned by Winsor et al[91] and a solution, though quite complex, was offered by Gilbart et al[22].

Most other designs of PAMRS are based on a gradient approach which usually results in systems that are only locally stable, and therefore, their convergence is only guaranteed if the state and the parameters of the model are always close to those of the plant's[25]. This characteristic makes these approaches unreliable during the initial stages of the adaptive process when the state and parameters of the plant and the model may not be close. For the same reasons, the rate of adaptation of these gradient methods has to be always kept very small. Different gradient-based nonlinear programming methods can be combined in a unified framework and may be applied to the adaptation algorithm via the maximum likelihood principle[25]. The use of maximum likelihood estimation in practice leads to difficult nonlinear programming problems[14]. In a lot

of cases the likelihood function has multiple maxima in the parameter space and the use of the gradient techniques may lead to convergence to the wrong stationary points. It is important to locate the absolute maximum of the likelihood function since it provides the unbiased estimate of the parameters. It should be clear that the difficulties in obtaining the absolute maximum of the likelihood function does not invalidate the likelihood principle[14]. The anomalies in the likelihood function are usually caused by either overparameterization (leading to nearly singular information matrix), or underparameterization (leading to saddle points). These problems have been considered by Edwards[14], Astrom and Bohlin[3], and Bohlin[8].

The starting values for the iterations used to maximize the likelihood function are very important to ensure convergence to the absolute maximum. The computation of the gradients of the likelihood function with respect to the adjustable parameters usually require the knowledge of the sensitivities of the model states with respect to the parameters which is the most time consuming part in the adaptation algorithm.

For this reason, research has been done on the computation of state sensitivities using reduced order models. Astrom and Bohlin[3] have proposed techniques for the model reduction in the case of single-input single-output systems in a canonical form. For the multi-input multi-output case little research has been done to develop techniques to reduce the order of the model, except of finding bounds on the order of the model[12,90].

The previous discussion suggests that one should consider and study the usefulness of other identification and modeling methods. One

of the recently more advanced techniques for this purpose can be considered to be the adaptive learning control system concept. Therefore, in the following section, background information about learning control systems is discussed.

2.3. Learning Control Systems

Published literature[18] on the theoretical state of the art of learning control systems has grown substantially within the past ten years. Practical applications however, are not nearly so great in number nor as widely distributed and read. This may be due to the cost and difficulty of implementation and that previous levels of research and development efforts in this area have not been maintained as a result of the national economy.

This section attempts to give a brief background of the various types of learning control systems and to describe the present state of learning control applications through the use of both, mini and general purpose digital computers.

The behavior or performance of certain types of advanced control systems have been labeled adaptive and learning. Learning is most widely used and accepted as describing the appropriate use of past experience and the resulting improvement in overall system performance.

A learning controller can be described as any control system that a) collects pertinent information (past and present), about the process it controls, and the environment it works in and then b) processes this information to optimize a certain performance index. The order of the hierarchy is the distinguishing factor between learning and adaptive

systems. Control systems using information contained in their past input, output and environmental feedback signals which improve their own performance are termed adaptive. A self-organizing or learning control system is consequently one which demonstrates both, adaptive and memory capabilities. A learning system has the capability of changing its basic structure (including the adapting logic and the performance index) as a function of its experience and/or its environment. Such a system is usually expected to learn the solution to a control problem on-line, a process required because of, and despite, incomplete a priori knowledge of the plant and its environment. Theoretically, a learning system is also capable of overcoming failures of the adaptive loop.

There are many variations of learning concepts which have been proposed, not all of them agreeing with the other. Many have been labeled learning when they do not conform to this definition and are simply adaptive control systems.

In the field of learning systems for automatic control, there is not any one single theory which forms the base-line. A mixture of theories and techniques must be used.

The most prominent mathmatical techniques to formulate a learning system are described below:

1) Decision Theory[10,19,32]. In this method one tries to specify a decision surface so as to minimize the probability of error. The system is called a pattern classifier and the simplest one is the linear case where the decision surface is a hyperplane. A modification of this algorithm has been suggested[32] that tries to arrive at a piecewise linear decision surface from a given set of classified feature vectors. This modified

method is called the trainable controller method. It quantizes the state space to elementary hypercubes in which control action is assumed constant. During the training process the trainable controller makes changes in its weight based on the training pattern being "shown" to it, together with the output of that pattern. This is done until the number of classification errors has reached a steady state value. It is shown[79] that this method can approximate a decision surface to an arbitrary degree of accuracy (by increasing the number of quantum zones).

2) Markov Chain Theory[65,76]. This method provides an approach to modelling the dynamics of learning controllers. This method is also called learning with reinforcement[64] even though this is a more general concept. By learning with reinforcement is meant the process where there is a continuous scale of rewards with strict reward and strict punishment representing the upper and lower bounds respectively of this scale. The engineering system is then designed to extremize reward. This method is used when there are n distinct control actions and the system chooses one of them by a specific probability. The effect of learning in this system can be viewed as an iteration of probabilities; hence, from one trial to the next a transition in the probabilities occurs. In general, it can be proved that the probability of correct action will converge to its maximum in the mean[20].

3) Bayesian Learning In Control Systems[1,33]. This is an on-line approach to improve the performance of a linear stochastic system by reducing the uncertainties about the plant parameters belonging to a finite set; if not, discretization of the parameter space should be done, which is a serious shortcoming of the method. A class of estimators and controllers is formed among which the stochastically optimal combination is

a member. Baye's rule is then applied to reduce the uncertainty of the unknown parameters by sequentially computing their respective a posteriori probabilities. The learning feature of the a posteriori probabilities is utilized in order to select the feedback controller among the possible combinations available. This algorithm is designed for linear Gaussian systems with quadratic performance criteria and unknown system parameters belonging to a finite set.

4) The Stochastic Approximation Method[84,85]. This method has been introduced by Tsypkin. The method utilizes a procedure where the unknown system dynamics as well as the control action are modeled by linearly independent functions weighted by adjustable coefficients. The learning scheme consists of updating the weighting coefficients to match the approximate combination of stochastic and optimal control. This method requires the evaluation of sensitivity matrices which, in the case of a linear plant, depend on the unknown system parameters. A difficulty arises with the choice of appropriate matrix functions which should span the corresponding space. This method is also called "hill climbing", since one perturbs the adjustable parameters in the direction of increasing performance index.

Having examined adaptive and learning control systems, in the following sections we will discuss the advancements of flight control systems.

2.4. Analog and Digital Flight Control Systems

From a meager start in sensors, the digital revolution has spread through avionics until it has now reached the central core of the automatic flight control system. The realignment of industry from analog

systems to digital systems is based on expectations that a number of problems associated with existing analog systems will be eliminated both for the designer and the user.

Many characteristics attributed to digital systems are said to solve the analog problems. Digital automatic flight control systems are a reality and, while they may not yet be perfect, they offer substantial advantages in capability, reliability and cost effectiveness over another generation of analog systems.

In terms of capability, the functional requirements for automatic flight control systems have been a joint function of basic electronic technology, packaging and the evolution of commercial transports. An automatic flight control system (AFCS) that can provide automatic control virtually from lift-off is basic to the aircraft. In conjunction with sophisticated navigation and sensor subsystems, the pilot is able to engage the AFCS shortly after take-off, climb to cruise altitude, fly along a predetermined route, and automatically land in near zero visibility conditions at the end of the flight by doing little more than pressing the correct buttons at the appropriate time.

The continuing trend is toward each generation of AFCS being more complex than its predecessor. The interface requirements have arisen from the number of sensors, actuators and logic data required to support the AFCS computer in accomplishing the various pilot-selected modes. The large amount of interface connections is significant to the user, since each connection represents a point where malfunctions or misfunctions can occur.

A factor that influences analog system capability and maintainability is the nature of the analog computer and its dedicated circuitry.

For each branch of the system control laws, a separate computational path comprising dedicated circuitry must be utilized. This has led to much difficulty in identifying and isolating system failures so that appropriate maintenance activity can be conducted. To alleviate these difficulties, research has been directed towards digital control systems.

Numerous studies in the past several years have been conducted to determine the applicability of digital computers to automatic flight control. The benefits most commonly attributed to digital flight controls can be categorized as improvements in computational accuracy, design flexibility, improved cost and reliability integration of functions, and improved capability for self-testing.

A digital computer is not inherently an accurate computer. There is a finite resolution to each calculation made that is a function of the scaling and digital word length. (Analog resolution is theoretical infinite). The digital computer's primary characteristic is that the calculations are repeatable. Two computers given the same input, will provide precisely the same output because the computers are not subject to internal analog errors such as gain tolerances or shifting null voltages. Repeatability of calculation is a distinct advantage in achieving virtually perfect mutual comparison or tracking between the outputs of computers operating in parallel-redundant systems.

A major aspect of digital computer flexibility is the commonality of the processor with many different applications. The processor nonrecurring costs are then spread out over several different systems. This supposition is felt to be in particular contrast to the experience with analog systems where it is unusual for a system designed initially for

installation on one airplane type to be used for a subsequent airplane model. The prime motivation factor, however, for changing auto-pilots from one model to the next is the changing electronic technology and not the inability of simple adaptation of one system to all the models.

One of the major advantages of a digital computer is the capability to time share the computational equipment. That is, unlike the analog system in which computational elements are mainly dedicated to one task, a digital system can use the same equipment to perform several unrelated computations within a given time frame. Failure to apply this capability will impair the cost-effectiveness of a digital flight control system.

The potential for self-test within a digital flight control system is substantially higher than for a similar analog system. The main problem in the analog case is that the built-in test equipment (BITE) requires dedicated circuits and directly affects complexity, reliability and cost. Such is not the case with a digital system. Self-test does require additional program to implement but no other dedicated circuitry need be required. The next section presents a brief overview of the F-8 Digital Fly-By-Wire (DFBW) study.

2.5. The F-8 Digital Fly-By-Wire (DFBW) Program

The broad objective of the NASA F-8 Digital Fly-By-Wire program is to provide the technology required for implementation of advanced, reliable, digital fly-by-wire (DFBW) flight control systems which will permit greater operational capability and increased performance of future aircraft. The program makes use of an F-8C naval fighter test aircraft which

has been modified by removal of the mechanical flight control system and its replacement with an electronic flight control system.

The program has been conducted in two phases. Phase I explored pilot acceptability and technical feasibility of digital fly-by-wire using a single channel digital system constructed from components developed previously for the Apollo Space Program. Phase II objectives include establishing a design base for practical multiple channel DFBW systems using a triplex digital system, to flight test the system and certain selected space shuttle flight control system concepts and to conduct research into and evaluate advanced control law concepts suitable for digital implementation.

Research to investigate and promote advanced control laws for possible flight experimentation has been motivated by the greater flexibility and logic capability of digital systems as compared to analog systems and by the increased complexity and sophistication expected of future aircraft flight control systems.

There are two major types of adaptive control. One type, sometimes called analytical redundancy, has to do with adaptation to failures in control system components internal to the aircraft such as sensors and actuators. The idea is to take advantage of the kinematic or dynamic relationships which exist between the sensors and/or actuators of a moving physical system such as an aircraft to complement or reduce the hardware redundancy needs of the physical system[11,30].

The second type of adaptive control has to do with the adaptation to the changing external environment of the aircraft, such as changes in dynamic pressure, mach number and altitude, etc.

These adaptive systems have not gained wide acceptance partly due to the success of gain scheduling technology and also due to the existence of both theoretical and practical problems that are still unresolved in the field of adaptive control. Most important is the problem of guaranteeing stability of the adaptive and control loops of the system under operation[42,59]. Another practical problem is the frequent need for a dithering signal to excite the system during periods of control inactivity. The signal must be subliminal to the pilot and crew. The need to limit the amplitude of this signal usually requires that the adaptive loops operate with un favorable signal-to-noise ratio.

The problems mentioned above indicate that a requirement needs to be imposed on any adaptive system regarding when to allow gain adjustments to be made. The system should allow gain adjustments to be made only when the adaptive system passed certain tests. This restriction, however, may preclude rapid gain adjustments and if such adjustments are required, only a gain scheduling system would be able to handle the problem. Seemingly, the next advance in flight control systems should take the best of the two worlds of gain scheduling and adaptive control and eliminate the undesirable features of each. This dissertation describes a system intended to accomplish that objective. The described system is called a learning control system[55]. It is, in fact, an adjustable blend of a gain scheduling system and an adaptive control system.

Having considered background information on adaptive learning control systems and flight control systems, our Learning Control System (LCS)

will be developed in general terms in the following chapter. We will then consider the F-8C aircraft to be the plant and apply our LCS to control its dynamics in chapters 4 and 5.

CHAPTER 3

THE LEARNING CONTROL SYSTEM

3.1. Introduction

The basic problem to be considered in this chapter is that of designing a Learning Control System (LCS) that is capable to meet design requirements over many possible operating conditions of the plant by adjusting, in a prescribed manner, the feedforward and feedback gains of the plant. Figure 3.1 shows the functional organization of the learning control system that consists of three basic subsystems: 1. The Information Acquisition Subsystem (IAS), 2. The Learning Algorithm Subsystem (LAS) and 3. The Memory and Control Process Subsystem (MCPS). Two techniques are described for developing the IAS. The first technique makes use of Liapunov's direct method and the second technique is based on Newton-Raphson method. Each IAS may be combined with the LAS and MCPS to form a LCS. The LAS is developed using a sequential coefficient estimator technique which is based on iterative least-square algorithms. The MCPS consist of the collection of updated coefficients which are used to compute the feedforward and feedback gains via a set of control laws. In the next sections we will describe general mathematical techniques used to develop the above mentioned subsystems.

3.2. The Information Acquisition Subsystem (IAS), Liapunov's Direct Method

The basic problem to be considered in this section is that of designing an adaptive algorithm that will result in a stable Information Acquisition Subsystem (IAS). Liapunov's stability theorems offer possible solutions to this design problem, the particular solution depending in part upon the form of the Liapunov function selected.

Consider the Information Acquisition Subsystem (IAS) of Fig. 3.2 where the linear multi-input multi-output plant with constant or slowly time varying parameters is described by the system of differential equations

$$\dot{y} = A_p(p)y + B_p(p)\mathcal{S}_e \tag{3.2.1}$$

where y is the n - dimensional state vector and $\mathcal{S}_e$ is the r - dimensional input vector. Matrices $A_p(p)$ and $B_p(p)$ describe the dynamic characteristics of the plant. Let $\mathcal{S}_e$ be a linear combination of the states and the control input given by

$$\mathcal{S}_e = Ky + G\mathcal{S}_s \tag{3.2.2}$$

where $\mathcal{S}_s$ is the control input and G and K are the feedforward and feedback gain matrices of the plant respectively. Substituting Eg. (3.2.1) yields

$$\dot{y} = \left[A_p(p) + B_p(p)K\right] y + \left[B_p(p)G\right]\cdot\mathcal{S}_s = A_p'(p)y + B_p'(p)\mathcal{S}_s \tag{3.2.3}$$

Let the plant described by Eq. (3.2.3) be represented by a model of the form

$$\dot{z} = Fz + \left[A_m(\hat{p}) - F\right] y + B_m(\hat{p})\mathcal{S}_s \tag{3.2.4}$$

where F is a stable matrix, z denotes the n - dimensional model state vector and $A_m(\hat{p})$ and $B_m(\hat{p})$ describe the model closed loop dynamic characteristics

as a function of parameter $(\hat{p})$. Note that $(\hat{p})$ and matrices $A_m(\hat{p})$ and $B_m(\hat{p})$ must satisfy the following conditions:

$$A_m(\hat{p} = p) = \left[A_p(p) + B_p(p)K\right] = A_p'(p) \tag{3.2.5}$$

$$B_m(\hat{p} = p) = B_p(p)G = B_p'(p) \tag{3.2.6}$$

The dimensionality of the model is assumed to be the same as that of the plant. Let the model-plant state error be defined as

$$e = z - y \tag{3.2.7}$$

The model-plant error differential equation yields

$$\dot{e} = Fe + \left(\sum_{i=1}^{n} b_i u_i^T\right)y + \left(\sum_{i=1}^{n} d_i w_i^T\right)\int_s \tag{3.2.8}$$

where

$$\sum_{i=1}^{n} b_i u_i^T = A_m(\hat{p}) - A_p'(p) \tag{3.2.9}$$

$$\sum_{i=1}^{n} d_i w_i^T = B_m(\hat{p}) - B_p'(p) \tag{3.2.10}$$

Vectors b_i and d_i are constant for all i and u_i and w_i are vectors whose elements are the misalignments of parameters $(\hat{p})$ and (p) of the i-th row.

In the Liapunov approach a Liapunov function V is chosen which is a quadratic form of the system error e and the parameter misalignments u_i and w_i. Let

$$V = e^T P e + \sum_{i=1}^{n} u_i^T N_i u_i + \sum_{i=1}^{n} w_i^T Q_i w_i \tag{3.2.11}$$

where P, N_i and Q_i are symmetric positive matrices with constant elements. The time derivative of the Liapunov function yields

$$\dot{V} = e^T(F^TP + PF)e + 2\sum_{i=1}^{n}\left[\dot{u}_i^T N_i + y^T(b_i^T Pe)\right]u_i + \tag{3.2.12}$$

$$+ 2\sum_{i=1}^{n}\left[\dot{w}_i^T Q_i + \mathcal{S}_s^T(d_i^T Pe)\right]w_i$$

The matrix P can be found as the unique solution of

$$F^TP + PF = -Q \tag{3.2.13}$$

where Q is any n x n symmetric positive definite matrix[27]

Applying Liapunov's stability criterion $V > 0$ and $\dot{V} \leq 0$ and integrating yields

$$u_i^T = -\int_o^t y^T(b_i^T Pe)N_i^{-1}dt + u_{io}^T \tag{3.2.14}$$

$$w_i^T = -\int_o^t \mathcal{S}_s^T(d_i^T Pe)Q_i^{-1}dt + w_{io}^T \tag{3.2.15}$$

Substituting Eqs. (3.2.14) and (3.2.15) into Eqs. (3.2.9) and (3.2.10) and rearranging the resulting equations one obtains

$$A_m(\hat{p}) = A_m(\hat{p}_o) - \sum_{i=1}^{n}\int_o^t b_i y^T(b_i^T Pe)N_i^{-1}dt \tag{3.2.16}$$

$$B_m(\hat{p}) = B_m(\hat{p}_o) - \sum_{i=1}^{n}\int_o^t d_i \mathcal{S}_s^T(d_i^T Pe)Q_i^{-1}dt \tag{3.2.17}$$

where

$$A_m(\hat{p}_o) = A_p'(p) - \sum_{i=1}^{n} b_i u_{io}^T \tag{3.2.16a}$$

$$B_m(\hat{p}_o) = B_p'(p) - \sum_{i=1}^{n} d_i w_{io}^T \qquad (3.2.17a)$$

Note that $\hat{p}_o$ is an initial estimate of vector p and u_{io}, w_{io} are the initial misalignments at t = 0. After this initial choice, we proceed to solve Eqs. (3.2.16) and (3.2.17) to obtain vector $\hat{p}$.

Substituting Eqs. (3.2.13), (3.2.14) and (3.2.15) into Eq. (3.2.12) yields

$$\dot{V} = - e^T Q e \qquad (3.2.18)$$

The form of $\dot{V}$ is negative definite with respect to e because Q is positive definite. Therefore, the error differential Eq. (3.2.8) is asymptotically stable in the whole for e which means that after an initial disturbance the Euclidean norm $\|e\| \longrightarrow 0$ for $t \rightarrow \infty$. Since $\dot{V}$ is indefinite with respect to u_i and w_i, the parameter misalignments do not necessarily go to zero, which means that the identification is not exact. To overcome this difficulty, another input is applied to the plant, if possible, after the model-plant state error has reached the steady state. Under certain circumstances, there may be a need to apply several inputs in order to obtain a better identification.

As we pointed out earlier, the adaptive algorithm may vary according to the Liapunov function selected. To illustrate this, let us choose a somewhat different Liapunov function

$$V = e^T P e + \sum_{i=1}^{n} \left[u_i + (b_i^T P e) y\right]^T N_i \left[u_i + (b_i^T P e) y\right] + \sum_{i=1}^{n} \left[w_i + (d_i^T P e) \delta_s\right]^T Q_i \left[w_i + (d_i^T P e) \delta_s\right] \qquad (3.2.19)$$

The time derivative of the Liapunov function following from Eg. (3.2.19) is

$$\dot{V} = e^T(F^TP + PF)e + 2\sum_{i=1}^{n}\left\{\dot{u}_i + d/dt\left[(b_i^TPe)y\right]\right\}^T \cdot N_i\left[u_i + (b_i^TPe)y\right]$$

$$+ 2\sum_{i=1}^{n}\left\{\dot{w}_i + d/dt\left[(d_i^TPe)\,\zeta_s\right]\right\}^T \cdot Q_i\left[w_i + (d_i^TPe)\,\zeta_s\right]$$

$$+ 2\sum_{i=1}^{n} y^T(b_i^TPe)u_i + 2\sum_{i=1}^{n}\zeta_s^T\,(d_i^TPe)w_i \qquad (3.2.20)$$

Again, applying Liapunov's stability criterion $V > 0$ and $\dot{V} \leq 0$ yields

$$u_i^T = -\int_0^t y^T(b_i^TPe)N_i^{-1}dt - y^T(b_i^TPe) + u_{io}^T \qquad (3.2.21)$$

$$w_i^T = -\int_0^t \zeta_s^T(d_i^TPe)Q_i^{-1}dt - \zeta_s^T(d_i^TPe) + w_{io}^T \qquad (3.2.22)$$

The adaptive algorithm equations resulting by substituting Eqs. (3.2.21) and (3.2.22) into Eqs. (3.2.9) and (3.2.10) are different from the previously obtained Eqs. (3.2.16) and (3.2.17) because of the different choice of the Liapunov's function and are given below by

$$A_m(\hat{p}) = A_m(\hat{p}_o) - \sum_{i=1}^{n}\int_0^t b_i y^T(b_i^TPe)N_i^{-1}dt - \sum_{i=1}^{n} b_i y^T(b_i^TPe) \qquad (3.2.23)$$

$$B_m(\hat{p}) = B_m(\hat{p}_o) - \sum_{i=1}^{n}\int_0^t d_i \zeta_s^T(d_i^TPe)Q_i^{-1}dt - \sum_{i=1}^{n} d_i \zeta_s^T(d_i^TPe) \qquad (3.2.24)$$

Substitution of Eqs. (3.2.21) and (3.2.22) into Eq. (3.2.20) yields

$$\dot{V} = - e^T Q e - 2 \sum_{i=1}^{n} y^T (b_i^T P e)^2 y - 2 \sum_{i=1}^{n} \zeta_s^T (d_i^T P e)^2 \zeta_s \qquad (3.2.25)$$

Since Eq. (3.2.25) contains more negative terms than Eq. (3.2.18) the adaptive algorithm defined by Eqs. (3.2.23) and (3.2.24) results in an accelerated error convergence[88] even though $\dot{V}$ is still negative definite in error e only. Note that Eqs. (3.2.23) and (3.2.24) are solved in a similar manner as Eqs. (3.2.16) and (3.2.17).

The performance of the IAS is monitored by a convergence criterion defined by

$$\eta = V(t)/V(0) \leq \eta_{min} \qquad (3.2.26)$$

where η_{min} is prescribed by the designer according to the desired accuracy between vectors p and p for a prescribed length of time while the system is subject to sufficient excitation. Since the plant parameters are unknown we have no knowledge of u_i and w_i which means that we cannot calculate the Liapunov function V(t) and consequently the convergence criterion η. To overcome this difficulty let us rewrite Eq. (3.2.26) as

$$\eta = V(t)/V(0) = 1 + \left[V(t) - V(0)\right] /V(0) = 1 + \int_0^t \dot{V}(t)dt/V(0) \qquad (3.2.27)$$

The Liapunov function may be viewed as being composed of three parts, i.e.

$$V = V_1 + V_2 + V_3 \qquad (3.2.28)$$

Consider Eq. (3.2.11) and let

$$V_1 = e^T P e$$

$$V_2 = \sum_{i=1}^{n} u_i^T N_i u_i \tag{3.2.29}$$

$$V_3 = \sum_{i=1}^{n} w_i^T Q_i w_i$$

If matrices N_i and Q_i are chosen such that

$$P \gg N_i \quad \text{and} \quad P \gg Q_i \qquad \text{(for every i)} \tag{3.2.30}$$

then V(0) may be approximated by

$$V(0) \cong V_1(T_m) - \int_0^{T_m} \dot{V}(t)dt \tag{3.2.31}$$

where T_m is the time at which V_1 reaches its maximum value, V_{1max}. Substituting Eq. (3.2.31) into Eq. (3.2.27) yields

$$\eta = 1 + \left\{ \int_0^t \dot{V}(t)dt \Big/ \left[V_{1max} - \int_0^{T_m} \dot{V}(t)dt \right] \right\} \tag{3.2.32}$$

which is the approximation of Eq. (3.2.26) used to calculate the convergence criterion η. For the adaptive algorithm given by Eqs. (3.2.23) and (3.2.24) the same approximation, Eq. (3.2.32), may be used to calculate the convergence criterion η, but in this case $\dot{V}(t)$ should be used as indicated by Eq. (3.2.25).

When the output measurements of the plant are corrupted with noise, this noise appears both in the plant output and in the error signal. Because

of the multiplication in the adaptive law Eq. (3.2.16), the computed $\hat{p}_i$ will be biased*. To overcome this, one may choose a model of the form

$$\dot{z} = A_m(\hat{p})z + B_m(\hat{p})\zeta_s \tag{3.2.33}$$

leading to an error differential equation of the form

$$\dot{e} = A_p(p)e + (\sum_{i=1}^{n} b_i u_i^T)y + (\sum_{i=1}^{n} d_i w_i^T)\zeta_s \tag{3.2.34}$$

A similar type of development as before, will produce the following adaptive algorithm equation

$$A_m(\hat{p}) = A_m(\hat{p}_o) - \sum_{i=1}^{n} \int_0^t b_i z^T (b_i^T P e) N_i^{-1} dt \tag{3.2.35}$$

which is to be used instead of Eq. (3.2.16) in the case of small signal to noise ratio. In this case the elements $\hat{p}_i$ will not be biased since one uses the outputs of the model, denoted by z, which are not directly affected by noise, while in Eq. (3.2.16) one directly uses the noise obscured measurements of the plant to be identified.

Parameters $\hat{p}_i$ after they have passed the convergence criterion, defined by Eq. (3.2.26), are packed into a 1 - dimensional parameter vector $\hat{p}$ which will be used as an input to the Learning Algorithm Subsystem (LAS).

The next section describes an alternate approach to develop the LAS, namely the Newton-Raphson method.

---

* Note that $\hat{p}_i$ are the elements of matrix $A_m(\hat{p})$

3.3. The Information Acquisition Subsystem (IAS), Newton-Raphson Method

In this section the adaptive algorithm of the (IAS) will be designed by using a gradient-based nonlinear programming method that can be used for computing maximum likelihood estimates. Let the plant described by Eq. (3.2.3) be represented by a model

$$\dot{x} = A_m(\hat{p})x + B_m(\hat{p})\int_s \tag{3.3.1}$$

where x is the n - dimensional model state vector and all other variables are as defined before. The dimensionality of the model is assumed to be the same as that of the plant. Note that $\hat{p}$ is an estimate of p and matrices $A_m(\hat{p})$ and $B_m(\hat{p})$ must satisfy the conditions given by Eqs. (3.2.5) and (3.2.6).

Let the model-plant error be defined as

$$e = y - x \tag{3.3.2}$$

In the parameter estimation problems, when the maximum likelihood method is used, it is usually more convenient to work with the negative of the logarithm of the likelihood function. It is possible to do so because the logarithm is a monotonic function. It can be shown[51] that the negative log-likelihood function $J(\hat{p})$ is

$$J(\hat{p}) = \tfrac{1}{2}\sum_{i=1}^{N}\left\{e_i^T B_i e_i + \log\left|B_i^{-1}\right|\right\} \tag{3.3.3}$$

where B_i is an n x n matrix whose inverse is the covariance matrix of the plant's state, that is

$$B_i^{-1} = E\left[(y_i - \bar{y}_i)\ (y_i - \bar{y}_i)^T\right] \tag{3.3.4}$$

and N is a fixed number which denotes the amount of data that need to be

collected before the minimization process can begin. Note that $\bar{y}_i$ is the expected value of y_i; $\bar{y}_i = E(y_i)$.

It is important to have good starting values of the parameters since this considerably improves the probability of convergence and of locating the absolute maximum of the likelihood function. It is also useful to determine if an appropriate model is being used and all parameters are identifiable from the data.

The basic iteration of gradient-type methods have the form

$$\hat{P}_{j+1} = \hat{P}_j - \rho_j S_j f_j \tag{3.3.5}$$

where $\hat{P}_j$ is the parameter vector at the j-th iteration, f_j is a vector of gradients of the negative log-likelihood function $J(\hat{p})$, i.e.,

$$f_j = \partial J / \partial \hat{p} \Big|_{\hat{p}=\hat{p}_j} \tag{3.3.6}$$

and S_j is an approximation to the second partial matrix i.e.,

$$S_j = \left[\partial^2 J(\hat{p}) / \partial \hat{p}^2\right]^{-1} \Big|_{\hat{p} = \hat{p}_j} \tag{3.3.7}$$

Note that ρ_j is a scalar step size parameter chosen to ensure that $J(\hat{p}_{j+1}) < J(\hat{p}_j) - \epsilon$, where ϵ is a positive number that can be chosen in a variety of ways[25].

The class of the gradient-type methods differ mainly in the selection of S_j, and in some cases ρ_j and f_j. It is shown[48] that the convergence rate near the minimum for algorithm (3.3.5) with ρ_j chosen

by a one - dimensional search is

$$J(\hat{p}_{j+1}) \leq (\mu_{max} - \mu_{min})/(\mu_{max} + \mu_{min})^2 J(\hat{p}_j) \qquad (3.3.8)$$

where μ_{max} and μ_{min} are the maximum and minimum eigenvalues of $S_j(\partial^2 J/\partial \hat{p}^2)$. It is clear from (3.3.8) that the best convergence is achieved by making S_j as nearly as possible equal to $(\partial^2 J/\partial \hat{p}^2)^{-1}$. In developing our IAS we use Newton-Raphson technique as a member of the gradient-type methods.

For the Newton-Raphson technique S_j is chosen as $(\partial^2 J/\partial \hat{p}^2)^{-1}\Big|_{\hat{p}=\hat{p}_j}$ and $\rho_j = 1$ except when this choice of ρ_j gives an increase in cost. When this method converges, the convergence is quadratic. However, the method has the following drawbacks: a) It fails to converge to the desired optimum whenever $(\partial^2 J/\partial \hat{p}^2)$ has some negative eigenvalues. b) If $(\partial^2 J/\partial \hat{p}^2)$ is nearly singular, there are numerical problems in inverting it. This may result in slow or no convergence at all. c) Generally, the computation of $(\partial^2 J/\partial \hat{p}^2)$ is very expensive. This is the main reason that we will consider various modifications of this algorithm by doing some approximations in order to save on computation load.

The first modification will be to get an approximation of $(\partial^2 J/\partial p^2)$ rather than computing its exact value. Differentiating Eq. (3.3.3) with respect to $\hat{p}$ we get (assuming B_i constant),

$$f_j = \partial J/\partial \hat{p}\,\Big|_{\hat{p}=\hat{p}_j} = \left[-\sum_{i=1}^{N} (\partial x/\partial \hat{p})_i^T B_i e_i\right]_j \qquad (3.3.9)$$

where $\partial x/\partial \hat{p}$ is the sensitivity matrix of dimension n x ℓ (ℓ is the number of unknown parameters) whose form is

$$\partial x/\partial \hat{p} = \begin{bmatrix} \partial x_1/\partial \hat{p}_1 & \partial x_1/\partial \hat{p}_2 & \cdots & \partial x_1/\partial \hat{p}_\ell \\ \partial x_2/\partial \hat{p}_1 & \partial x_2/\partial \hat{p}_2 & \cdots & \partial x_2/\partial \hat{p}_\ell \\ \vdots & \vdots & & \vdots \\ \partial x_n/\partial p_1 & \partial x_n/\partial \hat{p}_2 & \cdots & \partial x_n/\partial \hat{p}_\ell \end{bmatrix} \tag{3.3.10}$$

Differentiating Eq. (3.3.9) with respect to $\hat{p}$ we get

$$S_j^{-1} = \left[\sum_{i=1}^{N} (\partial x/\partial \hat{p})^T B_i (\partial x/\partial \hat{p})_i\right]_j \cong (\partial^2 J/\partial \hat{p}^2)\Big|_{\hat{p} = \hat{p}_j} \tag{3.3.11}$$

Then substituting Eqs. (3.3.11) and (3.3.9) into Eq. (3.3.5) yields

$$\hat{p}_{j+1} = \hat{p}_j + \left[\sum_{i=1}^{N} (\partial x/\partial \hat{p})_i^T B_i (\partial x/\partial \hat{p})_i\right]_j^{-1} \left[\sum_{i=1}^{N} (\partial x/\partial \hat{p})^T B_i e_i\right]_j \tag{3.3.12}$$

where $(\partial x/\partial \hat{p})$, the sensitivity matrix, can be obtained by differentiating Eq. (3.3.1) with respect to $\hat{p}$ and interchanging $\partial/\partial \hat{p}$ with d/dt. This yields

$$d/dt(\partial x/\partial \hat{p}) = A_m(\hat{p})(\partial x/\partial \hat{p}) + \partial/\partial \hat{p}\left[A_m(\hat{p})x + B_m(\hat{p})\delta_s\right] \text{ x constant} \tag{3.3.13}$$

Since the initial conditions of the model, x(0), can be selected independently of $\hat{p}_o$, the initial condition for the sensitivity matrix $(\partial x/\partial \hat{p})$ is set to zero, (0). Hence, $(\partial x/\partial \hat{p})$ can be obtained by solving the set of differential equations given by Eq. (3.3.13). Since S_j^{-1} is

non-negative definite, one can always find a ρ_j such that $J(\hat{p}_{j+1}) < J(\hat{p}_j)$. The method, however, runs into the problem when S_j^{-1} is singular or nearly singular, that when inverting S_j^{-1} we may obtain an indefinite S_j, so that $J(\hat{p}_{j+1}) > J(\hat{p}_j)$ for all $\rho_j > 0$. For these cases it is better to obtain the parameter step by solving the following linear equations

$$S_j^{-1}(\hat{p}_{j+1} - \hat{p}_j) = - f_j \tag{3.3.14}$$

Several schemes[25] are available for selecting ρ_j. Since the calculation of $J(\hat{p})$ is very expensive[25], methods which require several trial values of ρ_j during each iteration are not desirable. A simple procedure is to use $\rho_j = 1$ in those cases where

$$J(\hat{p}_{j+1}) - J(\hat{p}_j) < \tfrac{1}{4} \rho_j f_j^T S_j f_j \tag{3.3.15}$$

If condition (3.3.15) is not satisfied, $J(\hat{p}_j)$, f_j, $J(\hat{p}_{j+1})$ and f_{j+1} are used to obtain a quadratic fit in ρ and the stationary value $\rho^{(1)}$ that minimizes the quadratic fit is computed using $\rho_j = \rho^{(1)}$.

The convergence criterion for this IAS is satisfied when the following conditions are met: a) The cost function $J(\hat{p}_{j+1})$ is below some quantity ϵ_1 fixed by the designer, i.e.

$$J(\hat{p}_{j+1}) \leq \epsilon_1 \tag{3.3.16}$$

b) The vector $\hat{p}_{j+1}$ is close to its previous iterate $\hat{p}_j$ in the Euclidean norm sense i.e.

$$\| \hat{p}_{j+1} - \hat{p}_j \| \leq \epsilon_2 \tag{3.3.17}$$

where ϵ_2 is determined by the designer. c) As we shall show in the following section (3.4) S_{j+1} is the covariance matrix of $\hat{p}_{j+1}$. Hence, its i-th diagonal element is checked to be smaller than the allowable covariance of the parameter $\hat{p}_i$ i.e.

$$(S_{j+1})_{ii} \leq \text{cov } \hat{p}_i \tag{3.3.18}$$

where cov $\hat{p}_i$ is determined by the designer and is the maximum tolerable covariance of the coefficient $\hat{p}_i$.

Parameters $\hat{p}_i$ after they have passed the convergence criterion are packed into a parameter vector $\hat{p}$ of dimension $\ell \times 1$ to be used in conjunction with the Learning Algorithm Subsystem (LAS).

3.4. The Learning Algorithm Subsystem (LAS)

The values of parameter vector $\hat{p}$ affecting the dynamics of the plant are fitted to predetermined analytical expressions which describe the behavior of $\hat{p}$ over a range of the plant's operating conditions, denoted by vector h . Assume the relationship between the parameter vector $\hat{p}$ and the plant's operating condition vector h be described by an unknown memoryless system

$$\hat{p} = f(h) + \lambda \tag{3.4.1}$$

where λ is the uncertainty vector of $\hat{p}$ with properties $E(\lambda) = 0$ and the covariance matrix

$$R = E(\lambda\lambda^T) = E\left\{\left[\hat{p} - E(\hat{p})\right].\left[\hat{p} - E(\hat{p})\right]^T\right\} \tag{3.4.2}$$

where $E(\hat{p}) = f(h)$

A model is assumed of the form

$$f(h) = H(h)C \tag{3.4.3}$$

where H(h) is the operating condition matrix whose elements in any row are linearly independent functions of h spanning the space f(h). The values of $\hat{p}$ and H(h) to be used in the evaluation of the coefficient vector C are received sequentially from the information acquisition subsystem. Hence, an iterative form of the least-square method is appropriate for obtaining the coefficient vector C each time new information ($\hat{p}$, h) is received from the IAS. The problem is to select an estimate of C, denoted by C_k, which minimizes the quadratic criterion ϕ_k given by

$$\phi_k = \sum_{i=1}^{k} \left[\hat{p}_i - H(h_i)C_k\right]^T R_i^{-1} \left[\hat{p}_i - H(h_i)C_k\right] \tag{3.4.4}$$

The subscript on C_k is used to emphasize that we are using k vector observations to compute the estimate. At present, the subscript is superfluous, but it will be helpful when we develop the sequential format in the sequel. Because the minimization of ϕ_k is an ordinary deterministic minimization problem, the least-squares estimate C_k is obtained by setting

$$\partial \phi_k / \partial C_k = 0 \tag{3.4.5}$$

Differentiating Eq. (3.4.4) with respect to C_k yields

$$\partial \phi_k / \partial C_k = -2 \sum_{i=1}^{k} H^T(h_i) R_i^{-1} \left[\hat{p}_i - H(h_i) C_k \right] = 0 \tag{3.4.6}$$

Solving Eq. (3.4.6) for C_k we obtain

$$C_k = \left[\sum_{i=1}^{k} H^T(h_i) R_i^{-1} H(h_i) \right]^{-1} \left[\sum_{i=1}^{k} H^T(h_i) R_i^{-1} \hat{p}_i \right] \tag{3.4.7}$$

Note that the solution requires the inversion of the matrix $\sum_{i=1}^{k} H^T(h_i) R_i^{-1} H(h_i)$. The existence of this inverse is essentially an observability requirement[69]. For notational convenience, let us define P_k as

$$P_k \triangleq \left[\sum_{i=1}^{k} H^T(h_i) R_i^{-1} H(h_i) \right]^{-1} \tag{3.4.8}$$

In view of Eq. (3.4.8), Eq. (3.4.7) becomes

$$C_k = P_k \left[\sum_{i=1}^{k} H^T(h_i) R_i^{-1} \hat{p}_i \right] \tag{3.4.9}$$

It is desired to establish an iterative formula to simplify the computations involved in Eqs. (3.4.7)and (3.4.9). To do so, suppose the data $\hat{p}_{k+1}$, h_{k+1} is available, then C_{k+1} will be

$$C_{k+1} = P_{k+1} \sum_{i=1}^{k+1} H^T(h_i) R_i^{-1} \hat{p}_i \tag{3.4.10}$$

where

$$P_{k+1} = \left[\sum_{i=1}^{k+1} H^T(h_i) R_i^{-1} H(h_i) \right]^{-1} \tag{3.4.11}$$

Taking the inverse of Eq. (3.4.11) yields

$$P_{k+1}^{-1} = \sum_{i=1}^{k+1} H^T(h_i) R_i^{-1} H(h_i) = \sum_{i=1}^{k} H^T(h_i) R_i^{-1} H(h_i) + H^T(h_{k+1}) R_{k+1}^{-1} H(h_{k+1}) \tag{3.4.12}$$

Inverting Eq. (3.4.8) and then substituting into Eq. (3.4.12) yields

$$P_{k+1}^{-1} = P_k^{-1} + H^T(h_{k+1}) R_{k+1}^{-1} H(h_{k+1}) \tag{3.4.13}$$

Since matrices P_{k+1}, P_k, $H(h_{k+1})$, R_{k+1} satisfy Eq. (3.4.13) and P_{k+1}^{-1}, P_k^{-1}, R_{k+1}^{-1} are nonsingular and $H(h_{k+1})$ is of maximum rank, then P_{k+1} is given by[69]

$$P_{k+1} = P_k - P_k H^T(h_{k+1}) \left[H(h_{k+1}) P_k H^T(h_{k+1}) + R_{k+1} \right]^{-1} H(h_{k+1}) P_k \tag{3.4.14}$$

Equation (3.4.10) may also be written in the form

$$C_{k+1} = P_{k+1}\left[\sum_{i=1}^{k} H^T(h_i)R_i^{-1}\hat{p}_i + H^T(h_{k+1})R_{k+1}^{-1}\hat{p}_{k+1}\right] \tag{3.4.15}$$

Substituting Eq. (3.4.14) into Eq. (3.4.15) and rearranging terms yields the iterative equation for C_{k+1}

$$C_{k+1} = C_k + P_k H^T(h_{k+1})\left[H(h_{k+1})P_k H^T(h_{k+1}) + R_{k+1}\right]^{-1}\left[\hat{p}_{k+1} - H(h_{k+1})C_k\right] \tag{3.4.16}$$

The initial values of vector C_o may be selected as the coefficients of the interpolation polynomials over some apriori available data about the variation of parameters $\hat{p}_i$'s over some range of admissible operating condition h. This is done in order to start with a finite uncertainty about the coefficients C which is a necessary condition to guarantee stability of Eqs. (3.4.14) and (3.4.16). The matrix P_o may be chosen initially as any positive definite matrix, and this choice influences considerably the rate of convergence and stability of the algorithm[71].

To provide an estimate of the covariance matrix R of vector $\hat{p}$ let

$$\hat{p} - E(\hat{p}) \cong \hat{p}_{j+1} - \hat{p}_j \tag{3.4.17}$$

Substituting Eq. (3.3.12) into Eq. (3.4.2) and using the approximation given by Eq. (3.4.17) yields

$$R = \left[\sum_{i=1}^{N}(\partial x/\partial \hat{p})_i^T B(\partial x/\partial \hat{p})_i\right]^{-1}\left[\sum_{i=1}^{N}\sum_{k=1}^{N}(\partial x/\partial \hat{p})_i^T B\overline{e_i e_k^T}B(\partial x/\partial \hat{p})_k\right]$$
$$\left[\sum_{i=1}^{N}(\partial x/\partial \hat{p})_i^T B(\partial x/\partial \hat{p})_i\right]^{-1} \tag{3.4.18}$$

where the bar denotes expectation. Letting

$$\overline{e_i e_k^T} = B^{-1}\delta_{ik} \tag{3.4.19}$$

where

$$\delta_{ik} = \begin{cases} 0 & \text{for } i \neq k \\ 1 & \text{for } i = k \end{cases} \tag{3.4.20}$$

the covariance matrix R of vector $\hat{p}$ reduces to

$$R = \left[\sum_{i=1}^{N} (\partial x/\partial \hat{p})_i^T B (\partial x/\partial \hat{p})_i\right]^{-1} \tag{3.4.21}$$

Equations (3.4.14), (3.4.16) and (3.4.21) constitute the Learning Algorithm Subsystem (LAS).

To obtain the goodness of the least-squares estimate C_k let us define the estimation error as

$$\tilde{C}_k \triangleq C - C_k \tag{3.4.22}$$

Substitution of Eq. (3.4.9) into Eq. (3.4.22) yields

$$\tilde{C}_k = C - P_k \sum_{i=1}^{k} H^T(h_i) R_i^{-1} \hat{p}_i \tag{3.4.23}$$

since

$$\hat{p}_i = H(h_i)C + \lambda_i \tag{3.4.24}$$

Therefore, substituting Eq. (3.4.24) into Eq. (3.4.23) gives

$$\tilde{C}_k = C - P_k \sum_{i=1}^{k} H^T(h_i) R_i^{-1} \left[H(h_i)C + \lambda_i\right] \tag{3.4.25}$$

In view of Eq. (3.4.8)

$$\tilde{C}_k = - P_k \sum_{i=1}^{k} H^T(h_i) R_i^{-1} \lambda_i \tag{3.4.26}$$

Taking the expectation of Eq. (3.4.26) we obtain the expected value of $\tilde{C}_k$ as

$$E(\tilde{C}_k) = - P_k \sum_{i=1}^{k} H^T(h_i) R_i^{-1} \lambda_i = 0 \tag{3.4.27}$$

Hence, C_k is an unbiased estimator. The covariance of the least-squares estimation error is given by

$$(\mathrm{Cov})\tilde{C}_k = P_k \left[\sum_{i=1}^{k} \sum_{j=1}^{k} H^T(h_i) R_i^{-1} \overline{\lambda_i \lambda_j^T} R_j^{-1} H(h_j) \right] P_k \tag{3.4.28}$$

In view of Eq. (3.4.2), Eq. (3.4.28) becomes

$$(\mathrm{Cov})\tilde{C}_k = P_k \left[\sum_{i=1}^{k} H^T(h_i) R_i^{-1} H(h_i) \right] P_k = P_k \tag{3.4.29}$$

A necessary test for the LAS must be to continually evaluate the validity of the information in vector C_k. This test is performed by the confidence criterion which is satisfied when the following conditions are met: a) The mean square error is below some quantity ε_1 fixed by the designer i.e.

$$\phi_{k+1} \leq (k + 1) \varepsilon_1 \tag{3.4.30}$$

b) The vector C_{k+1} is close to its previous iterate C_k in the Euclidean norm sense i.e.

$$\left\| C_{k+1} - C_k \right\| \leq \varepsilon_2 \tag{3.4.31}$$

where again ε_2 is a number determined by the designer and depends upon the desired accuracy. c) The i-th diagonal element of matrix P_k is smaller than the allowable covariance of the coefficient C_i. Since

$$(P_k)_{ii} \cong E\left[(C_k)_i - C\right]^2 \tag{3.4.32}$$

then condition (c) reduces to

$$(P_k)_{ii} \leq \text{cov } C_i \tag{3.4.33}$$

where the quantity cov C_i is fixed by the designer and is the maximum tolerable covariance of the coefficient C_i.

Note that ϕ_{k+1} used in Eq. (3.4.30) is given iteratively by

$$\phi_{k+1} = \phi_k + \left[\hat{p}_{k+1} - H(h_{k+1})C_{k+1}\right]^T R_{k+1}^{-1} \left[\hat{p}_{k+1} - H(h_{k+1})C_{k+1}\right] \tag{3.4.34}$$

where ϕ_k is defined by Eq. (3.4.4).

3.5. The Memory and Control Process Subsystem (MCPS)

The plant's dynamic characteristics vary over different operating conditions h, therefore, the overall objective of the learning control system is to maintain uniform dynamic quality parameters over all possible operating conditions insofar as possible. That objective might be compromised because the feedback gains required to maintain uniform dynamic quality characteristics may be excessive. Excessive feedback gains can excite instabilities caused by nonlinearities of the plant.

In order to alleviate this possibility, the memory stores the values of vector C_k after they have passed the confidence criterion test. The control process subsystem, which consists of control laws, then computes the corrections $\triangle G$ and $\triangle K$ needed for the feedforward and feedback gain matrices G and K respectively using the stored values of vector C_k. In order to design the control laws for maintaining uniform dynamic quality parameters a design criterion is selected that yields a relation between the feedforward and feedback gains as a function of the parameter vector $\hat{p}$ and hence a function of the coefficient vector C_k. In summary, the control law is designed to meet a design criterion over a range of operating conditions to yield an operationally feasible control system.

Imposing the constraint that the plant's handling qualities remain the same over all possible flight conditions we get from Eqs. (3.2.5) and (3.2.6)

$$\begin{aligned} A_p(p) + B_p(p)K &= \text{constant} \\ B_p(p)G &= \text{constant} \end{aligned} \qquad (3.5.1)$$

Applying the difference operator Δ on both sides of Eq. (3.5.1) gives

$$\Delta A_p(p) + \left[\Delta B_p(p)\right] K + \left[B_p(p)\right] \Delta K = 0$$
$$\left[\Delta B_p(p)\right] G + \left[B_p(p)\right] \Delta G = 0 \qquad (3.5.2)$$

The solution of Eq. (3.5.2) for ΔK and ΔG yields relationships which constitute the control laws given by

$$\Delta K_i = - \left[B_p^T(p) B_p(p)\right]^{-1} B_p^T(p) \left[\Delta A_p^i(p) + \Delta B_p(p) K_i\right] \qquad (3.5.3)$$

where $i = 1,2,\ldots\ldots,n$ and

$$\Delta G = - \left[B_p^T(p) B_p(p)\right]^{-1} B_p^T(p) \left[\Delta B_p(p)\right] G \qquad (3.5.4)$$

Note that superscript i on the matrix $\Delta A_p(p)$ denotes the i-th column vector matrix $\Delta A_p(p)$. Equations (3.5.3) and (3.5.4) readily apply as the control laws for the longitudinal dynamics but not for the lateral dynamics since in the latter case the two inputs to the plant are not linear combinations of all the states. The lateral control laws will be developed in sections 4.5 and 5.4 accroding to the specific application.

The next chapter presents the application of the LCS to a high order representation of the F-8 DFBW aircraft dynamics.

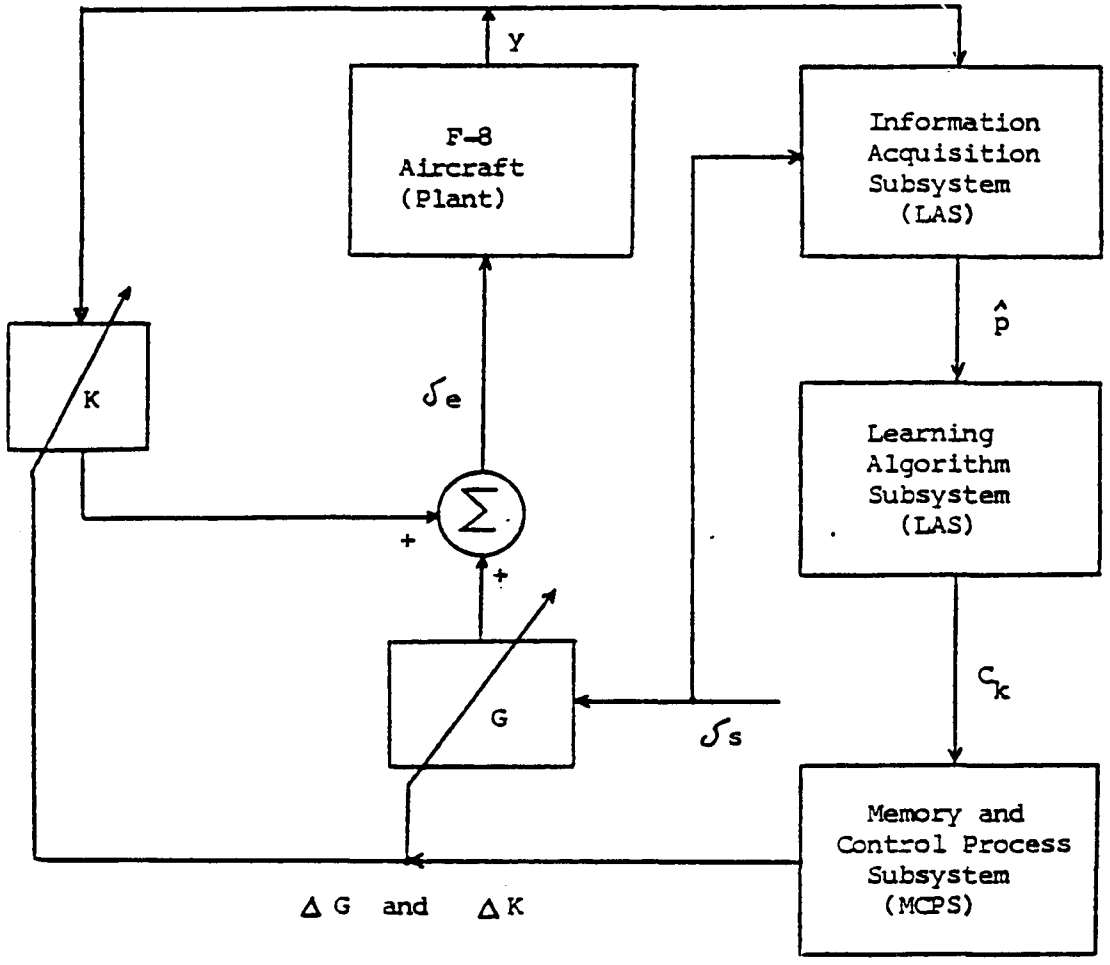

Fig. 3.1 Functional Organization of Learning Control System For The F-8 DFBW Aircraft.

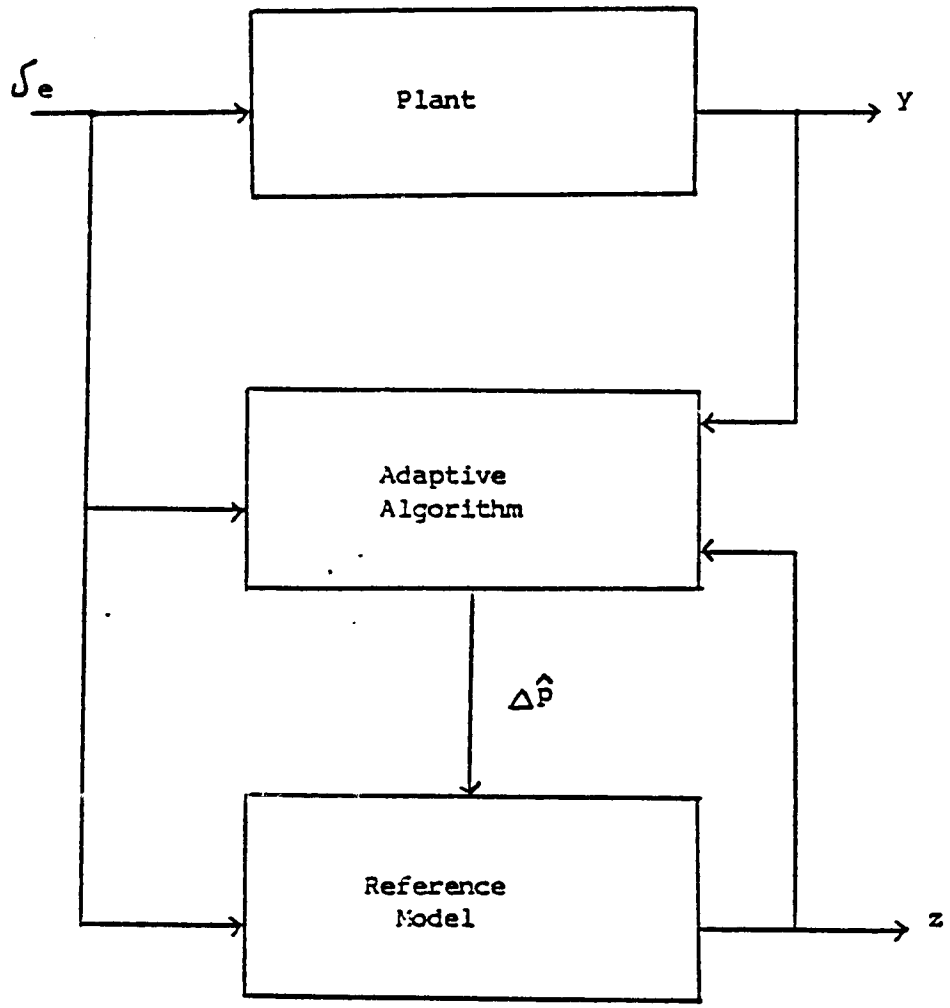

Fig. 3.2 Functional Organization of the Information Acquisition Subsystem (IAS)

CHAPTER 4

CASE STUDY I; THE APPLICATION OF THE LCS TO A HIGH ORDER REPRESENTATION OF THE F-8 DFBW AIRCRAFT DYNAMICS

4.1. Introduction

To describe the behavior of an aircraft, one must study the nonlinear equations of motion of the aircraft. A solution for these equations may be obtained by the use of analog or digital computers or by manual numerical integration. In most cases, however, by the use of proper assumptions, the nonlinear equations can be decoupled into two sets of equations describing the longitudinal and lateral dynamics separately. In order to obtain the two sets of equations, one may consider the aircraft to be in straight and level unaccelerated flight and then to be disturbed either by deflection of the elevator or by the aileron and rudder. The elevator deflection applies a pitching moment (longitudinal) but does not cause a rolling or yawing moment (lateral). On the other hand, a rolling and a yawing moment generated by the aileron and rudder disturbance excites angular velocities about all three axes; thus, for certain cases the equation cannot be decoupled. The pitching moment that is generated from a lateral motion results from second order terms of yaw rate and roll rate thus, if the perturbations are small, and if one assumes that yaw rate and roll rate are so small that their products and squares can be neglected, then the equations can be decoupled.

This chapter describes a simulation of our learning control system (LCS) on a digital computer as applied to the decoupled longitudinal and lateral dynamics of the F-8 DFBW aircraft. The simulation is not concerned with real-time while the aircraft is flying. In this study, as a first

attempt of applying the LCS system, fourth order linearized representations were used both for the modeling of the longitudinal and lateral dynamics of the plant. The main concern was to get insight into the properties and the behavior of the LCS.

Another aim of the work described in this chapter was to compare two different learning control systems based upon two different Information Acquisition Subsystems (IAS): (1) Liapunov Method and (2) Newton-Raphson Method.

We will consider a more realistic application of our LCS in the following chapter (Chapter 5) where we use non-linearized equations for the plant and we are concerned with the real time application.

This chapter is divided into five sections. The first two sections will describe the longitudinal dynamics and the LCS as applied to the longitudinal dynamics. The next two sections will describe the lateral dynamics and the LCS as applied to the lateral dynamics. The last section will discuss the simulation with the associated results and some concluding remarks.

4.2. The Longitudinal Dynamics

For the longitudinal case the state variables of the aircraft system are pitch rate q, forward velocity v, angle of attack α and pitch angle θ. The linearized equations of motion at selected flight conditions have the matrix form

$$\begin{bmatrix} \dot{q} \\ \dot{v} \\ \dot{\alpha} \\ \dot{\theta} \end{bmatrix} = \begin{bmatrix} p_1 & p_{10} & p_2 & 0 \\ 0 & p_3 & p_4 & -g \\ 1 & p_5 & p_6 & 0 \\ 1 & 0 & 0 & 0 \end{bmatrix} \begin{bmatrix} q \\ v \\ \alpha \\ \theta \end{bmatrix} + \begin{bmatrix} p_7 \\ p_8 \\ p_9 \\ 0 \end{bmatrix} \times \delta_e \qquad (4.2.1)$$

where δ_e is a linear combination of the states and the pilot's input given by the following equation

$$\delta_e = Ky + G\delta_s \qquad (4.2.1a)$$

Note that δ_s is the pilot's (stick) input and K and G are gain matrices as defined in Chapter 3. Parameters p_1 through p_{10} are functions of the aircraft's stability derivatives given by the following equations[21]:

$$p_1 = (qSC/2V_oI_y)\,(C_{m_q} + C_{m_{\dot{\alpha}}})$$

$$p_{10} = (qSC/V_oI_y)\left[C_{m_u} - (qSC/2mV_o^2)C_{m_{\dot{\alpha}}}C_{L_u}\right]$$

$$p_2 = (57.3qSC/I_y)\left[C_{m_\alpha} - (qSC/2mV_o^2)C_{m_{\dot{\alpha}}}C_{L_\alpha}\right]$$

$$p_3 = -(qS/mV_o^2)C_{D_u} \qquad p_4 = (57.3qS/m)C_{D_\alpha}$$

$$p_5 = (qS/mV_o^2)C_{L_u} \qquad p_6 = (57.3qS/mV_o^2)C_{L_\alpha}$$

$$p_7 = (57.3qSC/I_y)\left[C_{m_{\delta_e}} - (qSC/2mV_o^2)C_{m_{\dot{\alpha}}} C_{L_{\delta_e}}\right] \tag{4.2.2}$$

$$p_8 = (57.3qS/m)C_{D_{\delta_e}} \qquad p_9 = (57.3qS/mV_o)C_{L_{\delta_e}}$$

The stability derivatives affect the dynamics of the aircraft and as an example we will discuss the effects of C_{m_α}.

The static longitudinal stability of the aircraft is determined by the term C_{m_α} which is the change in the pitching moment due to a change in the angle of attack. For a "statically stable aircraft" this term must be negative. A statically stable aircraft is one that tends to return to its equilibrium condition after a disturbance has occurred. A negative C_{m_α} means that as the angle of attack increases positively, the pitching moment becomes more negative tending to decrease the angle of attack. The opposite is true for a positive C_{m_α}.

Although all aircraft are designed to be statically stable, C_{m_α} negative, certain flight conditions can result in large changes in the longitudinal stability. A severe shift in the longitudinal stability results in some high performance aircraft at high angles of attack, a phenomenon referred to as "pitch-up". As long as the slope of the C_m versus α curve is negative the aircraft is stable but as the angle of attack is increased, the slope changes sign and the aircraft becomes unstable. If corrective action is not taken, the angle of attack increases until the aircraft stalls. This usually happens so rapidly that the pilot is unable to control or stop the pitch-up. A practical solution of the pitch-up

problem is to limit the aircraft to angles of attack below the critical angle of attack; however, this also limits the performance of the aircraft. In order not to limit the aircraft's performance, the longitudinal control system is designed to make the aircraft flyable at angles of attack greater than the critical angle of attack. To design properly the longitudinal control system, we need a good estimate of the longitudinal parameters which is provided by our Learning Algorithm Subsystem (LAS). Our method of development of the longitudinal LCS is described in the following section.

4.3. Realization of the LCS as Applied to the Longitudinal Dynamics

As indicated in Chapter 3, to implement Liapunov's LAS, a model described by Eq. (3.2.4) is used which for the longitudinal dynamics has the form

$$\begin{bmatrix} \dot{z}_1 \\ \dot{z}_2 \\ \dot{z}_3 \\ \dot{z}_4 \end{bmatrix} = \begin{bmatrix} -10 & 0 & 0 & 0 \\ 0 & -10 & 0 & 0 \\ 0 & 0 & -10 & 0 \\ 0 & 0 & 0 & -10 \end{bmatrix} \times \begin{bmatrix} z_1 \\ z_2 \\ z_3 \\ z_4 \end{bmatrix} +$$

$$+ \begin{bmatrix} \hat{p}_1+10 & \hat{p}_{10} & \hat{p}_2 & 0 \\ 0 & \hat{p}_3+10 & \hat{p}_4 & -g \\ 1 & \hat{p}_5 & \hat{p}_6+10 & 0 \\ 1 & 0 & 0 & 10 \end{bmatrix} \times \begin{bmatrix} q \\ v \\ \alpha \\ \theta \end{bmatrix} + \begin{bmatrix} \hat{p}_7 \\ \hat{p}_8 \\ \hat{p}_9 \\ 0 \end{bmatrix} \times \delta_s \qquad (4.3.1)$$

or in equivalent form

$$\begin{bmatrix} \dot{z}_1 \\ \dot{z}_2 \\ \dot{z}_3 \\ \dot{z}_4 \end{bmatrix} = \begin{bmatrix} \hat{p}_1 & \hat{p}_{10} & \hat{p}_2 & 0 \\ 0 & \hat{p}_3 & \hat{p}_4 & -g \\ 1 & \hat{p}_5 & \hat{p}_6 & 0 \\ 1 & 0 & 0 & 0 \end{bmatrix} \times \begin{bmatrix} q \\ v \\ \alpha \\ \theta \end{bmatrix} + \begin{bmatrix} \hat{p}_7 \\ \hat{p}_8 \\ \hat{p}_9 \\ 0 \end{bmatrix} \times \delta_s +$$

$$+ \begin{bmatrix} -10 & 0 & 0 & 0 \\ 0 & -10 & 0 & 0 \\ 0 & 0 & -10 & 0 \\ 0 & 0 & 0 & -10 \end{bmatrix} \times \begin{bmatrix} e_1 \\ e_2 \\ e_3 \\ e_4 \end{bmatrix} \qquad (4.3.2)$$

where $\hat{p}_i$ is an estimate of p_i and

$$\begin{bmatrix} e_1 \\ e_2 \\ e_3 \\ e_4 \end{bmatrix} = \begin{bmatrix} z_1 - q \\ z_2 - v \\ z_3 - \alpha \\ z_4 - \theta \end{bmatrix} \tag{4.3.3}$$

The matrices P, N_i and Q_i appearing in the Liapunov function are chosen as

$$P = \begin{bmatrix} 30 & 0 & 0 \\ 0 & 30 & 0 \\ 0 & 0 & 30 \end{bmatrix} \tag{4.3.4}$$

$$N_1 = \begin{bmatrix} 0.01 & 0 & 0 \\ 0 & 10 & 0 \\ 0 & 0 & 0.0001 \end{bmatrix} \tag{4.3.4a}$$

$$N_2 = \begin{bmatrix} \infty & 0 & 0 \\ 0 & 10 & 0 \\ 0 & 0 & 0.001 \end{bmatrix} \tag{4.3.4b}$$

$$N_3 = \begin{bmatrix} \infty & 0 & 0 \\ 0 & 10 & 0 \\ 0 & 0 & 0.0001 \end{bmatrix} \tag{4.3.4c}$$

$$Q_1 = Q_2 = Q_3 = 0.00001 \tag{4.3.4d}$$

Note that even though we consider a fourth order system, matrices P and N_i

are of third order because there are no unknown parameters in the fourth differential equation therefore, $e_4 \equiv 0$. The matrices Q_1, Q_2, Q_3 reduce to be scalars because there is only one column in matrix $B_m(\hat{p})$. The infinity elements in N_2 and N_3 matrices indicate that the corresponding elements of the $A_m(\hat{p})$ matrix is known. For example, the first diagonal element of matrix N_3 being ∞ shows that the first element of the third row of the $A_m(\hat{p})$ matrix is known, namely 1. After these choices have been made (Eqs. 4.3.4) the adaptive algorithm equations given by Eqs. (3.2.16) and (3.2.17) reduce to

$$
\begin{aligned}
\hat{p}_1 &= \hat{p}_1^{(o)} - \int_0^t (30e_1 q/.01)\, dt \\
\hat{p}_{10} &= \hat{p}_{10}^{(o)} - \int_0^t (30e_1 v/10)\, dt \\
\hat{p}_2 &= \hat{p}_2^{(o)} - \int_0^t (30e_1 \alpha/.0001)\, dt \\
\hat{p}_3 &= \hat{p}_3^{(o)} - \int_0^t (30e_2 v/10)\, dt \\
\hat{p}_4 &= \hat{p}_4^{(o)} - \int_0^t (30e_2 \alpha/.001)\, dt \\
\hat{p}_5 &= \hat{p}_5^{(o)} - \int_0^t (30e_3 v/10)\, dt \\
\hat{p}_6 &= \hat{p}_6^{(o)} - \int_0^t (30e_3 \alpha/.0001)\, dt \\
\hat{p}_7 &= \hat{p}_7^{(o)} - \int_0^t (30e_1 \delta_s/.00001)\, dt
\end{aligned}
\qquad (4.3.5)
$$

$$\hat{p}_8 = \hat{p}_8^{(o)} - \int_o^t (30e_2 \delta_s/.00001)\, dt$$

$$\hat{p}_9 = \hat{p}_9^{(o)} - \int_o^t (30e_3 \delta_s/.00001)\, dt$$

where $\hat{p}_i^{(o)}$ is an initial estimate of parameter p_i.

For the Newton-Raphson IAS a model described by Eq. (3.3.1) is used which for the longitudinal dynamics has the form

$$\begin{bmatrix} \dot{x}_1 \\ \dot{x}_2 \\ \dot{x}_3 \\ \dot{x}_4 \end{bmatrix} = \begin{bmatrix} \hat{p}_1 & \hat{p}_{10} & \hat{p}_2 & 0 \\ 0 & \hat{p}_3 & \hat{p}_4 & -g \\ 1 & \hat{p}_5 & \hat{p}_6 & 0 \\ 1 & 0 & 0 & 0 \end{bmatrix} \begin{bmatrix} x_1 \\ x_2 \\ x_3 \\ x_4 \end{bmatrix} + \begin{bmatrix} \hat{p}_7 \\ \hat{p}_8 \\ \hat{p}_9 \\ 0 \end{bmatrix} \times \delta_s \qquad (4.3.6)$$

In this case the sensitivity matrix (Eq. 3.3.10) has the dimension 3 x 10 with a typical element (the i-j element) $\partial x_i/\partial \hat{p}_j$ ($i \leq 3$, $j \leq 10$). Each element of the sensitivity matrix satisfies the differential equation (3.3.13) which is used to evaluate that element. For example, the elements $\partial x_2/\partial \hat{p}_3$ and $\partial x_3/\partial \hat{p}_1$ satisfy the following differential equations respectively

$$d/dt(\partial x_2/\partial \hat{p}_3) = \hat{p}_3(\partial x_2/\partial \hat{p}_3) + \hat{p}_4(\partial x_3/\partial \hat{p}_3) + x_2$$

$$d/dt(\partial x_3/\partial \hat{p}_1) = (\partial x_1/\partial \hat{p}_1) + \hat{p}_5(\partial x_2/\partial \hat{p}_1) + \hat{p}_6(\partial x_3/\partial \hat{p}_1) \qquad (4.3.7)$$

Note that the other elements of the sensitivity matrix are not shown here but are obtained in a similar way. After all sensitivity elements are obtained, they are substituted into Eq. (3.3.12) to yield an improved

estimate of vector p.

In this study we used data from reference [21] and considered the four wing-down (CO) configurations. The simulated flights were at three different altitudes (L = sea level, L = 20,000 ft., L = 40,000 ft.) and three different mach numbers (M = 0.5, M = 0.7, M = 0.9). The first step was to interpolate polynomials through the data in the least square sense and determine a functional representation of the model system parameter $\hat{p}_i$ with respect to mach number M and altitude L for the purpose of establishing the model as a function of M and L. These functional representations are used for the Learning Algorithm Subsystem (LAS) and were determined so that the mean square error between the curves and the data was below a pre-specified bound. The functional representations of the $\hat{p}_i$ parameters are of the form

$$\hat{p}_1 = \hat{p}_1(M,L) = C_1 + C_2M + C_3L + C_4M\,L$$

$$\hat{p}_2 = \hat{p}_2(M,L) = C_5 + C_6M + C_7L + C_8M\,L + C_9M^2 + C_{10}L^2$$

$$\hat{p}_3 = \hat{p}_3(M,L) = C_{11} + C_{12}M + C_{13}L + C_{14}M\,L + C_{15}M^2 + C_{16}L^2$$

$$\hat{p}_4 = \hat{p}_4(M,L) = C_{17} + C_{18}M + C_{19}L + C_{20}M\,L + C_{21}M^2 + C_{22}L^2$$

$$\hat{p}_5 = \hat{p}_5(M,L) = C_{23} + C_{24}M + C_{25}L + C_{26}M\,L + C_{27}M^2 + C_{28}M^3$$

$$\hat{p}_6 = \hat{p}_6(M,L) = C_{29} + C_{30}M + C_{31}L + C_{32}M\,L + C_{33}M^2 + C_{34}L^2$$

$$\hat{p}_7 = \hat{p}_7(M,L) = C_{35} + C_{36}M + C_{37}L + C_{38}M\,L + C_{39}M^2 + C_{40}L^2 \qquad (4.3.8)$$

$$\hat{p}_8 = \hat{p}_8(M,L) = C_{41} + C_{42}M + C_{43}L + C_{44}M\,L + C_{45}M^2 + C_{46}L^2 + C_{47}M^3 + C_{48}L\,M^2 + C_{49}M\,L^2$$

$$\hat{p}_9 = \hat{p}_9(M,L) = C_{50} + C_{51}M + C_{52}L + C_{53}M\,L + C_{54}M^2 + C_{55}L^2$$

$$\hat{p}_{10} = \hat{p}_{10}(M,L) = C_{56} + C_{57}M + C_{58}L + C_{59}M\,L + C_{60}M^2 + C_{61}L^2 + \\ + C_{62}L\,M^2 + C_{63}M\,L^2 + C_{64}M^3 + C_{65}M^4 + C_{66}L\,M^3$$

After establishing the model as a function of M and L we applied our LCS as described in the previous chapter and the results are discussed in section 4.6.

As an illustration of the LAS consider one parameter curve $\hat{p}_1(M,L)$ and assume for simplicity that

$$\hat{p}_1(M,L) = C_1 + C_2M + C_3L = \begin{bmatrix} 1 & M & L \end{bmatrix}^{\prime} \begin{bmatrix} C_1 \\ C_2 \\ C_3 \end{bmatrix} = H(M,L)C \qquad (4.3.9)$$

Now assume the aircraft flies at mach number M_1 and altitude L_1 and the LAS generates $\hat{p}_1(M_1,L_1)$. Interpolating wind tunnel data we have an a priori knowledge of vector C; namely

$$C_o = \begin{bmatrix} C_1 \\ C_2 \\ C_3 \end{bmatrix}^{(0)} \qquad (4.3.10)$$

Let $P_o = I_3$ (Identity matrix and initial covariance matrix of vector C). The LAS updates vector C according to Eq. (3.4.16)

$$\begin{bmatrix} C_1 \\ C_2 \\ C_3 \end{bmatrix}^{(1)} = \begin{bmatrix} C_1 \\ C_2 \\ C_3 \end{bmatrix}^{(0)} + \begin{bmatrix} 1 \\ M_1 \\ L_1 \end{bmatrix} (r_{11} + 1 + M_1^2 + L_1^2)^{-1} \left\{ \hat{p}_1(M_1,L_1) - \begin{bmatrix} 1 & M_1 & L_1 \end{bmatrix}^{\prime} \begin{bmatrix} C_1 \\ C_2 \\ C_3 \end{bmatrix}^{(0)} \right\} \qquad (4.3.11)$$

where r_{11} is the first diagonal element of matrix R (covariance of λ given by Eq. 3.4.2).

For simplicity let $r_{11} = 1$. Equation (4.3.11) yields

$$C_1^{(1)} = C_1^{(o)} + \left[\hat{p}_1(M_1,L_1) - (C_1^{(o)} + C_2^{(o)}M_1 + C_3^{(o)}L_1)\right] /(2 + M_1^2 + L_1^2)$$

$$C_2^{(1)} = C_2^{(o)} + M_1\left[\hat{p}_1(M_1,L_1) - (C_1^{(o)} + C_2^{(o)}M_1 + C_3^{(o)}L_1)\right] /(2 + M_1^2 + L_1^2) \qquad (4.3.12)$$

$$C_3^{(1)} = C_3^{(o)} + L_1\left[\hat{p}_1(M_1,L_1) - (C_1^{(o)} + C_2^{(o)}M_1 + C_3^{(o)}L_1)\right] /(2 + M_1^2 + L_1^2)$$

The updated covariance matrix P_1 is computed according to Eq. (3.4.14)

$$P_1 = \begin{bmatrix} 1 & 0 & 0 \\ 0 & 1 & 0 \\ 0 & 0 & 1 \end{bmatrix} - \begin{bmatrix} 1 \\ M_1 \\ L_1 \end{bmatrix} * (r_{11} + 1 + M_1^2 + L_1^2)^{-1} * \begin{bmatrix} 1 & M_1 & L_1 \end{bmatrix} \qquad (4.3.13)$$

Equation (4.3.13) yields (for $r_{11} = 1$)

$$P_1 = \begin{bmatrix} 1 + M_1^2 + L_1^2 & -M_1 & -L_1 \\ -M_1 & 2 + L_1^2 & -M_1L_1 \\ -L_1 & -M_1L_1 & 2 + M_1^2 \end{bmatrix} /(2 + M_1^2 + L_1^2) \qquad (4.3.14)$$

Next assume the aircraft flies at mach number M_2 and altitude L_2 and the IAS generates $\hat{p}_1(M_2,L_2)$. Applying the second iteration of the learning algorithm (Eqs. 3.4.14 and 3.4.16) we obtain an updated vector C with elements

$$C_1^{(2)} = C_1^{(1)} + \left\{\hat{P}_1(M_2,L_2) - (C_1^{(1)} + C_2^{(1)}M_2 + C_3^{(1)}L_2)\right\}(1+M_1^2+L_1^2-M_1M_2-L_1L_2)/D$$

$$C_2^{(2)} = C_2^{(1)} + \left\{\hat{P}_1(M_2,L_2) - (C_1^{(1)} + C_2^{(1)}M_2 + C_3^{(1)}L_2)\right\}(2M_2 - M_1 + M_2L_1^2 - M_1L_1L_2)/D \quad (4.3.15)$$

$$C_3^{(2)} = C_3^{(1)} + \left\{\hat{P}_1(M_2,L_2) - (C_1^{(1)} + C_2^{(1)}M_2 + C_3^{(1)}L_2)\right\}(2L_2 - L_1 + L_2M_1^2 - L_1M_1M_2)/D$$

where

$$D = 2 + M_2^2 + L_2^2 + (M_1 - M_2)^2 + (L_1 - L_2)^2 + (L_1M_2 - M_1L_2)^2 \quad (4.3.16)$$

and matrix P_2

$$P_2 = P_1 - \begin{bmatrix} J_1^2 & J_1J_2 & J_1J_3 \\ J_1J_2 & J_2^2 & J_2J_3 \\ J_1J_3 & J_2J_3 & J_2^2 \end{bmatrix} / D \quad (4.3.17)$$

where

$$\begin{aligned} J_1 &= 1 + M_1^2 + L_1^2 - M_1M_2 - L_1L_2 \\ J_2 &= 2M_2 - M_1 + M_2L_1^2 - M_1L_1L_2 \\ J_3 &= 2L_2 - L_1 + L_2M_1^2 - L_1M_1M_2 \end{aligned} \quad (4.3.18)$$

and P_1 is given by Eq. (4.3.14).

The confidence criterion gives according to Eqs. (3.4.30) and (3.4.34)

$$\begin{aligned} \phi_1 &= \left\{\hat{P}_1(M_1,L_1) - (C_1^{(1)} + C_2^{(1)}M_1 + C_3^{(1)}L_1)\right\}^2 \leq \varepsilon_1 \\ \phi_2 &= \phi_1 + \left\{\hat{P}_1(M_2,L_2) - (C_2^{(1)} + C_2^{(2)} + M_2 + C_3^{(2)}L_2)\right\}^2 \leq 2\varepsilon_1 \end{aligned} \quad (4.3.19)$$

For the longitudinal LCS the elevator command structure is

$$\delta_e = k_1q + k_2v + k_3\alpha + G\delta_s \quad (4.3.20)$$

Imposing the constraint that the plant's handling qualities remain the same over all possible operating conditions, Eqs. (3.5.1) and (4.3.20) are used to obtain relationships which constitute the control laws given by

$$\Delta k_1 = -\left[\hat{p}_8(k_1\Delta p_8 + \Delta p_1) + \hat{p}_4 k_1 \Delta p_9 + \hat{p}_{10} k_1 \Delta p_{10}\right] / (\hat{p}_8^2 + \hat{p}_9^2 + \hat{p}_{10}^2)$$

$$\Delta k_2 = -\left[\hat{p}_8(k_2\Delta p_8+\Delta p_2)+\hat{p}_9(k_2\Delta p_9+\Delta p_4)+\hat{p}_{10}(k_2\Delta p_{10}+\Delta p_6)\right] / (\hat{p}_8^2+\hat{p}_9^2+\hat{p}_{10}^2) \tag{4.3.21}$$

$$\Delta k_3 = -\left[\hat{p}_8(k_3\Delta p_8+\Delta p_3)+\hat{p}_9(k_3\Delta p_9+\Delta p_5)+\hat{p}_{10}(k_3\Delta p_{10}+\Delta p_7)\right]/(\hat{p}_8^2+\hat{p}_9^2+\hat{p}_{10}^2)$$

$$\Delta G = -(\hat{p}_8 G\Delta p_8 + \hat{p}_9 G\Delta p_9 + \hat{p}_{10} G\Delta p_{10})/(\hat{p}_8^2 + \hat{p}_9^2 + \hat{p}_{10}^2)$$

where the $\hat{p}_i$ are the learned parameters obtained from LAS and Δp_i is the difference between the learned $\hat{p}_i$ at the current time and the previous time. Note that the $\hat{p}_i$ are computed using the C_k's stored in the memory.

In the next two sections we will discuss the lateral dynamics and the development of our LCS as applied to the lateral dynamics.

4.4. The Lateral Dynamics

For the lateral case the state variables of the aircraft system are roll rate p, yaw rate r, side slip angle and roll angle . The linearized equations of motion at selected flight conditions have the matrix form

$$\begin{bmatrix} \dot{p} \\ \dot{r} \\ \dot{\beta} \\ \dot{\phi} \end{bmatrix} = \begin{bmatrix} p_1 & p_2 & p_3 & 0 \\ p_4 & p_5 & p_6 & 0 \\ p_7 & p_8 & p_9 & g/v_o \\ \cos a_f & \sin a_f & 0 & 0 \end{bmatrix} \times \begin{bmatrix} p \\ r \\ \beta \\ \phi \end{bmatrix} + \begin{bmatrix} p_{10} & p_{11} \\ p_{12} & p_{13} \\ 0 & p_{14} \\ 0 & 0 \end{bmatrix} \times \begin{bmatrix} \delta_a \\ \delta_r \end{bmatrix} \qquad (4.4.1)$$

where δ_a is the aileron displacement and δ_r the rudder displacement. Angle a_f is the trimmed angle of attack at each flight condition and the parameters p_1 through p_{14} are functions of the aircraft's stability derivatives and angle a_f and are given by the following equations

$$\begin{aligned}
p_1 &= L_r' \cos^2 a_f - L_r' \sin a_f \cos a_f - N_p' \cos a_f \sin a_f + N_r' \sin^2 a_f \\
p_2 &= L_p' \sin a_f \cos a_f + L_r' \cos^2 a_f - N_p' \sin^2 a_f - N_r' \cos a_f \sin a_f \\
p_3 &= L_\beta' \cos a_f - N_\beta' \sin a_f \\
p_4 &= L_p' \cos a_f \sin a_f - L_r' \sin^2 a_f + N_p' \cos^2 a_f - N_p' \sin a_f \cos a_f \\
p_5 &= L_p' \sin^2 a_f + L_r' \cos a_f \sin a_f + N_p' \sin a_f \cos a_f + N_r' \cos^2 a_f \\
p_6 &= L_\beta' \sin a_f + N_\beta' \cos a_f \\
p_7 &= Y_p \cos a_f - Y_r \sin a_f \\
p_8 &= Y_p \sin a_f + Y_r \cos a_f
\end{aligned} \qquad (4.4.2)$$

$$p_9 = Y_\beta$$

$$p_{10} = L'_{\zeta_a} \cos a_f - N'_{\zeta_a} \sin a_f$$

$$p_{11} = L'_{\zeta_r} \cos a_f - N'_{\zeta_r} \sin a_f$$

$$p_{12} = L'_{\zeta_a} \sin a_f + N'_{\zeta_a} \cos a_f$$

$$p_{13} = L'_{\zeta_r} \sin a_f + N'_{\zeta_r} \cos a_f$$

$$p_{14} = Y_{\zeta_r}$$

where

$$L'_i = \left[L_i + (I_{xz}/I_x)N_i\right] / \left[1 - (I_{xz}/I_x I_z)\right]$$

$$N'_i = \left[N_i + (I_{xz}/I_z)L_i\right] / \left[1 - (I_{xz}^2/I_x I_z)\right] \qquad (4.4.3)$$

and $i = p, r, \beta, \zeta_a, \zeta_r$

The unprimed derivatives are defined as

$$L_p = (qSb^2/2V_o I_x)C_{l_p}, \qquad L_r = qSb^2/2V_o I_x)C_{l_r}$$

$$L_\beta = (57.3qSb/I_x)C_{l_\beta}, \qquad L_{\zeta_a} = (57.3qSb/I_x)C_{l_{\zeta_a}}$$

$$L_{\zeta_r} = (57.3qSb/I_x)C_{l_{\zeta_r}}, \qquad N_p = (qSb^2/2V_o I_z)C_{n_p}$$

$$N_r = (qSb^2/2V_o I_z)C_{n_r}, \qquad N_\beta = (57.3qSb/I_z)C_{n_\beta} \qquad (4.4.4)$$

$$N_{\zeta_a} = (57.3qSb/I_z)C_{n_{\zeta_a}}, \qquad N_{\zeta_r} = (57.3qSb/I_z)C_{n_{\zeta_r}}$$

$$Y_p = (qSb/2mV_o^2)C_{Y_p}, \qquad Y_r = (qSb/2mV_o^2)C_{Y_r}$$

$$Y_{\beta} = (57.3qSb/mV_o)C_{Y_{\beta}} \quad , \quad Y_{\delta_a} = (57.3qSb/mV_o)C_{Y_{\delta_a}}$$

$$Y_{\delta_r} = (57.3qSb/mV_o)C_{Y_{\delta_r}}$$

As an example, we will discuss the stability derivative C_{l_p} and how it affects the dynamics at the aircraft. C_{l_p} is the change in the rolling moment due to a rolling velocity, arising from the change in the angle of attack on the wings caused by a rolling velocity. The down-going wing experiences an increase in angle of attack while the up-going wing is subjected to a decrease in angle of attack. These changes in angle of attack cause changes in the lift and drag of the up and down going wings which, in turn, produces a moment opposing the rolling velocity.

Analytical results show that the rudder input (δ_r) excites mainly the side slip angle β and yaw rate r. This is called the Dutch roll mode. In the same manner aileron displacement (δ_a) mainly excites the roll angle ϕ and roll rate p. This is called the Rolling mode.

There exists a coupling between the Dutch roll mode and the Rolling mode mainly due to the existence of C_{n_p} (which is the change in the yawing moment due to a rolling velocity) and C_{l_r} (which is the change in the rolling moment due to a yawing velocity).

The cause for C_{n_p} is the same as that of C_{l_p}. The change in the angle of attack as mentioned previously, will result in the lift vector being tilted forward on the down-going wing and rearward on the up-going wing therefore producing a negative yawing moment (an adverse yaw) for a positive roll rate.

C_{l_r} arises from the changes in the lift on the wings resulting from a yawing velocity. If the aircraft is subject to a yawing velocity, the

relative velocity of the left and right wing panels changes with respect to the air mass. The forward going wing experiences an increase in lift while the lift on the rearward going wing decreases. This factor caused a positive rolling moment for a positive yawing velocity.

One of the functions of the lateral control system is to provide artificial damping of the Dutch roll. To do so, we need to have the lateral parameters as a function of mach number M and altitude L, since the transient response of the aircraft varies considerably with changes in airspeed and altitude. The lateral parameters are provided by our lateral LAS whose development in conjunction with the IAS is presented in the following section.

4.5. Realization of the LCS as Applied to the Lateral Dynamics

The model used to implement Liapunov's IAS for the lateral dynamics of the F-8 DFBW aircraft has the form

$$\begin{bmatrix}\dot{z}_1\\ \dot{z}_2\\ \dot{z}_3\\ \dot{z}_4\end{bmatrix} = \begin{bmatrix}-10 & 0 & 0 & 0\\ 0 & -10 & 0 & 0\\ 0 & 0 & -10 & 0\\ 0 & 0 & 0 & -10\end{bmatrix}\begin{bmatrix}z_1\\ z_2\\ z_3\\ z_4\end{bmatrix} +$$

$$+ \begin{bmatrix}\hat{p}_1+10 & \hat{p}_2 & \hat{p}_3 & 0\\ \hat{p}_4 & \hat{p}_5+10 & \hat{p}_6 & 0\\ \hat{p}_7 & \hat{p}_8 & \hat{p}_9+10 & g/v_o\\ \cos a_f & \sin a_f & 0 & 10\end{bmatrix}\begin{bmatrix}p\\ r\\ \beta\\ \phi\end{bmatrix} + \begin{bmatrix}\hat{p}_{10} & \hat{p}_{11}\\ \hat{p}_{12} & \hat{p}_{13}\\ 0 & \hat{p}_{14}\\ 0 & 0\end{bmatrix}\begin{bmatrix}\delta_a\\ \delta_r\end{bmatrix} \qquad (4.5.1)$$

or in equivalent form

$$\begin{bmatrix}\dot{z}_1\\ \dot{z}_2\\ \dot{z}_3\\ \dot{z}_4\end{bmatrix} = \begin{bmatrix}\hat{p}_1 & \hat{p}_2 & \hat{p}_3 & 0\\ \hat{p}_4 & \hat{p}_5 & \hat{p}_6 & 0\\ \hat{p}_7 & \hat{p}_8 & \hat{p}_9 & g/v_o\\ \cos a_f & \sin a_f & 0 & 0\end{bmatrix}\begin{bmatrix}p\\ r\\ \beta\\ \phi\end{bmatrix} +$$

$$+ \begin{bmatrix}\hat{p}_{10} & \hat{p}_{11}\\ \hat{p}_{12} & \hat{p}_{13}\\ 0 & \hat{p}_{14}\\ 0 & 0\end{bmatrix}\begin{bmatrix}\delta_a\\ \delta_r\end{bmatrix} + \begin{bmatrix}-10 & 0 & 0 & 0\\ 0 & -10 & 0 & 0\\ 0 & 0 & -10 & 0\\ 0 & 0 & 0 & -10\end{bmatrix}\begin{bmatrix}e_1\\ e_2\\ e_3\\ e_4\end{bmatrix} \qquad (4.5.2)$$

where $\hat{p}_i$ is an estimate of p_i and

$$\begin{bmatrix} e_1 \\ e_2 \\ e_3 \\ e_4 \end{bmatrix} = \begin{bmatrix} z_1 - p \\ z_2 - r \\ z_3 - \beta \\ z_4 - \phi \end{bmatrix} \qquad (4.5.3)$$

The matrices P, N_i and Q_i involved in the Liapunov function are chosen as follows:

$$P = \begin{bmatrix} 30 & 0 & 0 \\ 0 & 30 & 0 \\ 0 & 0 & 30 \end{bmatrix}$$

$$N_1 = \begin{bmatrix} 0.01 & 0 & 0 \\ 0 & 0.0001 & 0 \\ 0 & 0 & 0.00001 \end{bmatrix}$$

$$N_2 = \begin{bmatrix} 0.001 & 0 & 0 \\ 0 & 0.00001 & 0 \\ 0 & 0 & 0.000001 \end{bmatrix}$$

$$N_3 = \begin{bmatrix} 0.01 & 0 & 0 \\ 0 & 0.0001 & 0 \\ 0 & 0 & 0.00001 \end{bmatrix} \qquad (4.5.4)$$

$$Q_1 = Q_2 = \begin{bmatrix} 0.00001 & 0 \\ 0 & 0.00001 \end{bmatrix}$$

$$Q_3 = \begin{bmatrix} \infty & 0 \\ 0 & 0.00001 \end{bmatrix}$$

The same reasoning as before (see longitudinal dynamics) indicates that the P and N_i matrices are of third order. Note that $e_4 = 0$, Q_i matrices are of second order and matrix $B_m(\hat{p})$ has two columns. The infinity element of matrix Q_3 indicates that the first element of the third row of matrix $B_m(\hat{p})$ is known, namely 0. The adaptive algorithm equation used to identify the parameters of the lateral dynamics are obtained by substituting Eqs. (4.5.4) into Eqs. (3.2.16) and (3.2.17) and are given by

$$\hat{p}_1 = \hat{p}_1^{(o)} - \int_o^t (30e_1 p/0.01)dt$$

$$\hat{p}_2 = \hat{p}_2^{(o)} - \int_o^t (30e_1 r/0.0001)dt$$

$$\hat{p}_3 = \hat{p}_3^{(o)} - \int_o^t (30e_1 \beta/0.00001)dt$$

$$\hat{p}_4 = \hat{p}_4^{(o)} - \int_o^t (30e_2 p/0.001)dt$$

$$\hat{p}_5 = \hat{p}_5^{(o)} - \int_o^t (30e_2 r/0.00001)dt$$

$$\hat{p}_6 = \hat{p}_6^{(o)} - \int_o^t (30e_2 \beta/0.000001)dt$$

$$\hat{p}_7 = \hat{p}_7^{(o)} - \int_o^t (30e_3 p/0.01)dt$$

$$\hat{p}_8 = \hat{p}_8^{(o)} - \int_o^t (30e_3 r/0.0001)dt \qquad (4.5.5)$$

$$\hat{p}_9 = \hat{p}_9^{(o)} - \int_o^t (30e_3 \beta/0.00001)dt$$

$$\hat{p}_{10} = \hat{p}_{10}^{(o)} - \int_o^t (30e_1 \delta_a/0.00001)dt$$

$$\hat{p}_{11} = \hat{p}_{11}^{(o)} - \int_o^t (30e_1 \delta_r/0.00001)dt$$

$$\hat{p}_{12} = \hat{p}_{12}^{(o)} - \int_o^t (30e_2 \delta_a/0.00001)dt$$

$$\hat{p}_{13} = \hat{p}_{13}^{(o)} - \int_o^t (30e_2 \delta_r/0.00001)dt$$

$$\hat{p}_{14} = \hat{p}_{14}^{(o)} - \int_o^t (30e_3 \delta_r/0.00001)dt$$

Again $\hat{p}_i^{(o)}$ is an initial estimate of parameter p_i.

In order to implement the Newton-Raphson IAS for the lateral dynamics, a model of the following form is used

$$\begin{bmatrix} \dot{x}_1 \\ \dot{x}_2 \\ \dot{x}_3 \\ \dot{x}_4 \end{bmatrix} = \begin{bmatrix} \hat{p}_1 & \hat{p}_2 & \hat{p}_3 & 0 \\ \hat{p}_4 & \hat{p}_5 & \hat{p}_6 & 0 \\ \hat{p}_7 & \hat{p}_8 & \hat{p}_9 & g/v_o \\ \cos a_f & \sin a_f & 0 & 0 \end{bmatrix} \begin{bmatrix} x_1 \\ x_2 \\ x_3 \\ x_4 \end{bmatrix} + \begin{bmatrix} \hat{p}_{10} & \hat{p}_{11} \\ \hat{p}_{12} & \hat{p}_{13} \\ 0 & \hat{p}_{14} \\ 0 & 0 \end{bmatrix} \begin{bmatrix} \delta a \\ \delta r \end{bmatrix} \qquad (4.5.6)$$

In this case, the sensitivity matrix has dimension 3 x 14 whose i - j element is $\partial x_i/\partial \hat{p}_j$ $(i \leq 3, \quad j \leq 14)$. The differential Eq. (3.3.13) is solved to evaluate the elements of the sensitivity matrix. Once the sensitivity elements are obtained, they are substituted into Eq. (3.3.12) to yield an improved estimate of vector $\hat{p}$.

For the lateral simulation, we once again used data from reference (21) and considered the four wing-down (CO) configurations at three different altitudes (L = sea level, L = 20,000 ft., L = 40,000 ft.) and three different mach numbers (M = 0.5, M = 0.7, M = 0.9). The same procedure used for the longitudinal case was followed through the lateral case except that the interpolation polynomials used to represent the system parameters $\hat{p}_i$ with respect to mach number M and altitude L were only

expanded up to second order terms resulting in the following equations:

$$\hat{p}_1 = \hat{p}_1(M,L) = C_1 + C_2M + C_3L + C_4ML + C_5M^2 + C_6L^2$$

$$\hat{p}_2 = \hat{p}_2(M,L) = C_7 + C_8M + C_9L + C_{10}ML + C_{11}M^2 + C_{12}L^2$$

$$\hat{p}_3 = \hat{p}_3(M,L) = C_{13} + C_{14}M + C_{15}L + C_{16}ML + C_{17}M^2 + C_{18}L^2$$

$$\hat{p}_4 = \hat{p}_4(M,L) = C_{19} + C_{20}M + C_{21}L + C_{22}ML + C_{23}M^2 + C_{24}L^2$$

$$\hat{p}_5 = \hat{p}_5(M,L) = C_{25} + C_{26}M + C_{27}L + C_{28}ML + C_{29}M^2 + C_{30}L^2$$

$$\hat{p}_6 = \hat{p}_6(M,L) = C_{31} + C_{32}M + C_{33}L + C_{34}ML + C_{35}M^2 + C_{36}L^2$$

$$\hat{p}_7 = \hat{p}_7(M,L) = C_{37} + C_{38}M + C_{39}L + C_{40}ML + C_{41}M^2 + C_{42}L^2 \qquad (4.5.7)$$

$$\hat{p}_8 = \hat{p}_8(M,L) = C_{43} + C_{44}M + C_{45}L + C_{46}ML + C_{47}M^2 + C_{48}L^2$$

$$\hat{p}_9 = \hat{p}_9(M,L) = C_{49} + C_{50}M + C_{51}L + C_{52}ML + C_{53}M^2 + C_{54}L^2$$

$$\hat{p}_{10} = \hat{p}_{10}(M,L) = C_{55} + C_{56}M + C_{57}L + C_{58}ML + C_{59}M^2 + C_{60}L^2$$

$$\hat{p}_{11} = \hat{p}_{11}(M,L) = C_{61} + C_{62}M + C_{63}L + C_{64}ML + C_{65}M^2 + C_{66}L^2$$

$$\hat{p}_{12} = \hat{p}_{12}(M,L) = C_{67} + C_{68}M + C_{69}L + C_{70}ML + C_{71}M^2 + C_{72}L^2$$

$$\hat{p}_{13} = \hat{p}_{13}(M,L) = C_{73} + C_{74}M + C_{75}L + C_{76}ML + C_{77}M^2 + C_{78}L^2$$

$$\hat{p}_{14} = \hat{p}_{14}(M,L) = C_{79} + C_{80}M + C_{81}L + C_{82}ML + C_{83}M^2 + C_{84}L^2$$

Once the relationship between the lateral parameters as a function of mach number M and altitude L has been established Eqs. (4.5.7) the application of the LAS is implemented by the iterative application of Eqs. (3.4.14) and (3.4.16).

For the lateral LCS the aileron and rudder command structures are

$$\delta_a = K_1p + G_1\delta_{s1}$$
$$\delta_r = K_2r + K_3\beta + G_2\delta_{s2} \qquad (4.5.8)$$

Imposing the constraint that the plant's handling qualities remain the same over all possible operating conditions, Eqs. (3.5.1) and (4.5.8) are used to obtain relationships which constitute the control laws given by

$$\Delta K_1 = -\left[\hat{p}_{10}(K_1\Delta p_{10} + \Delta p_1) + \hat{p}_{12}(K_1\Delta p_{12} + \Delta p_4)\right] /(\hat{p}_{10}^2 + \hat{p}_{12}^2)$$

$$\Delta K_2 = -\left[\hat{p}_{11}(K_2\Delta p_{11} + \Delta p_2) + \hat{p}_{13}(K_2\Delta p_{13} + \Delta p_5) + \right.$$
$$\left. + \hat{p}_{14}(K_2\Delta p_{14} + \Delta p_8)\right] /(\hat{p}_{11}^2 + \hat{p}_{13}^2 + \hat{p}_{14}^2)$$

$$\Delta K_3 = -\left[\hat{p}_{11}(K_3\Delta p_{11} + \Delta p_3) + \hat{p}_{13}(K_3\Delta p_{13} + \Delta p_6) + \right. \qquad (4.5.9)$$
$$\left. + \hat{p}_{14}(K_3\Delta p_{14} + \Delta p_9)\right] /(\hat{p}_{11}^2 + \hat{p}_{13}^2 + \hat{p}_{14}^2)$$

$$\Delta G_1 = -(\hat{p}_{10}G_1\Delta p_{10} + \hat{p}_{12}G_1\Delta p_{12})/(\hat{p}_{10}^2 + \hat{p}_{12}^2)$$

$$\Delta G_2 = -(\hat{p}_{11}G_2\Delta p_{11} + \hat{p}_{13}G_2\Delta p_{13} + \hat{p}_{14}G_2\Delta p_{14})/(\hat{p}_{11}^2 + \hat{p}_{13}^2 + \hat{p}_{14}^2)$$

where $\hat{p}_i$ are the learned parameters obtained from the LAS and Δp_i is the difference between the learned $\hat{p}_i$ at the current time and the previous time. Note that $\hat{p}_i$ are computed using the $C'_k s$ stored in the memory. This process was illustrated in section 4.3 and is carried out for the lateral case in the same fashion.

4.6. Results and Discussion

Our LCS was applied to the longitudinal and lateral dynamics of the F-8 DFBW aircraft. The complete system was simulated on a digital computer as shown by the flow diagrams of figures 4-1a (Liapunov's IAS) and 4-1b (Newton-Raphson IAS). The learning of twenty four aircraft parameters (ten for the longitudinal dynamics and fourteen for the lateral dynamics) have been evaluated. Six of these parameters (longitudinal p_1, p_3, p_8 and lateral p_2, p_4, p_{11}) are presented in Figs. 4.2-4.13 to emphasize the learning performance of the two different LCS.

A comparison between Figs. 4-2 & 4-5 and 4-4 & 4-7 show that the learned parameter curves using Newton-Raphson IAS give a better approximation to the plant parameter curves than the ones obtained by using Liapunov's IAS. A comparison between Figs. 4-3 & 4-6 show that where Liapunov's IAS failed to obtain a better approximation of the initial parameters, Newton-Raphson IAS did not. These comparisons are based upon equal time operation of the two learning control systems, while both the information acquisition subsystems passed the convergence criterion. Since the convergence criterion has been satisfied in both IAS's there is no need to further extend the monitoring of the adjusted parameters. It is assumed that once the parameters pass the convergence criterion little or not additional information is gained by further operation of the system.

These observations indicate that the performance of the learning control system is strongly affected by the accuracy of the IAS. The comparative results show that the LCS using the IAS based on Newton-Raphson method produces better learning of the parameters. This, in turn, means that the gain schedule adjustments were more accurate than the adjustments

obtained from the LCS based on Liapunov's direct method IAS. These experimental results and the comparative observations were described and presented at the NASA session of the 1976 IEEE Decision and Control Conference, Clearwater, Florida, December 1976. The presentation is published in the Proceedings of this Conference[56].

It was also observed experimentally that for a low amplitude input signal $\mathcal{S}_s$ in both Liapunov's and Newton-Raphson's IAS the measurement information content, y, is not adequate to obtain a useful estimate vector $\hat{p}$ because the process attempts to fit the noise. This indicates that there exists a need to make tests on measurement information prior to modifying the estimate of parameter vector $\hat{p}$. For the Liapunov IAS this test was incorporated in the convergence criterion described in Chapter 3. For the Newton-Raphson's IAS lower bounds were placed on the diagonal elements of the information matrix I, given by

$$I = \sum_{i=1}^{N} (\partial x/\partial \hat{p})_i^T B_i (\partial x/\partial \hat{p})_i \qquad (4.6.1)$$

prior to allowing adjustments of the estimate of parameter vector $\hat{p}$. The bounds were determined by examining the variation of the appropriate information matrix elements during steady-state conditions with no input signal applied. In that case, the variations were caused by measurement noise so that any variations of the elements below the selected bounds were regarded as being caused by measurement noise and therefore, the estimate of parameter vector $\hat{p}$ was not adjusted.

Since Newton-Raphson method proved to give better results for the IAS therefore, this information acquisition procedure is incorporated with the LAS and the Memory and Control Process subsystem (MCPS) to form

a LCS which is applied to NASA's real-time simulation of the F-8 DFBW aircraft. This LCS has been evaluated on NASA's real-time computer and is presented in the next chapter.

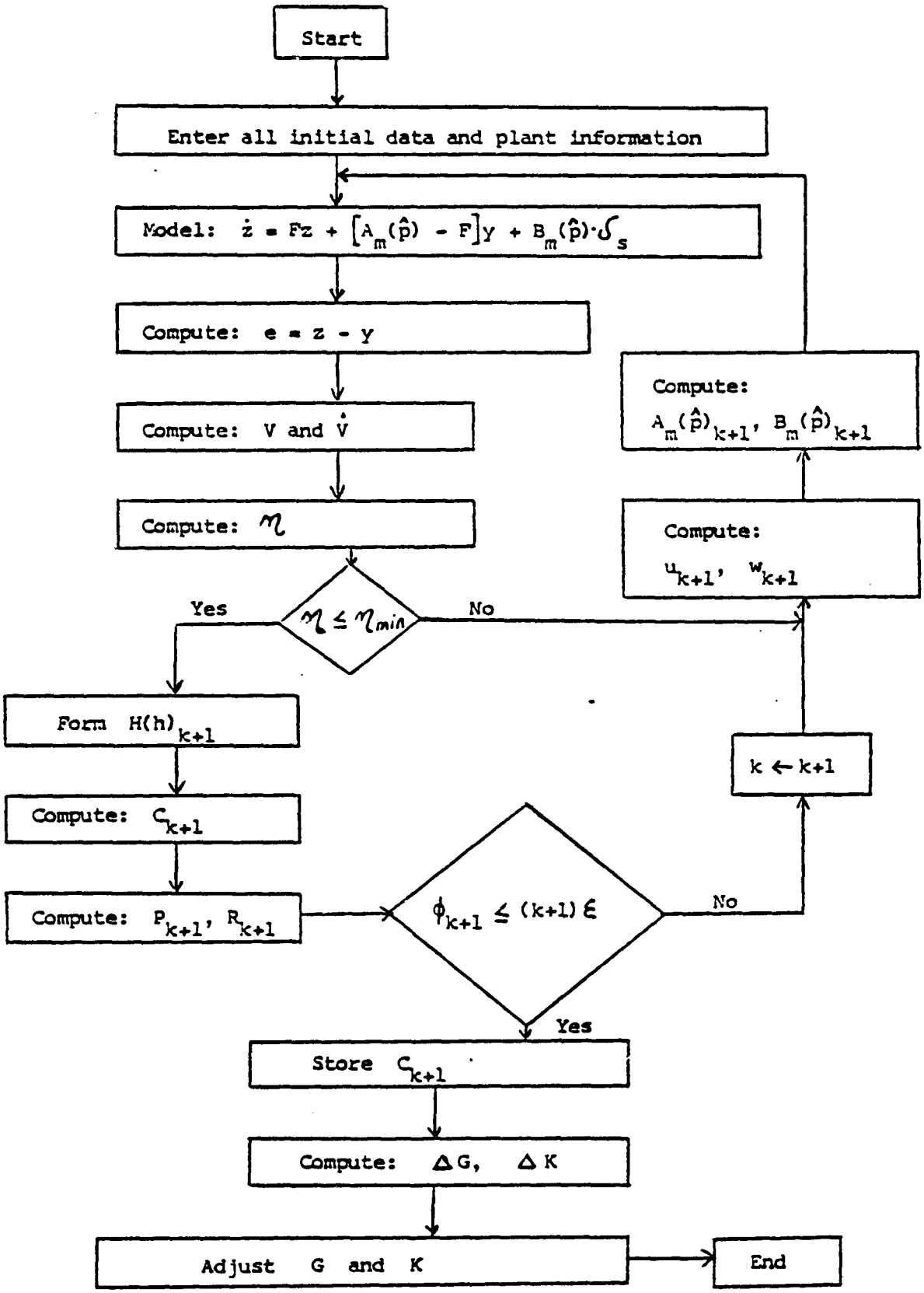

Fig. 4.1a Logic Flow Diagram. (IAS - Liapunov Method)

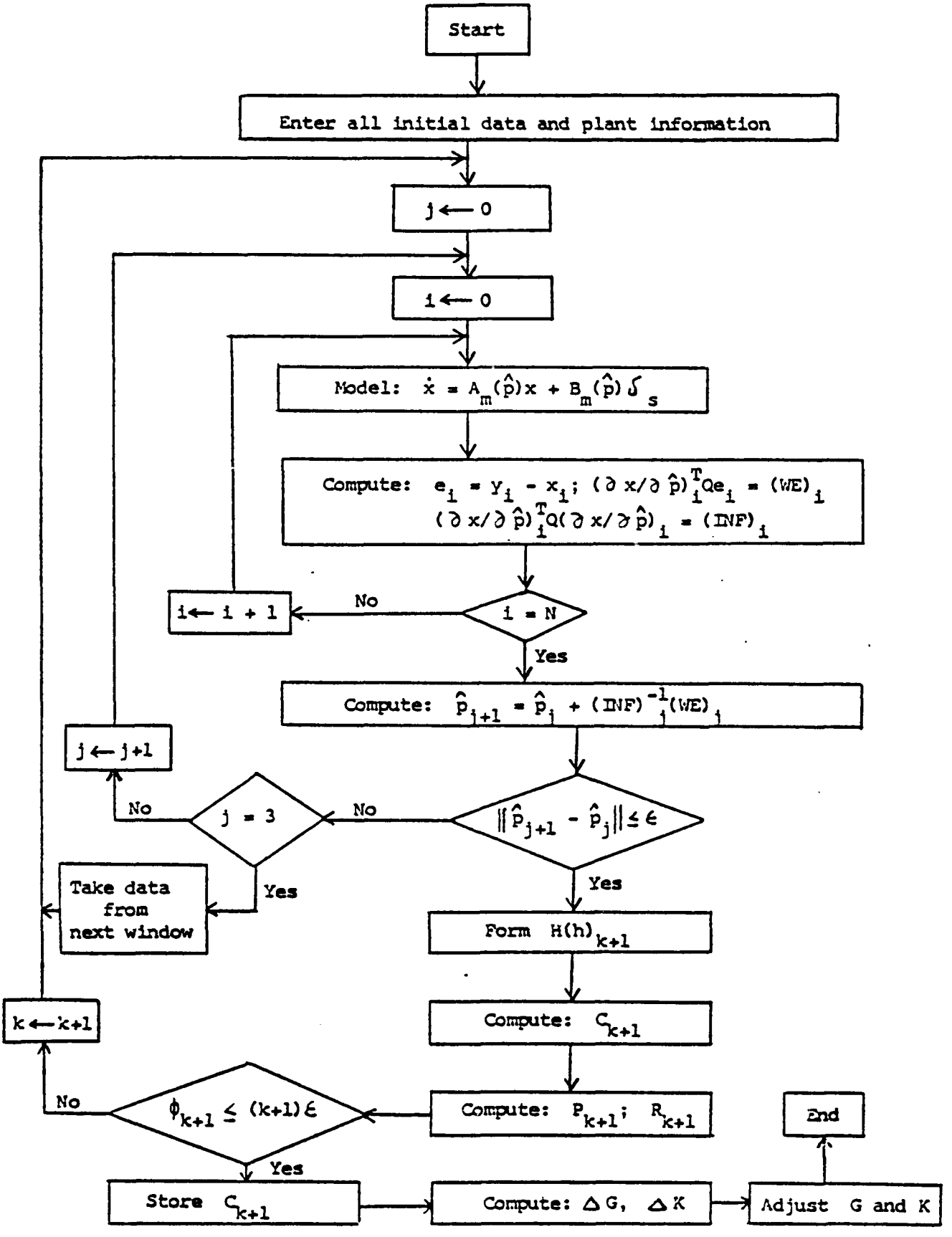

Fig. 4.1b Logic Flow Diagram (IAS - Newton-Raphson Method)

Fig. 4.2 LONG. P1 VS. MACH (Liapunov IAS)

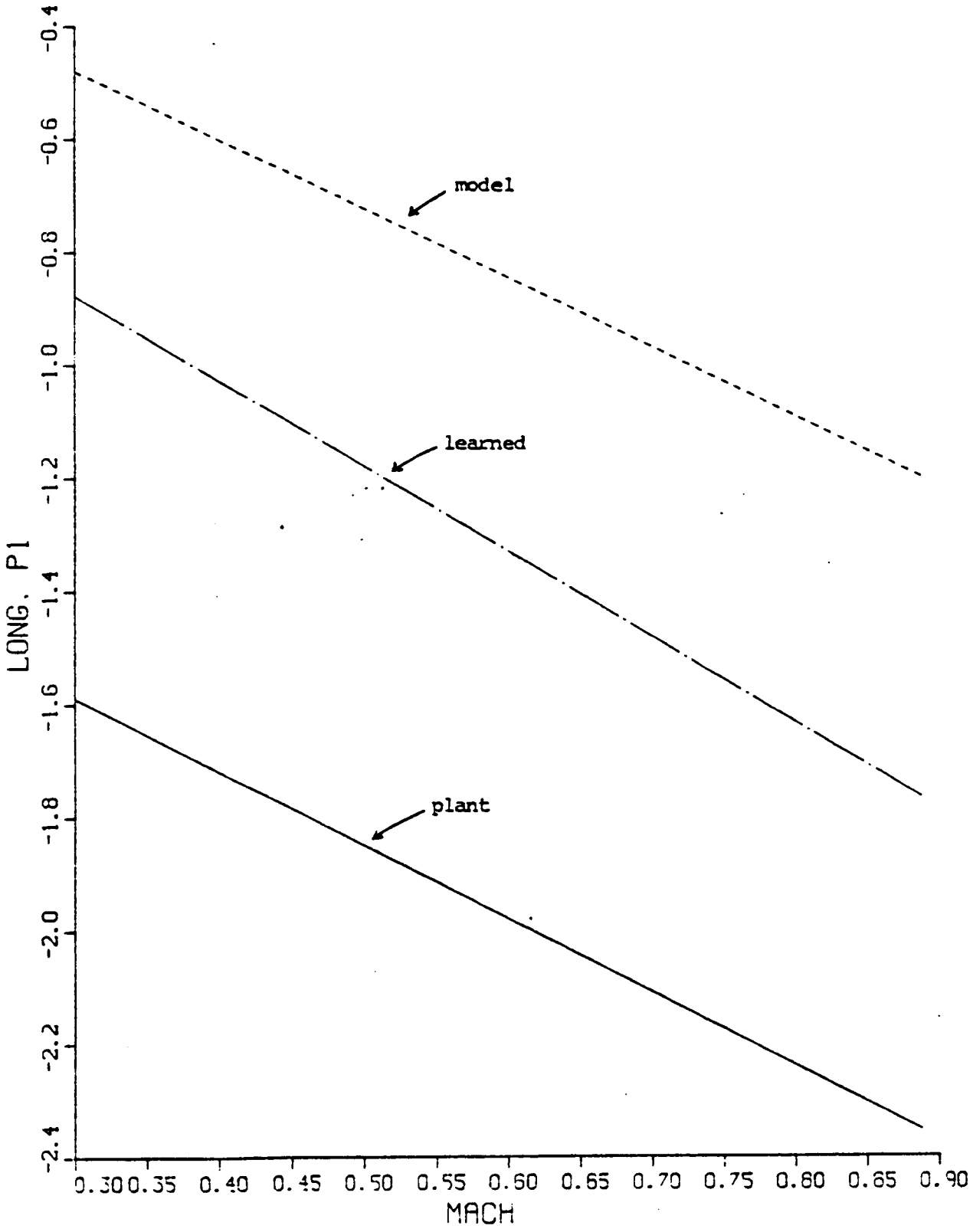

Fig. 4.3 LONG. P3 VS. MACH (Liapunov IAS)

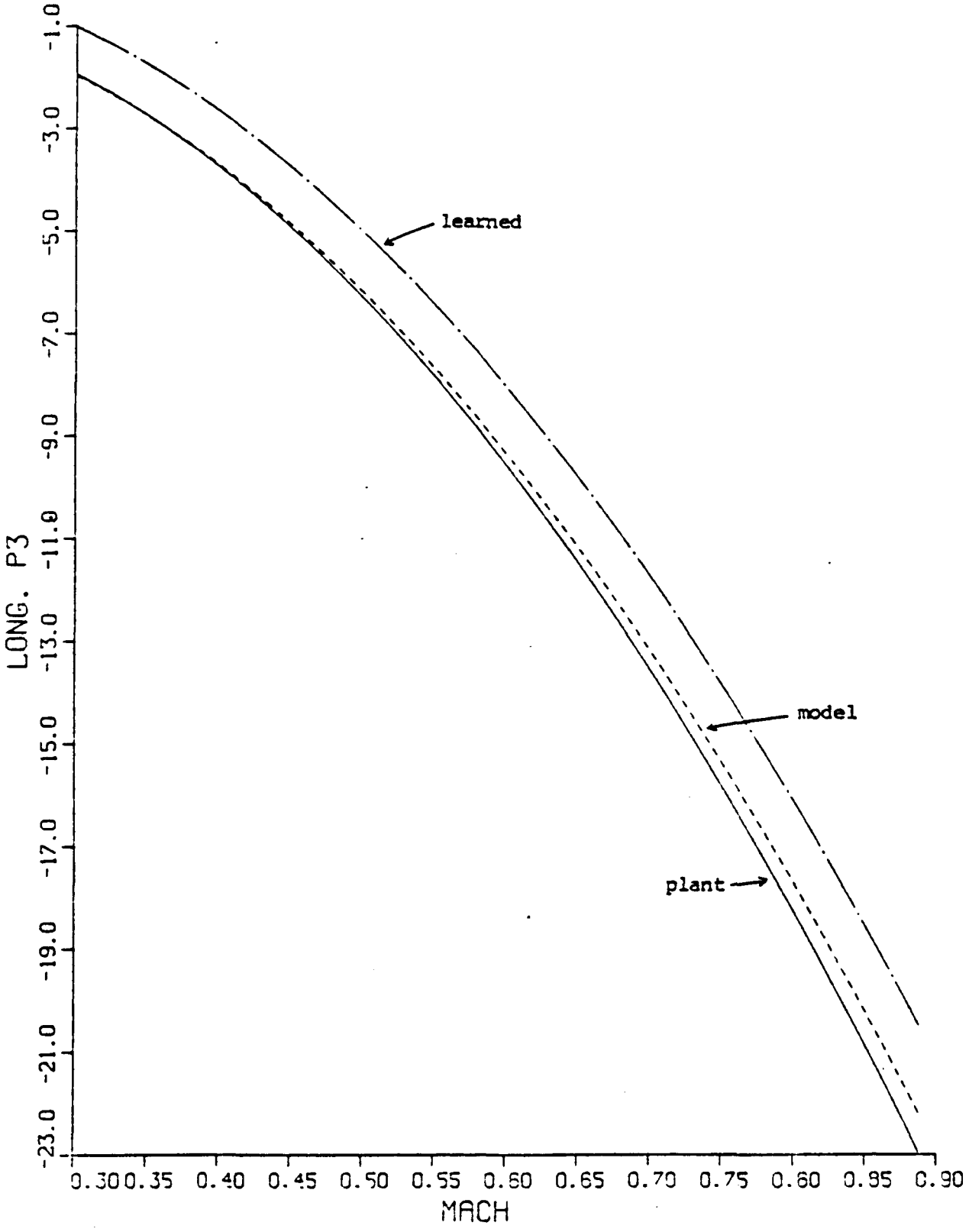

Fig. 4.4 LONG. P8 VS. MACH (Liapunov IAS)

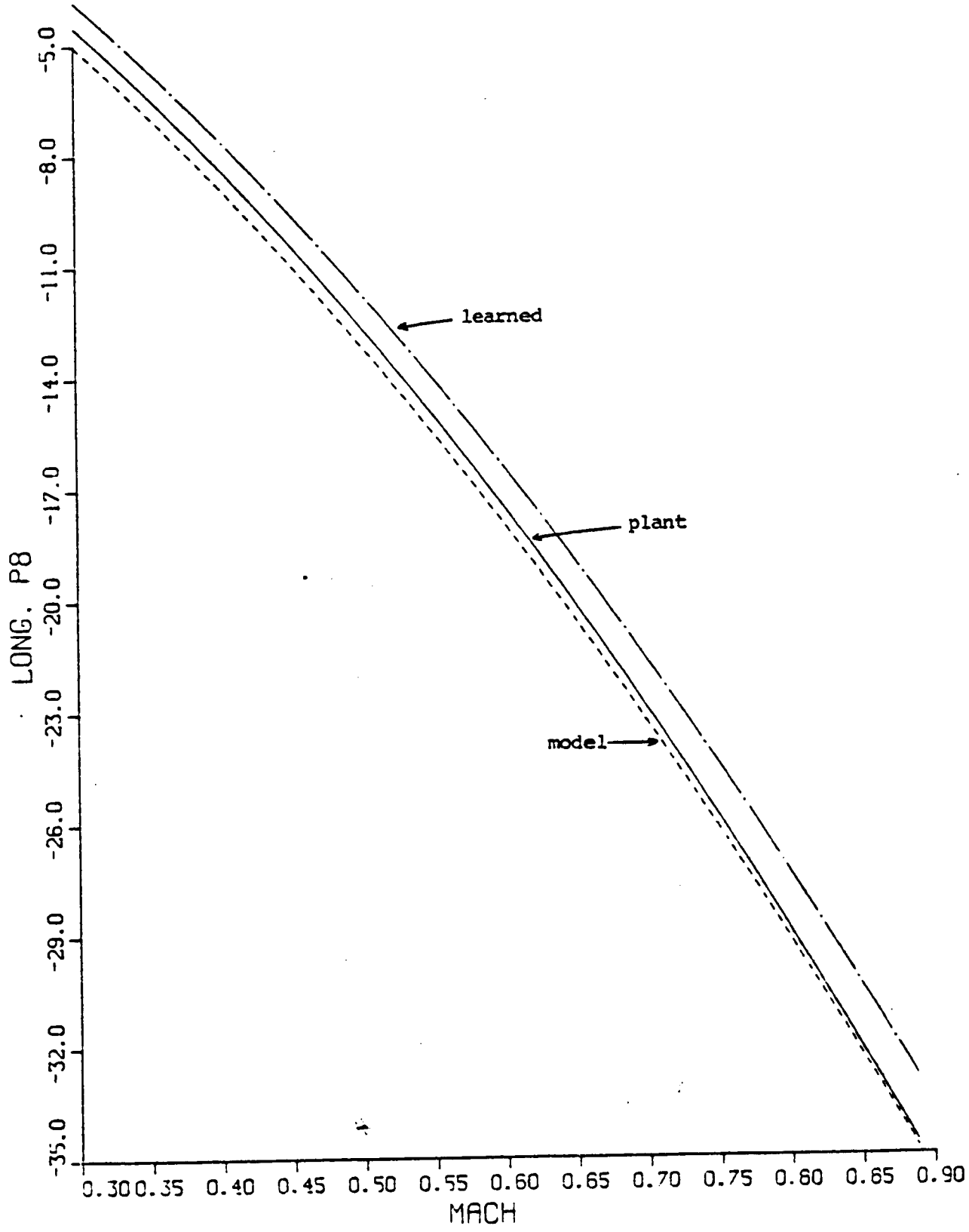

Fig. 4.5 LONG. P1 VS. MACH (Newton-Raphson IAS)

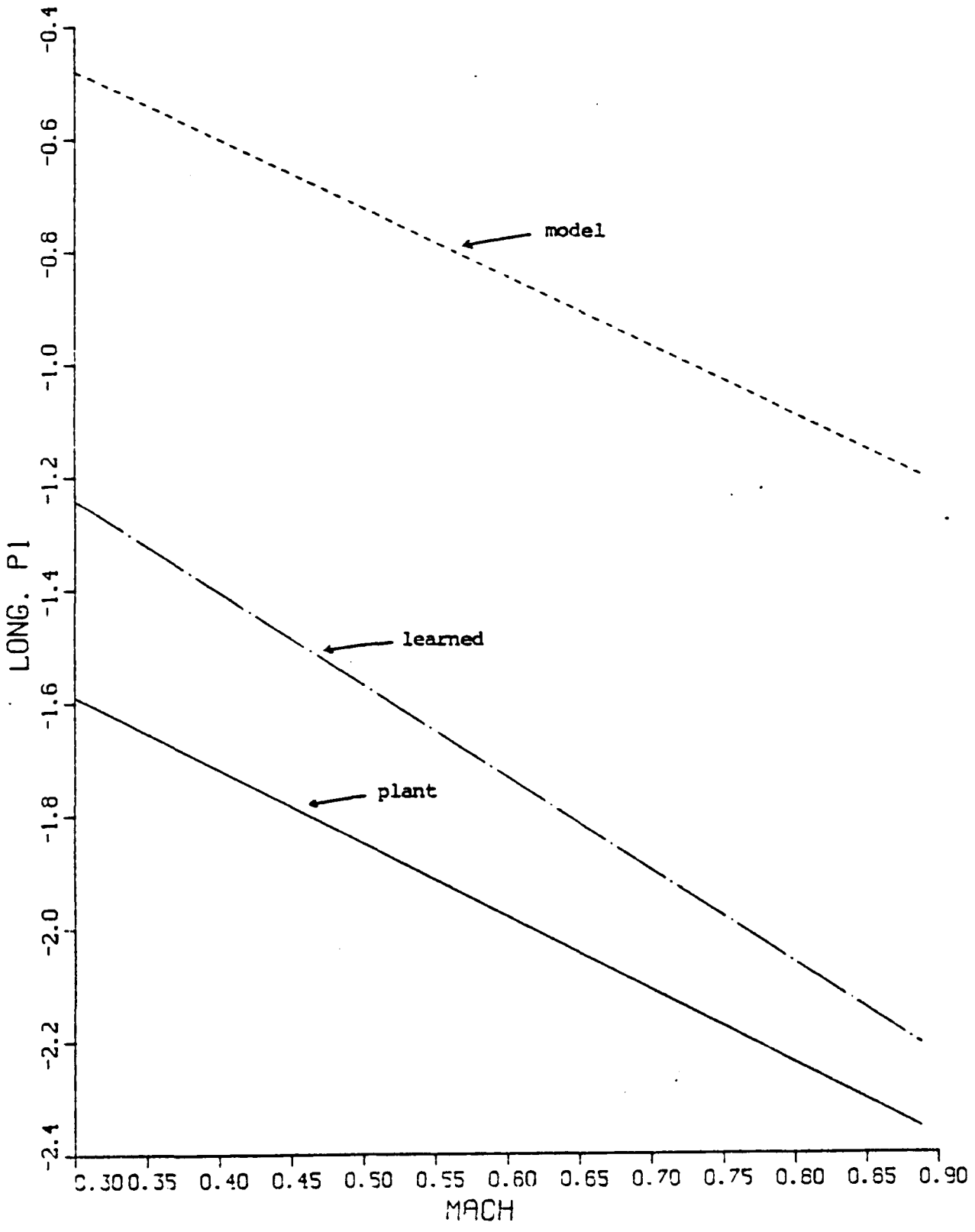

Fig. 4.6 LONG. P3 VS. MACH (Newton-Raphson IAS)

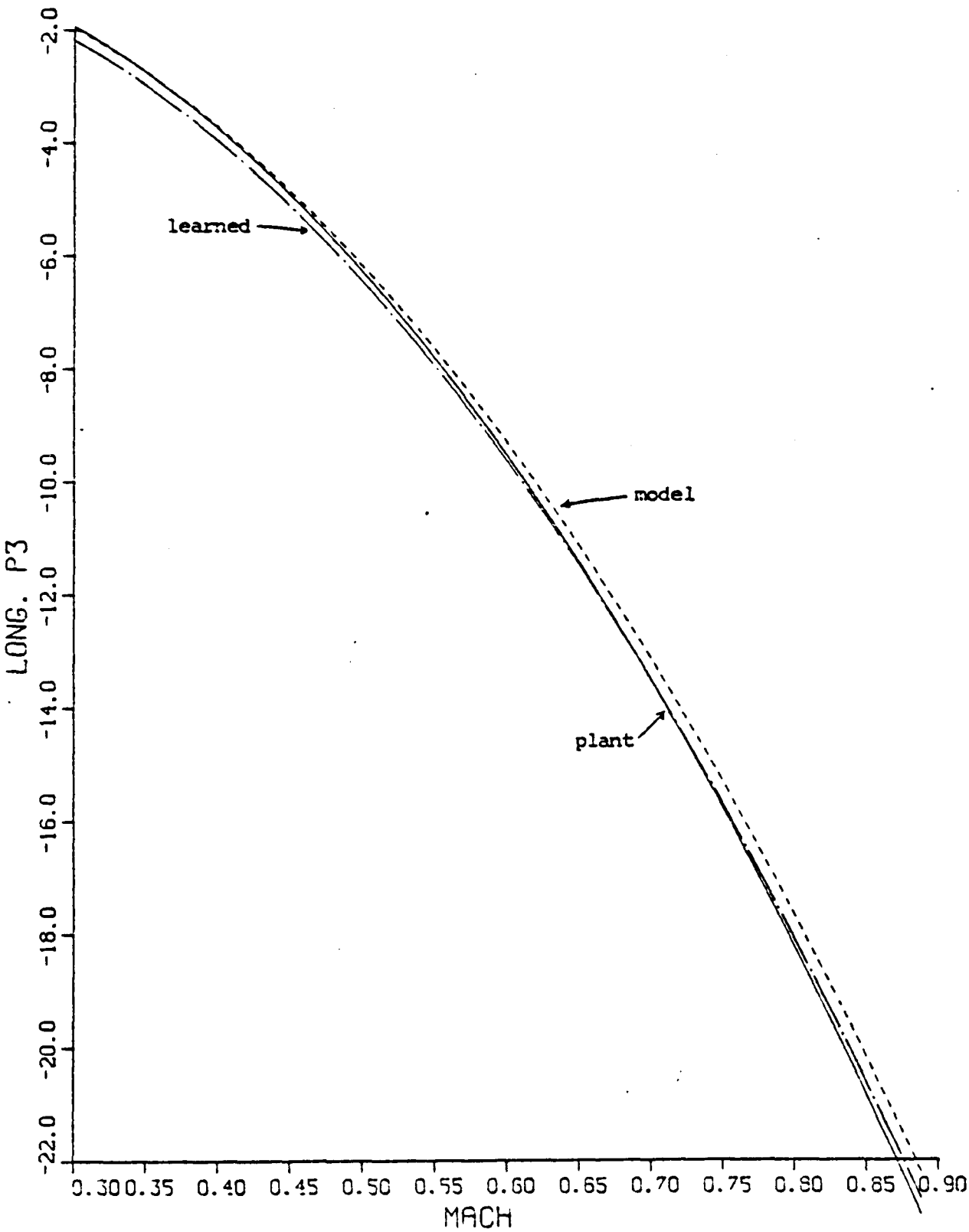

Fig. 4.7 LONG. P8 VS. MACH (Newton-Raphson IAS)

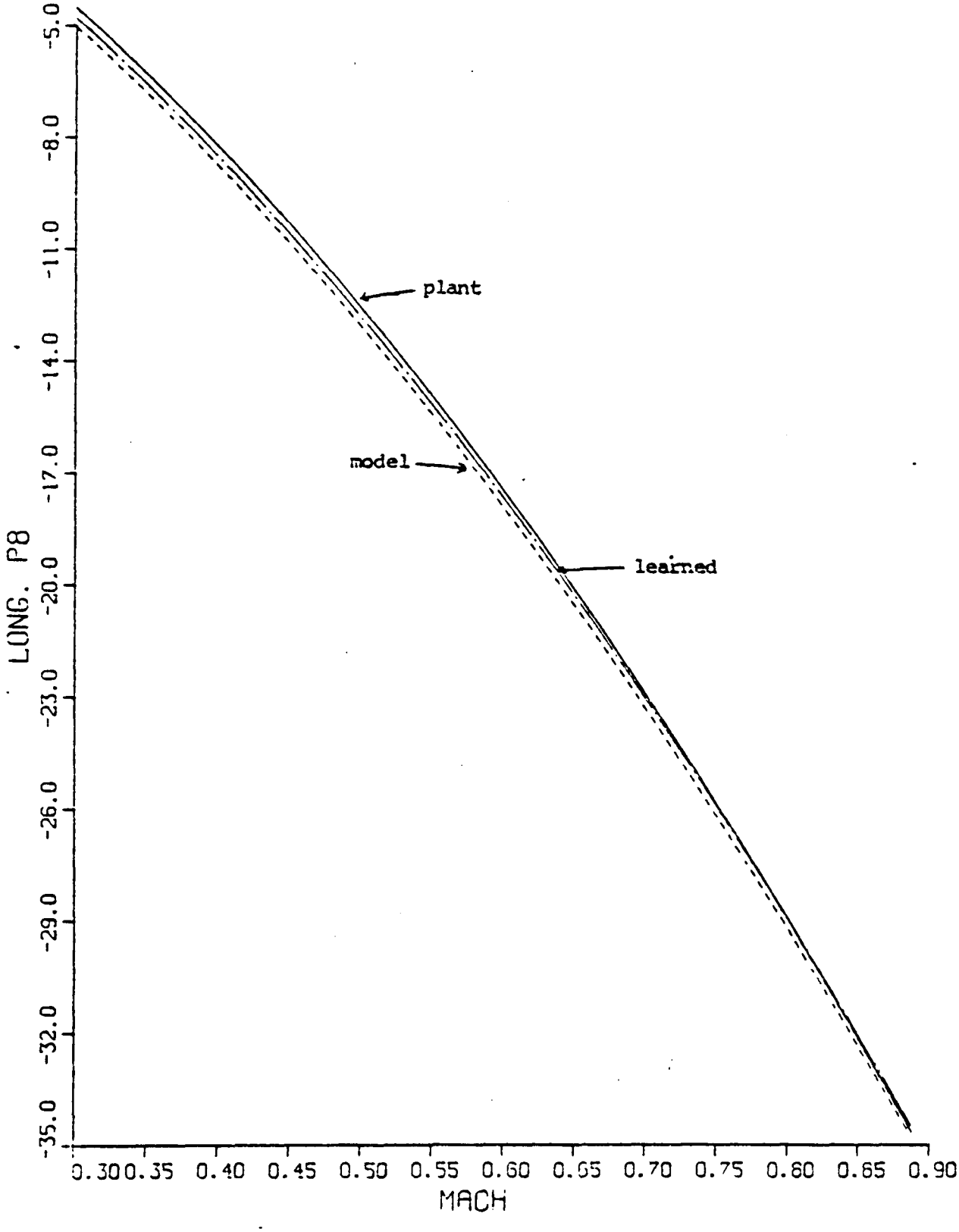

Fig. 4.8 LATR. P2 VS. MACH (Liapunov IAS)

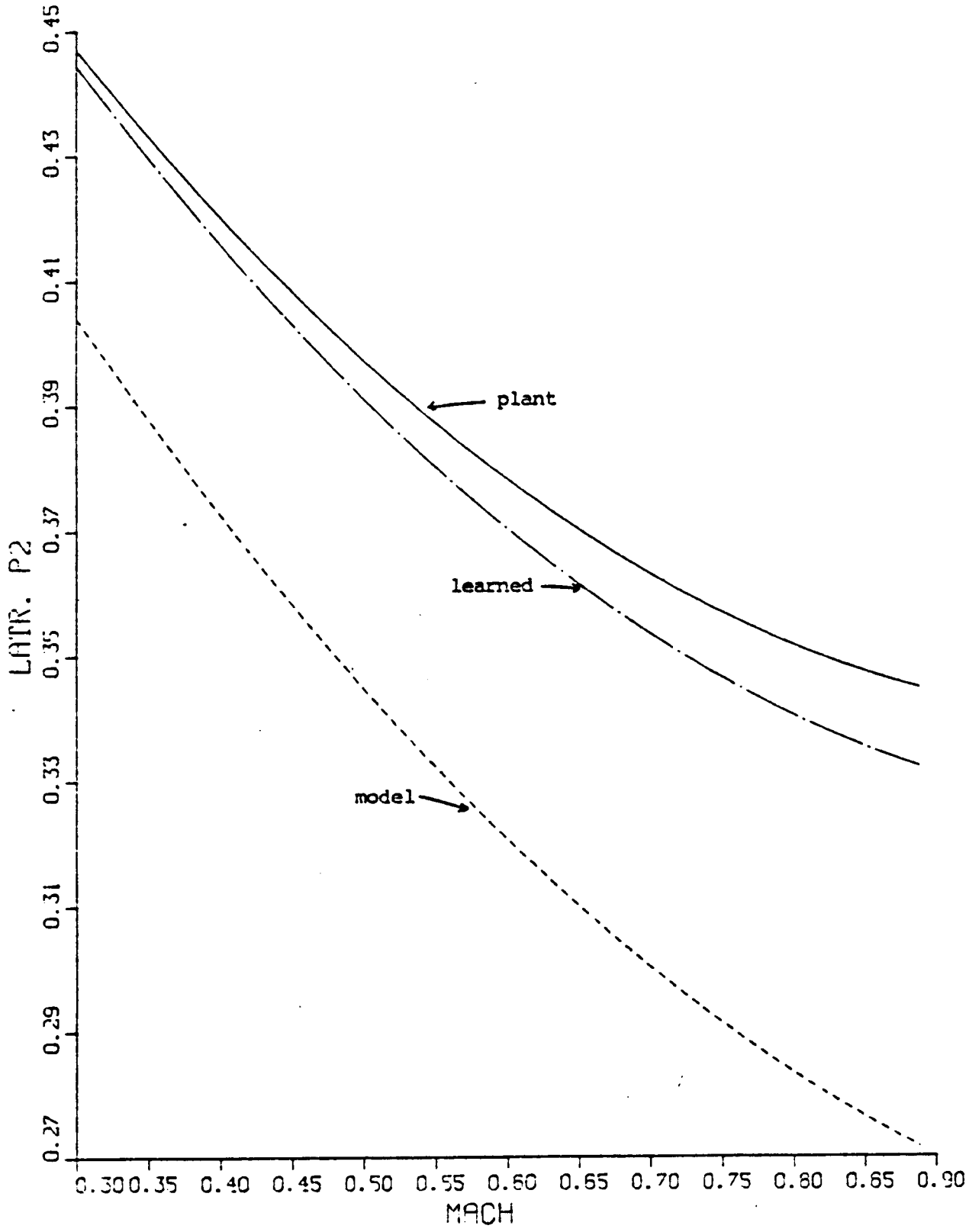

Fig. 4.9 LATR. P4 VS. MACH (Liapunov IAS)

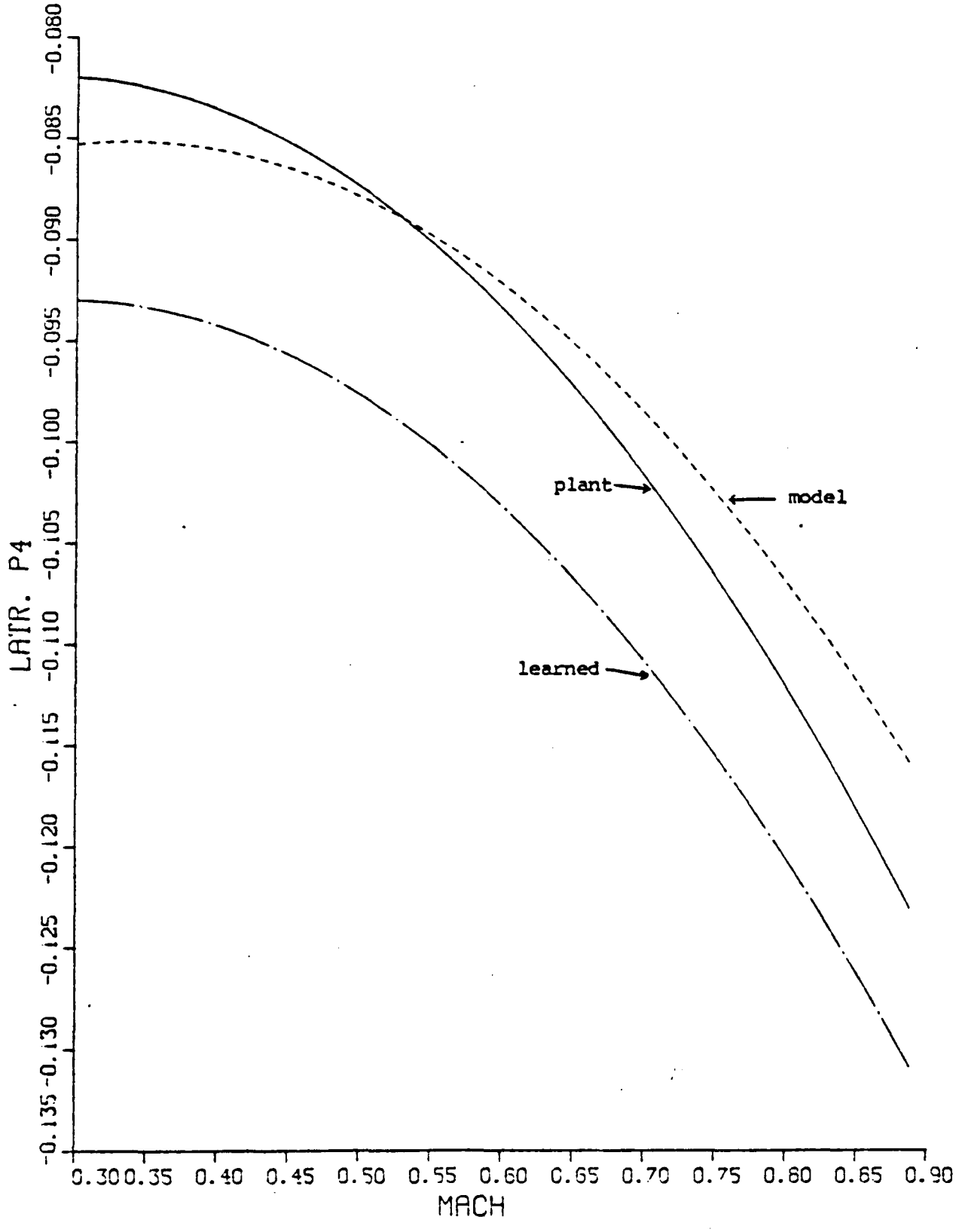

Fig. 4.10 LATR. P11 VS. MACH (Liapunov IAS)

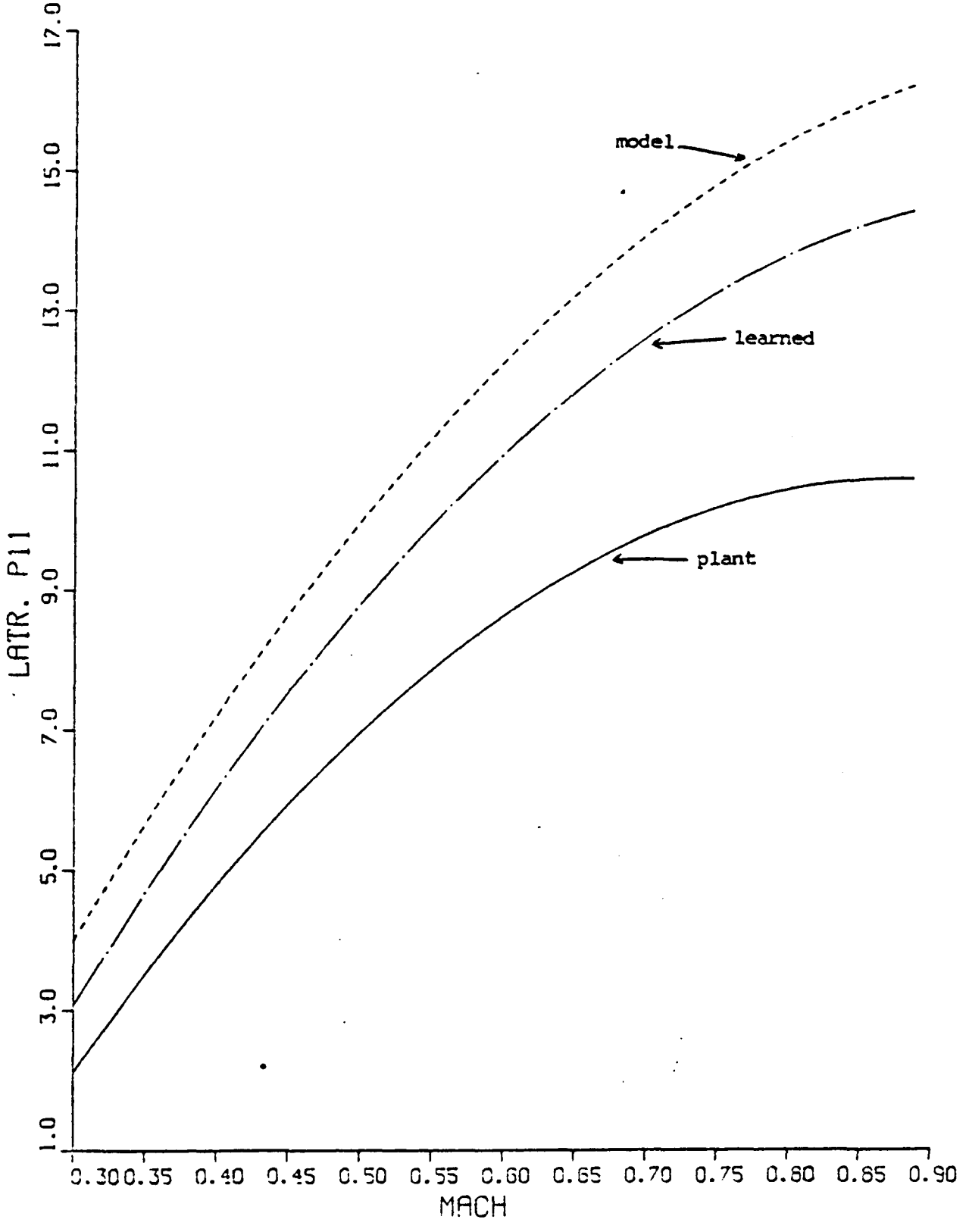

Fig. 4.11 LATR. P2 VS. MACH (Newton-Raphson IAS)

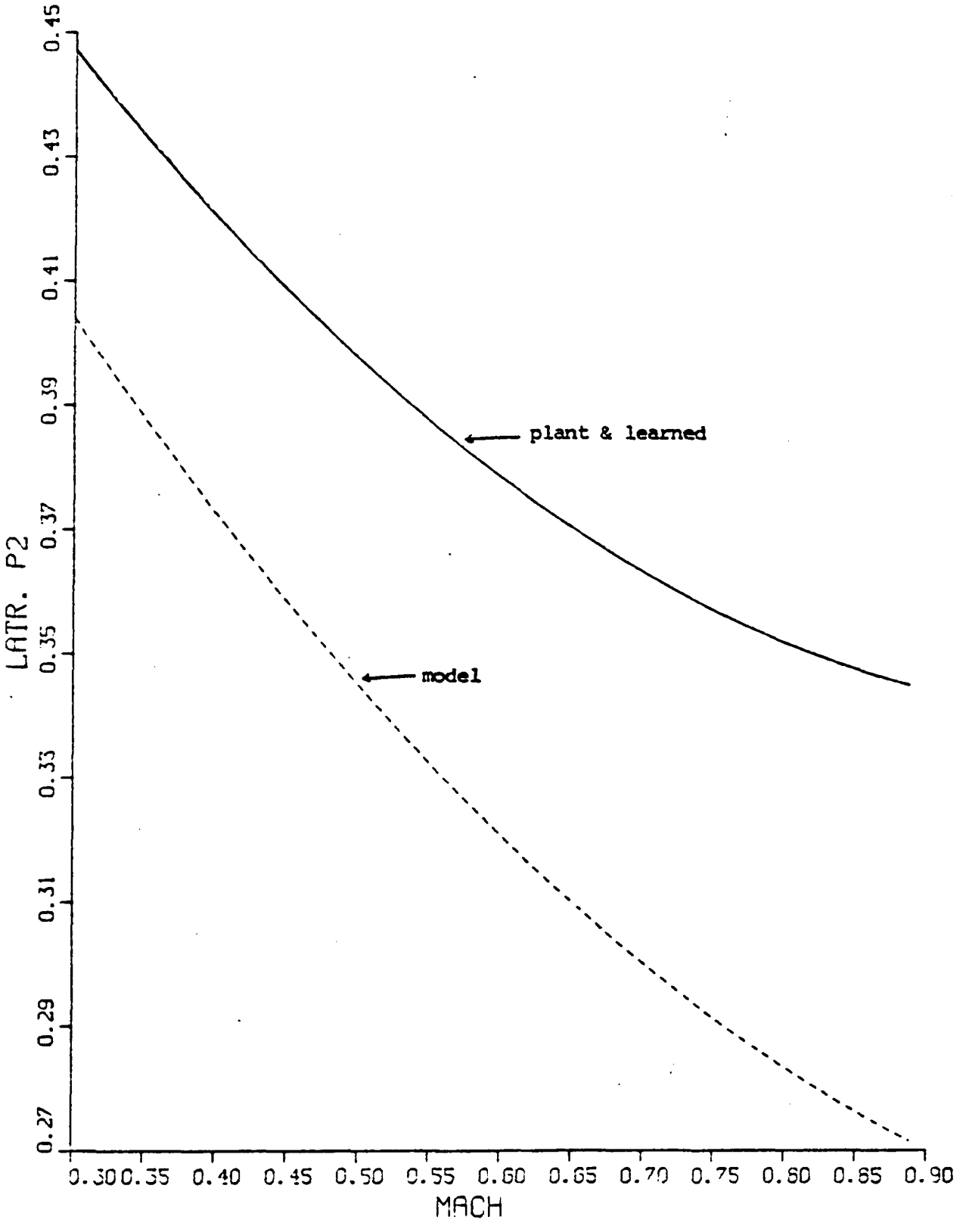

Fig. 4.12 LATR. P4 VS. MACH (Newton-Raphson IAS)

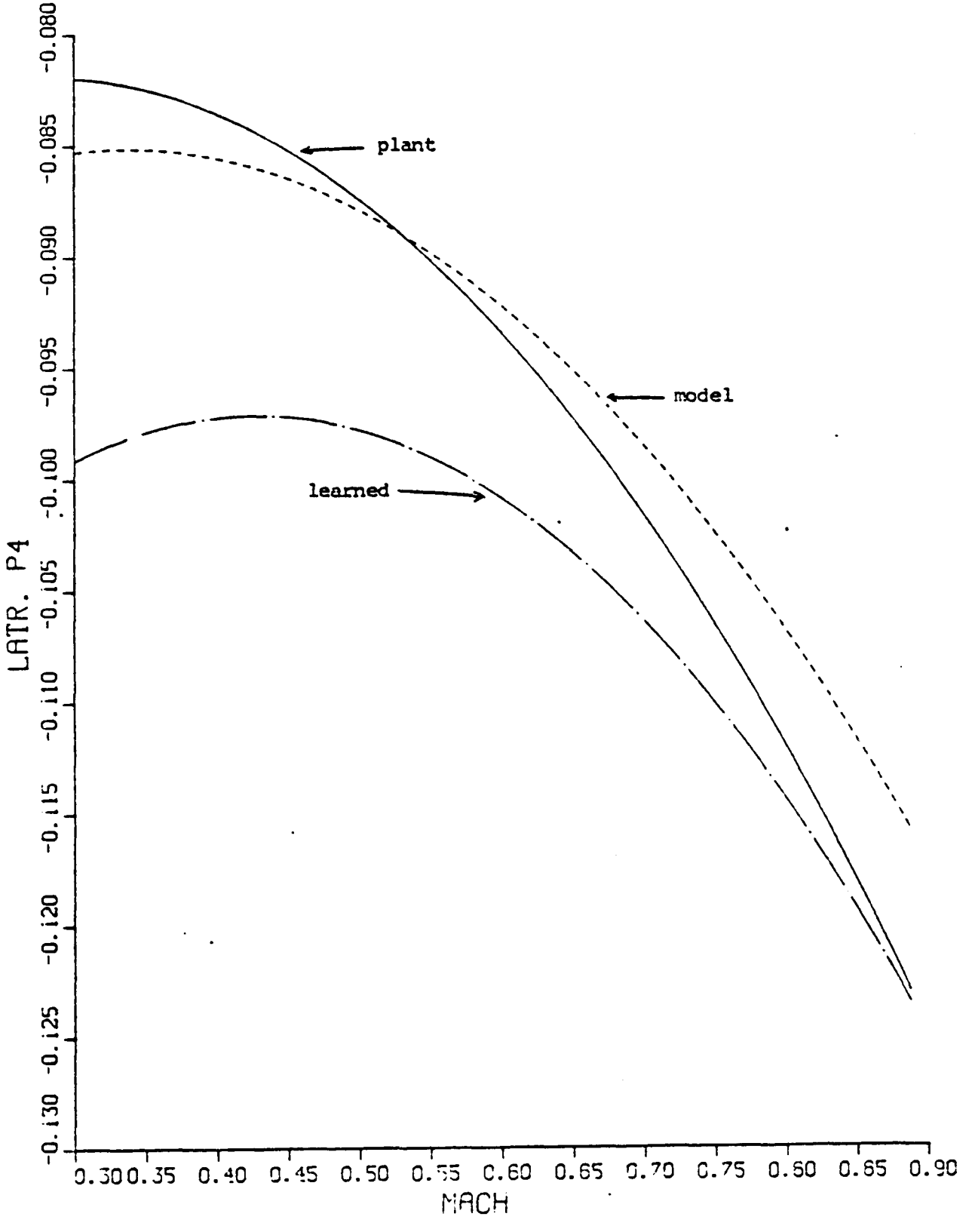

Fig. 4.13 LATR. P11 VS. MACH (Newton-Raphson IAS)

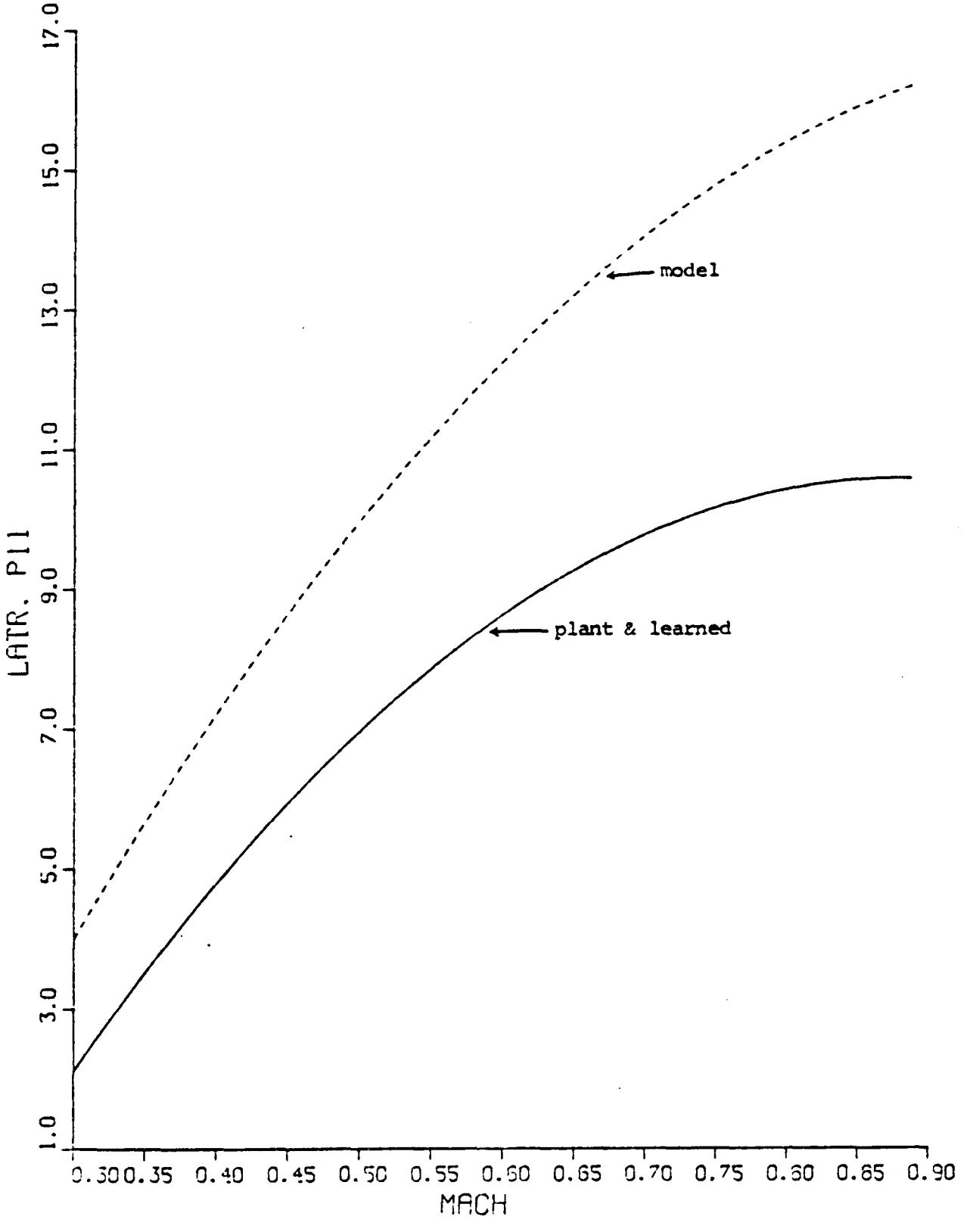

CHAPTER 5

CASE STUDY II; THE REAL-TIME APPLICATION OF THE LCS TO THE F-8 DFBW AIRCRAFT*

5.1. Introduction

As indicated in the previous chapter, the Learning Control System (LCS) using the Newton-Raphson IAS had better performance than the LCS using Liapunov IAS. Our main concern in this chapter is to apply the LCS using Newton-Raphson IAS to the piloted six degree of freedom simulation of the F-8 DFBW aircraft. This was performed at NASA, LRC, on the real-time simulator.

Liapunov's IAS appears to have a convergence problem when applied in real-time. This is in contrast to the fact that Liapunov's IAS is by construction stable, i.e. the convergence of the IAS and hence of the LCS is always guaranteed. The reason for this discrepancy is that the integration routine involved in the adaptive loop requires integration stepsize as small as a hundredth of the smallest time constant of the aircraft dynamics. Since with such a small stepsize, the approximation of Liapunov's function derivative is no longer semi-definite therefore, one becomes confronted with a covergence problem.

The Learning Control System (LCS) designed using Newton-Raphson IAS has been modified for application for real-time control of the F-8 DFBW aircraft. A problem of the Newton-Raphson IAS is the requirement to to determine the sensitivities of the system state to unknown parameters, which is the most time consuming part in the IAS. For this reason, research has been done on the computation of state sensitivities using

---

* This study has been conducted at NASA, Langley Research Center.

reduced order models.[12,90] In our application, described in this chapter, we use first or second order models which generate a modeling error noise. This indicates the need to make tests on information prior to modifying parameter estimates. These tests and convergence tests are in corporated in the convergence criterion.

In the next two sections we will describe the real-time application of our LCS to the longitudinal and lateral dynamics of the F-8 DFBW aircraft, respectively and in the final section, we will discuss our results.

5.2. The Real-Time Longitudinal LCS

For the longitudinal LCS the dynamics of the plant were simulated according to the equations

$$\begin{aligned}
\dot{v} &= -\bar{q}\, S/(C_D - C_T \cos\alpha)/m - g \sin\gamma \\
\dot{\gamma} &= \bar{q}\, S(C_L + C_T \sin\alpha)/mv - g \cos\gamma/v \\
\dot{q} &= \bar{q}\, S\bar{c}\, C_M/I_y \\
\dot{\theta} &= q \\
\dot{L} &= v \sin\gamma
\end{aligned} \tag{5.2.1}$$

where v is the air speed, γ is the flight path angle, q is the pitch rate, θ is the pitch angle, L is the altitude and $\alpha = \theta - \gamma$ is the angle of attack.

The model used for the longitudinal IAS has the form

$$\begin{aligned}
\dot{\alpha} &= q + \hat{p}_4 \alpha \\
\dot{q} &= \hat{p}_1 \alpha + \hat{p}_2 q + \hat{p}_3 \delta_e
\end{aligned} \tag{5.2.2}$$

The model given by Eq. (5.2.2) describes the short period longitudinal mode. The longitudinal phugoid mode was not modeled because its time

constant is normally large and its identification is not possible with a short term span data base. Also, its definition is not a major element in adjusting the feedback gains of the primary control loops. Therefore, our model given by Eq. (5.2.2) is only of second order in view of the plant being of fifth order.

For the real-time computation of Eq. (5.2.2) we utilized a discrete-time approximation. The discrete-time approximation is based on the division of the time axis into time intervals of T = 0.125 seconds each. Since the time increment T is sufficiently small compared with the time constants of the system, the response evaluated by discrete-time methods will be reasonably accurate

As it is shown in Appendix B, the difference equations that approximate a linear system of the form

$$\dot{x} = Ax + B\delta_s \tag{5.2.3}$$

are given by

$$x(k+1) = (TA + I)x(k) + TB\delta_s(k) \tag{5.2.4}$$

For our model described by Eq. (5.2.2) we have

$$A = \begin{bmatrix} \hat{p}_4 & 1 \\ \hat{p}_1 & \hat{p}_2 \end{bmatrix}$$

and (5.2.5)

$$B = \begin{bmatrix} 0 \\ \hat{p}_3 \end{bmatrix}$$

Therefore the real-time computation of Eq. (5.2.2) is evaluated using the discrete-time system

$$\begin{bmatrix} \alpha \\ q \end{bmatrix}_{k+1} = \begin{bmatrix} 1 + T\hat{p}_4 & T \\ T\hat{p}_1 & 1 + T\hat{p}_2 \end{bmatrix} * \begin{bmatrix} \alpha \\ q \end{bmatrix}_k + \begin{bmatrix} 0 \\ T\hat{p}_3 \end{bmatrix} * \delta_s \tag{5.2.6}$$

The fit error for the Newton-Raphson IAS is defined as

$$J(\hat{p}) = \tfrac{1}{2}\left[\sum_{k=1}^{25}(\bar{\alpha}-\alpha)_k^2\, b_{11} + (\bar{q}-q)_k^2\, b_{22}\right] \tag{5.2.7}$$

where $\bar{\alpha}$ and $\bar{q}$ are the sensor measurements of the angle of attack and pitch rate respectively, and b_{ii} are the elements of matrix B. Note that the number 25 (upper limit of summation) is the size of the data base over which the Newton-Raphson IAS iterates.

To develop the Newton-Raphson IAS, let us compute the gradient of the fit error with respect to $\hat{p}$. This yields

$$(\partial J/\partial \hat{p}) = -\sum_{k=1}^{25}\begin{bmatrix} e_1 b_{11}(\partial\alpha/\partial\hat{p}_1)_k + e_2 b_{22}(\partial q/\partial\hat{p}_1)_k \\ e_1 b_{11}(\partial\alpha/\partial\hat{p}_2)_k + e_2 b_{22}(\partial q/\partial\hat{p}_2)_k \\ e_1 b_{11}(\partial\alpha/\partial\hat{p}_3)_k + e_2 b_{22}(\partial q/\partial\hat{p}_3)_k \\ e_1 b_{11}(\partial\alpha/\partial\hat{p}_4)_k + e_2 b_{22}(\partial q/\partial\hat{p}_4)_k \end{bmatrix} \tag{5.2.8}$$

where

$$\begin{aligned} e_1 &= \bar{\alpha} - \alpha \\ e_2 &= \bar{q} - q \end{aligned} \tag{5.2.9}$$

To obtain an approximation of the second partial derivative of the fit error with respect to the parameters, let us differentiate Eq. (5.2.8) with respect to $\hat{p}$ and neglect the second order partials of the states with respect to $\hat{p}$. This yields the matrix $\partial^2 J/\partial\hat{p}^2$ whose elements are given by the following equation

$$(\partial^2 J/\partial\hat{p}^2)_{11} = \sum_{k=1}^{25} b_{11}(\partial\alpha/\partial\hat{p}_1)_k^2 + b_{22}(\partial q/\partial\hat{p}_1)_k^2$$

$$(\partial^2 J/\partial\hat{p}^2)_{12} = (\partial^2 J/\partial\hat{p}^2)_{21} = \sum_{k=1}^{25} b_{11}(\partial\alpha/\partial\hat{p}_1)_k(\partial\alpha/\partial\hat{p}_2)_k +$$

$$+ b_{22}(\partial q/\partial\hat{p}_1)_k(\partial q/\partial\hat{p}_2)_k$$

$$(\partial^2 J/\partial \hat{p}^2)_{13} = (\partial^2 J/\partial \hat{p}^2)_{31} = \sum_{k=1}^{25} b_{11}(\partial \alpha/\partial \hat{p}_1)_k(\partial \alpha/\partial \hat{p}_3)_k +$$

$$+ b_{22}(\partial q/\partial \hat{p}_1)_k(\partial q/\partial \hat{p}_3)_k$$

$$(\partial^2 J/\partial \hat{p}^2)_{14} = (\partial^2 J/\partial \hat{p}^2)_{41} = \sum_{k=1}^{25} b_{11}(\partial \alpha/\partial \hat{p}_1)_k(\partial \alpha/\partial \hat{p}_4)_k +$$

$$+ b_{22}(\partial q/\partial \hat{p}_1)_k(\partial q/\partial \hat{p}_4)_k$$

$$(\partial^2 J/\partial \hat{p}^2)_{22} = \sum_{k=1}^{25} b_{11}(\partial \alpha/\partial \hat{p}_2)_k^2 + b_{22}(\partial q/\partial \hat{p}_2)_k^2$$

$$(\partial^2 J/\partial \hat{p}^2)_{23} = (\partial^2 J/\partial \hat{p}^2)_{32} = \sum_{k=1}^{25} b_{11}(\partial \alpha/\partial \hat{p}_2)_k(\partial \alpha/\partial \hat{p}_3)_k +$$

$$+ b_{22}(\partial q/\partial \hat{p}_2)_k(\partial q/\partial \hat{p}_3)_k \qquad (5.2.10)$$

$$(\partial^2 J/\partial \hat{p}^2)_{24} = (\partial^2 J/\partial \hat{p}^2)_{42} = \sum_{k=1}^{25} b_{11}(\partial \alpha/\partial \hat{p}_2)_k(\partial \alpha/\partial \hat{p}_4)_k +$$

$$+ b_{22}(\partial q/\partial \hat{p}_2)_k(\partial q/\partial \hat{p}_4)_k$$

$$(\partial^2 J/\partial \hat{p}^2)_{33} = \sum_{k=1}^{25} b_{11}(\partial \alpha/\partial \hat{p}_3)_k^2 + b_{22}(\partial q/\partial \hat{p}_3)_k^2$$

$$(\partial^2 J/\partial \hat{p}^2)_{34} = (\partial^2 J/\partial \hat{p}^2)_{43} = \sum_{k=1}^{25} b_{11}(\partial \alpha/\partial \hat{p}_3)_k(\partial \alpha/\partial \hat{p}_4)_k +$$

$$+ b_{22}(\partial q/\partial \hat{p}_3)_k(\partial q/\partial \hat{p}_4)_k$$

$$(\partial^2 J/\partial \hat{p}^2)_{44} = \sum_{k=1}^{25} b_{11}(\partial \alpha/\partial \hat{p}_4)_k^2 + b_{22}(\partial q/\partial \hat{p}_4)_k^2$$

To compute the sensitivities involved in Eqs. (5.2.8) and (5.2.10) let us differentiate Eq. (5.2.6) with respect to $\hat{p}$. This yields

$$(\partial \alpha/\partial \hat{p}_1)_{k+1} = (1 + T\hat{p}_4)(\partial \alpha/\partial \hat{p}_1)_k + T(\partial q/\partial \hat{p}_1)_k$$

$$(\partial \alpha/\partial \hat{p}_2)_{k+1} = (1 + T\hat{p}_4)(\partial \alpha/\partial \hat{p}_2)_k + T(\partial q/\partial \hat{p}_2)_k$$

$$(\partial \alpha/\partial \hat{p}_3)_{k+1} = (1 + T\hat{p}_4)(\partial \alpha/\partial \hat{p}_3)_k + T(\partial q/\partial \hat{p}_3)_k \qquad (5.2.11)$$

$$(\partial \alpha/\partial \hat{p}_4)_{k+1} = (1 + T\hat{p}_4)(\partial \alpha/\partial \hat{p}_4)_k + T(\partial q/\partial \hat{p}_4)_k + T\alpha$$

$$(\partial q/\partial \hat{p}_1)_{k+1} = T\hat{p}_1(\partial \alpha/\partial \hat{p}_1)_k + (1 + T\hat{p}_2)(\partial q/\partial \hat{p}_1)_k + T\alpha$$

$$(\partial q/\partial \hat{p}_2)_{k+1} = T\hat{p}_1(\partial \alpha/\partial \hat{p}_2)_k + (1 + T\hat{p}_2)(\partial q/\partial \hat{p}_2)_k + Tq$$

$$(\partial q/\partial \hat{p}_3)_{k+1} = T\hat{p}_1(\partial \alpha/\partial \hat{p}_3)_k + (1 + T\hat{p}_2)(\partial q/\partial \hat{p}_3)_k + T\zeta_s$$

$$(\partial q/\partial \hat{p}_4)_{k+1} = T\hat{p}_1(\partial \alpha/\partial \hat{p}_4)_k + (1 + T\hat{p}_2)(\partial q/\partial \hat{p}_4)_k$$

The difference Eq. set (5.2.11) is solved starting with zero initial conditions, since the initial state is independent of the initial choice of the parameters.

After the first and second partials of the fit error are computed with respect to the parameters $\hat{p}_i$, the parameters are adjusted according to the following equation

$$\hat{p}_{j+1} = \hat{p}_j - (\partial^2 J/\partial p^2)_j^{-1}(\partial J/\partial \hat{p})_j \qquad (5.2.12)$$

During the iteration process defined by Eq. (5.2.12) the information content of the data base is checked by examining the determinant of the matrix $(\partial^2 J/\partial \hat{p}^2)$ prior to making iterations on the vector $\hat{p}$, especially, if the determinant is lower than 10^{-7}. This number was determined by examining the variation of the determinant of the matrix $(\partial^2 J/\partial \hat{p}^2)$ on the real-time computer during steady-state operation of the system with no input signal applied. In this case, the variation of the determinant is caused by measurement noise so that if the determinant is lower than 10^{-7} we considered that there was no adequate information in the processed data-base therefore, the parameter vector $\hat{p}$ was not adjusted. Another test incorporated in the convergence criterion did not allow more than 8 iterations over the data-base.* We also checked that the fit error should be lower than 0.1 and the Euclidean norm of the gradient vector $(\partial J/\partial \hat{p})$ be lower than 5×10^{-4}. Finally, the four diagonal elements of the matrix $(\partial^2 J/\partial \hat{p}^2)^{-1}$ were checked to be lower than 1,000, 300, 300 and 300 respectively. The numbers 1,000, 300, 300 and 300 denote the maximum allowable covariance of the parameters $\hat{p}_1$, $\hat{p}_2$, $\hat{p}_3$ and $\hat{p}_4$ respectively and were chosen experimentally using the real-time computer at NASA. When these tests were satisfied, the parameter vector $\hat{p}$ was passed to the Learning Algorithm Subsystem (LAS).

For the longitudinal application of the LAS, the relationship between the parameters $\hat{p}_i$'s as a function of mach number M and altitude L was represented by second order polynomials. This relationship is given by

* The reason for selecting only 8 iterations is that we wished to check the convergence during one second due to time limitation by the real-time simulator.

$$\hat{p}_1(M,L) = C_1 + C_2M + C_3L + C_4ML + C_5M^2 + C_6L^2$$

$$\hat{p}_2(M,L) = C_7 + C_8M + C_9L + C_{10}ML + C_{11}M^2 + C_{12}L^2 \qquad (5.2.13)$$

$$\hat{p}_3(M,L) = C_{13} + C_{14}M + C_{15}L + C_{16}ML + C_{17}M^2 + C_{18}L^2$$

$$\hat{p}_4(M,L) = C_{19} + C_{20}M + C_{21}L + C_{22}ML + C_{23}M^2 + C_{24}L^2$$

The LAS then produces the coefficient vector C by the iterative application of Eqs. (3.4.14) and (3.4.16). The obtained C_i's are then passed to the Memory and Control Process Subsystem (MCPS).

The design criterion for the longitudinal MCPS was to maintain a short period damping coefficient of 0.7 of critical damping independent of frequency. To meet this criterion, the elevator control was chosen in the following form

$$\delta_e = \delta_{e_{tr}} + K_1 q + K_2 \delta_s \qquad (5.2.14)$$

The first term on the right side of Eq. (5.2.14) is a trim integrator which allows the pilot to bias the total elevator position using a three-position switch (pitch up, off, pitch down). Figure (5.9) indicates the variation of the short-period root as a function of the feedback gain K_1. It also indicates the upper limit imposed on the gain. The limit is necessary to avoid instabilities resulting from rate limiting of surface actuators. Substituting Eq. (5.2.14) into Eq. (5.2.2) and rearranging terms yields

$$\dot{\alpha} = q + \hat{p}_4 \alpha$$
$$\dot{q} = \hat{p}_1 \alpha + (\hat{p}_2 + \hat{p}_3 K_1) q + \hat{p}_3 (\delta_{e_{tr}} + K_2 \delta_s) \tag{5.2.15}$$

The characteristic equation of the system described by Eq. (5.2.15) is obtained as

$$\begin{vmatrix} s - \hat{p}_4 & -1 \\ -\hat{p}_1 & s - (\hat{p}_2 + \hat{p}_3 K_1) \end{vmatrix} = 0 \tag{5.2.16}$$

or

$$s^2 - (\hat{p}_2 + \hat{p}_4 + \hat{p}_3 K_1) s - \hat{p}_1 + \hat{p}_4 (\hat{p}_2 + \hat{p}_3 K_1) = 0 \tag{5.2.17}$$

therefore

$$2\zeta = -(\hat{p}_2 + \hat{p}_4 + \hat{p}_3 K_1) / \sqrt{-\hat{p}_1 + \hat{p}_4 (\hat{p}_2 + \hat{p}_3 K_1)} \tag{5.2.18}$$

Solving Eq. (5.2.18) for K_1 and substituting the requirement $\zeta = 0.7$ yields

$$K_1 = (-\hat{p}_2 - \sqrt{-2\hat{p}_1 - \hat{p}_4^2}) / \hat{p}_3 \tag{5.2.19}$$

Equation (5.2.19) comprises the control law and the parameters $\hat{p}_i$'s are substituted using Eq. (5.2.13). The C_i's, M and L used in Eq. (5.2.13) are the current contents of the memory for which the gain scheduling is computed. The results obtained for the longitudinal case are discussed in section 5.4.

5.3. The Real-Time Lateral LCS

For the lateral LCS the dynamics of the plant were used utilizing the existing NASA's real-time simulation of the six-degree-of-freedom dynamics of the F-8 DFBW aircraft. The simulator is described in reference (92). The six-degree-of-freedom nonlinear equations can also be

found in several textbooks (7,17). The simulation was mechanized using a CDC 6600 computer operating in real-time. The simulation code was arranged to be consistent with the F-8 DFBW capability in that data samples were taken at 0.125 second intervals.

The performance of the plant during simulated flight over a wide range of conditions is given in reference (61). It represents a simulated flight to examine the lateral system characteristics. In the run, zero-mean Gaussian noise was added to the sensor measurements. The noise levels were 0.67°/second for rate measurements and 0.67° for angular measurements. The control law was not engaged at time intervals during the run to determine the characteristics of the unaugmented vehicle. Noise was propagated to the aircraft surface commands only during times when the control laws were engaged.

To develop a LCS for the lateral dynamics, we first need to consider a model that characterizes the predominant lateral modes. Note that for implementing the LCS on a flight computer, the primary control loop processing is assigned high priority while the IAS and LAS are processed in a time available basis. This indicates that the IAS and LAS apply to data taken in the past during the same flight.

The model used for the lateral IAS has the form

$$\begin{aligned} \dot{p} &= \hat{p}_1 p + \hat{p}_2 \beta + \hat{p}_6 \delta_a + b\hat{p}_7 \delta_r \\ \dot{r} &= \hat{p}_4 r + \hat{p}_3 \beta + \hat{p}_7 \delta_r \\ \dot{\beta} &= -r + \hat{p}_5 \beta + a\hat{p}_7 \delta_r \end{aligned} \qquad (5.3.1)$$

where p is the roll rate, r is the yaw rate, β is the angle of sideslip and $\hat{p}_i$ are the parameter to be identified and processed by the learning

algorithm. The terms a and b are constants which depend on the moment arm of the vertical stabilizer. These constants were included in order to reduce the number of parameters that must be identified. Note that δ_r is the rudder actuator and δ_a is the aileron actuator.

The model assumed by Eq. (5.3.1) describes the lateral roll mode and the lateral Dutch roll mode. The lateral spiral mode was not modeled because its time constant is normally large and its identification is not possible with a short time span data base. Additionally, its consideration is not a major element in adjusting the feedback gains of the primary control loops.

For the real-time computation of Eq. (5.3.1) we again utilized a discrete-time approximation. The discrete-time approximation is based on the division of the time axis into time intervals of T = 0.125 sec. each. The response evaluated by discrete-time methods will be reasonably accurate since the time increment, T, is sufficiently small compared with the time constants of the system.

As shown in Appendix B, the difference equation representation of the model is obtained, as before, by Euler's method. (See Eq. 5.2.4).

For our model described by Eq. (5.3.1) we have

$$A = \begin{bmatrix} \hat{p}_1 & 0 & \hat{p}_2 \\ 0 & \hat{p}_4 & \hat{p}_3 \\ 0 & -1 & \hat{p}_5 \end{bmatrix}$$

$$B = \begin{bmatrix} \hat{p}_6 & b\hat{p}_7 \\ 0 & \hat{p}_7 \\ 0 & a\hat{p}_7 \end{bmatrix} \qquad (5.3.2)$$

Therefore, the real time computation of Eq. (5.3.2) is evaluated using the discrete-time system

$$\begin{bmatrix} p \\ r \\ \beta \end{bmatrix}_{k+1} = \begin{bmatrix} 1 + T\hat{p}_1 & 0 & T\hat{p}_2 \\ 0 & 1 + T\hat{p}_4 & T\hat{p}_3 \\ 0 & -T & 1 + T\hat{p}_5 \end{bmatrix} \times \begin{bmatrix} p \\ r \\ \beta \end{bmatrix}_k + \tag{5.3.3}$$

$$+ \begin{bmatrix} T\hat{p}_6 & Tb\hat{p}_7 \\ 0 & T\hat{p}_7 \\ 0 & Ta\hat{p}_7 \end{bmatrix} \times \begin{bmatrix} \delta_a \\ \delta_r \end{bmatrix}$$

For the lateral dynamics to implement the Newton-Raphson IAS, we used two separate performance indices. This was done to reduce the onboard computations. The cost function for the roll mode was

$$J_1(\hat{p}) = \tfrac{1}{2} \sum_{k=1}^{25} (\bar{p} - p)_k^2 \tag{5.3.4}$$

and is minimized over the $\hat{p}_1$, $\hat{p}_2$ and $\hat{p}_5$ variables. Note that $\bar{p}$ denotes the sensor measurements of the roll rate. For the Dutch roll mode the cost function was

$$J_2(\hat{p}) = \tfrac{1}{2} \left[\sum_{k=1}^{25} (\bar{\beta} - \beta)_k^2 b_{11} + \sum_{k=1}^{25} (\bar{r} - r)_k^2 b_{22} \right] \tag{5.3.5}$$

and was minimized over the $\hat{p}_3$, $\hat{p}_4$, $\hat{p}_5$ and $\hat{p}_7$ variables. Note that $\bar{\beta}$ and $\bar{r}$ are the sensor measurements of the sideslip angle and the yaw rate respectively.

The partitioning results in the requirement of inverting one

3 x 3 matrix and one 4 x 4 matrix as opposed to one 7 x 7 matrix in the Newton-Raphson algorithm. To apply the lateral IAS we need to compute $\partial J_1/\partial \hat{p}$, $\partial^2 J_1/\partial \hat{p}^2$, $\partial J_2/\partial \hat{p}$, $\partial^2 J_2/\partial \hat{p}^2$. This is done by differentiating Eqs. (5.3.4) and (5.3.5) with respect to $\hat{p}$ which yields

$$\partial J_1/\partial \hat{p} = -\sum_{k=1}^{25} \begin{bmatrix} (\bar{p} - p)_k \, (\partial p/\partial \hat{p}_1)_k \\ (\bar{p} - p)_k \, (\partial p/\partial \hat{p}_2)_k \\ (\bar{p} - p)_k \, (\partial p/\partial \hat{p}_6)_k \end{bmatrix} \tag{5.3.6}$$

and

$$\partial J_2/\partial \hat{p} = -\sum_{k=1}^{25} \begin{bmatrix} e_1 b_{11} (\partial \beta/\partial \hat{p}_3)_k + e_2 b_{22} (\partial r/\partial \hat{p}_3)_k \\ e_1 b_{11} (\partial \beta/\partial \hat{p}_4)_k + e_2 b_{22} (\partial r/\partial \hat{p}_4)_k \\ e_1 b_{11} (\partial \beta/\partial \hat{p}_5)_k + e_2 b_{22} (\partial r/\partial \hat{p}_5)_k \\ e_1 b_{11} (\partial \beta/\partial \hat{p}_7)_k + e_2 b_{22} (\partial r/\partial \hat{p}_7)_k \end{bmatrix} \tag{5.3.7}$$

where

$$\begin{aligned} e_1 &= \bar{\beta} - \beta \\ e_2 &= \bar{r} - r \end{aligned} \tag{5.3.8}$$

To obtain $\partial^2 J_1/\partial \hat{p}^2$ and $\partial^2 J_2/\partial \hat{p}^2$ we differentiate Eqs. (5.3.6) and (5.3.7) with respect to $\hat{p}$ and neglect the second order partials of the states with respect to $\hat{p}$. This yields the following equations for the elements of the above matrices

$$(\partial^2 J_1/\partial \hat{p}^2)_{11} = \sum_{k=1}^{25} (\partial p/\partial \hat{p}_1)_k^2$$

$$(\partial^2 J_1/\partial \hat{p}^2)_{12} = (\partial^2 J_1/\partial \hat{p}^2)_{21} = \sum_{k=1}^{25} (\partial p/\partial \hat{p}_1)_k (\partial p/\partial \hat{p}_2)_k$$

$$(\partial^2 J_1/\partial \hat{p}^2)_{13} = (\partial^2 J_1/\partial \hat{p}^2)_{31} = \sum_{k=1}^{25} (\partial p/\partial \hat{p}_1)_k (\partial p/\partial \hat{p}_6)_k$$

$$(\partial^2 J_1/\partial \hat{p}^2)_{22} = \sum_{k=1}^{25} (\partial p/\partial \hat{p}_2)_k^2 \qquad (5.3.9)$$

$$(\partial^2 J_1/\partial \hat{p}^2)_{23} = (\partial^2 J_1/\partial \hat{p}^2)_{32} = \sum_{k=1}^{25} (\partial p/\partial \hat{p}_2)_k (\partial p/\partial \hat{p}_6)_k$$

$$(\partial^2 J_1/\partial \hat{p}^2)_{33} = \sum_{k=1}^{25} (\partial p/\partial \hat{p}_6)_k^2$$

and

$$(\partial^2 J_2/\partial \hat{p}^2)_{11} = \sum_{k=1}^{25} b_{11} (\partial \beta/\partial \hat{p}_3)_k^2 + b_{22} (\partial r/\partial \hat{p}_3)_k^2$$

$$(\partial^2 J_2/\partial \hat{p}^2)_{12} = (\partial^2 J_2/\partial \hat{p}^2)_{21} = \sum_{k=1}^{25} b_{11} (\partial \beta/\partial \hat{p}_3)_k (\partial \beta/\partial \hat{p}_4)_k +$$

$$+ b_{22} (\partial r/\partial \hat{p}_3)_k (\partial r/\partial \hat{p}_4)_k$$

$$(\partial^2 J_2/\partial \hat{p}^2)_{13} = (\partial^2 J_2/\partial \hat{p}^2)_{31} = \sum_{k=1}^{25} b_{11} (\partial \beta/\partial \hat{p}_3)_k (\partial \beta/\partial \hat{p}_5)_k +$$

$$+ b_{22} (\partial r/\partial \hat{p}_3)_k (\partial r/\partial \hat{p}_5)_k$$

$$(\partial^2 J_2/\partial \hat{p}^2)_{14} = (\partial^2 J_2/\partial \hat{p}^2)_{41} = \sum_{k=1}^{25} b_{11} (\partial \beta/\partial \hat{p}_3)_k (\partial \beta/\partial \hat{p}_7)_k +$$

$$+ b_{22} (\partial r/\partial \hat{p}_3)_k (\partial r/\partial \hat{p}_7)_k \qquad (5.3.10)$$

$$(\partial^2 J_2/\partial \hat{p}^2)_{22} = \sum_{k=1}^{25} b_{11} (\partial \beta/\partial \hat{p}_4)_k^2 + b_{22} (\partial r/\partial \hat{p}_4)_k^2$$

$$(\partial^2 J_2/\partial \hat{p}^2)_{23} = (\partial^2 J_2/\partial \hat{p}^2)_{32} = \sum_{k=1}^{25} b_{11} (\partial \beta/\partial \hat{p}_4)_k (\partial \beta/\partial \hat{p}_5)_k +$$

$$+ b_{22} (\partial r/\partial \hat{p}_4)_k (\partial r/\partial \hat{p}_5)_k$$

$$(\partial^2 J_2/\partial \hat{p}^2)_{24} = (\partial^2 J_2/\partial \hat{p}^2)_{42} = \sum_{k=1}^{25} b_{11}(\partial \beta/\partial \hat{p}_4)_k(\partial \beta/\partial \hat{p}_7)_k +$$

$$+ b_{22}(\partial r/\partial \hat{p}_4)_k(\partial r/\partial \hat{p}_7)_k$$

$$(\partial^2 J_2/\partial \hat{p}^2)_{33} = \sum_{k=1}^{25} b_{11}(\partial \beta/\partial \hat{p}_5)_k^2 + b_{22}(\partial r/\partial \hat{p}_5)_k^2$$

$$(\partial^2 J_2/\partial \hat{p}^2)_{34} = (\partial^2 J_2/\partial \hat{p}^2)_{43} = \sum_{k=1}^{25} b_{11}(\partial \beta/\partial \hat{p}_5)_k(\partial \beta/\partial \hat{p}_7)_k +$$

$$+ b_{22}(\partial r/\partial \hat{p}_5)_k(\partial r/\partial \hat{p}_7)_k$$

$$(\partial^2 J_2/\partial \hat{p}^2)_{44} = \sum_{k=1}^{25} b_{11}(\partial \beta/\partial \hat{p}_7)_k^2 + b_{22}(\partial r/\partial \hat{p}_7)_k^2$$

To compute the sensitivities involved in Eqs. (5.3.6) and (5.3.9) let us differentiate the first equation of the Eq. set (5.3.3) with respect to $\hat{p}_1$, $\hat{p}_2$ and $\hat{p}_6$. This yields

$$(\partial p/\partial \hat{p}_1)_{k+1} = (1 + T\hat{p}_1)(\partial p/\partial \hat{p}_1)_k + Tp$$

$$(\partial p/\partial \hat{p}_2)_{k+1} = (1 + T\hat{p}_1)(\partial p/\partial \hat{p}_2)_k + T\beta \qquad (5.3.11)$$

$$(\partial p/\partial \hat{p}_6)_{k+1} = (1 + T\hat{p}_1)(\partial p/\partial \hat{p}_6)_k + T\delta_a$$

In the same fashion we differentiate the last two equations of the Eq. set (5.3.3) with respect to $\hat{p}_3$, $\hat{p}_4$, $\hat{p}_5$ and $\hat{p}_7$ to compute the sensitivities involved in Eqs. (5.3.7) and (5.3.10). This yields

$$(\partial r/\partial \hat{p}_3)_{k+1} = (1 + T\hat{p}_4)(\partial r/\partial \hat{p}_3)_k + T\hat{p}_3(\partial \beta/\partial \hat{p}_3)_k + T\beta$$

$$(\partial r/\partial \hat{p}_4)_{k+1} = (1 + T\hat{p}_4)(\partial r/\partial \hat{p}_4)_k + T\hat{p}_3(\partial \beta/\partial \hat{p}_4)_k + Tr$$

$$(\partial r/\partial \hat{p}_5)_{k+1} = (1 + T\hat{p}_4)(\partial r/\partial \hat{p}_5)_k + T\hat{p}_3(\partial\beta/\partial \hat{p}_5)_k$$

$$(\partial r/\partial \hat{p}_7)_{k+1} = (1 + T\hat{p}_7)(\partial r/\partial \hat{p}_7)_k + T\hat{p}_3(\partial\beta/\partial \hat{p}_7)_k + T\delta_r$$

$$(\partial\beta/\partial \hat{p}_3)_{k+1} = -T(\partial r/\partial \hat{p}_3)_k + (1 + T\hat{p}_5)(\partial\beta/\partial \hat{p}_3)_k \qquad (5.3.12)$$

$$(\partial\beta/\partial \hat{p}_4)_{k+1} = -T(\partial r/\partial \hat{p}_4)_k + (1 + T\hat{p}_5)(\partial\beta/\partial \hat{p}_4)_k$$

$$(\partial\beta/\partial \hat{p}_5)_{k+1} = -T(\partial r/\partial \hat{p}_5)_k + (1 + T\hat{p}_5)(\partial\beta/\partial \hat{p}_5)_k + T\beta$$

$$(\partial\beta/\partial \hat{p}_7)_{k+1} = -T(\partial r/\partial \hat{p}_7)_k + (1 + T\hat{p}_5)(\partial\beta/\partial \hat{p}_7)_k + Ta\delta_r$$

After the first and second partials of the fit errors J_1 and J_2 given by Eqs. (5.3.6 - 5.3.10) are computed with respect to the parameters $\hat{p}_i$, the parameters $\hat{p}_1$, $\hat{p}_2$ and $\hat{p}_6$ are adjusted by the following

$$\hat{p}_{j+1} = \hat{p}_j - (\partial^2 J_1/\partial \hat{p}^2)^{-1}_j (\partial J_1/\partial \hat{p})_j \qquad (5.3.13)$$

and the parameters $\hat{p}_3$, $\hat{p}_4$, $\hat{p}_5$ and $\hat{p}_7$ are adjusted by

$$\hat{p}_{j+1} = \hat{p}_j - (\partial^2 J_2/\partial \hat{p}^2)^{-1}_j (\partial J_2/\partial \hat{p})_j \qquad (5.3.14)$$

The information content of the data base is considered to be adequate for adjusting the paramerers if the determinants of $(\partial^2 J_1/\partial \hat{p}^2)$ and $(\partial^2 J_2/\partial \hat{p}^2)$ are higher than 10^{-8}. This number was determined, as in the longitudinal case, by examining the variation of the two determinants on the real time computer during steady-state operation of the system with no input signal applied. Another test performed by the convergence criterion was to limit the number of iterations over any data-base up to 8.

The fit errors J_1 and J_2 were checked to be lower than 1 and the gradient vectors $(\partial J_1/\partial \hat{p})$ and $(\partial J_2/\partial \hat{p})$ were checked to have Euclidean norm lower than 3×10^{-4}. Finally, the maximum allowable covariance of all the lateral parameters $\hat{p}_1$ through $\hat{p}_7$ was set to be 200. This number was chosen experimentally using the real time computer at NASA. When these tests were satisfied, the parameter vector $\hat{p}$ was passed to the Learning Algorithm Subsystem (LAS).

For the lateral application of the LAS, the relationship between the parameters $\hat{p}_i$'s as a function of mach number M and altitude L was represented by second order polynomials. This relationship is given by

$$\begin{aligned}
\hat{p}_1(M,L) &= C_1 + C_2M + C_3L + C_4M\,L + C_5M^2 + C_6L^2 \\
\hat{p}_2(M,L) &= C_7 + C_8M + C_9L + C_{10}M\,L + C_{11}M^2 + C_{12}L^2 \\
\hat{p}_3(M,L) &= C_{13} + C_{14}M + C_{15}L + C_{16}M\,L + C_{17}M^2 + C_{18}L^2 \\
\hat{p}_4(M,L) &= C_{19} + C_{20}M + C_{21}L + C_{22}M\,L + C_{23}M^2 + C_{24}L^2 \\
\hat{p}_5(M,L) &= C_{25} + C_{26}M + C_{27}L + C_{28}M\,L + C_{29}M^2 + C_{30}L^2 \\
\hat{p}_6(M,L) &= C_{31} + C_{32}M + C_{33}L + C_{34}M\,L + C_{35}M^2 + C_{36}L^2 \\
\hat{p}_7(M,L) &= C_{37} + C_{38}M + C_{39}L + C_{40}M\,L + C_{41}M^2 + C_{42}L^2
\end{aligned} \tag{5.3.15}$$

The LAS then produces the coefficient vector C by the iterative application of Eqs. (3.4.14) and (3.4.16). The obtained C_i's are then passed to the Memory and Control Process Subsystem (MCPS).

The design criterion selected for the lateral characteristics of the Dutch roll mode was to maintain the damping coefficient of 0.7 of

critical damping independent of frequency. To meet this criterion the rudder control was chosen in the following form:

$$\zeta_r = K_3 r + K_4 \zeta_s \tag{5.3.16}$$

Substituting Eq. (5.3.16) into the last two equations of Eq. set (5.3.1) yields

$$\begin{aligned} \dot{r} &= (\hat{p}_4 + \hat{p}_7 K_3) r + \hat{p}_3 \beta + \hat{p}_7 K_4 \zeta_s \\ \dot{\beta} &= (-1 + a\,\hat{p}_7 K_3) r + \hat{p}_5 \beta + a\,\hat{p}_7 K_4 \zeta_s \end{aligned} \tag{5.3.17}$$

The characteristic equation of the system described by Eq. (5.3.17) is obtained as

$$\begin{vmatrix} s - (\hat{p}_4 + \hat{p}_7 K_3) & -\hat{p}_3 \\ 1 - a\hat{p}_7 K_3 & s - \hat{p}_5 \end{vmatrix} = 0 \tag{5.3.18}$$

or

$$s^2 - (\hat{p}_4 + \hat{p}_5 + \hat{p}_7 K_3)\, s + \hat{p}_3 (1 - a\hat{p}_7 K_3) = 0 \tag{5.3.19}$$

therefore

$$2\zeta = -(\hat{p}_4 + \hat{p}_5 + \hat{p}_7 K_3) / \sqrt{\hat{p}_3 (1 - a\hat{p}_7 K_3)} \tag{5.3.20}$$

Taking the square of both sides of Eq. (5.3.20), substituting for $\zeta = \sqrt{2}/2 \cong 0.7$ and rearranging terms yields

$$\hat{p}_7^2 K_3^2 + 2\hat{p}_7 \left[\hat{p}_4 + \hat{p}_3 (1 + a)\right] K_3 + (\hat{p}_4 + \hat{p}_5)^2 - 2\hat{p}_3 = 0 \tag{5.3.21}$$

The solution of Eq. (5.3.21) for K_3 that provides positive damping is taken, and this comprises the control law for the Dutch roll mode. For

the lateral characteristics of the roll mode, the design criterion was to keep the roll mode time constant at 0.2 sec. and to maintain uniform maneuver effectiveness of the lateral stick in producing roll rate[61]. To meet this criterion, the aileron control was chosen in the following form

$$\delta_a = K_5\, p + k_6 \delta_s \tag{5.3.22}$$

Substituting Eq. (5.3.22) into the first equation of Eq. set (5.3.1) yields

$$\dot{p} = (\hat{p}_1 + \hat{p}_6 K_5)\, p + \hat{p}_2 \beta + \hat{p}_6 K_6 \delta_s + b\hat{p}_7 \delta_r \tag{5.3.23}$$

For this first order system the time constant is given by

$$\tau = -1/(\hat{p}_1 + \hat{p}_6 K_5) = 0.2 \tag{5.3.24}$$

Solving Eq. (5.3.24) for K_5 yields

$$K_5 = -(5 + \hat{p}_1)/\hat{p}_6 \tag{5.3.25}$$

The lateral stick control effectiveness is required to be 5, therefore

$$K_6 = 5/\hat{p}_6 \tag{5.3.26}$$

By this choice, the maximum lateral stick deflection will produce 2π rad/sec. roll rate[61]. Eqs. (5.3.25) and (5.3.26) comprise the control law for the roll mode. The way to evaluate the control law which consists of the solution of Eq. (5.3.21) and Eqs. (5.3.25) and (5.3.26) is to substitute for the parameters $\hat{p}_i$'s using Eq. (5.3.15). The C_i's used in Eq. (5.3.15) are the current contents of the memory and M and L are the values of mach number and altitude for which the gain scheduling is computed, respectively. In the next section we present and

discuss the results obtained for the longitudinal and the lateral cases.

5.4. Results and Discussion

The learning control system was applied to the six-degree-of-freedom real-time simulation of the F-8 DFBW aircraft on NASA, Langley's CDC 6600 computer.

The results shown in Figs. 5.1 - 5.3 illustrate the learning of p_1, p_2 and p_3 of the longitudinal dynamics at sea level altitude over a range of Mach numbers M = .3 to M = .9 based on continuous flight as indicated by the Mach number and altitude time histories, shown in Fig. 5.4 (a,b). The associated angle of attack, pitch rate, elevator command, and pilot's command are shown in Fig. 5.4 (c,d,e,f). Figure 5.4 (g,h,i, j,k) shows the time histories of the variables associated with the convergence criterion during the same flight course. The convergence criterion consists of the monitoring of the values of the performance index (Fig. 5.4 (g)), the determinant of the information matrix (Fig. 5.4 (h)), and the three diagonal elements of the information matrix after it has been inverted (Fig. 5.4 (i,j,k)). When the determinant of the information matrix is low there is no information in the processed data base. In the portions of time when the determinant has high values, only then can we iterate through the Newton-Raphson algorithm and this corresponds to some control activity as indicated by the pilot command and the elevator command. Note that the diagonal elements of the inverse of the information matrix have low values when the determinant is high and high values when the determinant is low, as would be expected. The performance index has low values except at the final portion of time where the states of the aircraft are highly excited as shown by the angle of attack time history. This indicates that the model does not match the plant dynamics for big

perturbations since the model describes only some linearized modes of the dynamics. Note that the descending steps of the performance index result from the updating of the parameters done in the Newton-Raphson algorithm.

The learned curves shown in Figs. 5.5 - 5.7 illustrate the learning of p_1, p_2 and p_7 of the lateral dynamics at sea level altitude over a range of Mach numbers M = .3 to M = .8880 based on continuous flight as indicated by the Mach number and altitude time histories shown in Fig. 5.8 (a,b). The associated states of the Dutch roll mode, sideslip angle and yaw rate, are shown in Fig. 5.8 (c,d), and the rudder command is shown in Fig. 5.8 (e). The roll rate and the aileron command are shown in Fig. 5.8 (f,g). Finally, Fig. 5.8 (h) shows the determinant of the information matrix. Note that the determinant has high values only during periods of control activity. Although the flight was continuous, learning of the parameters has occurred only for particular flight conditions selected by the convergence criterion when it was satisfied.

The learned curves shown in Figs. 5.10 - 5.13 describe the learning of the longitudinal parameters p_1, p_2, p_3 and p_4 as a function of both, altitude and mach number (L,M) over the entire flight envelope. These curves are also based on continuous flight as shown in Fig. 5.4 (a,b). Note that the grid interval of those three dimensional curves is 5,000 ft. for altitude and .05 for mach number. Another interesting observation is that the intersection of the three dimensional curves with the plane L = 0 corresponds to the two dimensional curves shown in Figs. 5.1 - 5.3.

The learned curves shown in Figs. 5.14 - 5.20 describe the learning of the lateral parameters p_1 through p_7 over the entire flight

envelope based on continuous flight as shown in Fig. 5.8 (a,b).

In order to evaluate the performance of the learning control system, we computed from the real-time simulator the values of the partial derivatives of the moment with respect to angle of attack α, pitch rate q and elevator deflection δ_e (M_α, M_q, M_{δ_e}). The time histories of these partial derivatives during a flight as indicated by the mach number and altitude in Fig. 5.21 (a,b) are shown in Figs. 5.21 (h,i,j). The variation of the partial derivative of the lift with respect to angle of attack α (L_α) during the same flight is shown in Fig. 5.21 (k). The associated learned parameters (p_1, p_2, p_3 and p_4) are shown in Figs. 5.21 (d,e,f,g). It is interesting to note that the learned parameter p_1 does not have the spikes depicted by the real-time M_α since these spikes are due to elevator variations and in our learning control system we restricted p_1 to be a function only of mach number and altitude. Another observation is that the cost function (J) shown in Fig. 5.21 (c) has high values initially, meaning that the model is misaligned substantially from the plant. This is true if we note that p_2 initially has positive values where the real-time M_q is negative. As soon as an identification occurs p_2 has negative values and the cost function (J) is reduced.

The same comparisons are possible also for the lateral case, but were not carried out due to enormous additional amount of simulations.

In the next chapter we summarize the development of the learning control system as presented in this dissertation and present the final conclusions.

Fig. 5.1 LONG. PI VS. MACH

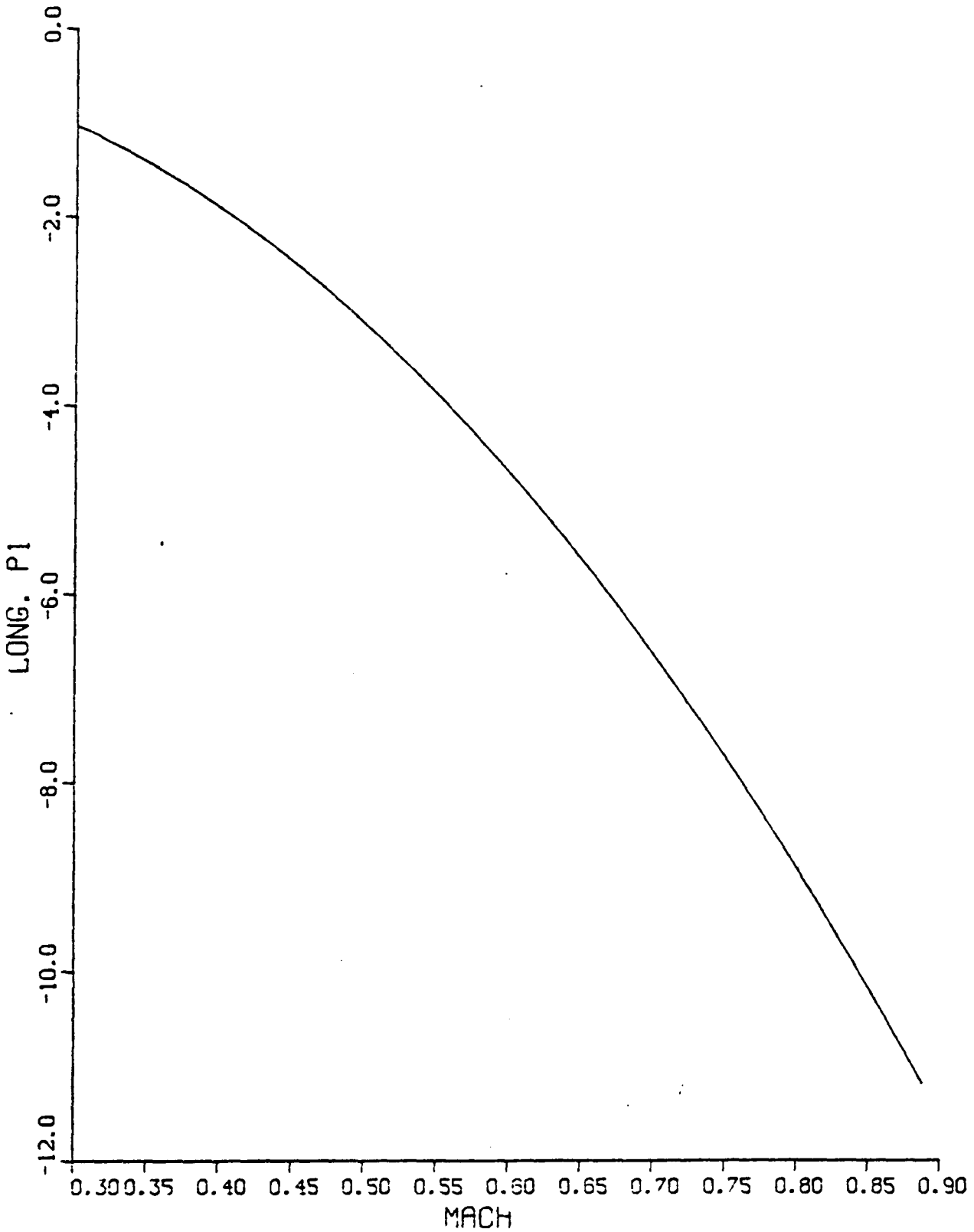

Fig. 5.2 LONG. P2 VS. MACH

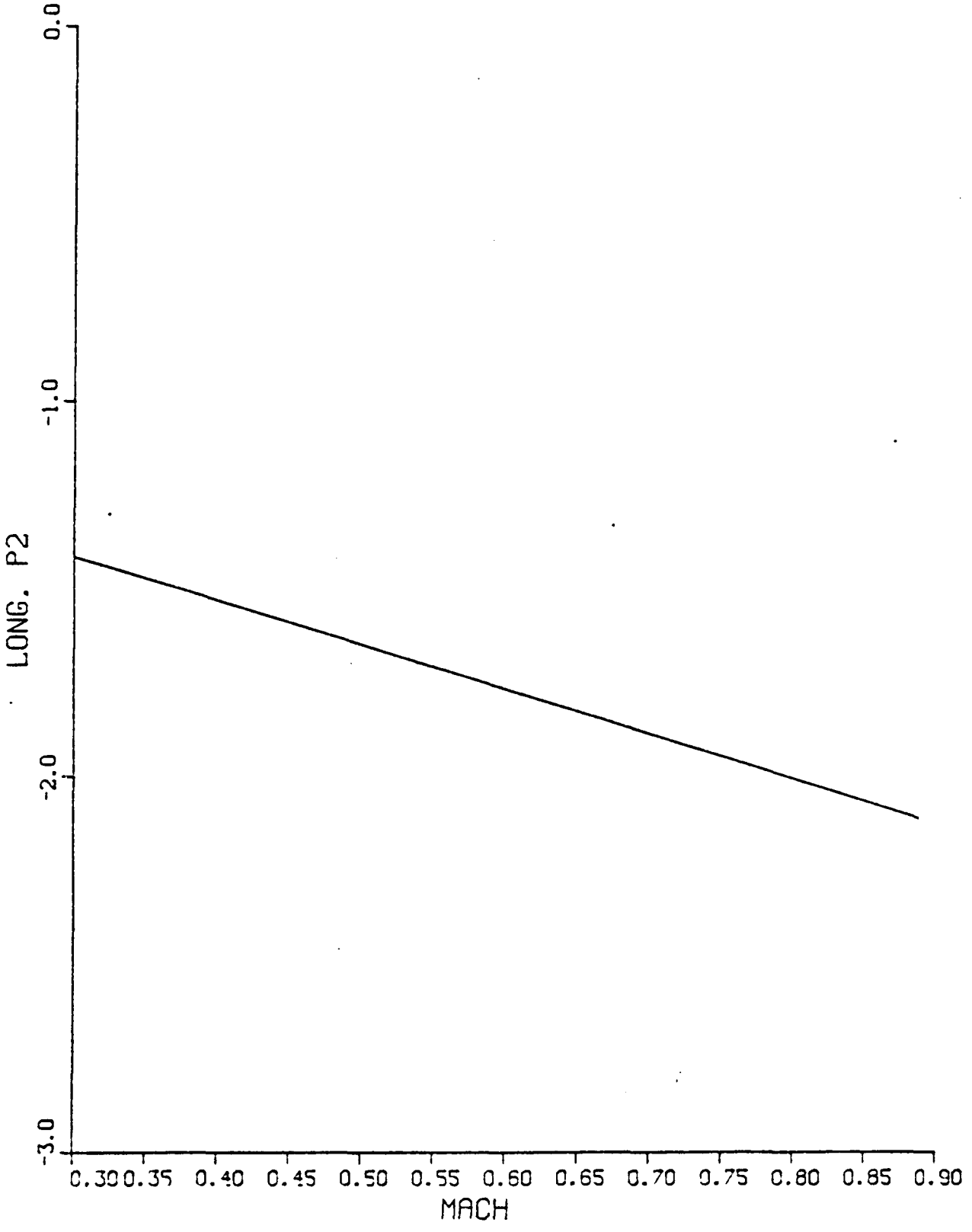

Fig. 5.3 LONG. P3 VS. MACH

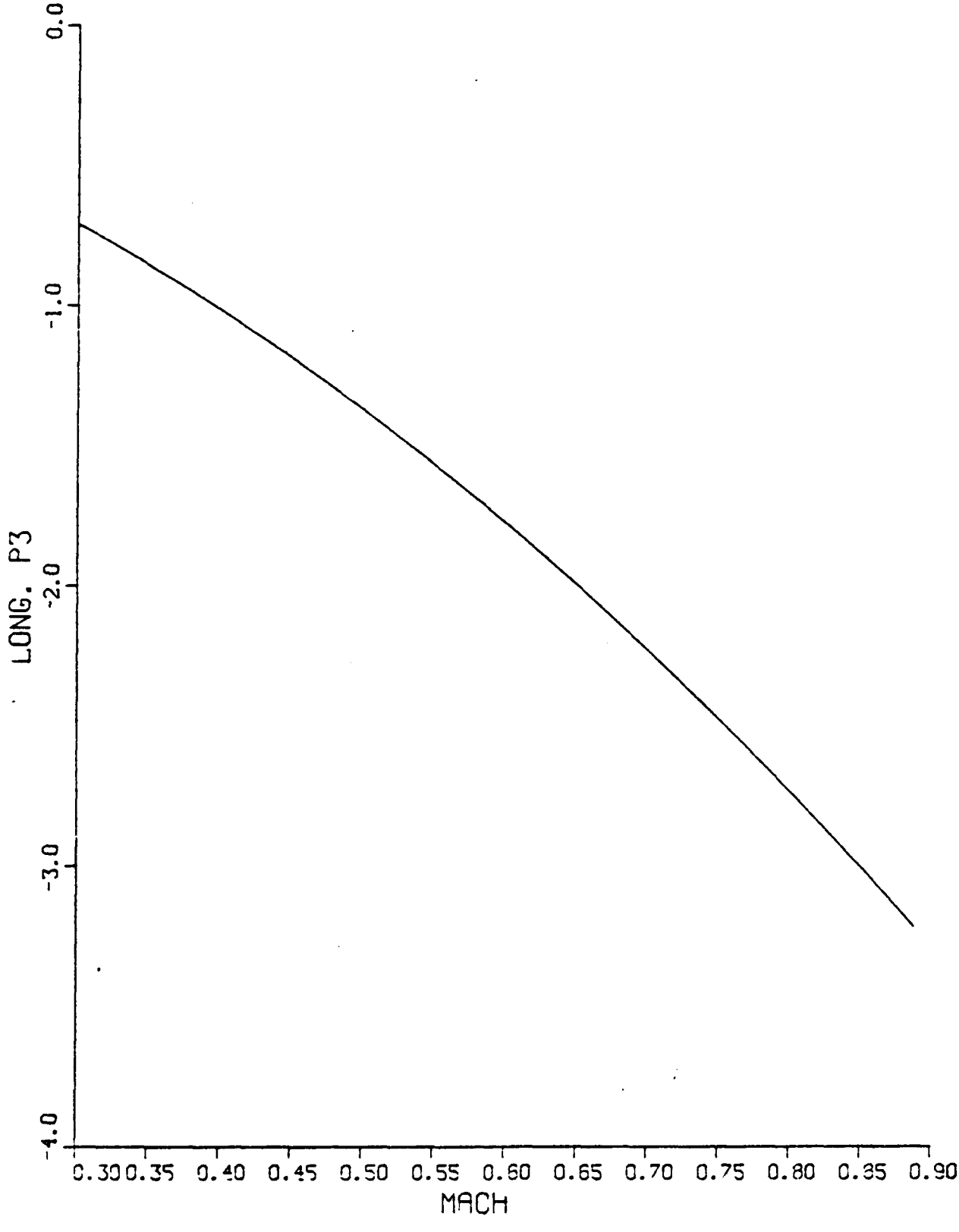

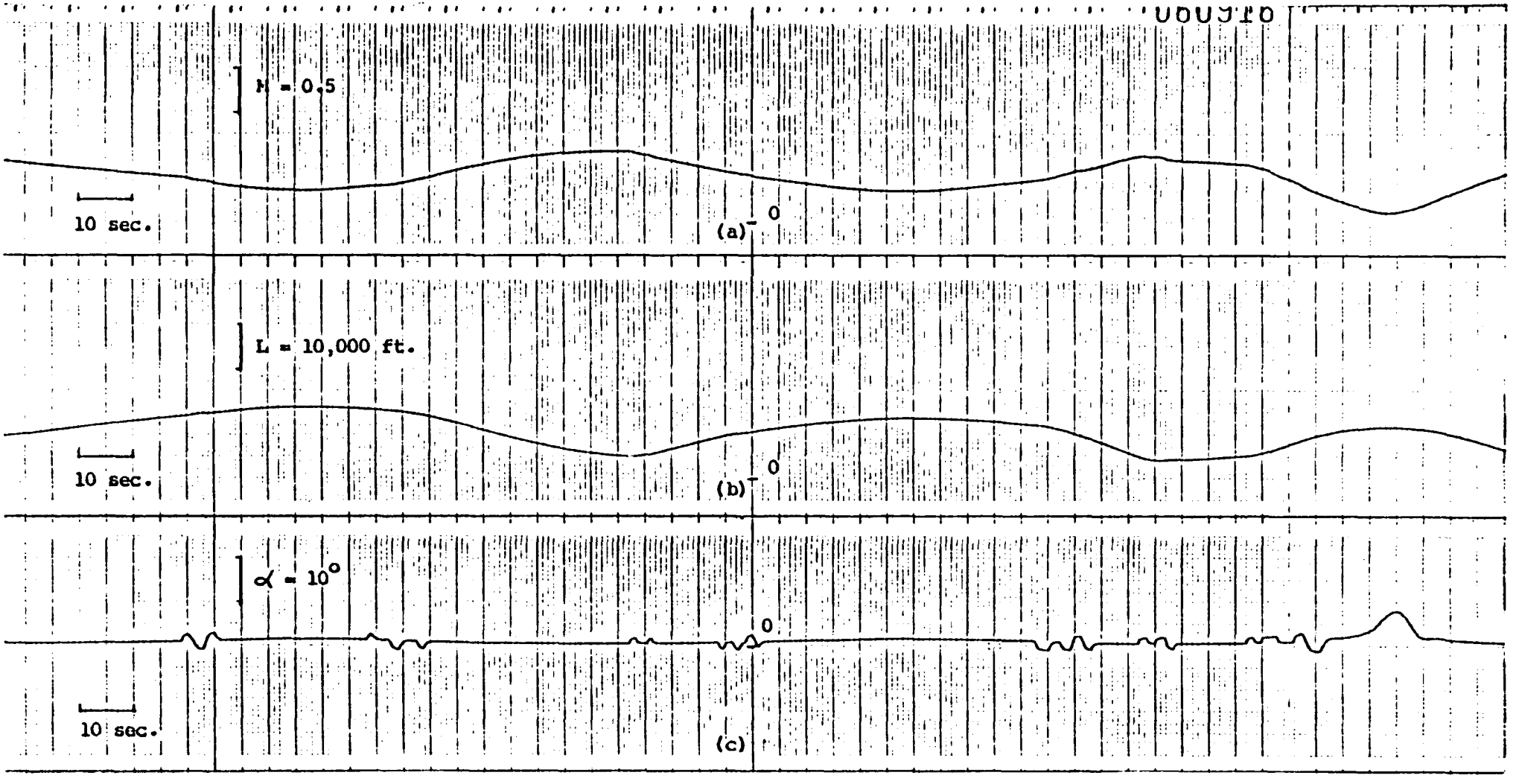

Fig. 5.4 Real-time simulation time histories of the longitudinal dynamics of F-8 DFBW aircraft (a) mach number (b) altitude (c) angle of attack.

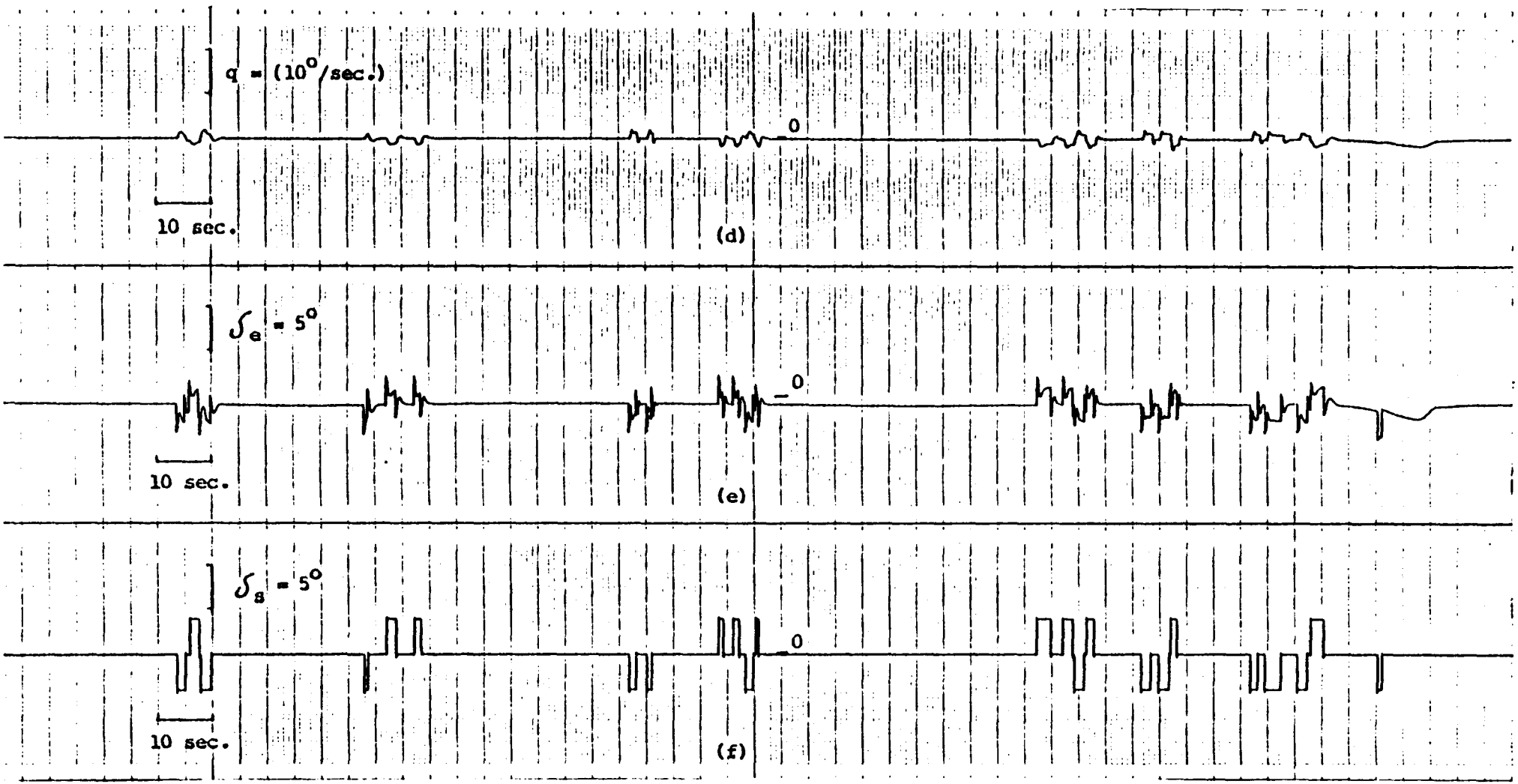

Fig. 5.4 continued: (d) pitch rate (e) elevator command (f) pilot's command.

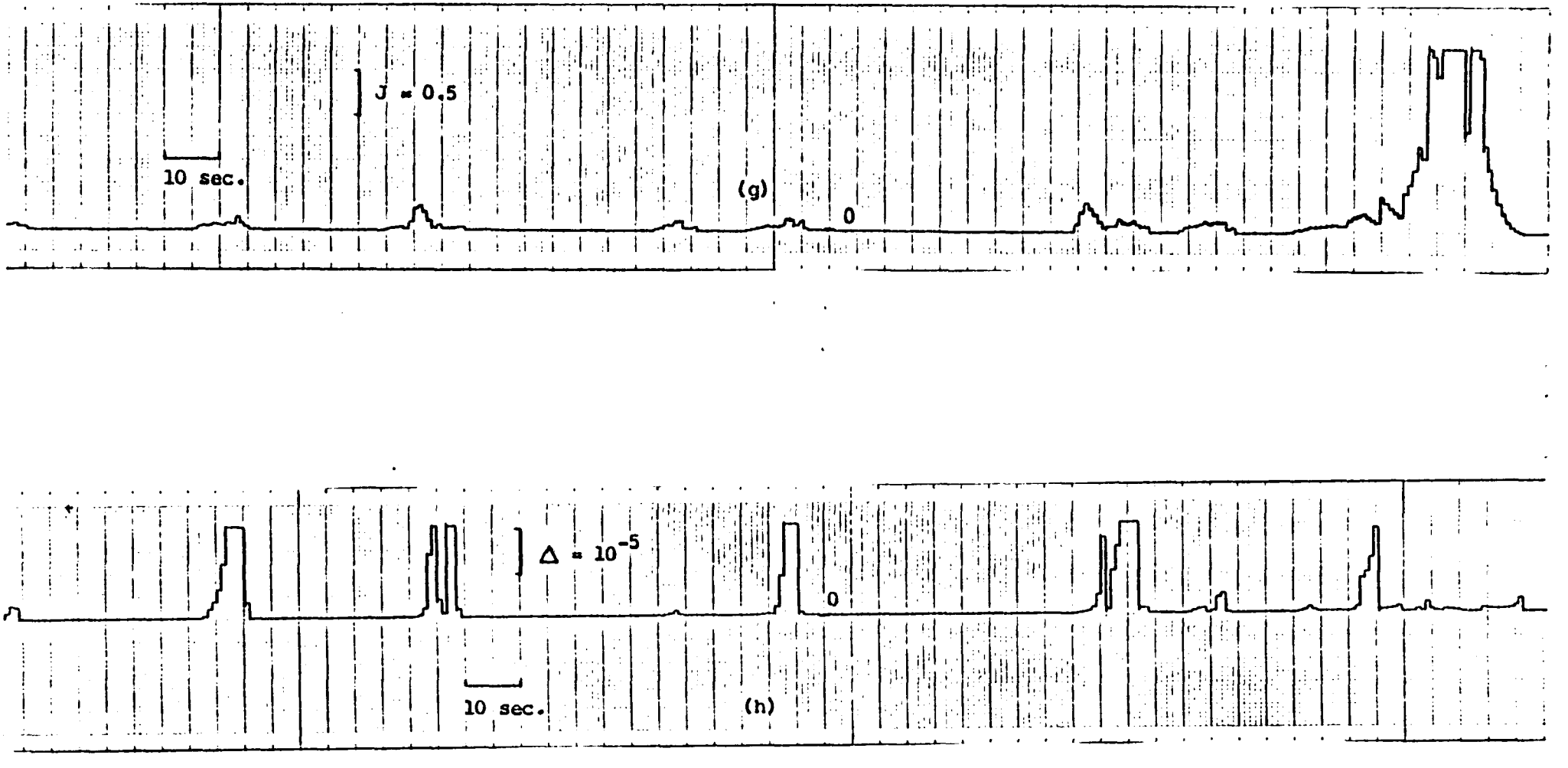

Fig. 5.4 continued: (g) performance index (h) determinant of the information matrix.

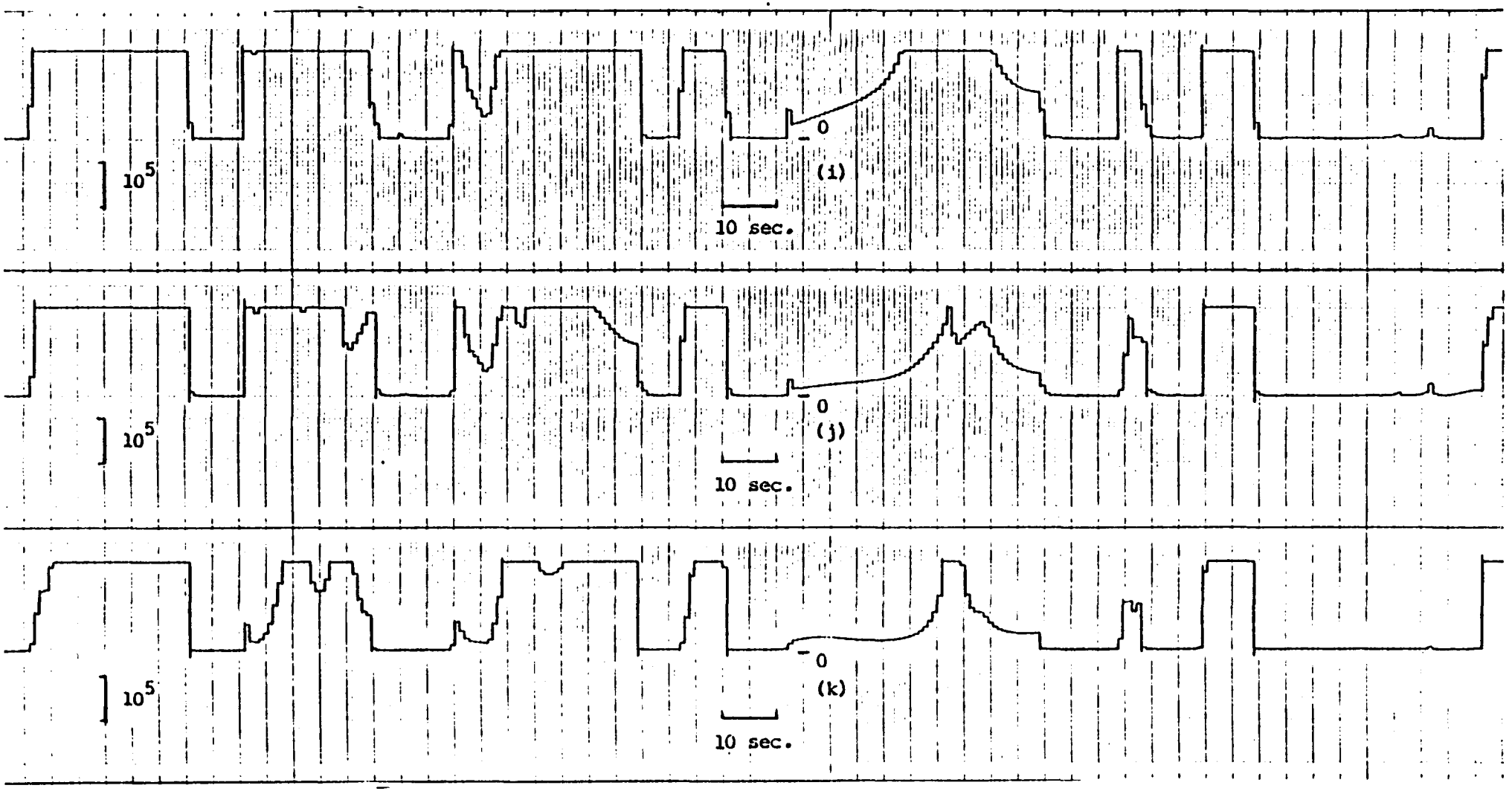

Fig. 5.4 continued: (i,j,k) the three diagonal elements of the inverted information matrix.

Fig. 5.5 LATR. P1 VS. MACH

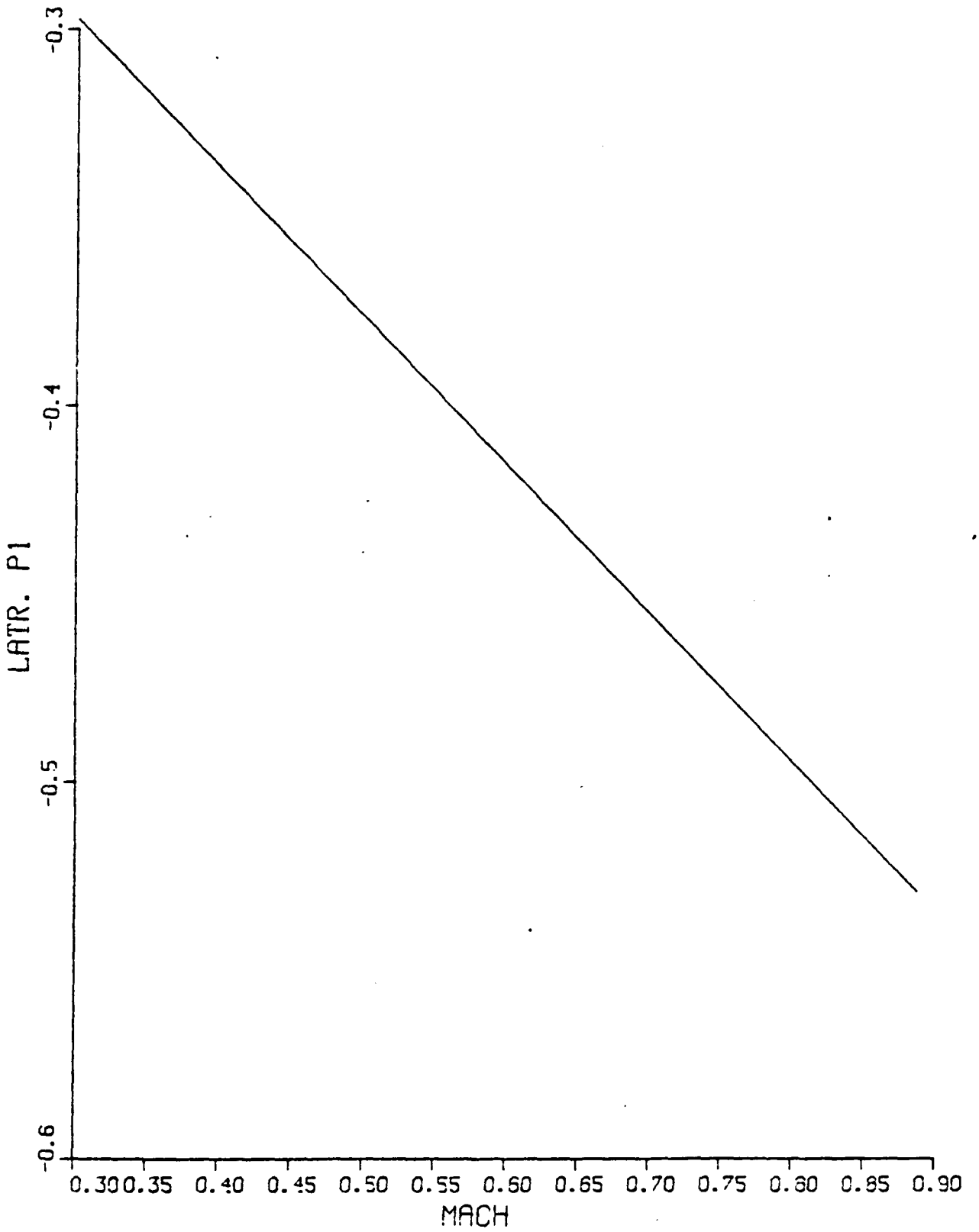

Fig. 5.6 LATR. P2 VS. MACH

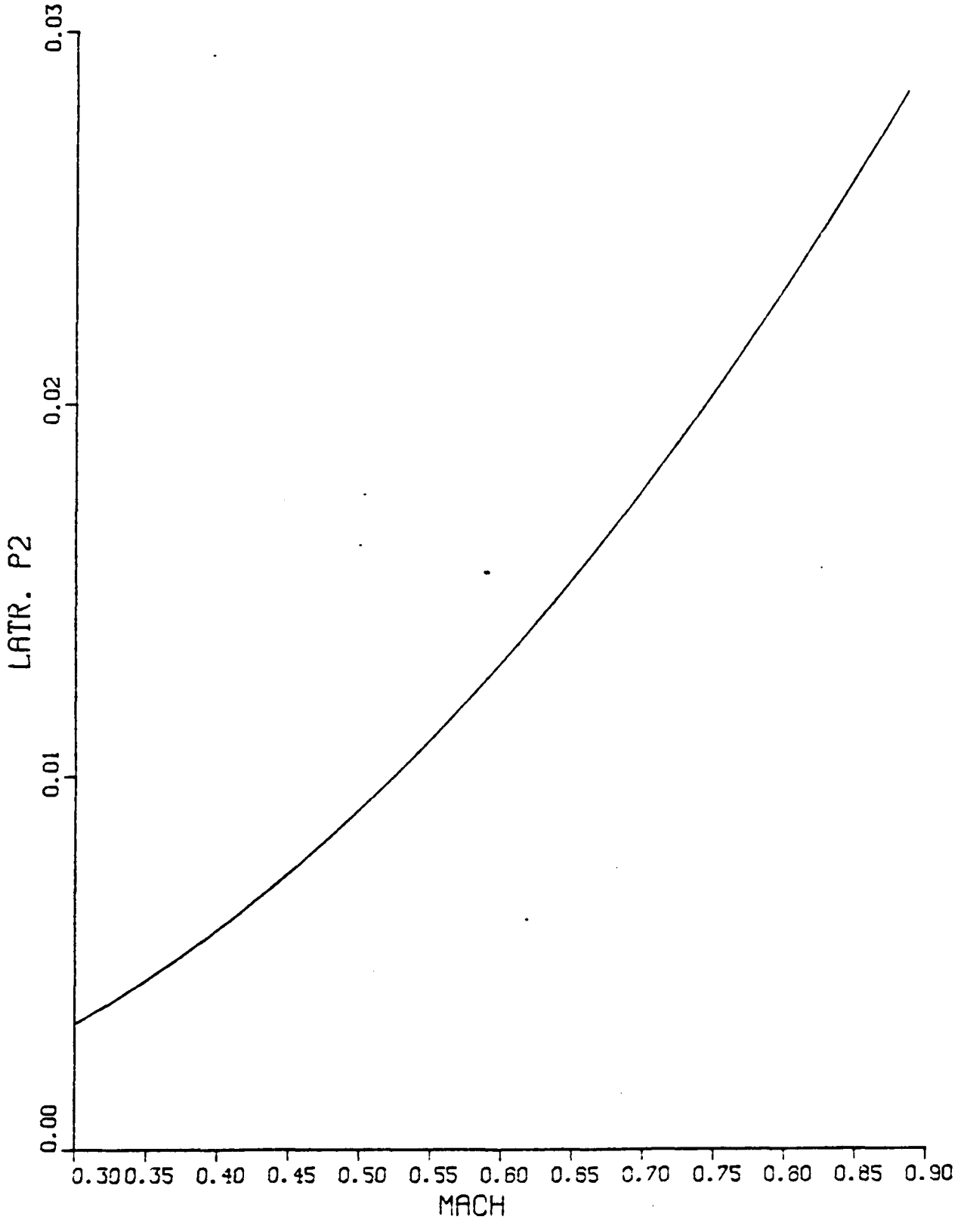

Fig. 5.7 LATR. P7 VS. MACH

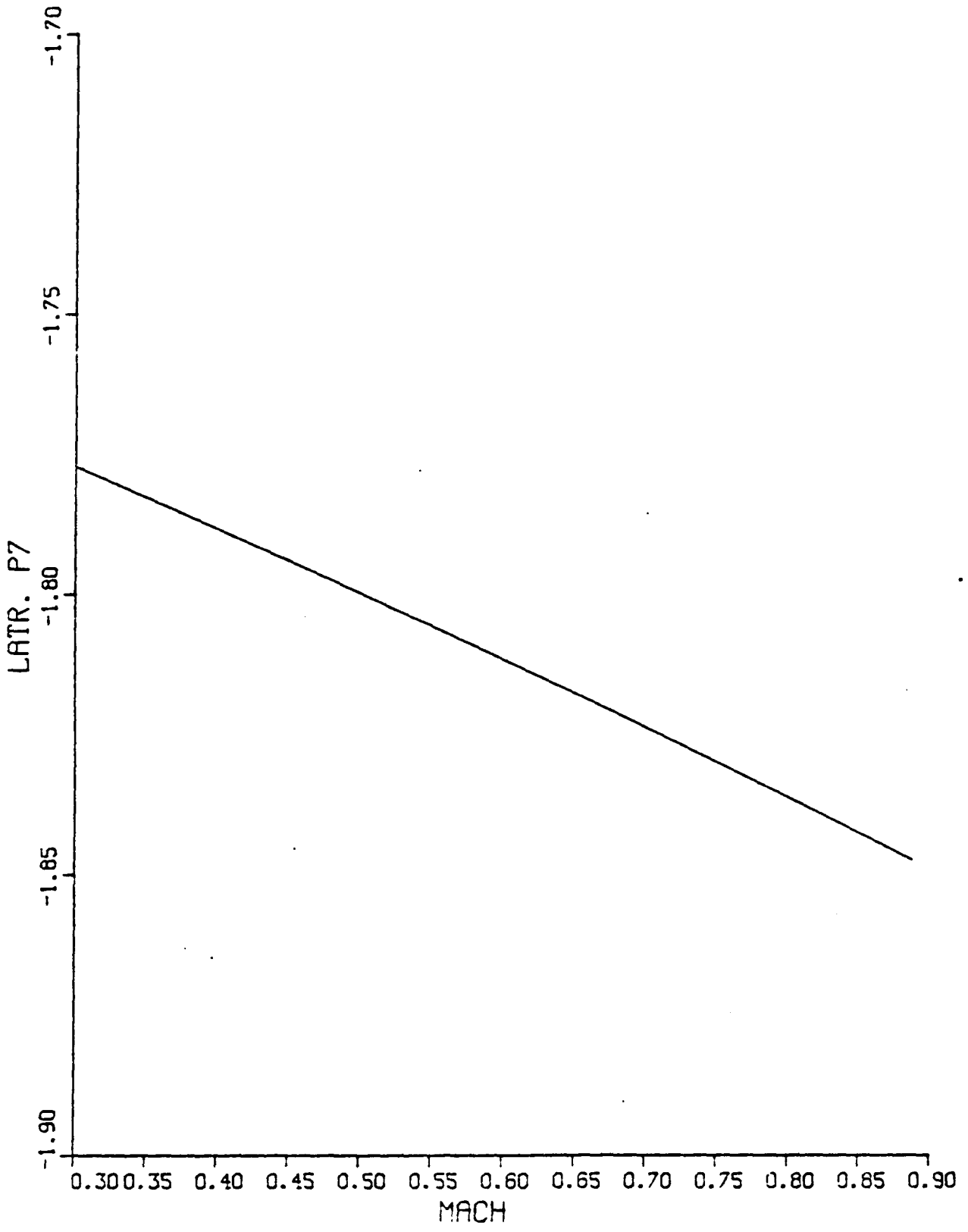

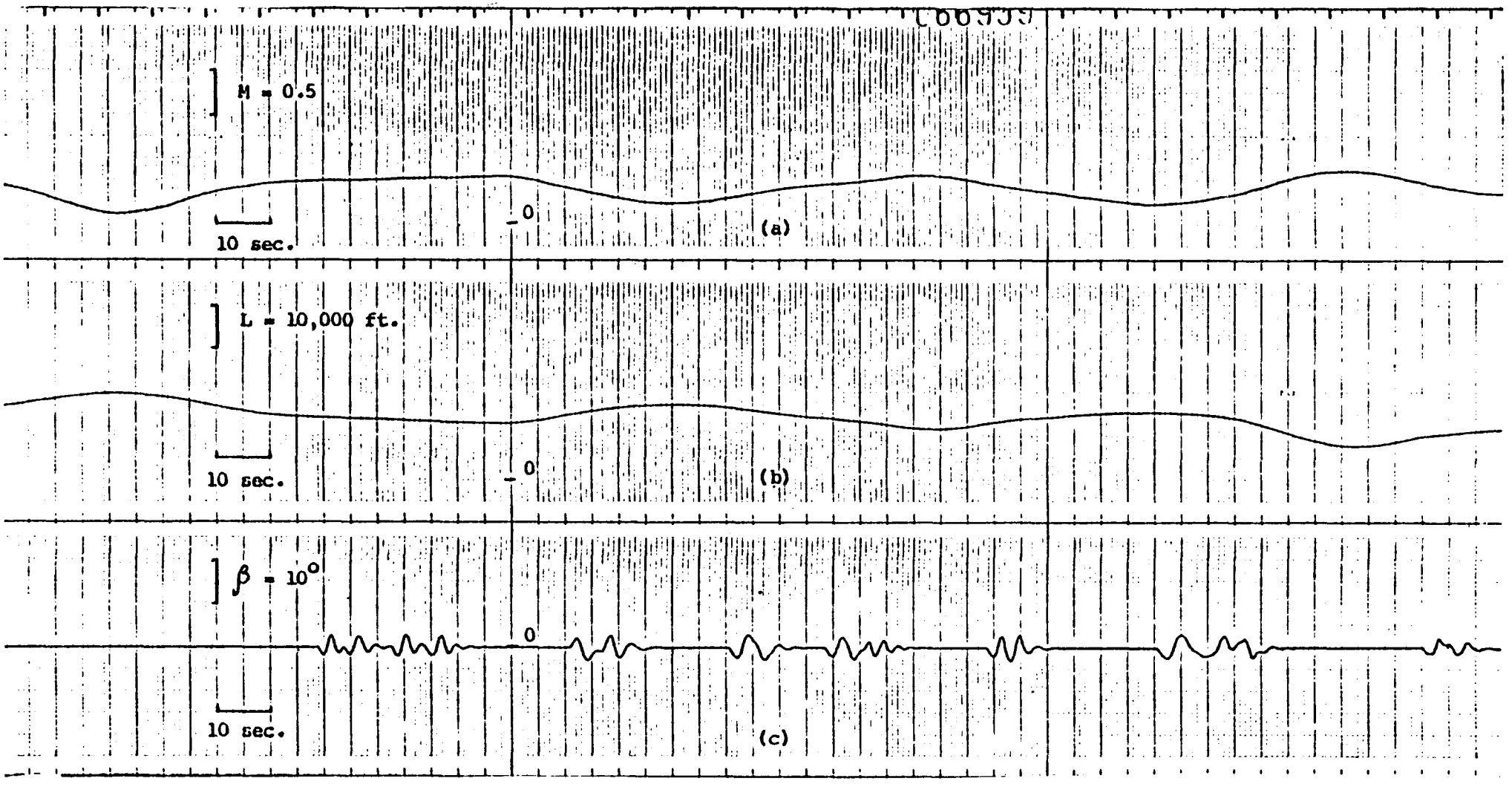

Fig. 5.8 Real-time simulation time histories of the lateral dynamics of F-8 DFBW aircraft
(a) mach number (b) altitude (c) sideslip angle.

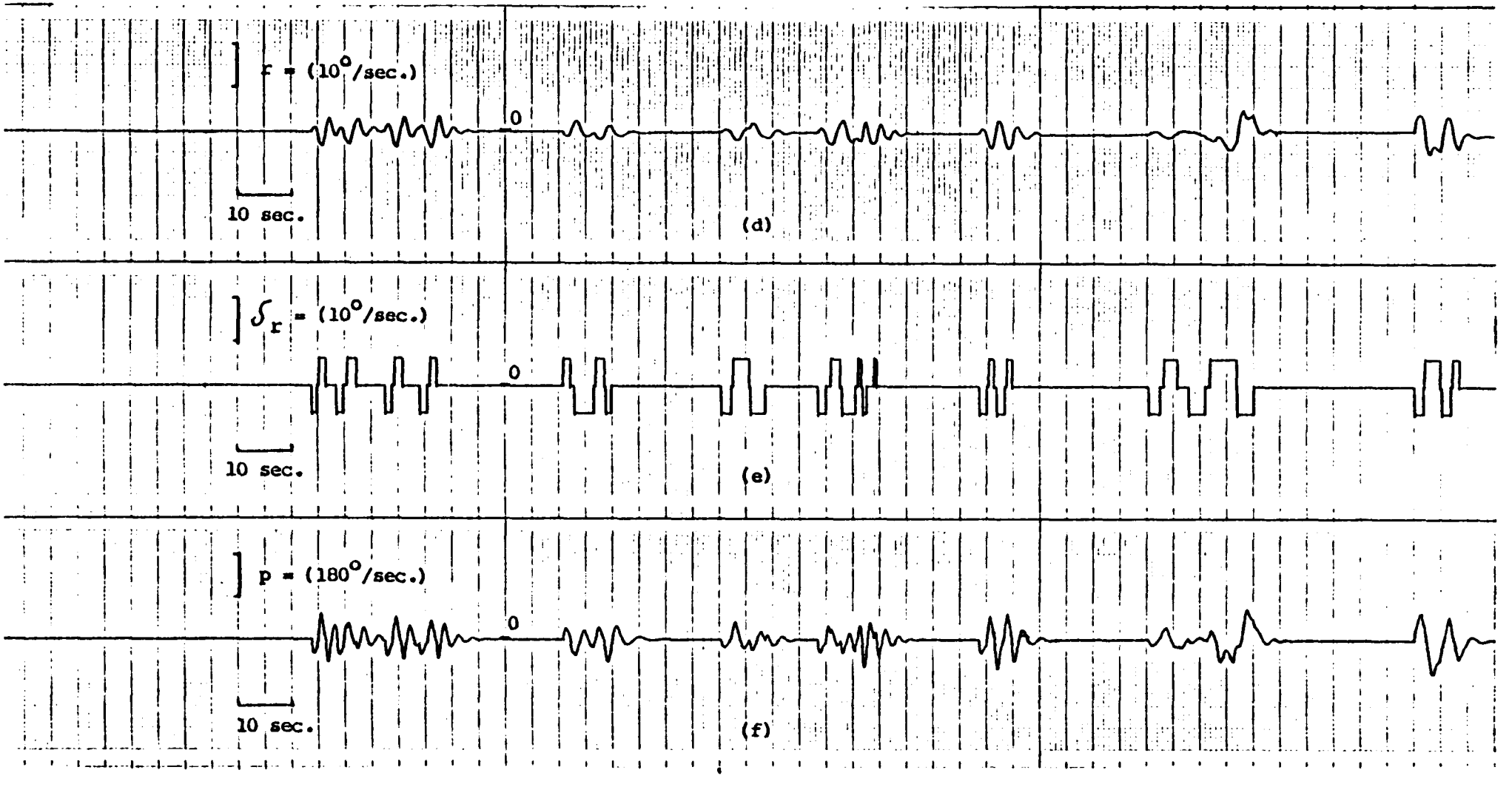

Fig. 5.8 continued: (d) yaw rate (e) rudder command (f) roll rate.

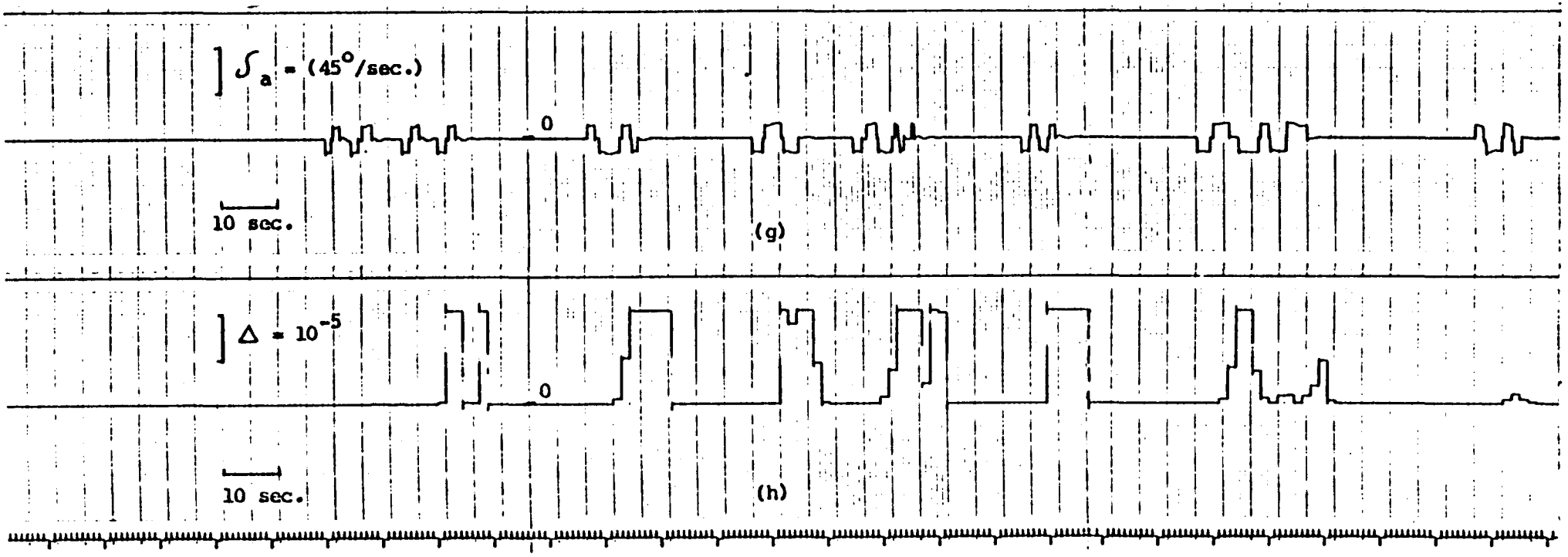

Fig. 5.8 continued: (g) aileron command (h) determinant of the information matrix.

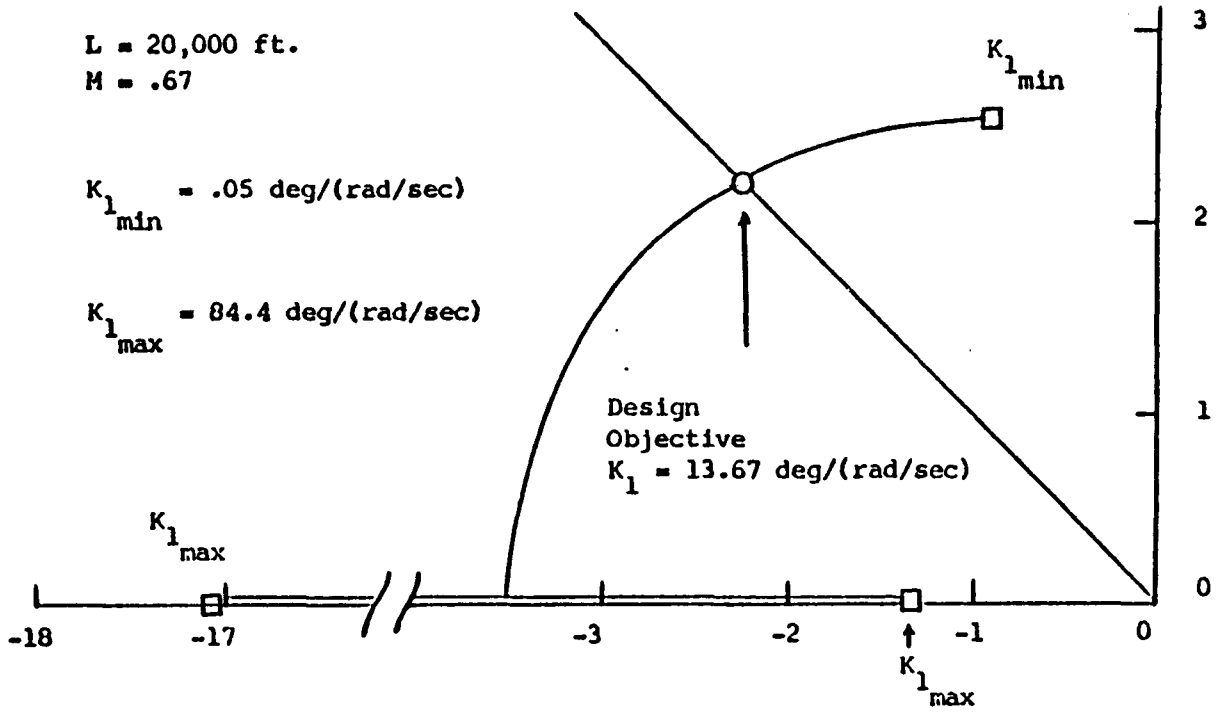

Fig. 5.9 Short Period Root Locus for Pitch Rate Feedback Gain Variations

Fig. 5.10 LONG. P1 VS. MACH, ALTIT.

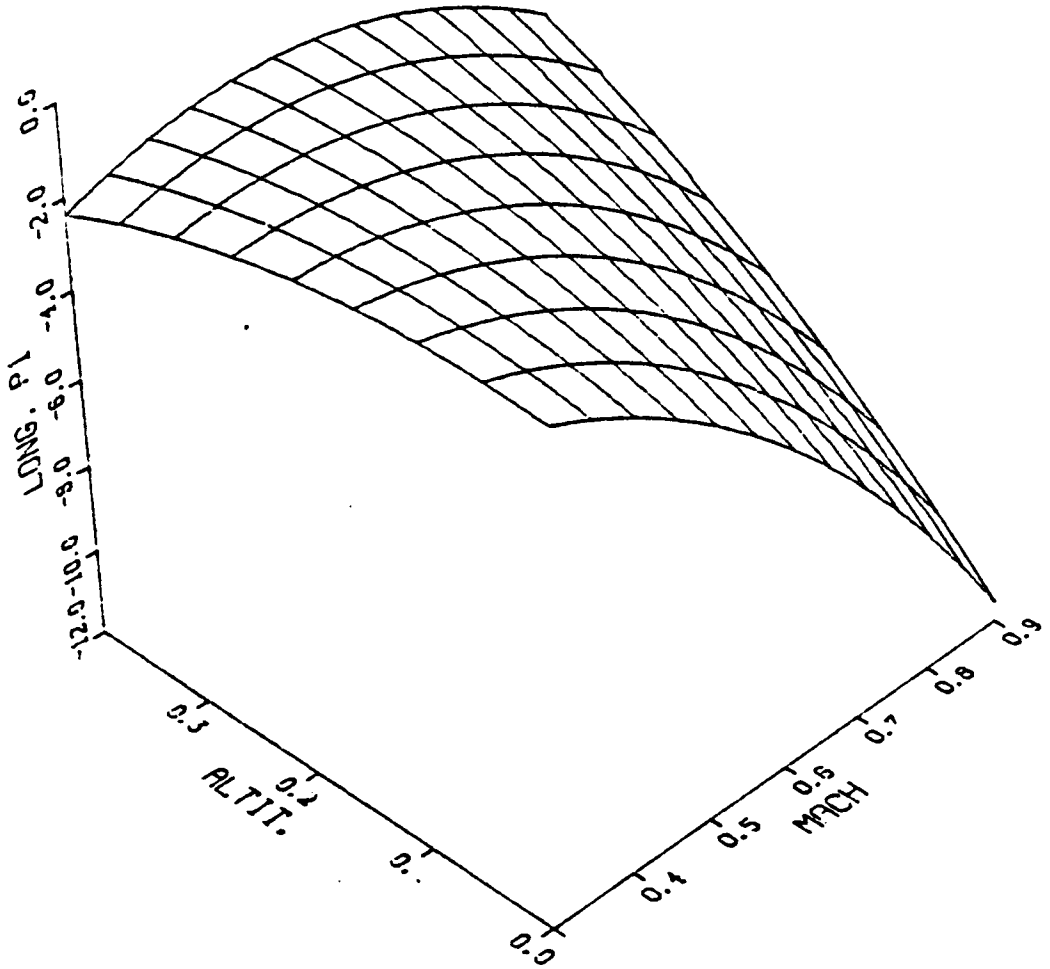

Fig. 5.11 LONG. P2 VS. MACH, ALTIT.

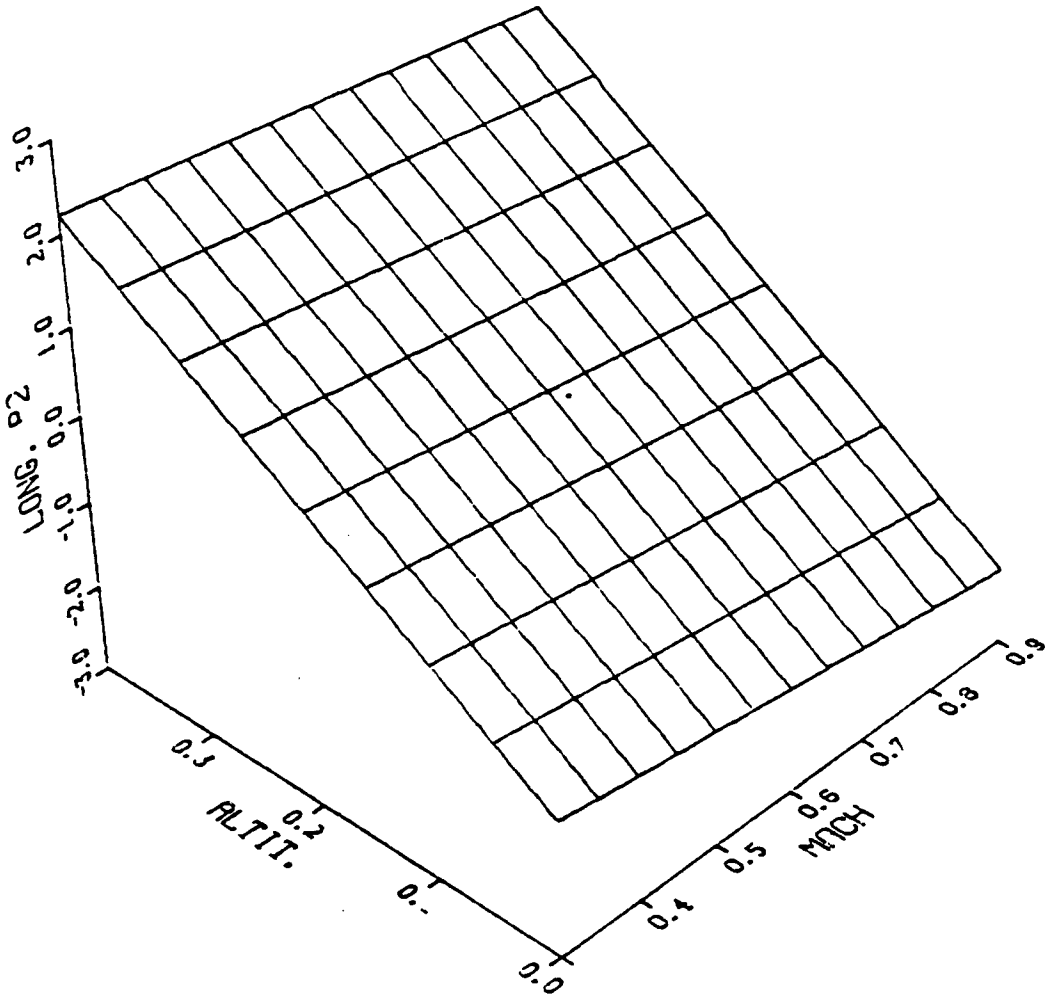

Fig. 5.12 LONG. P3 VS. MACH, ALTIT.

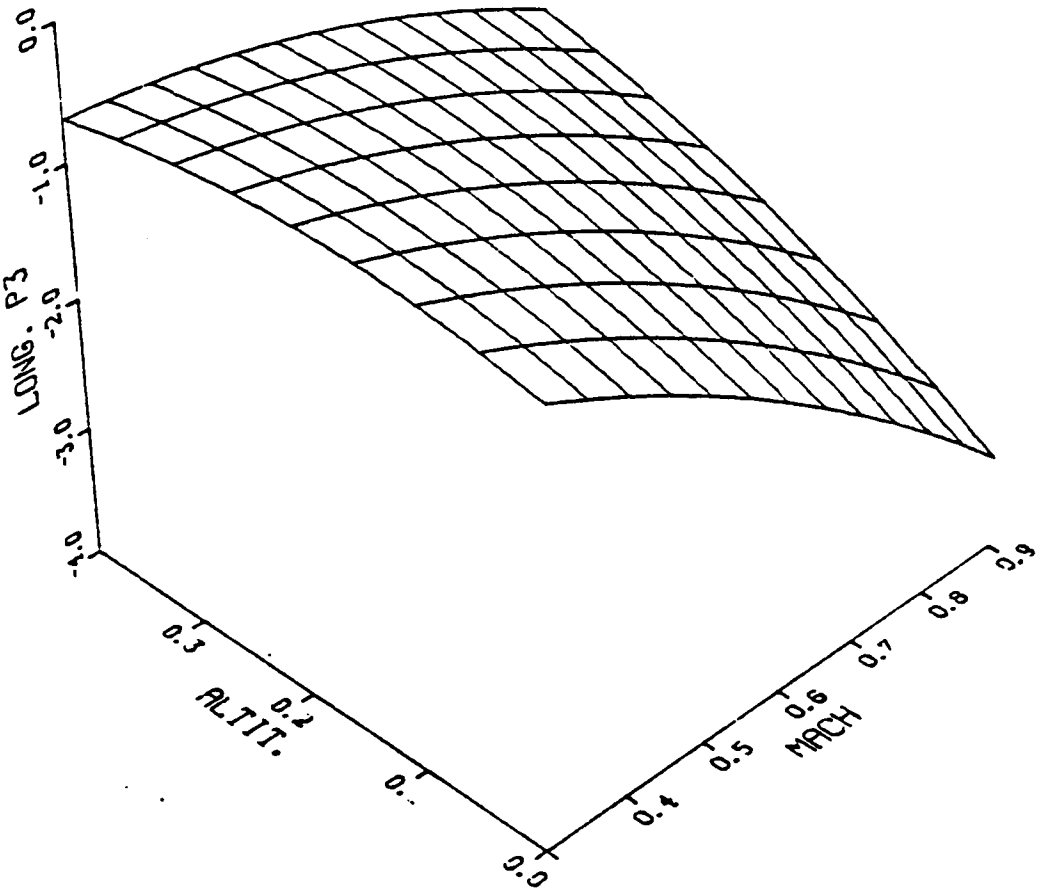

Fig. 5.13 LONG. P4 VS. MACH, ALTIT.

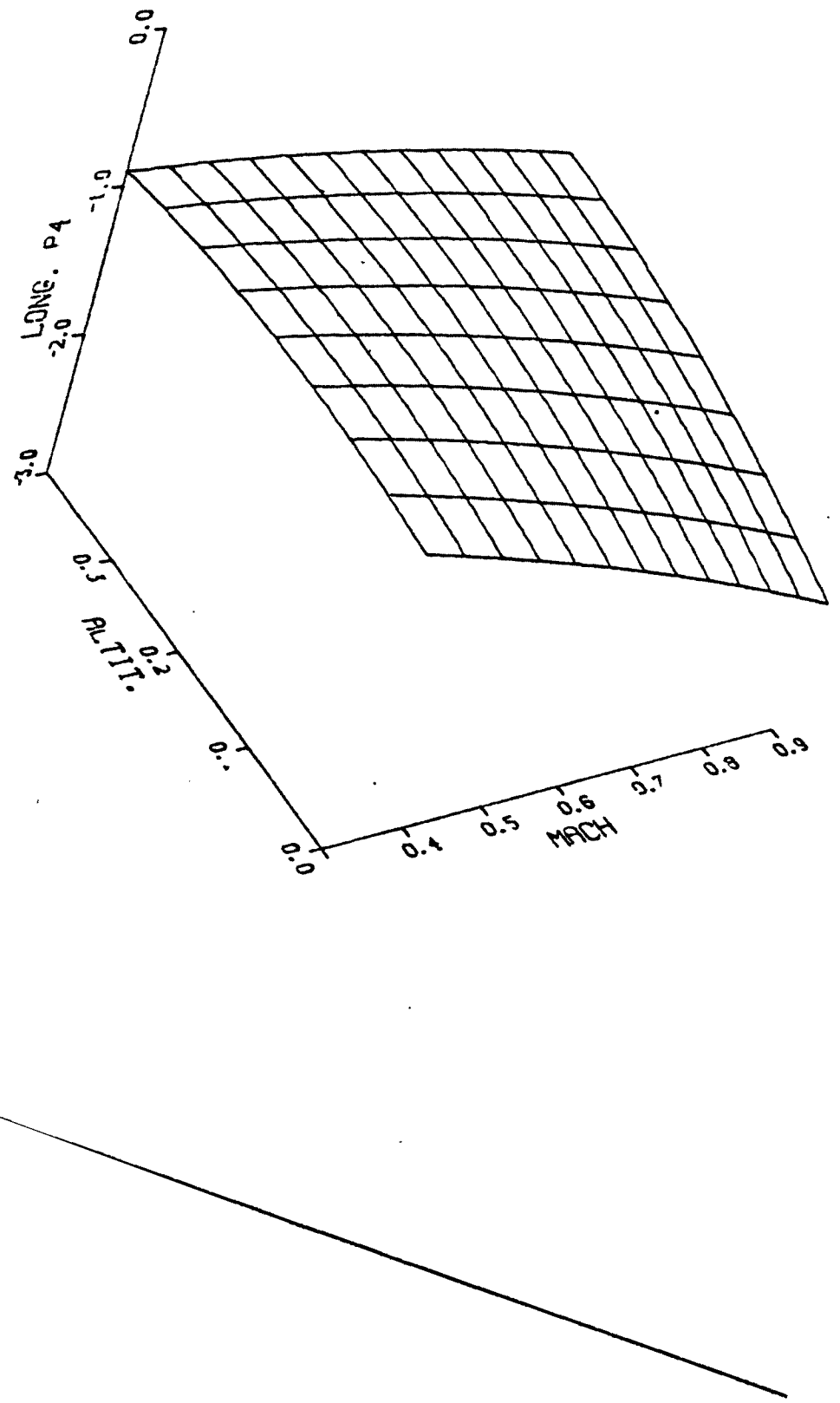

Fig. 5.14 LATR. P1 VS. MACH, ALTIT.

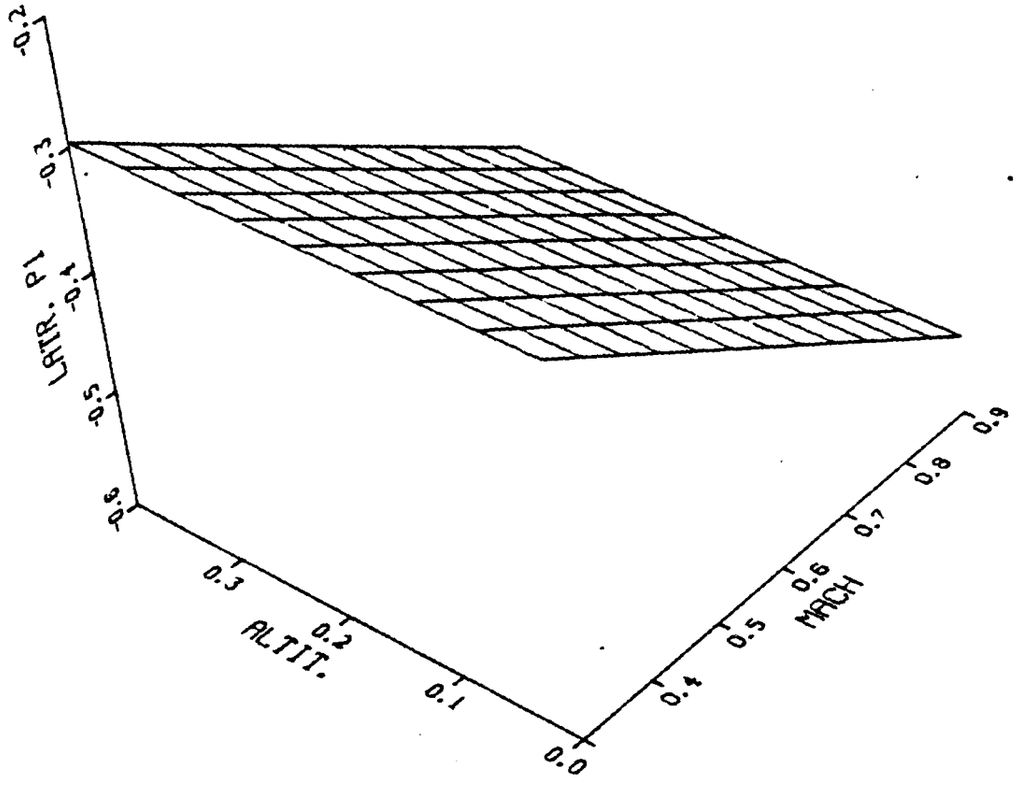

Fig. 5.15 LATR. P2 VS. MACH, ALTIT.

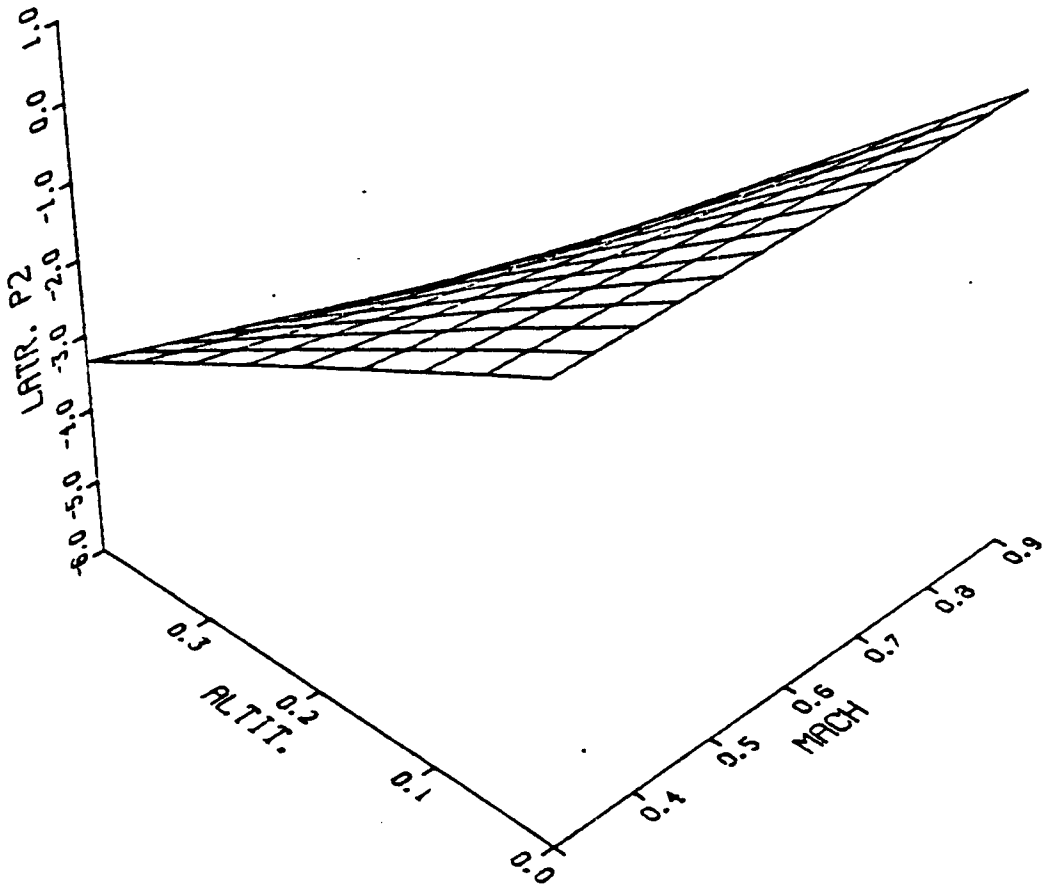

Fig. 5.16 LATR. P3 VS. MACH, ALTII.

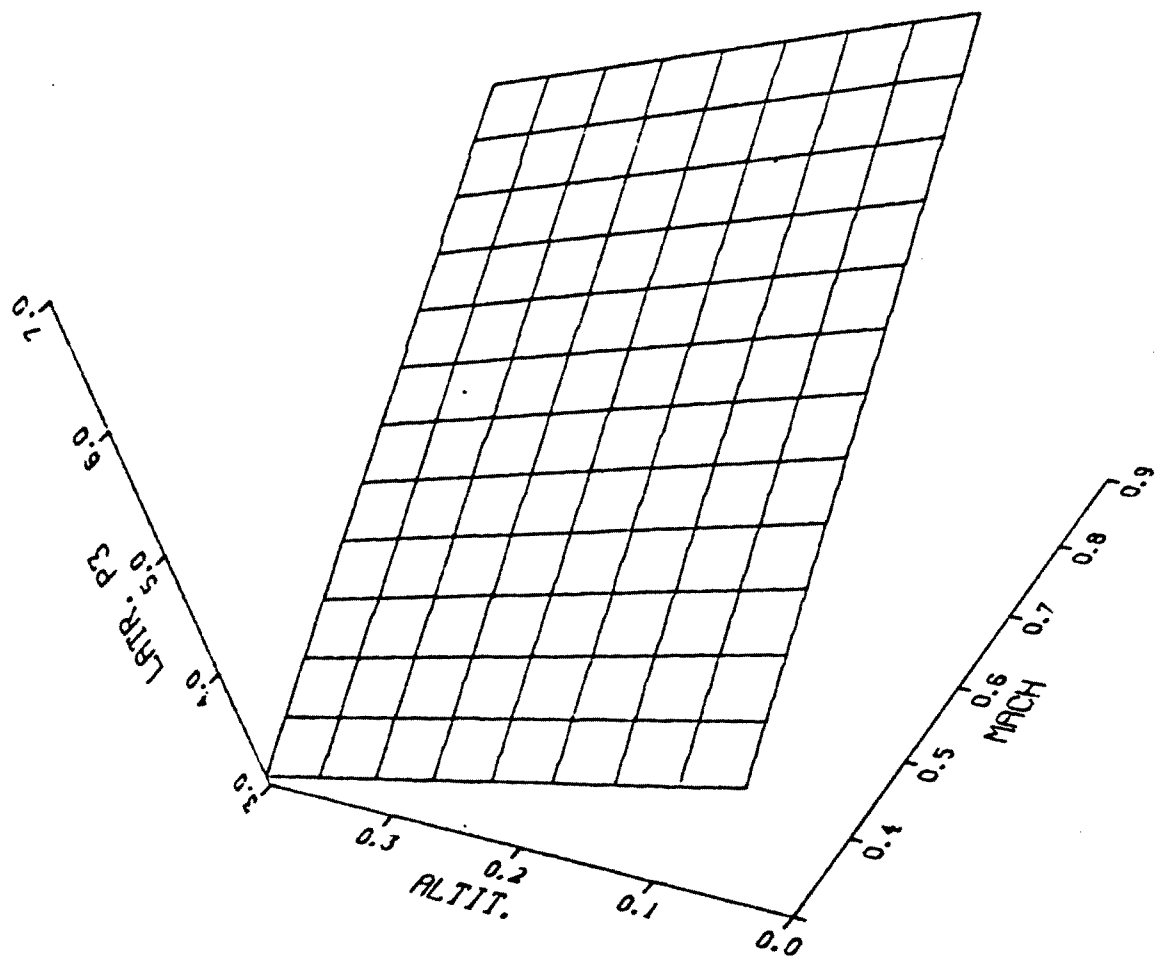

Fig. 5.17 LATR. P4 VS. MACH, ALTIT.

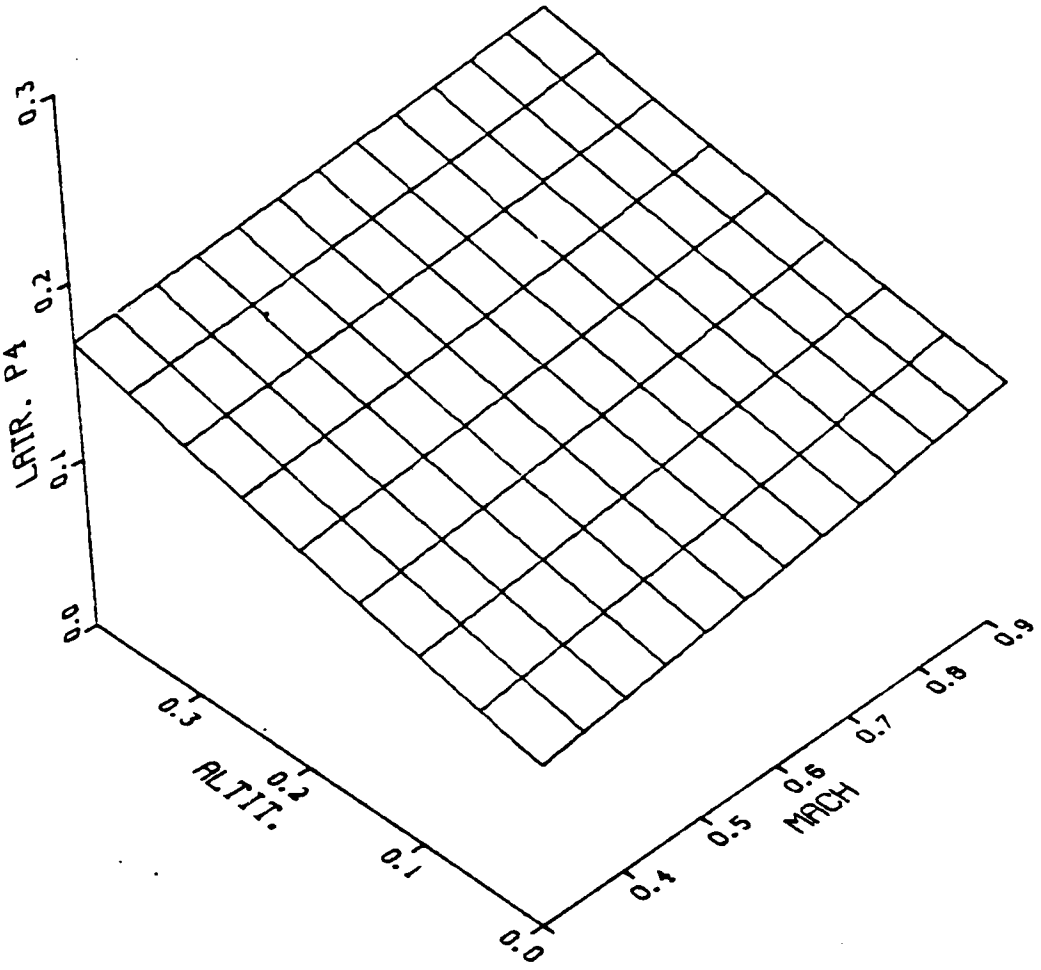

Fig. 5.18 LATR. P5 VS. MACH, ALTIT.

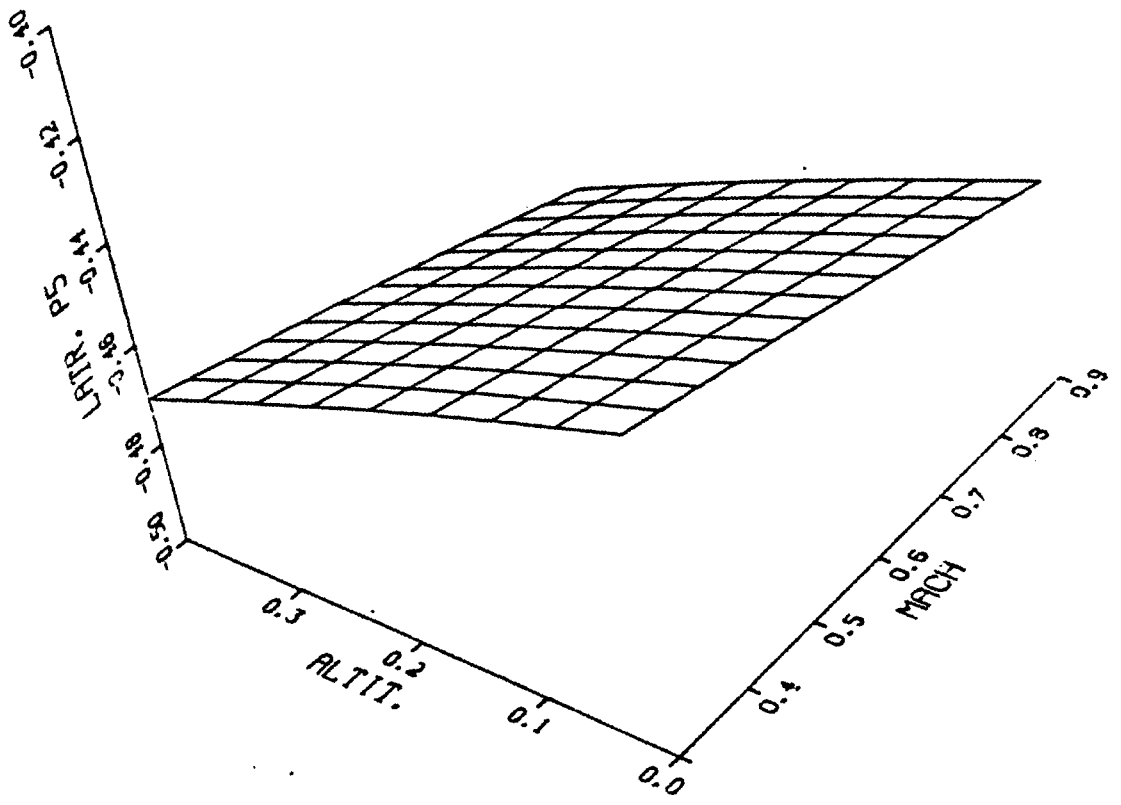

Fig. 5.19 LATR. P6 VS. MACH, ALTIT.

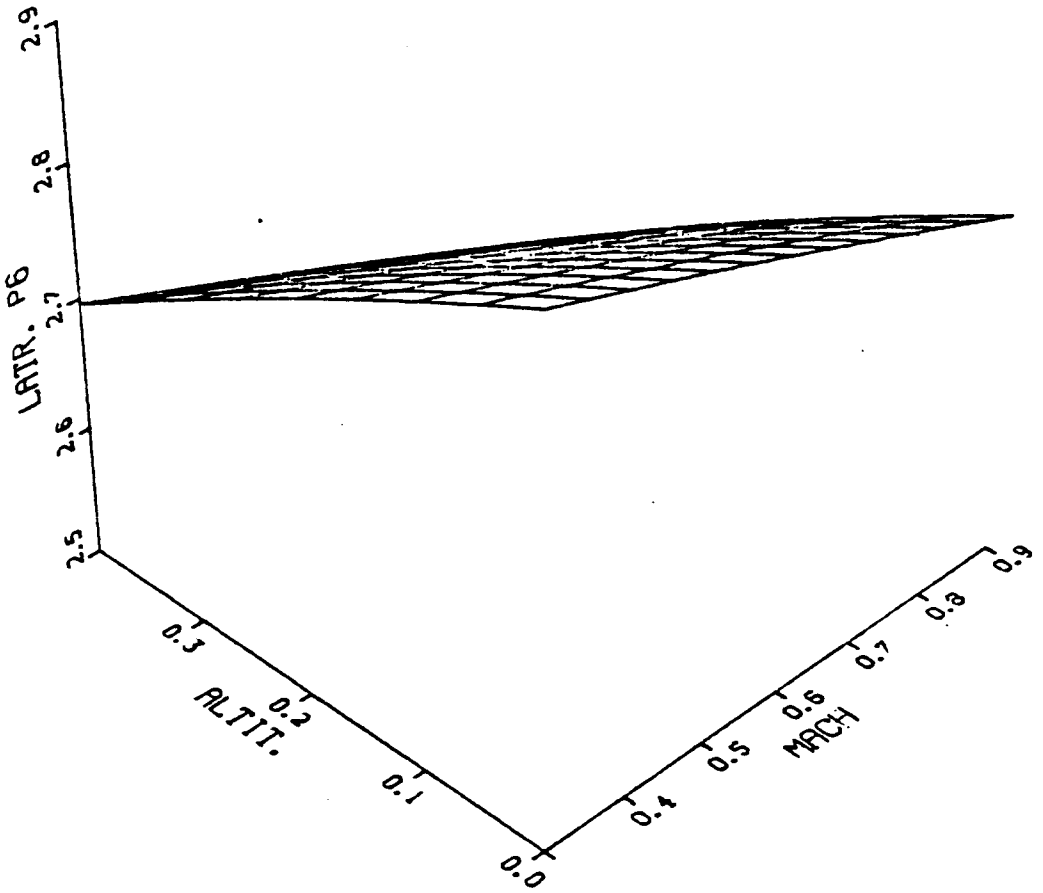

Fig. 5.20 LATR. P7 VS. MACH, ALTIT.

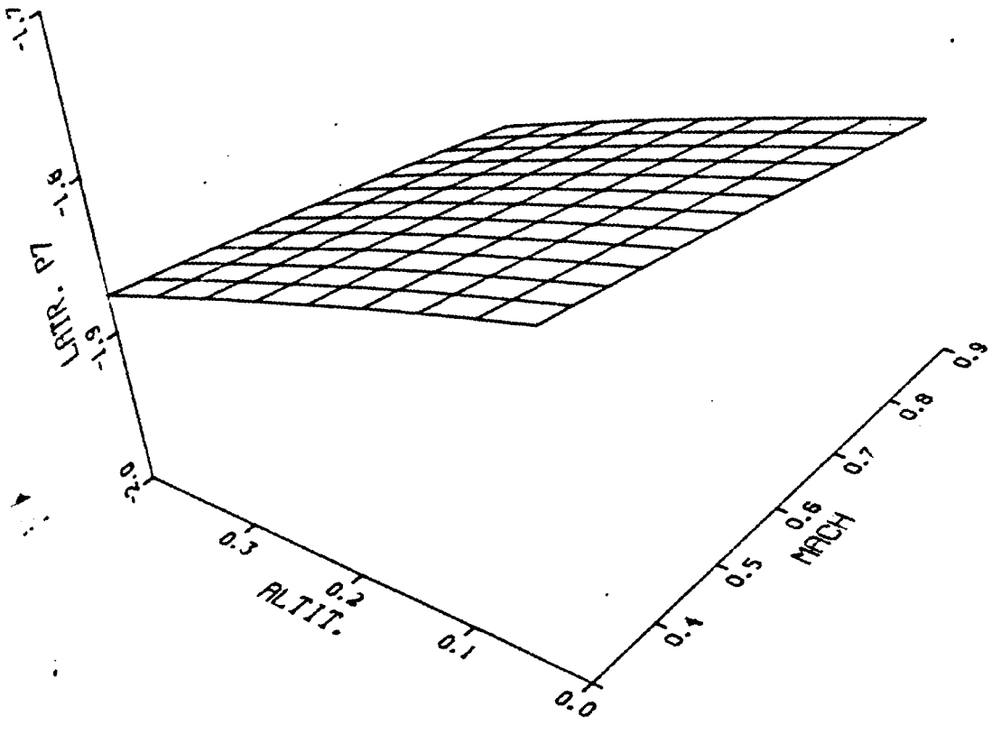

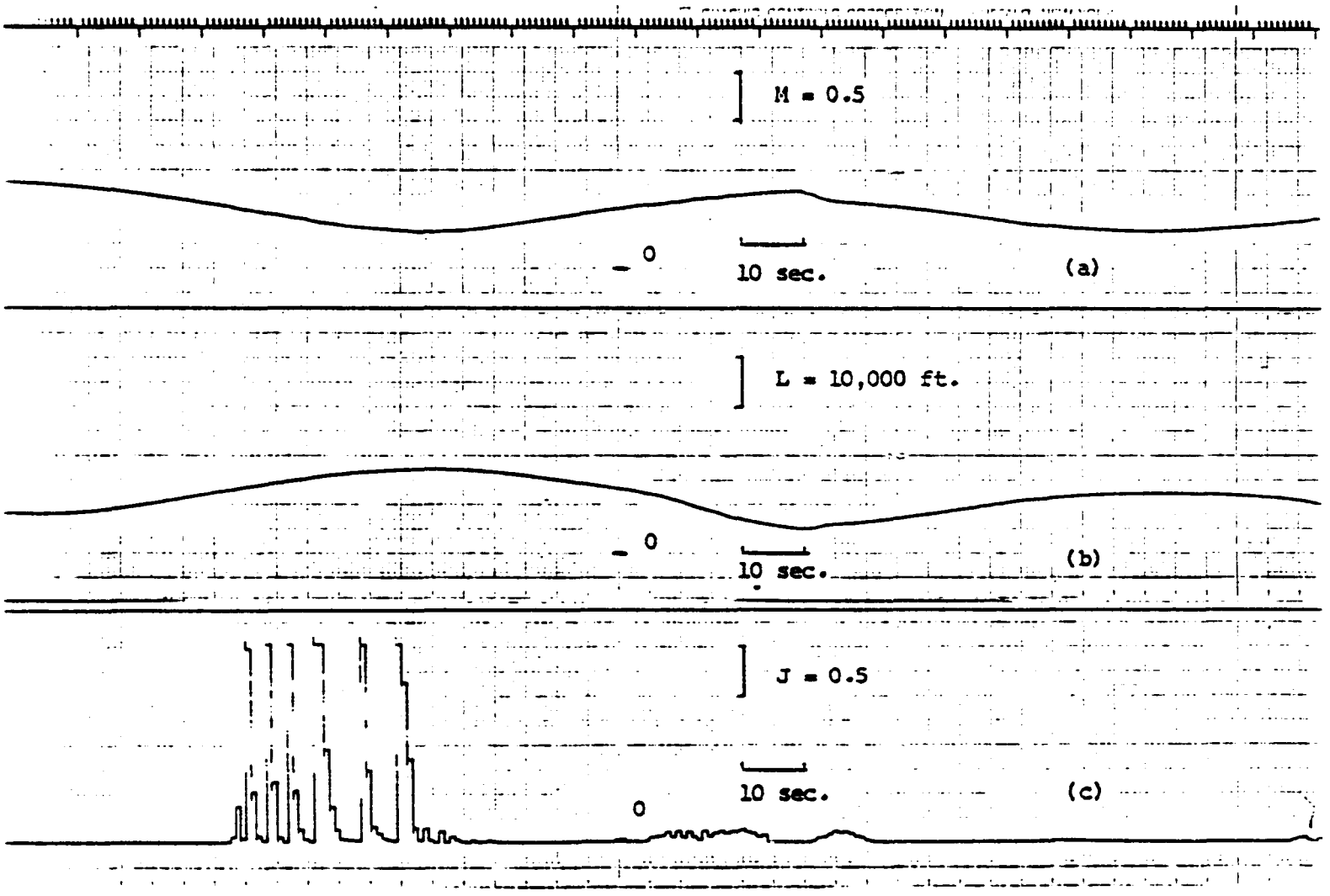

Fig. 5.21 Comparison of the learned parameters with the F-8 DFBW aircraft longitudinal parameters during a real-time simulation. (a) mach number (b) altitude (c) performance index

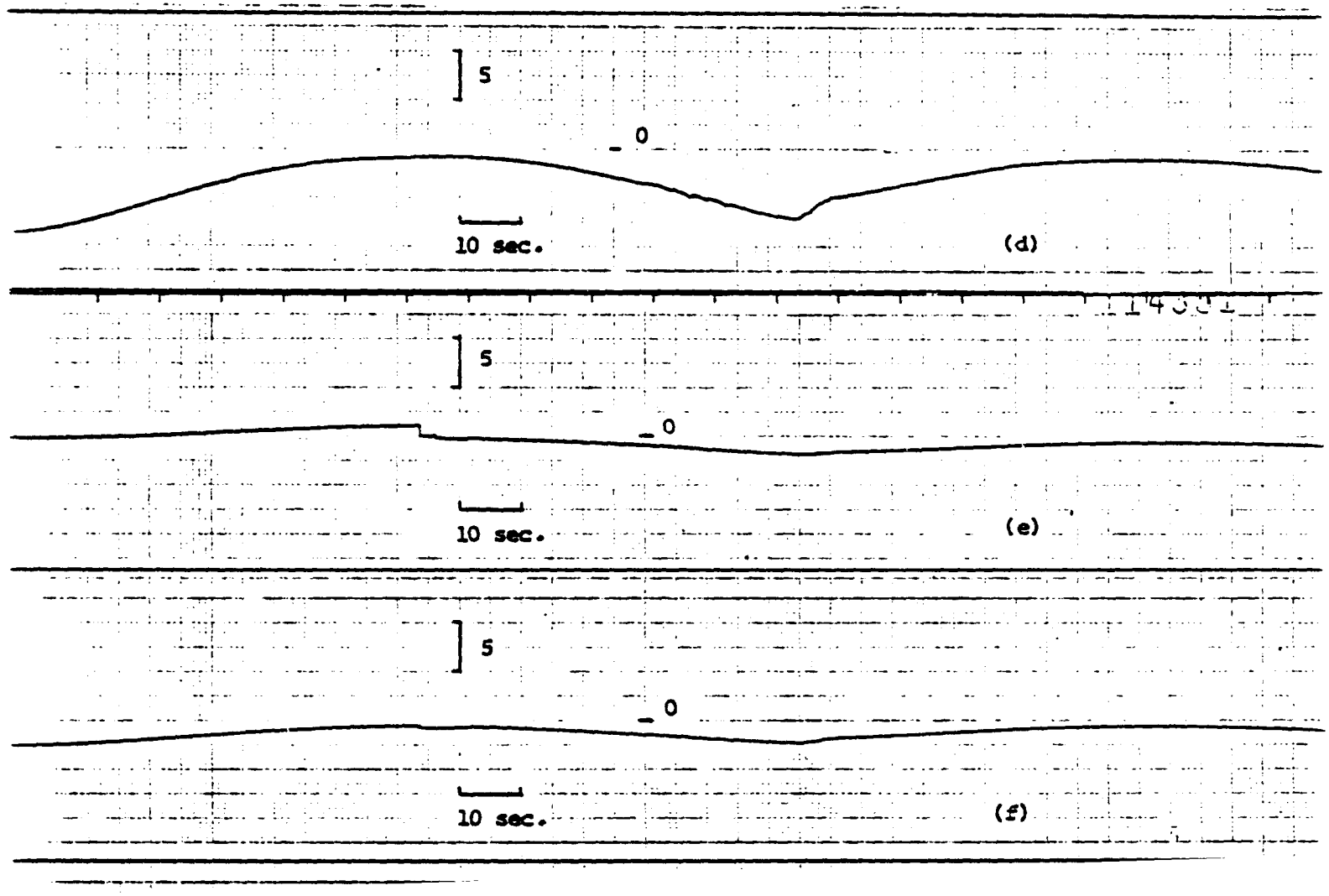
5
0
10 sec.
(d)
5
0
10 sec.
(e)
5
0
10 sec.
(f)

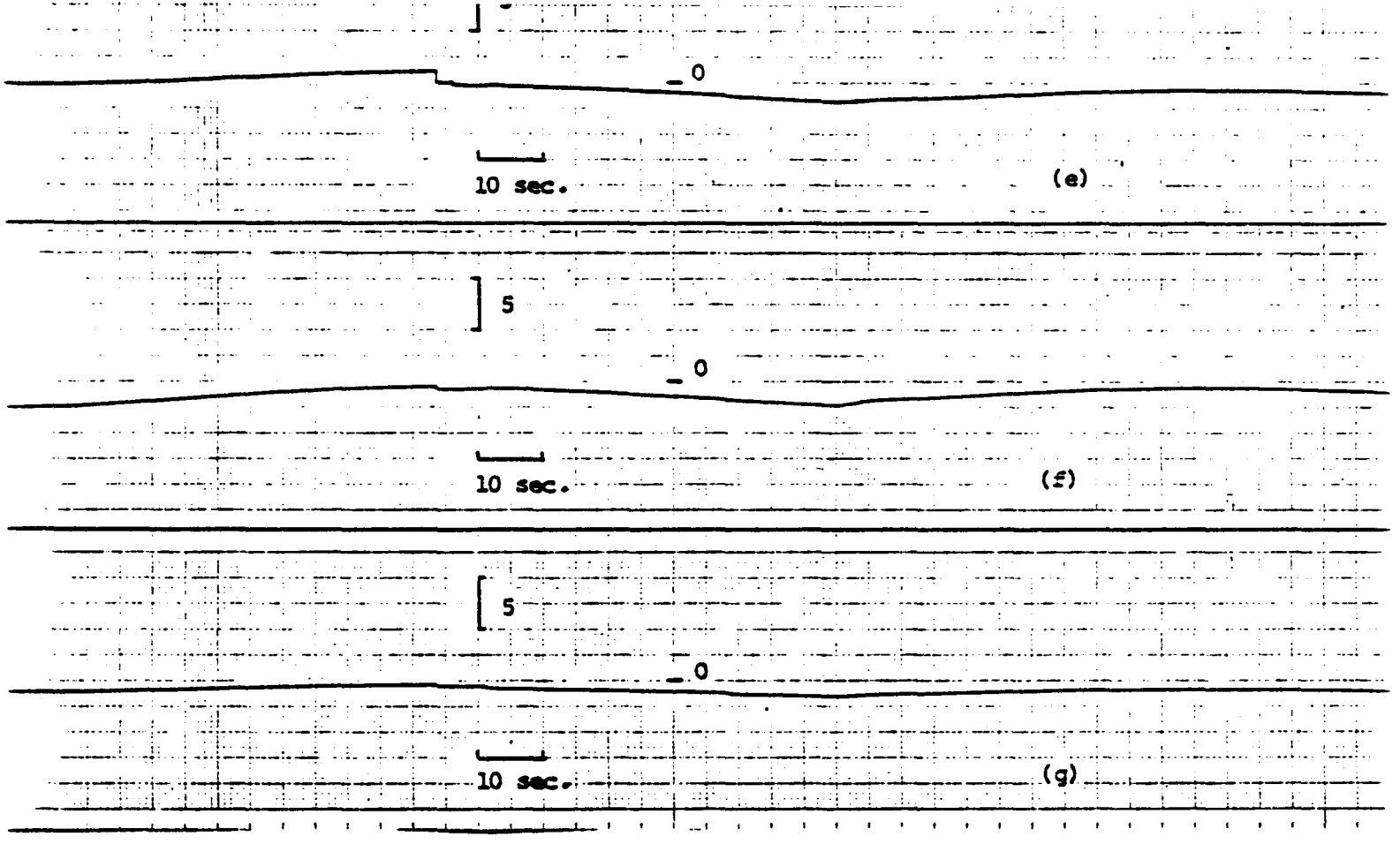

Fig. 5.21 Continued:

(d) Learned longitudinal parameter $\hat{p}_1$ (e) learned longitudinal parameter $\hat{p}_2$ (f) learned longitudinal parameter $\hat{p}_3$ (g) learned longitudinal parameter $\hat{p}_4$

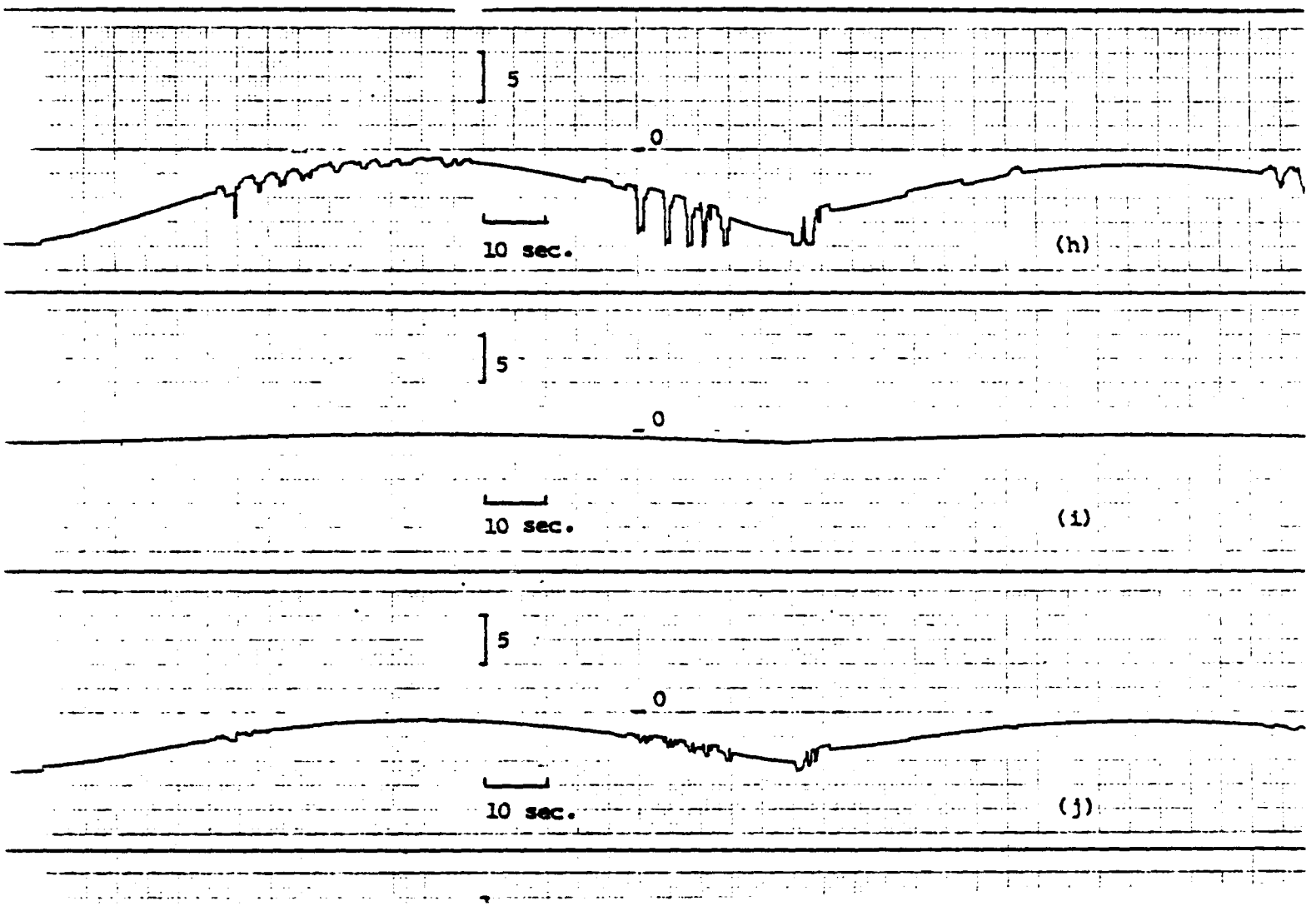
5
0
10 sec.
(h)
5
0
10 sec.
(i)
5
0
10 sec.
(j)

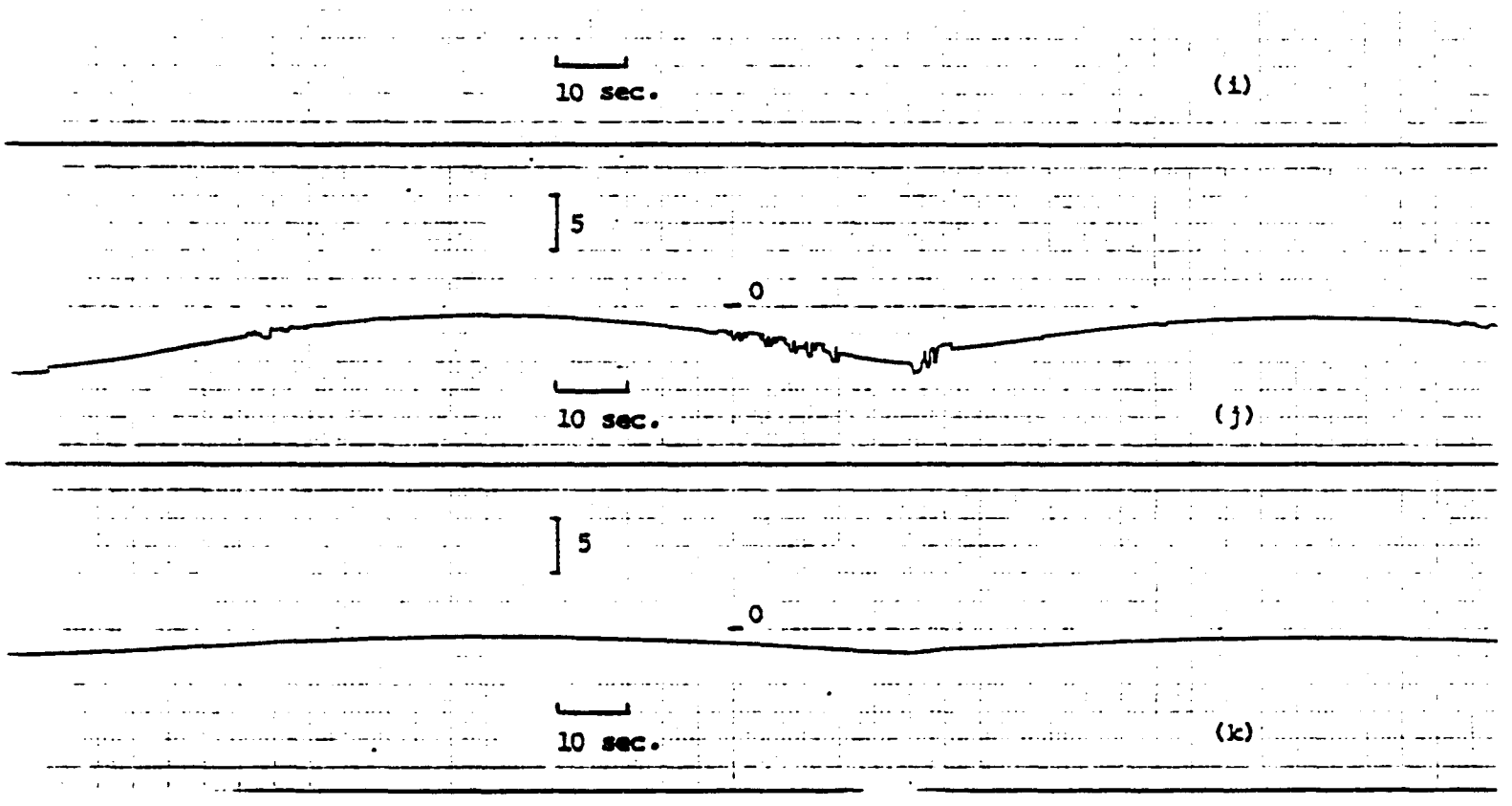

Fig. 5.21 Continued:

(h) Real (F-8) longitudinal parameter p_1 (M_α)
(i) Real (F-8) longitudinal parameter p_2 (M_q)
(j) Real (F-8) longitudinal parameter p_3 (M_{δ_e})
(k) Real (F-8) longitudinal parameter p_4 (L_α)

CHAPTER 6

SUMMARY AND CONCLUSIONS

6.1. Summary

This dissertation describes one of the many possible ways to develop an adaptive learning control system and its application as a flight control system for the F-8 DFBW aircraft. This learning control system blends the gain scheduling and adaptive control into a single system that has the advantages of both.

One important feature of this adaptive learning control system lies in its ability to adjust the gain schedule in a prescribed and learned manner to account for changing plant operating characteristics. Another important feature of the presented adaptive learning scheme is that one needs to identify the plant's parameters only at selected operating conditions in order to obtain reasonable adjustments for the gain schedule over a large range of operating conditions. This is done by the use of the coefficients, C_i's, (weights) produced by the learning algorithm subsystem and stored in the memory. The gain schedule for every possible operating condition is then determined by the weights. In this fashion, the learning control system makes practical the real-time computation of the gain schedule. Another feature of such an approach is that it may be implemented with sufficiently inexpensive technology to make use in control systems to be economical for a wide variety of industrial applications.

The functional organization of the learning control system with a general description of the task of each subsystem was presented in Chapter 3. More specifically, sections 3.2 and 3.3 describe two different mathematical techniques to implement the information acquisition

subsystem, one based on Liapunov's direct method and the second based on Newton-Raphson method. The next two sections (3.4 and 3.5) describe mathematical techniques to implement the learning algorithm subsystem and the memory and control process subsystem respectively.

Perusal of the existing literature about adaptive learning control systems and flight control systems was discussed in Chapter 2. Section 2.2 introduces a popular class of adaptive systems, namely the parameter adaptive model reference systems and discusses mathematical techniques to implement the adaptive algorithm based on Liapunov's function and on the gradient approach. Section 2.3 examines the present state of learning control systems and their applications and also presents the most prominent mathematical techniques to formulate a learning system. The advancements of flight control systems, as a result of the evolution of digital flight control systems, are examined in section 2.4. Section 2.5 gives particular reference to the NASA F-8 Digital Fly-By-Wire (DFBW) program.

Chapters 4 and 5 give the application of the learning control system to control two different simulations of the F-8 dynamics, and present the associated results. More specifically, in Chapter 4 we use fourth order simulations of the longitudinal and lateral dynamics of the F-8 DFBW aircraft and the model used for the learning control system is of the same order. The application considered in Chapter 5 is more realistic since it was done in real-time for the piloted six-degree-of-freedom simulation of the F-8 DFBW aircraft. Because of the real-time constraint* only the predominant motion modes were modeled, using first or second order analytical models.

In the next section, final conclusions are drawn about the

---

* as discussed in Chapter 5.

performance of the learning control system as evidenced from the research carried out in this dissertation and the LCS's applicability to model and control various other systems is also discussed.

6.2. Conclusions

The aircraft flight envelope used for the learning control system design is shown in Fig. 6.1. Symbols (o) indicate flight condition points in the flight envelope for which our models were developed.

The symbols on the horizontal line L = 0 = sea level indicate mach numbers .5, .7 and .9. At these flight conditions the aircraft was simulated to obtain the parameter curves shown in Chapter 4, Figs. 4.2-4.13. An important feature of the LCS, as evidenced in these curves, is that we obtain information about the parameters for different flight conditions which the aircraft has not experienced. This indicates that once the aircraft is in a new flight condition, we may adjust the gain scheduling with no need to identify the parameters for this new flight condition. This, in turn, shows that a dither signal to excite the system is not needed during periods of control inactivity, where in conventional adaptive schemes we would have to perturb the system at each different flight condition.

In Appendix A, the figures illustrate the learned parameter curves as a function of altitude obtained from the flight conditions indicated in Fig. 6.1 on the vertical line M = .7 (L = 0 = sea level, 20,000 ft., 40,000 ft.). Even though the curves shown in Appendix A were obtained from different flight patterns than those shown in Chapter 4, Figs. 4.2-4.13, the corresponding parameters have close values for the same flight conditions. By this, we may conclude that the performance of the LCS does not

depend on the particular choice of flight conditions experienced by the aircraft; i.e. corresponding parameters are the same independent of the selected flight conditions. Though not discussed in this dissertation, we may infer that the LCS may be generalized to incorporate variations of the parameters as a function of several other variables, e.g. the angle of attack.

The gain scheduling technique adjusts the gains at each different flight condition by having prestored the values of the parameters. This is practical for parameters that are functions of one to three variables however, for functions of four or more variables, the gain scheduling becomes impractical because of the extraordinary memory requirements. On the other hand, the LCS introduces a significant saving in storage thus requiring a memory of reasonable size and also makes practical the real-time computation of the parameters and the gains by a table look-up. By this, we may conclude that the LCS may be used to control plants that are affected by parameters that are multi-variant functions.

In view of the longitudinal models used in Chapters 4 and 5, namely Eqs. (4.3.2) and (5.2.2), one may observe a correspondence between the longitudinal parameters $\hat{p}_3$, $\hat{p}_1$ and $\hat{p}_8$ of Eq. (4.2.1) and the longitudinal parameters $\hat{p}_1$, $\hat{p}_2$ and $\hat{p}_3$ of Eq. (5.2.2) respectively. (See Table 6.1)

The comparison of Figs. 4.3 & 5.1, 4.2 & 5.2 and 4.4 & 5.3 show that the curves have the same approximate shape but the corresponding values are different. This may be attributed to two different reasons: (1) In Chapter 5 the simulation of the plant describes the entire six-degree-of-freedom dynamics of the F-8 DFBW aircraft while the plant simulation used in Chapter 4 describes only the linearized longitudinal & lateral dynamics. (2) In Chapter 5 we only modeled the short period longitudinal

mode, the Dutch roll mode and the roll mode, where in Chapter 4 the model was more elaborate. This simplification was done because of the real-time constraint*.

The correspondence of the lateral parameters used in Chapters 4 and 5 may be observed by comparing Eq.(4.5.2) with Eq. (5.3.1) and is given in table 6.2. The figures 6.2 and 6.3 indicate the learning of p_1 and p_{13} of Chapter 4, respectively and are included here for the sake of comparison. The comparison of Figs. 5.5 & 6.2 and 5.7 & 6.3 show again different values of the parameters for corresponding flight conditions, which is attributed to the two reasons described above.

For this reason, we do not have a way to evaluate the curves obtained from the real-time simulation so we will evaluate the performance of the LCS according to how the design criteria are met, namely 0.7 dampting ratio for the Dutch roll and short period longitudinal modes, and 0.2 seconds time constant for the roll mode. During the time intervals when the LCS is engaged, its performance can be observed. Figure 6.4 shows the response of the sideslip angle β to a rudder input. This figure indicates that when the LCS is engaged at times 30 sec., 60 sec., 80 sec. and 110 sec. the Dutch roll mode damping ratio is maintained at 0.7. Figure 6.5 shows the response of roll rate p due to an aileron input. By comparing the steady-state roll rate at times 20 sec., 60 sec., 80 sec. and 100 sec. the uniformity of the roll-rate response during engagement of the LCS may be noticed. By this, we may conclude that the LCS is capable to meet design requirements over the entire flight envelope, without the need to prestore or identify the parameters at each

* See Chapter 5

flight condition as would be required by the gain scheduling, or the conventional adaptive techniques, respectively. In the next section we will discuss possiblities for future research on learning control systems both from the theory and the applications points of view.

6.3 Recommendations for Future Research

Future research on learning control systems could be approached from two points of view: a) the mathematical approach and b) the application approach. From the mathematical point of view, the following areas of research are suggested:

1. To develop further criteria for the adequacy of the learning control system by improving on the convergence and confidence criteria.

2. Investigate the performance of the learning control system when different functional representations are used to implement the LAS.

3. Examine the learning control system design for distributed parameter systems.

From the application point of view, the following areas of research are recommended:

1. Modify the LAS to incorporate variations of the parameters as functions of more than two variables as shown in this dissertation. This will depend on the particular problem at hand.

2. Apply the learning control system to control systems such as chemical processes and physiological systems.

Chapter 4	Chapter 5
$\hat{p}_3$	$\hat{p}_1$
$\hat{p}_1$	$\hat{p}_2$
$\hat{p}_8$	$\hat{p}_3$
$\hat{p}_7$	$\hat{p}_4$

Table 6.1 Correspondence of the longitudinal parameters from Chapters 4 and 5

Chapter 4	Chapter 5
$\hat{p}_1$	$\hat{p}_1$
$\hat{p}_3$	$\hat{p}_2$
$\hat{p}_5$	$\hat{p}_4$
$\hat{p}_6$	$\hat{p}_3$
$\hat{p}_9$	$\hat{p}_5$
$\hat{p}_{10}$	$\hat{p}_6$
$\hat{p}_{11}$	$\hat{bp}_7$
$\hat{p}_{13}$	$\hat{p}_7$
$\hat{p}_{14}$	$\hat{ap}_7$

Table 6.2 Correspondence of the lateral parameters from Chapters 4 and 5

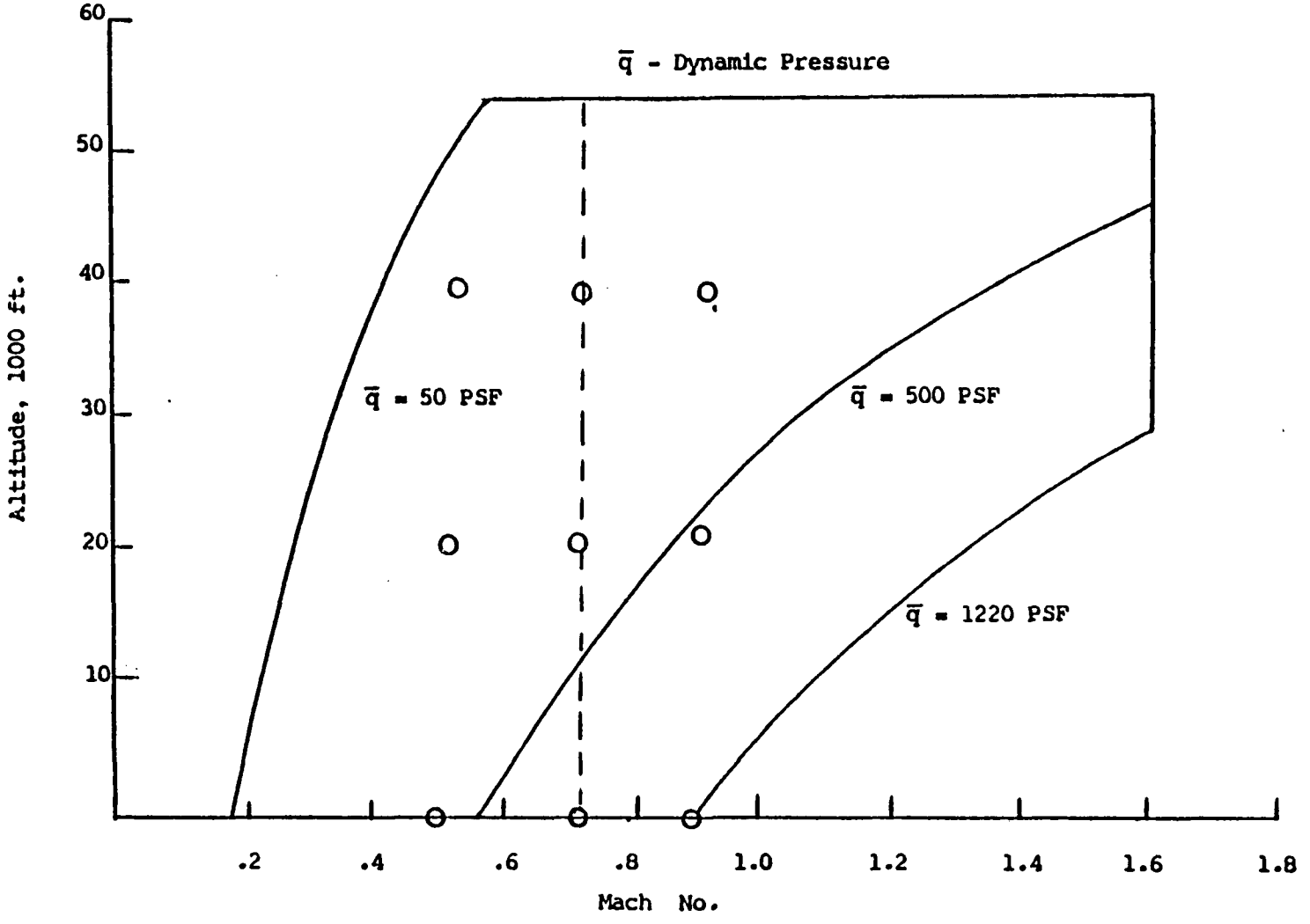

Fig. 6.1 F-8 Flight Envelope and Design Data Points

Fig. 6.2 LATR. P1 VS. MACH (Newton-Raphson IAS)

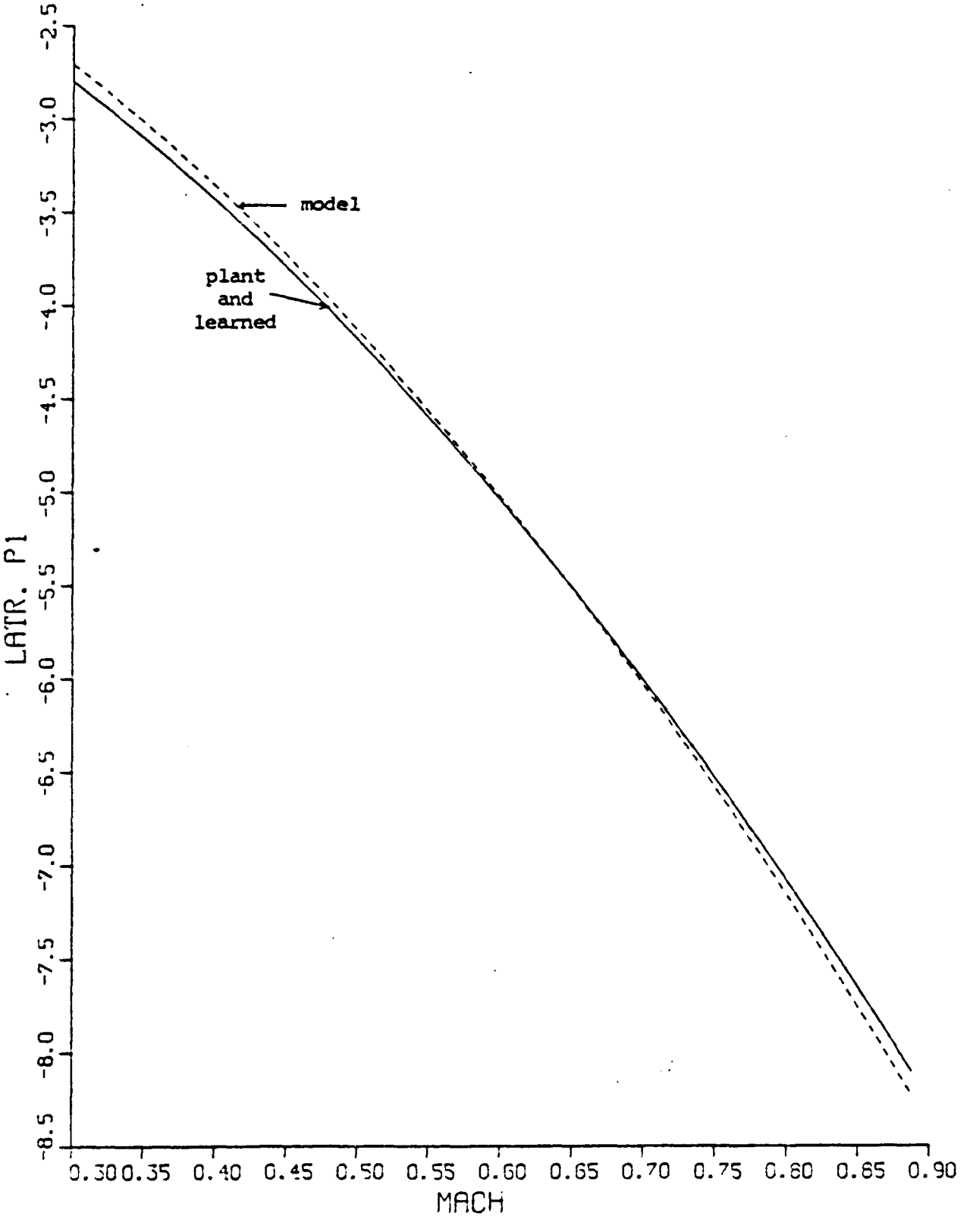

Fig. 6.3 LATR. P13 VS. MACH (Newton-Raphson Method)

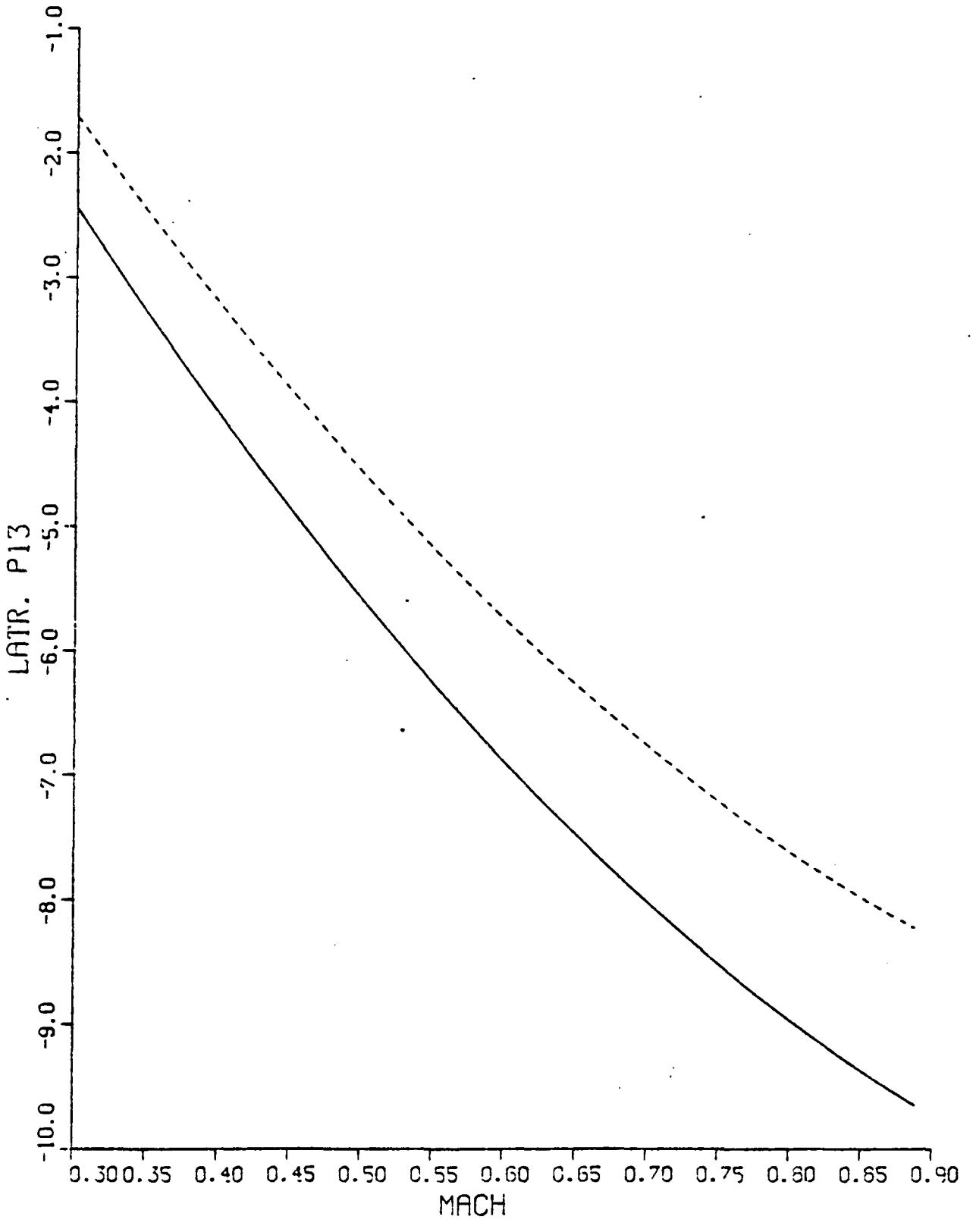

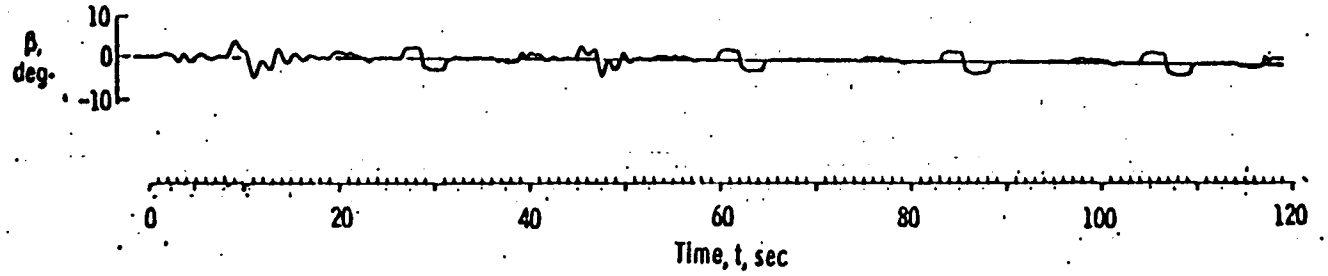

Fig. 6.4 Respone of the Sideslip Angle β to a Rudder Input.

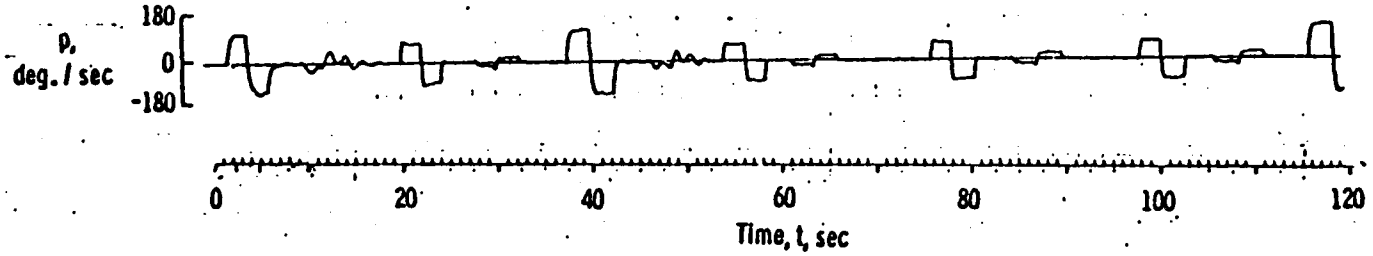

Fig. 6.5 Response of Roll Rate p to an Aileron Input.

APPENDIX A

LEARNED PARAMETER CURVES AS A FUNCTION OF ALTITUDE OBTAINED FROM CASE STUDY I (CHAPTER 4)

This appendix contains the graphs of the learned parameter curves as a function of altitude for mach number M = 0.7 for a high order representation of the F-8 DFBW aircraft dynamics. The first twenty figures show the longitudinal parameters p_1 to p_{10} obtained via two different LCS's one using Liapunov's IAS and the other, by the use of Newton-Raphson IAS. The latter twenty eight figures show the lateral parameters p_1 to p_{14} obtained via the above two mentioned LCS's.

These curves were obtained by simulating the operation of the aircraft at the following operating conditions: Mach number M = 0.7 and Altitude L = sea level, 20,000 ft., 40,000 ft. The following representations depict the plant's learned and model parameters.

_____ plant's parameter curve

_____ . _____ . _____ learned parameter curve

- model parameter curve

Fig. A.1 LONG. P1 VS. ALTIT. (Liapunov IAS)

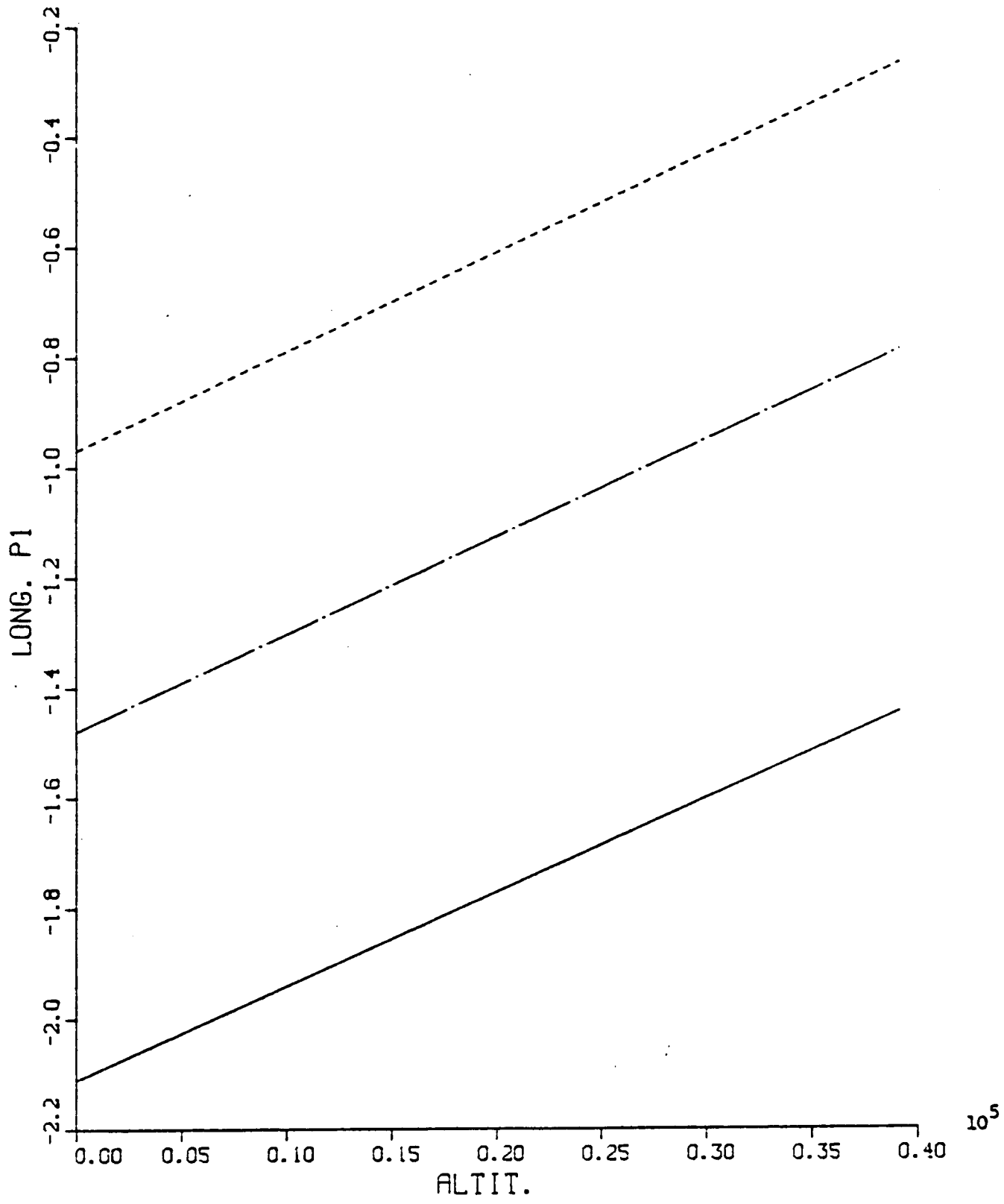

Fig. A.2 LONG. P2 VS. ALTIT. (Liapunov IAS)

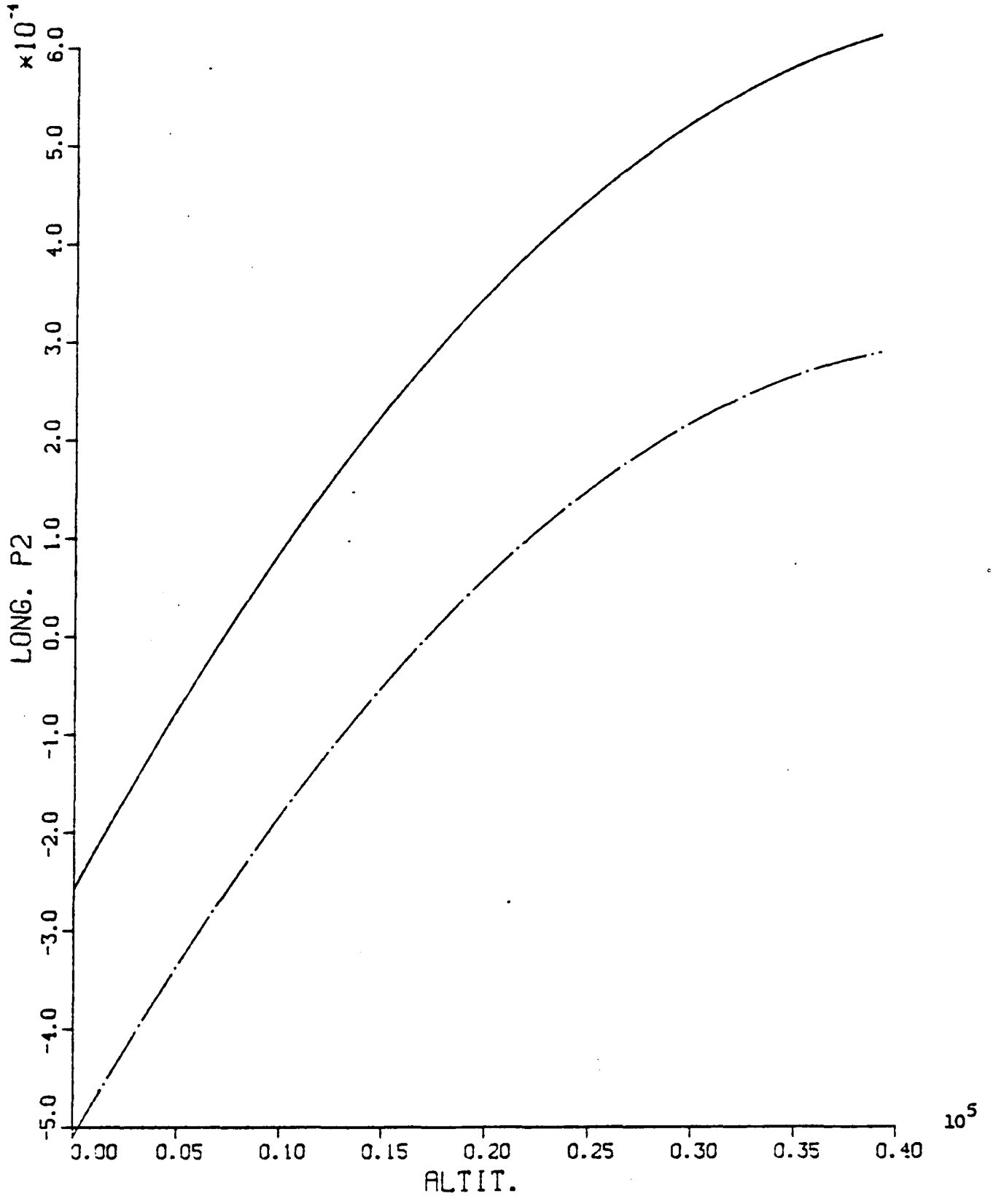

Fig. A.3 LONG. P3 VS. ALTIT. (Liapunov IAS)

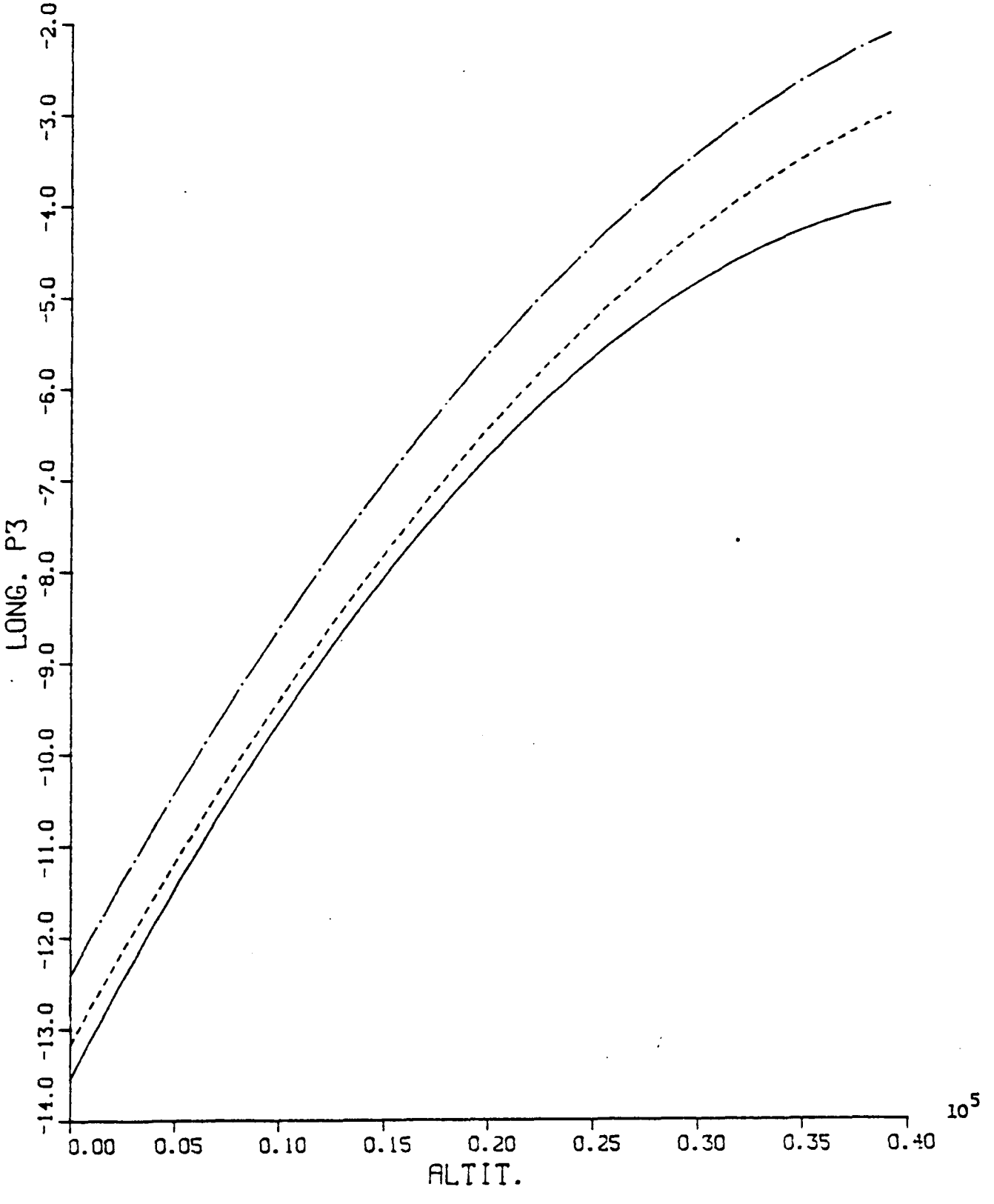

Fig. A.4 LONG. P4 VS. ALTIT. (Liapunov IAS)

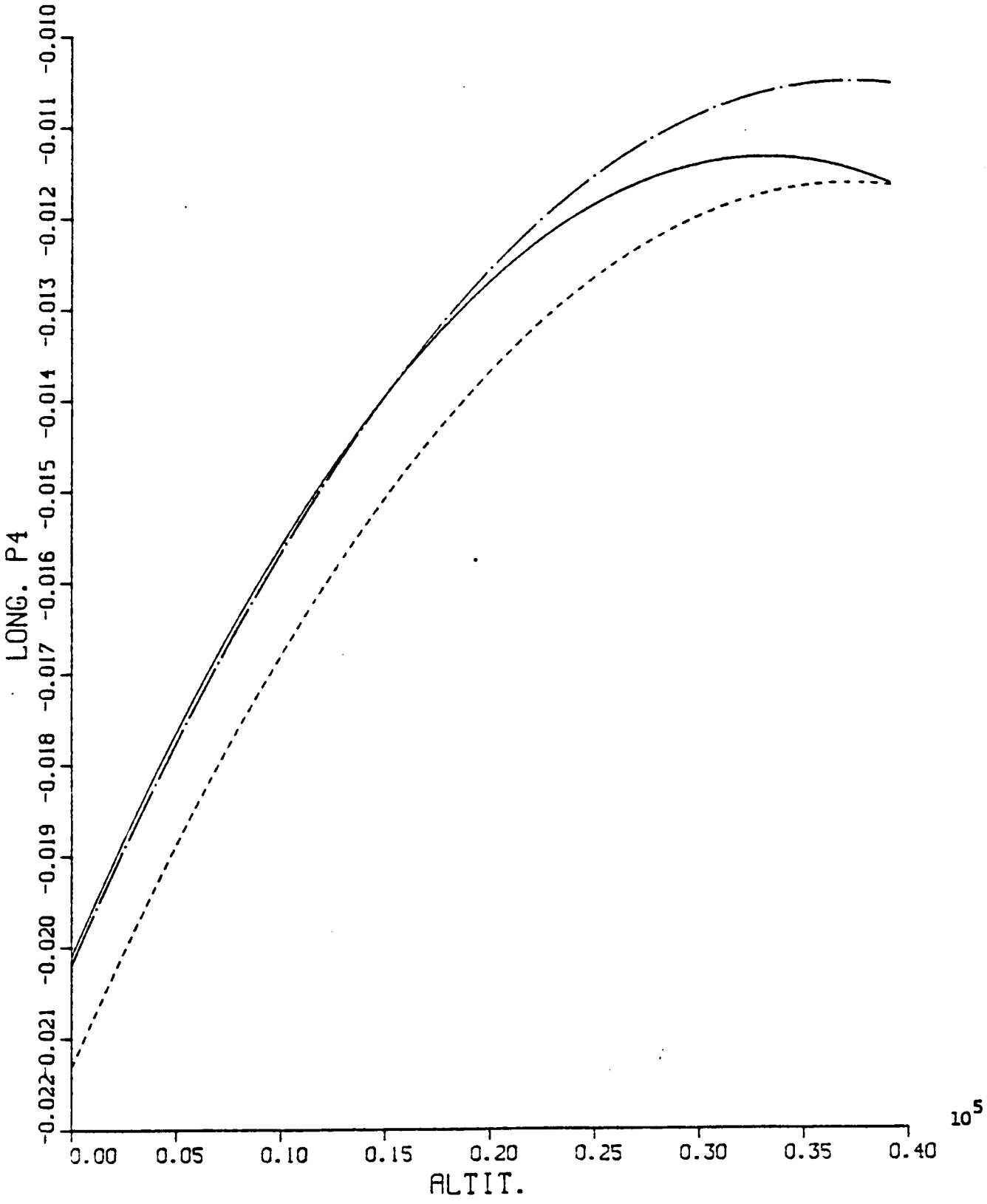

Fig. A.5 LONG. P5 VS. ALTIT. (Liapunov IAS)

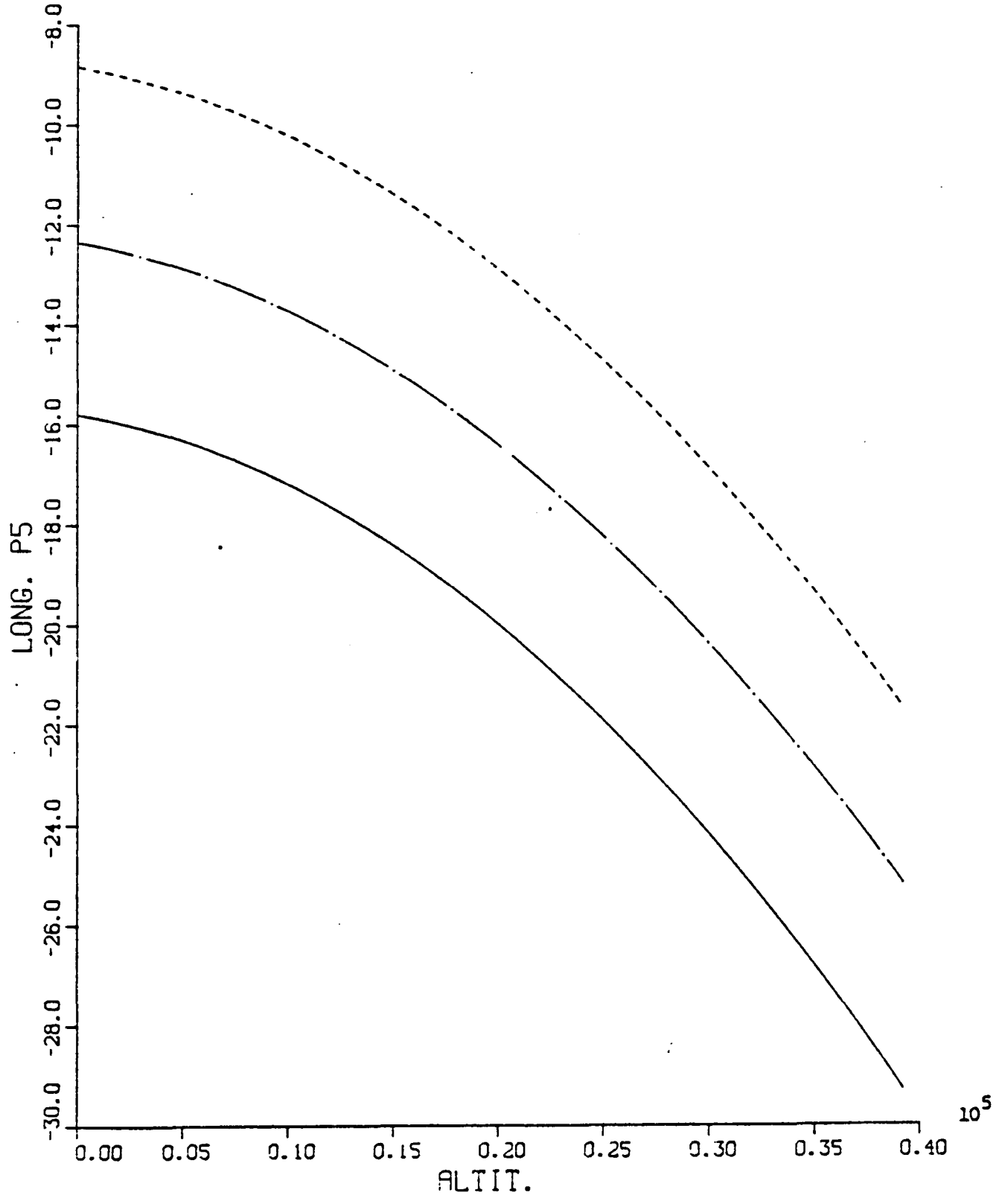

Fig. A.6 LONG. P6 VS. ALTIT. (Liapunov IAS)

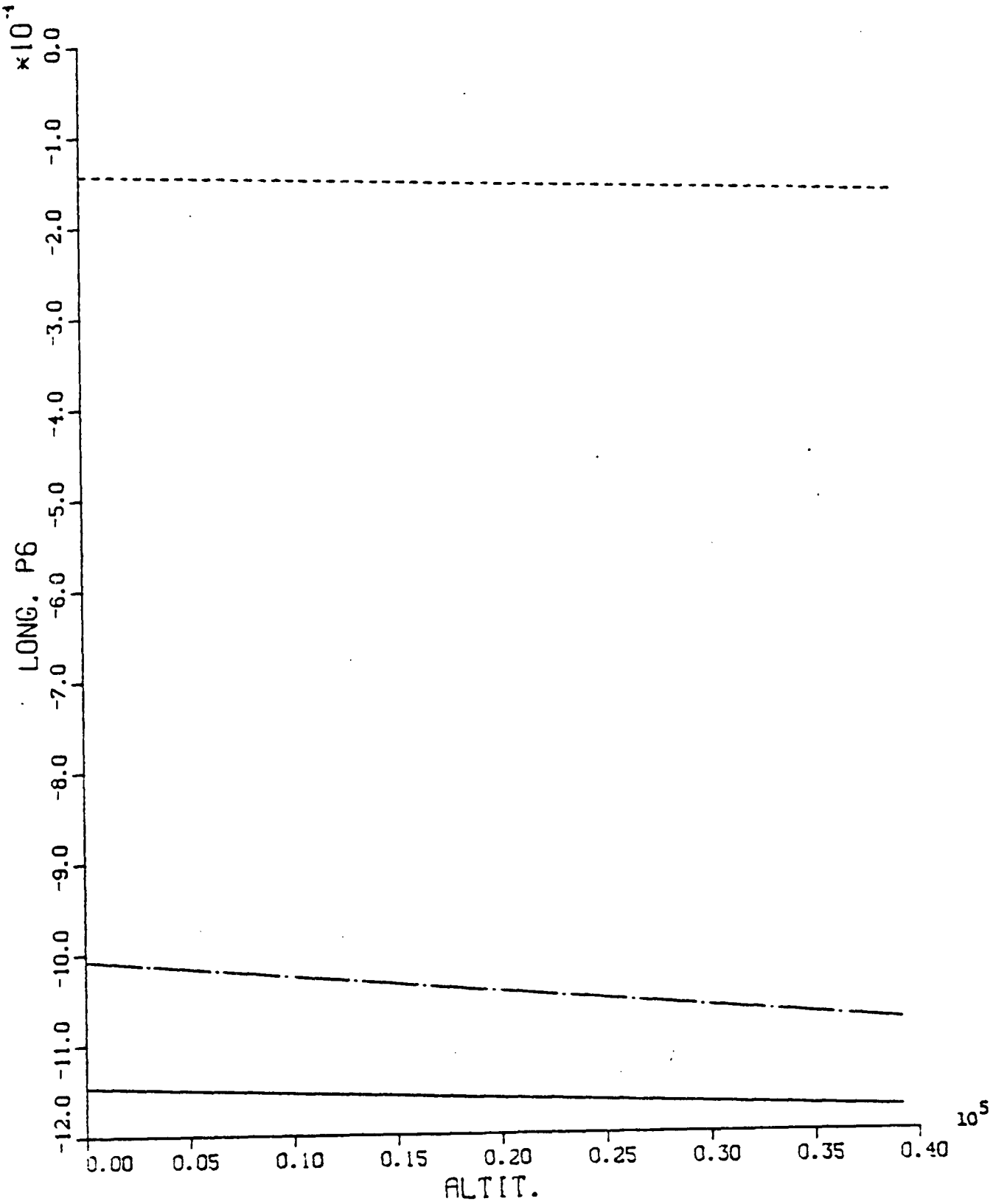

Fig. A.7 LONG. P7 VS. ALTIT. (Liapunov IAS)

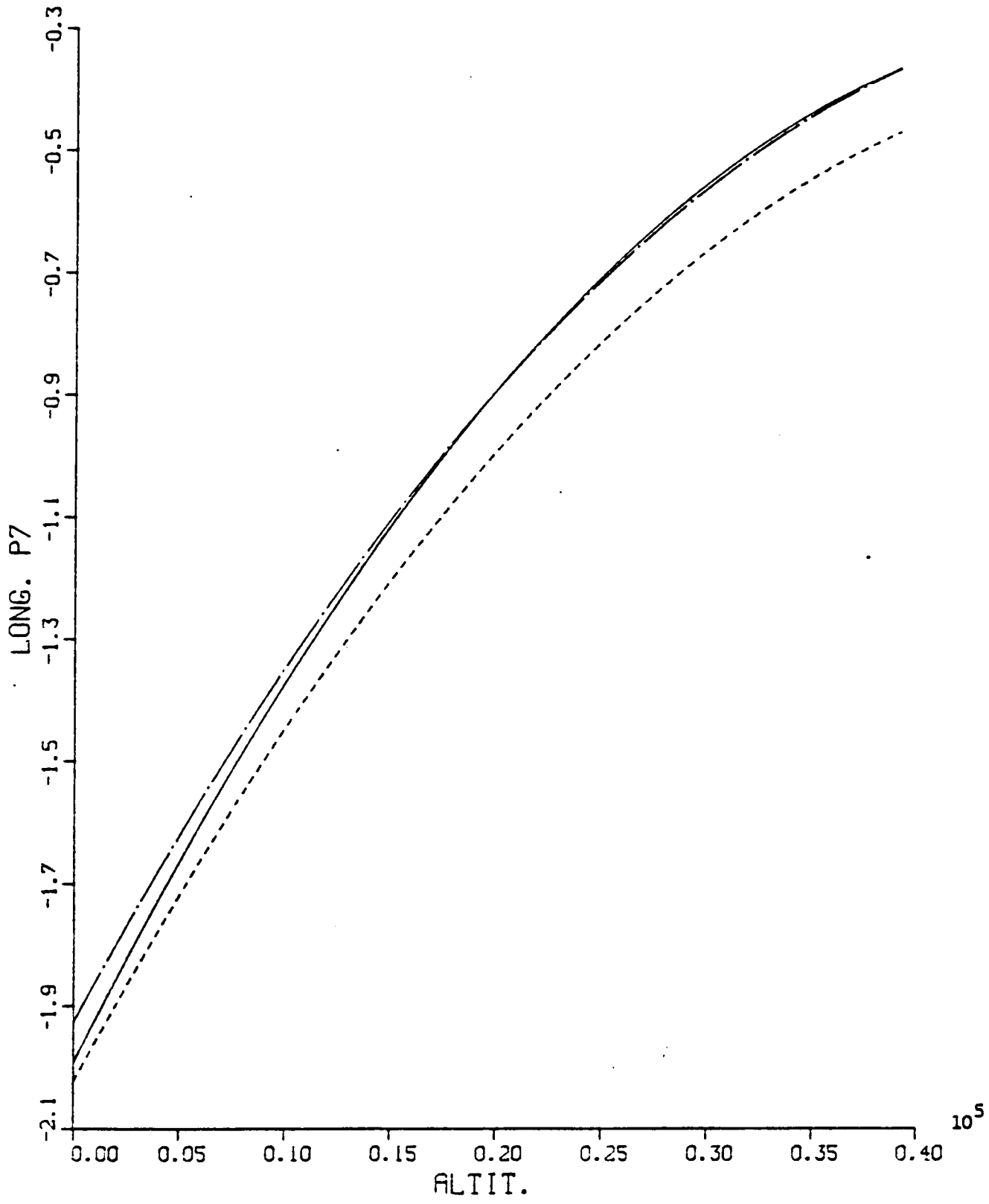

Fig. A.8 LONG. P8 VS. ALTIT. (Liapunov IAS)

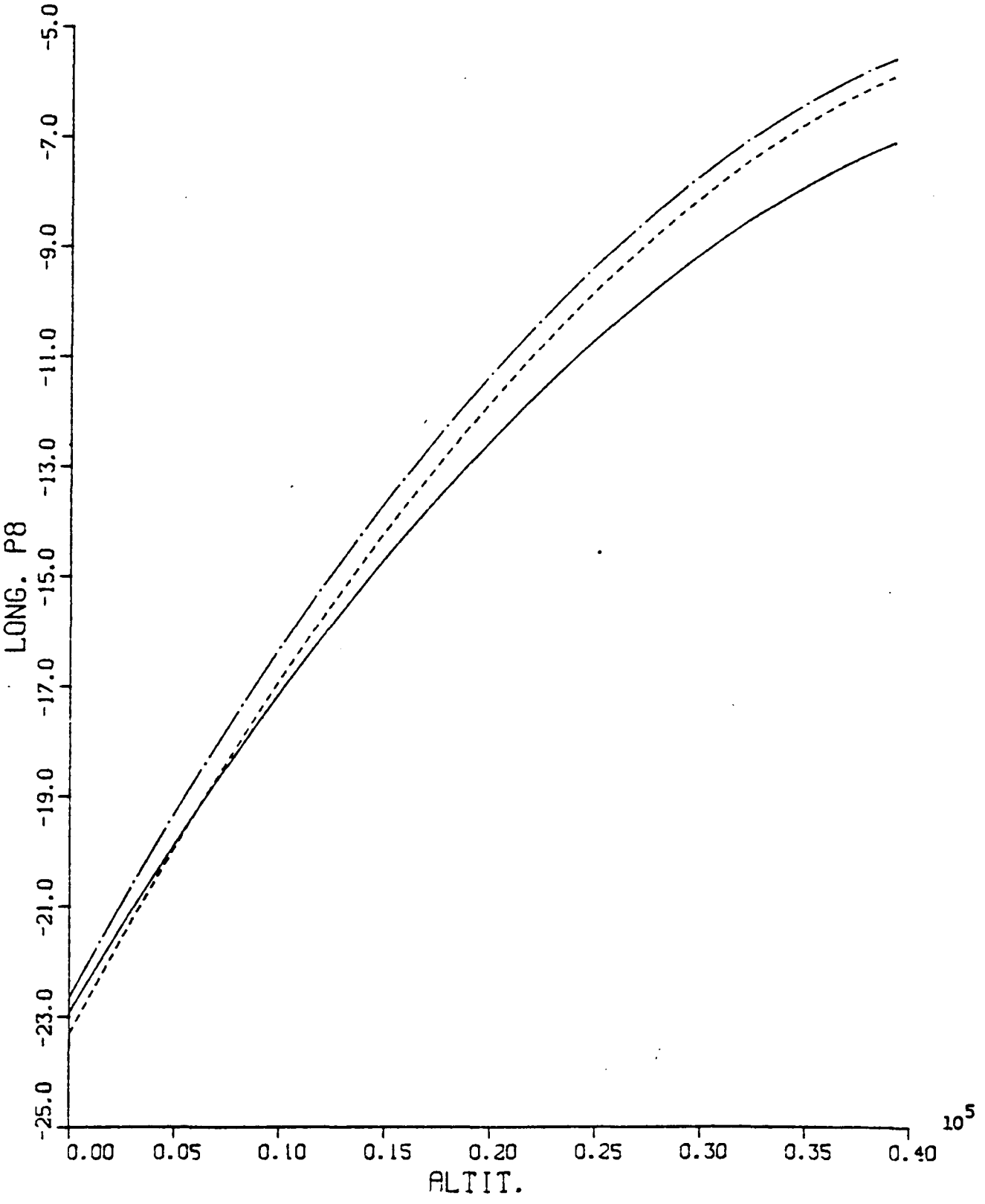

Fig. A.9 LONG. P9 VS. ALTIT. (Liapunov IAS)

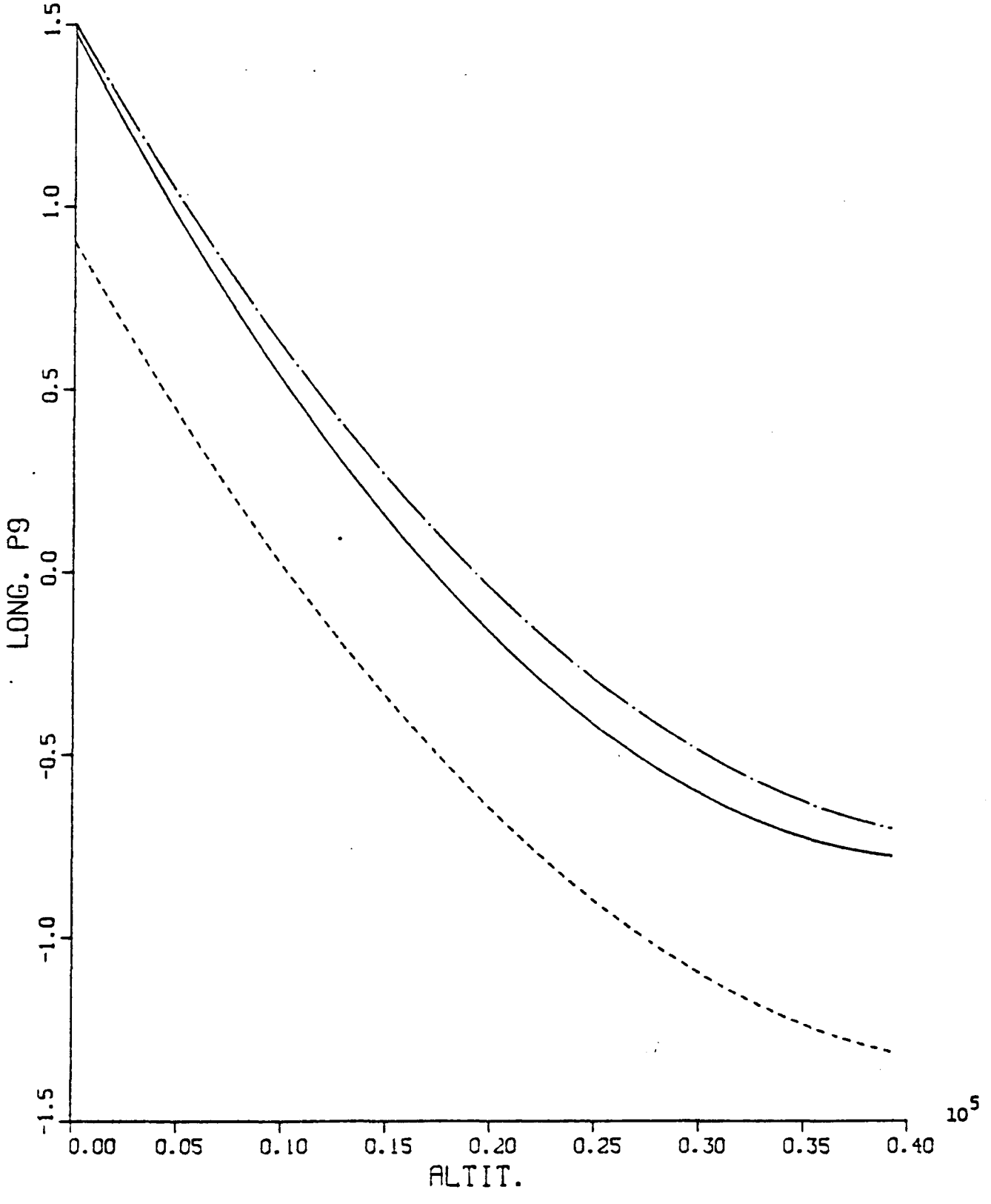

Fig. A.10 LONG. P10 VS. ALTIT. (Liapunov IAS)

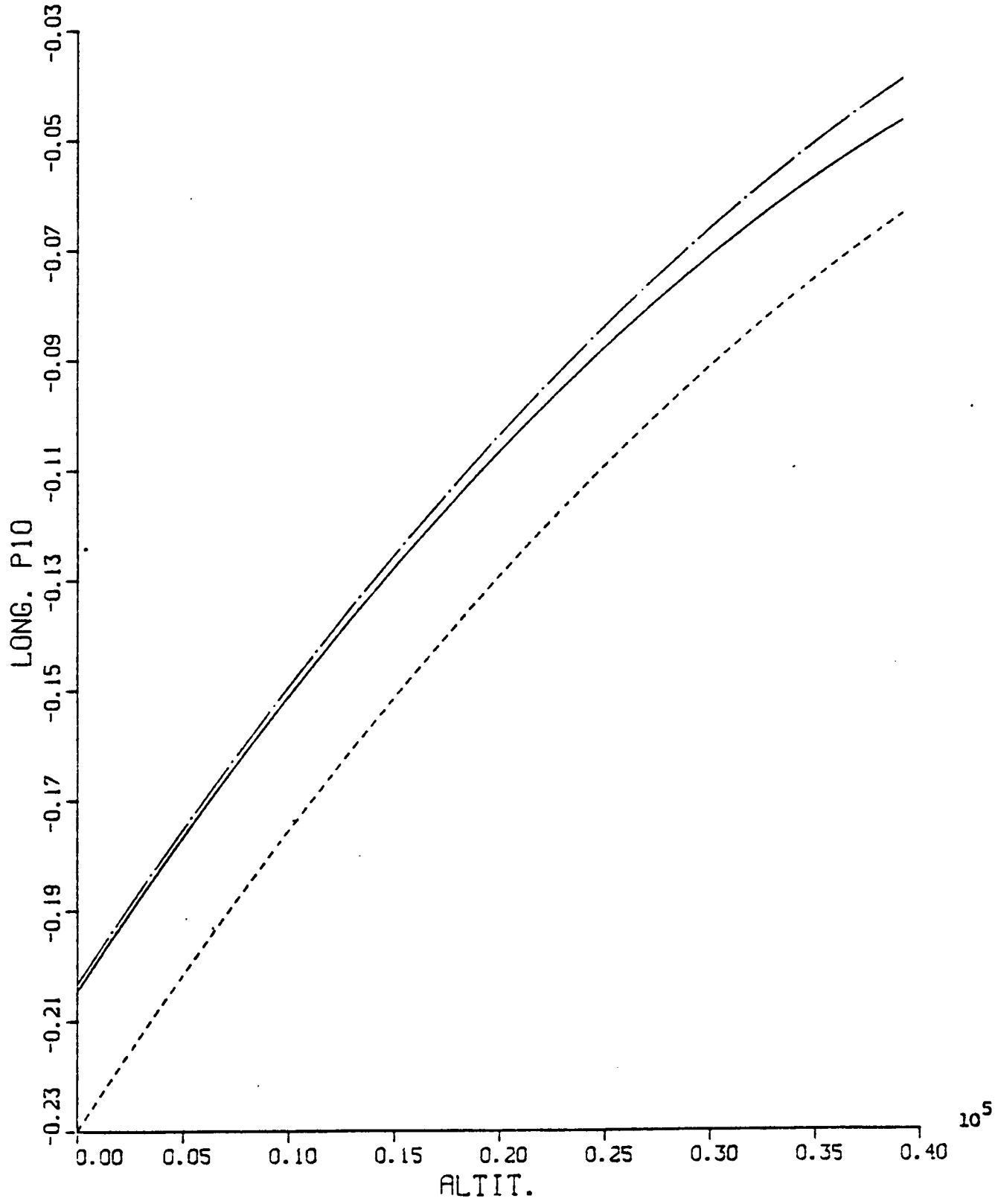

Fig. A.11 LONG. P1 VS. ALTIT. (Newton-Raphson IAS)

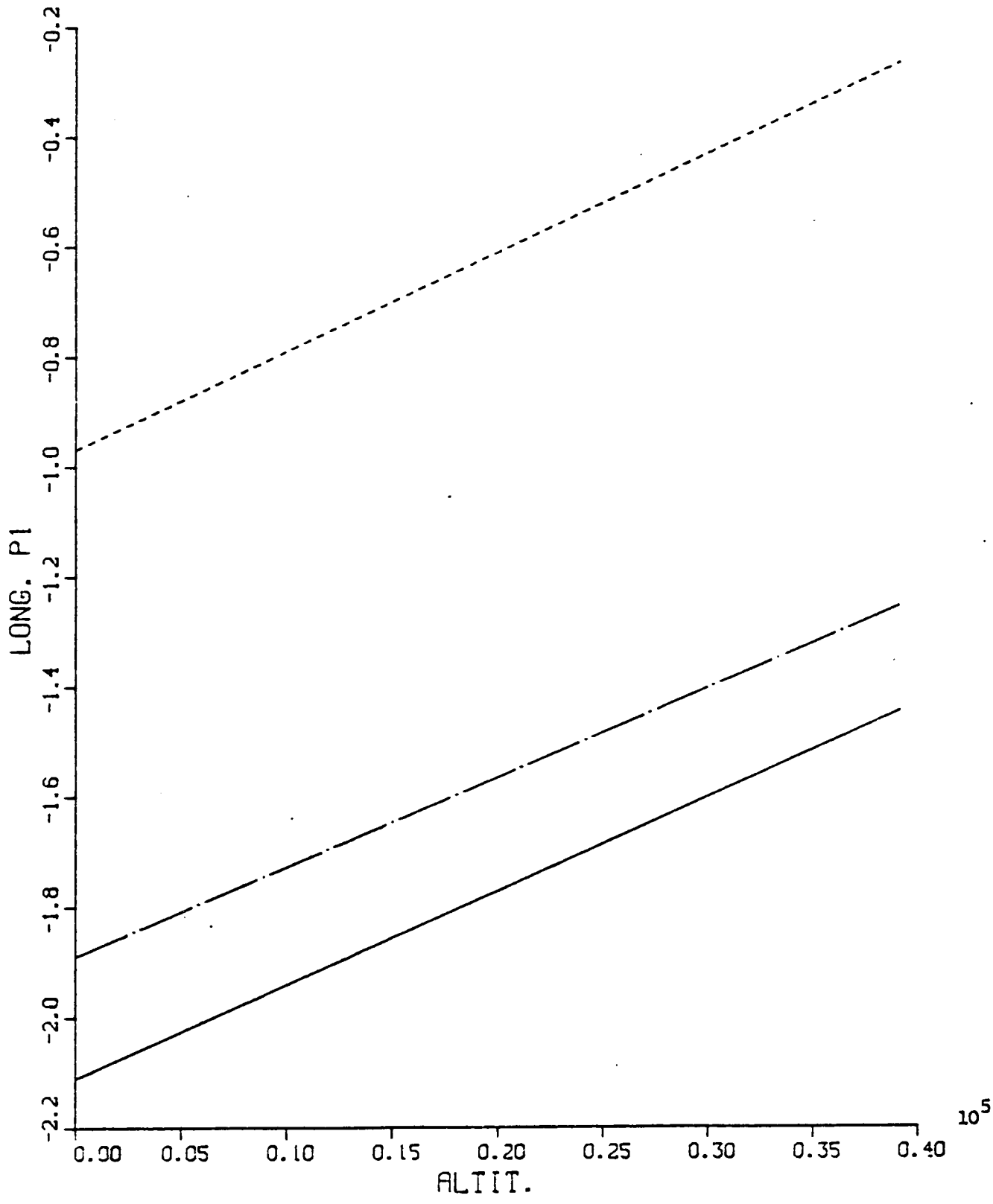

Fig. A.12 LONG. P2 VS. ALTIT. (Newton-Raphson IAS)

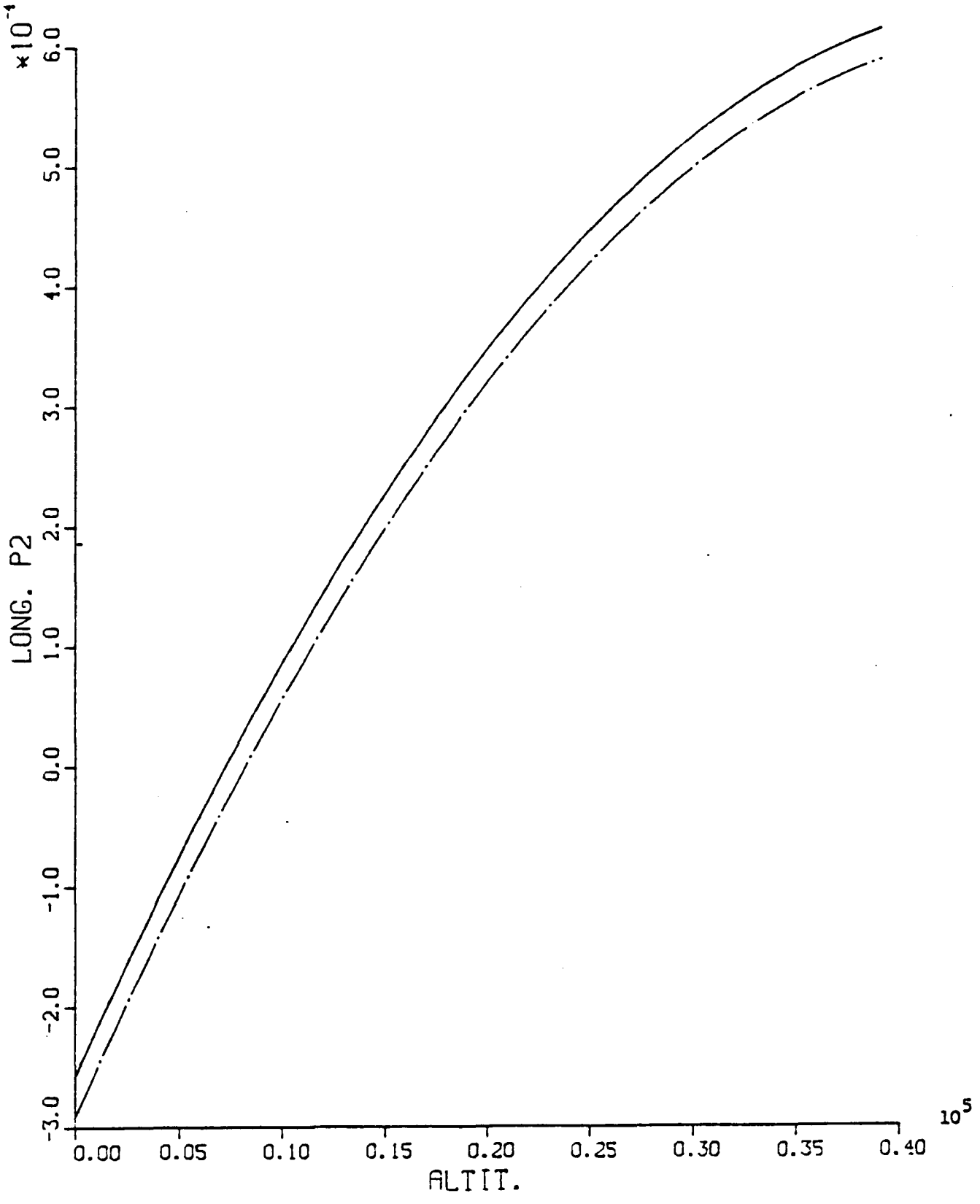

Fig. A.13 LONG. P3 VS. ALTIT. (Newton-Raphson IAS)

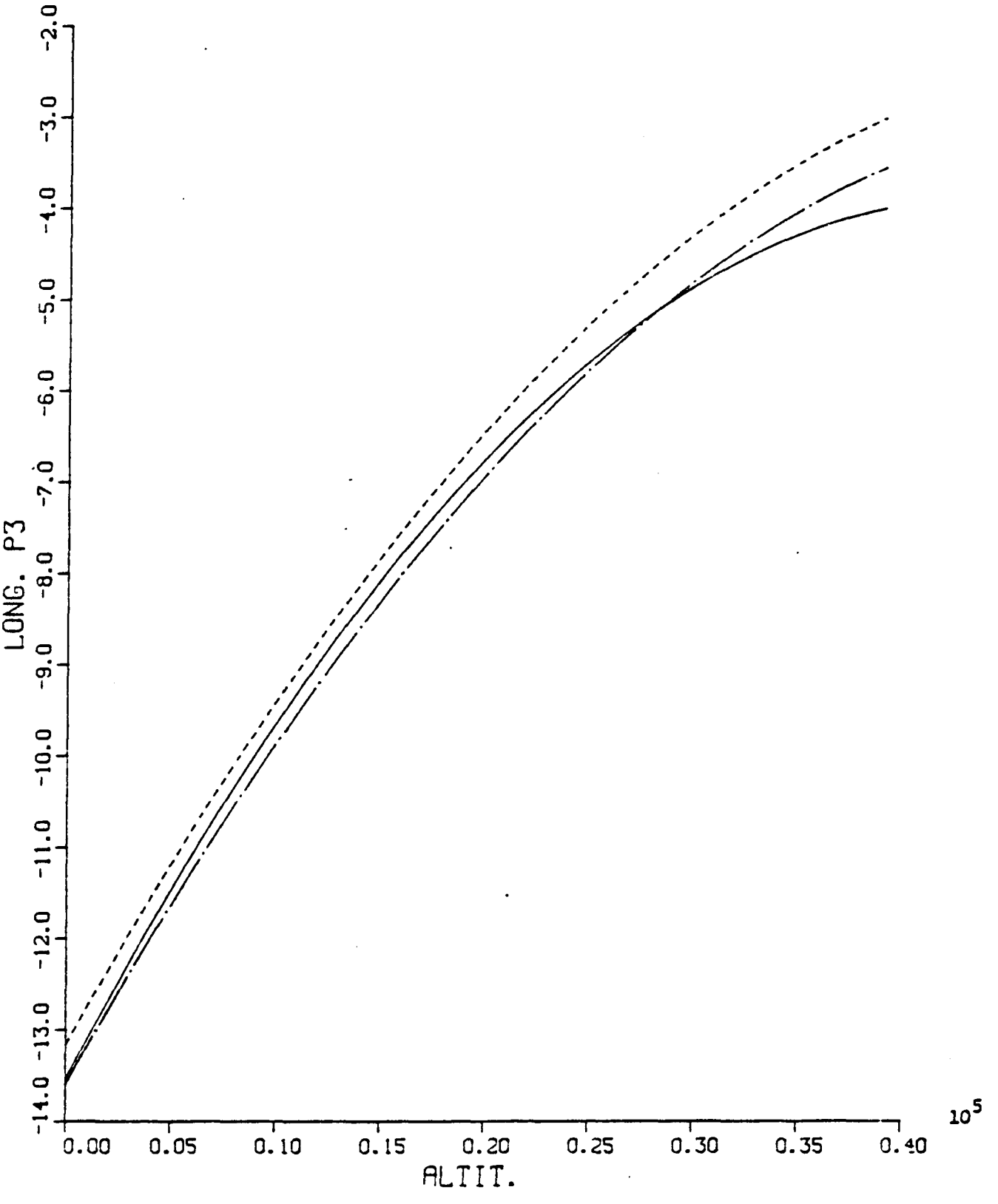

Fig. A.14 LONG. P4 VS. ALTIT. (Newton-Raphson IAS)

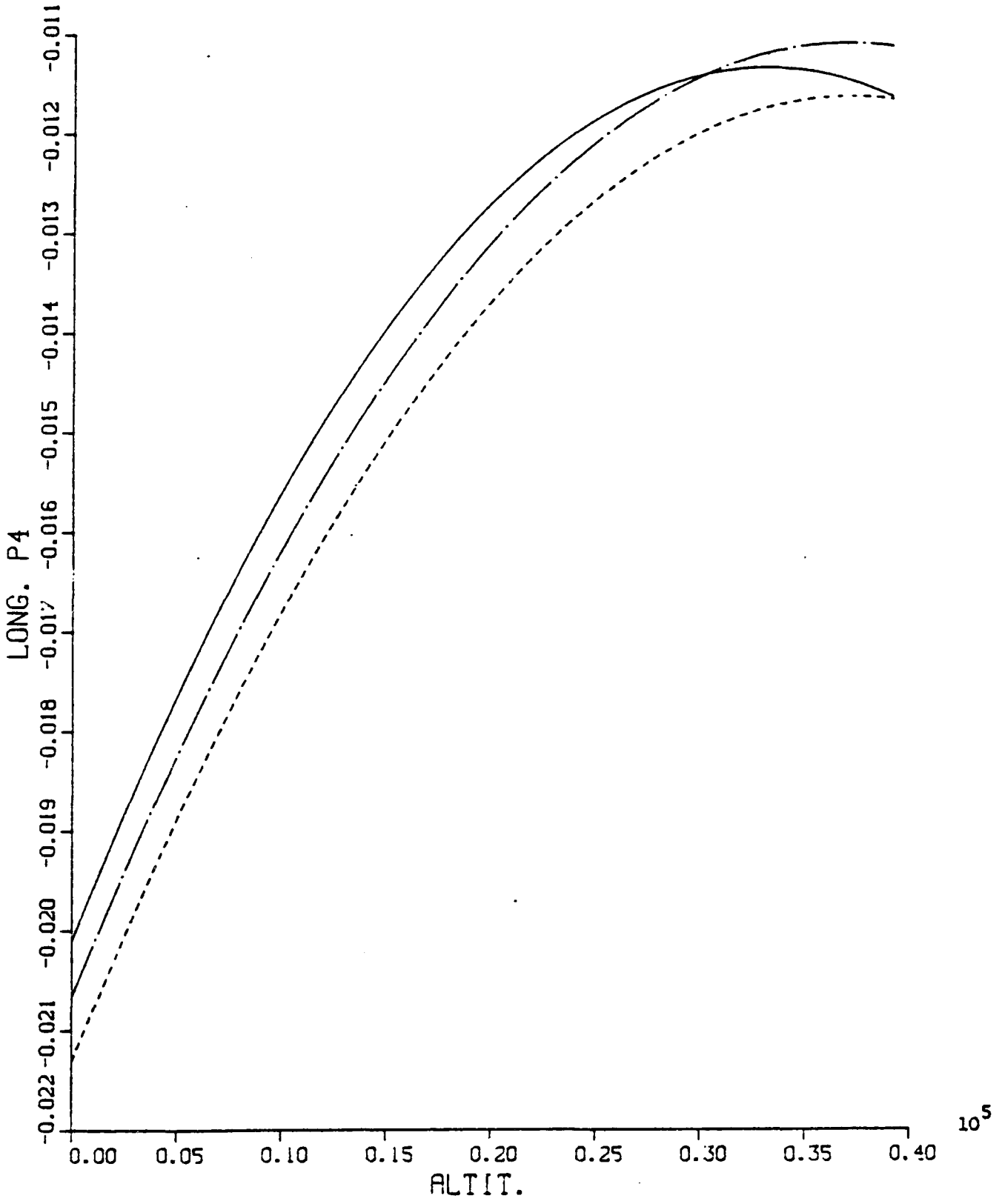

Fig. A.15 LONG. P5 VS. ALTIT. (Newton-Raphson IAS)

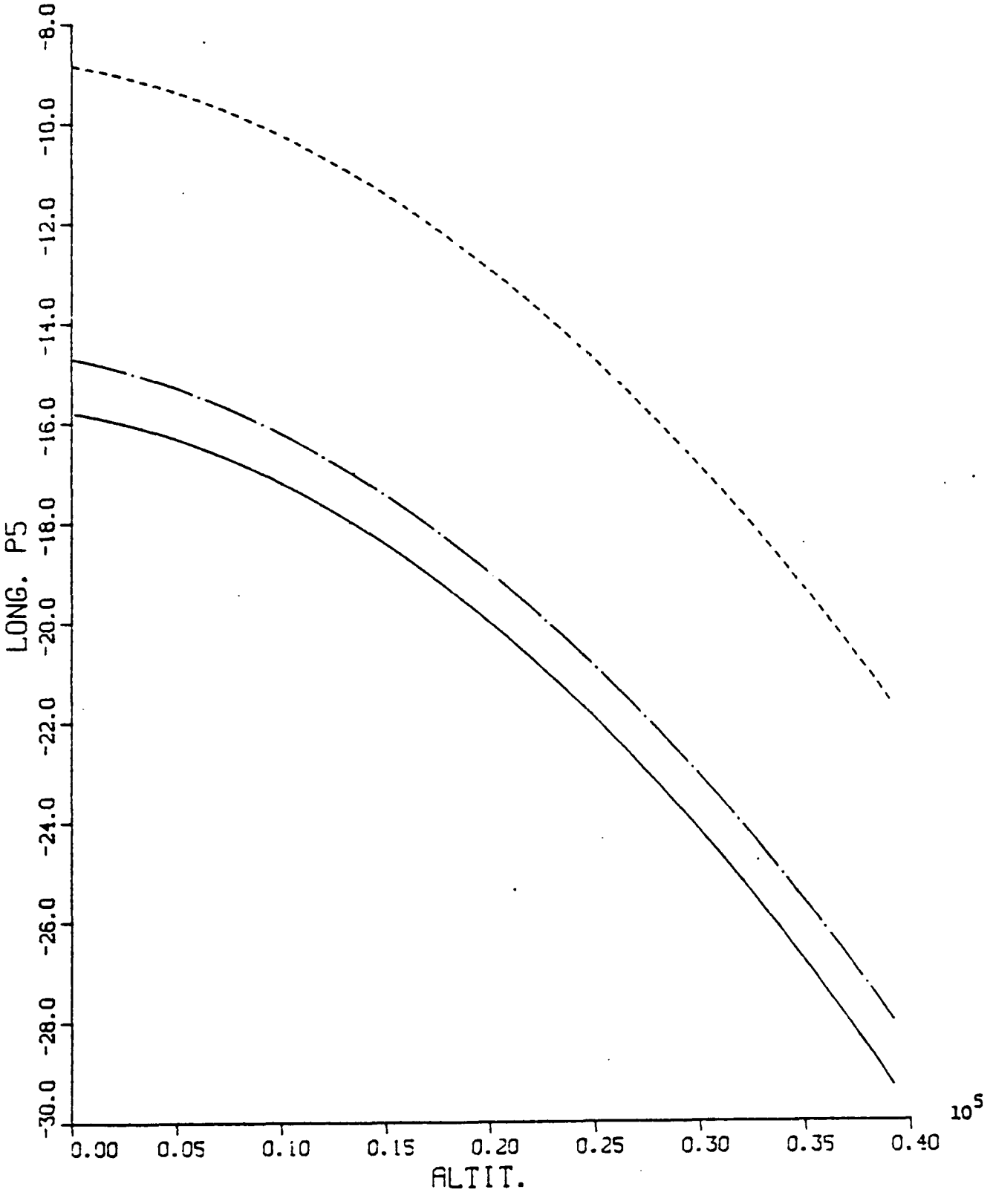

Fig. A.16 LONG. P6 VS. ALTIT. (Newton-Raphson IAS)

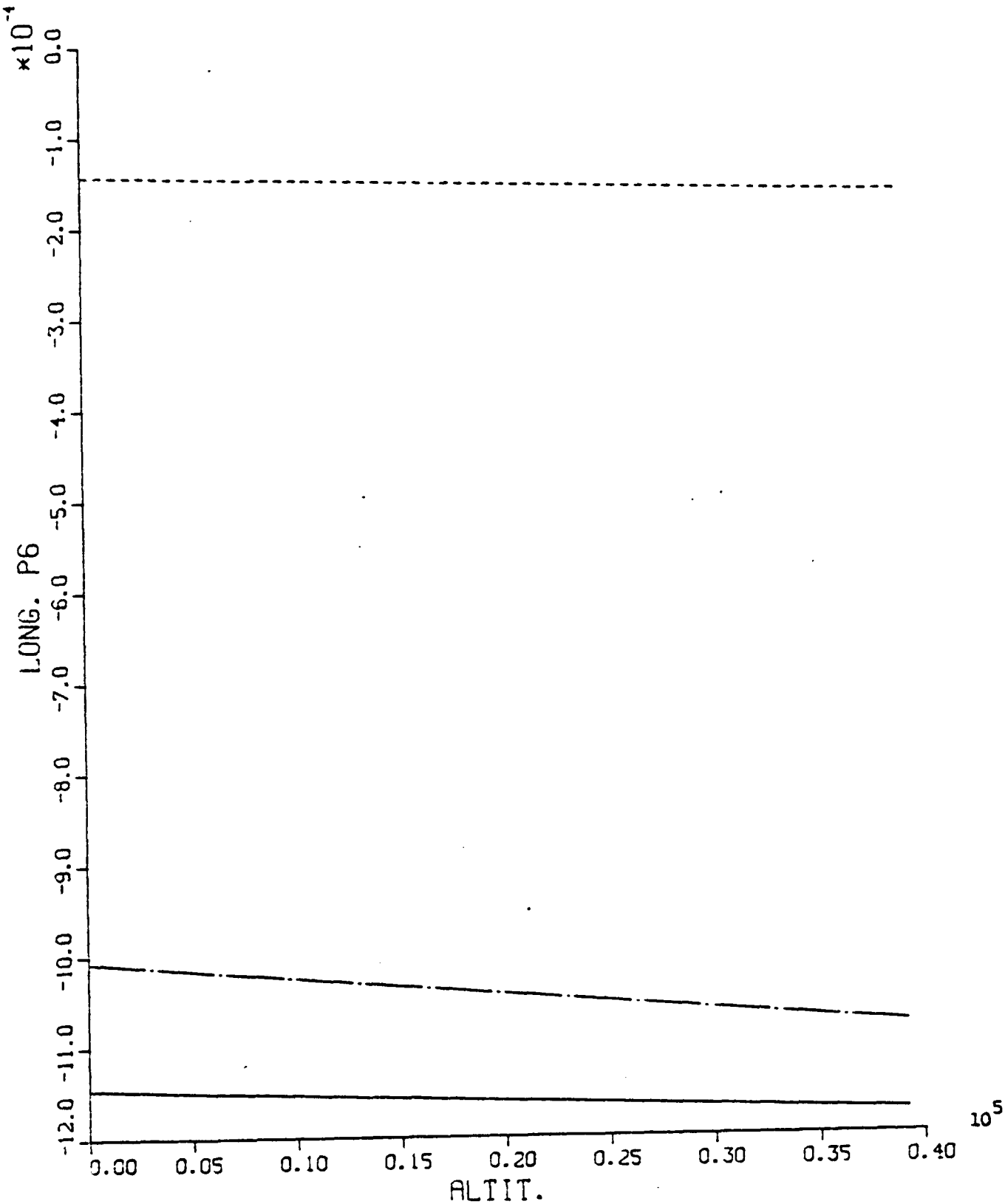

Fig. A.17 LONG. P7 VS. ALTIT. (Newton-Raphson IAS)

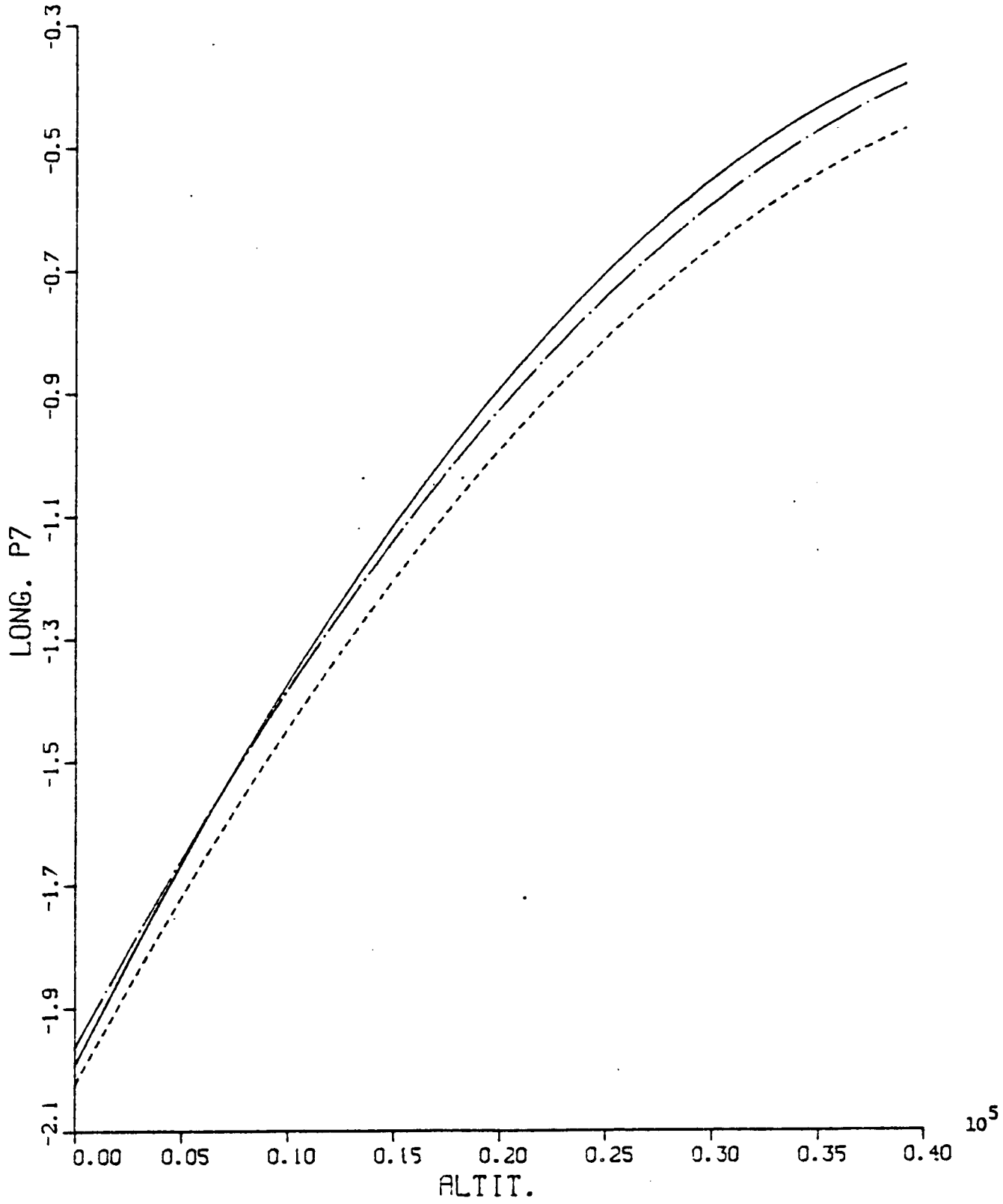

Fig. A.18 LONG. P8 VS. ALTIT. (Newton-Raphson IAS)

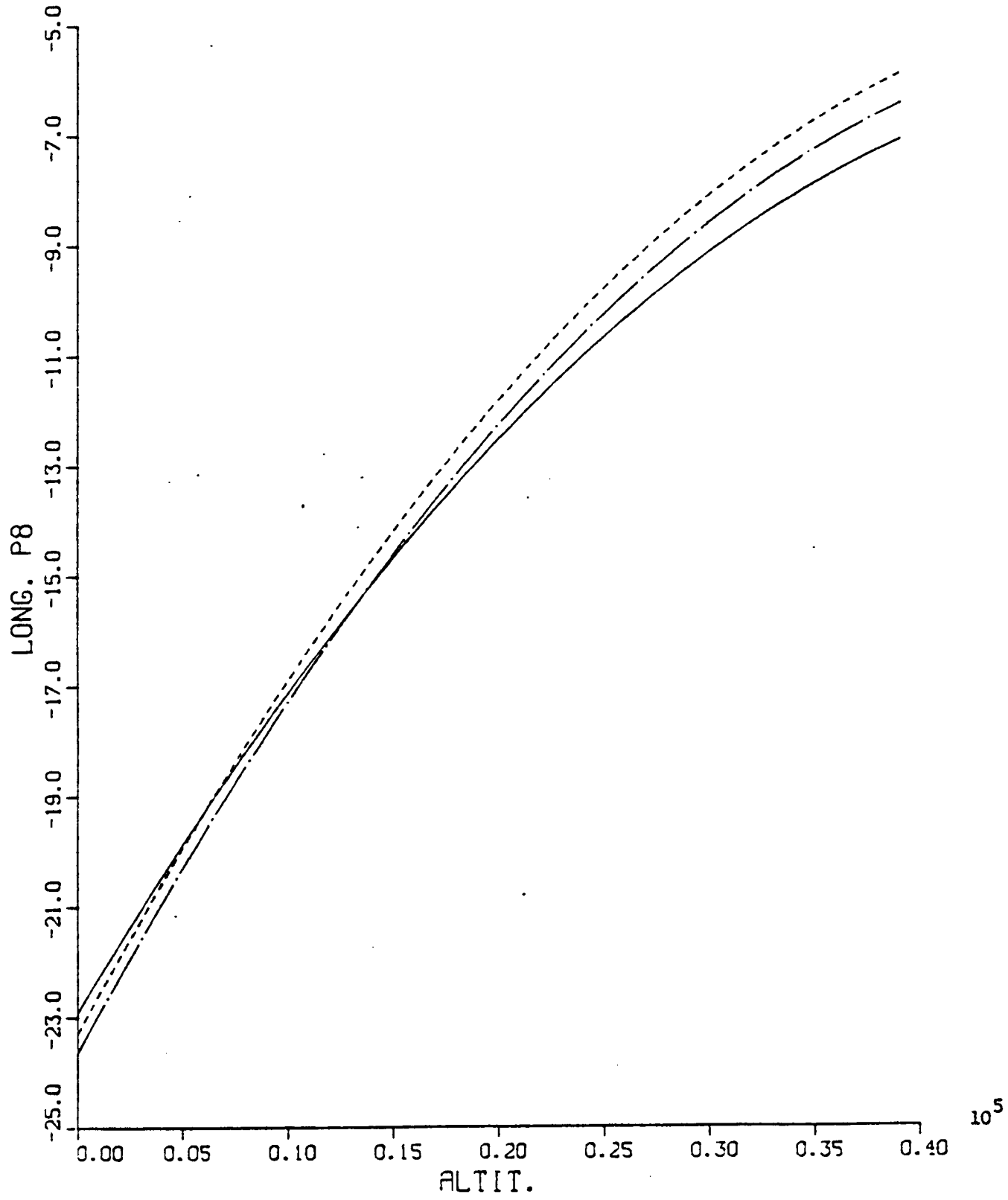

Fig. A.19 LONG. P9 VS. ALTIT. (Newton-Raphson IAS)

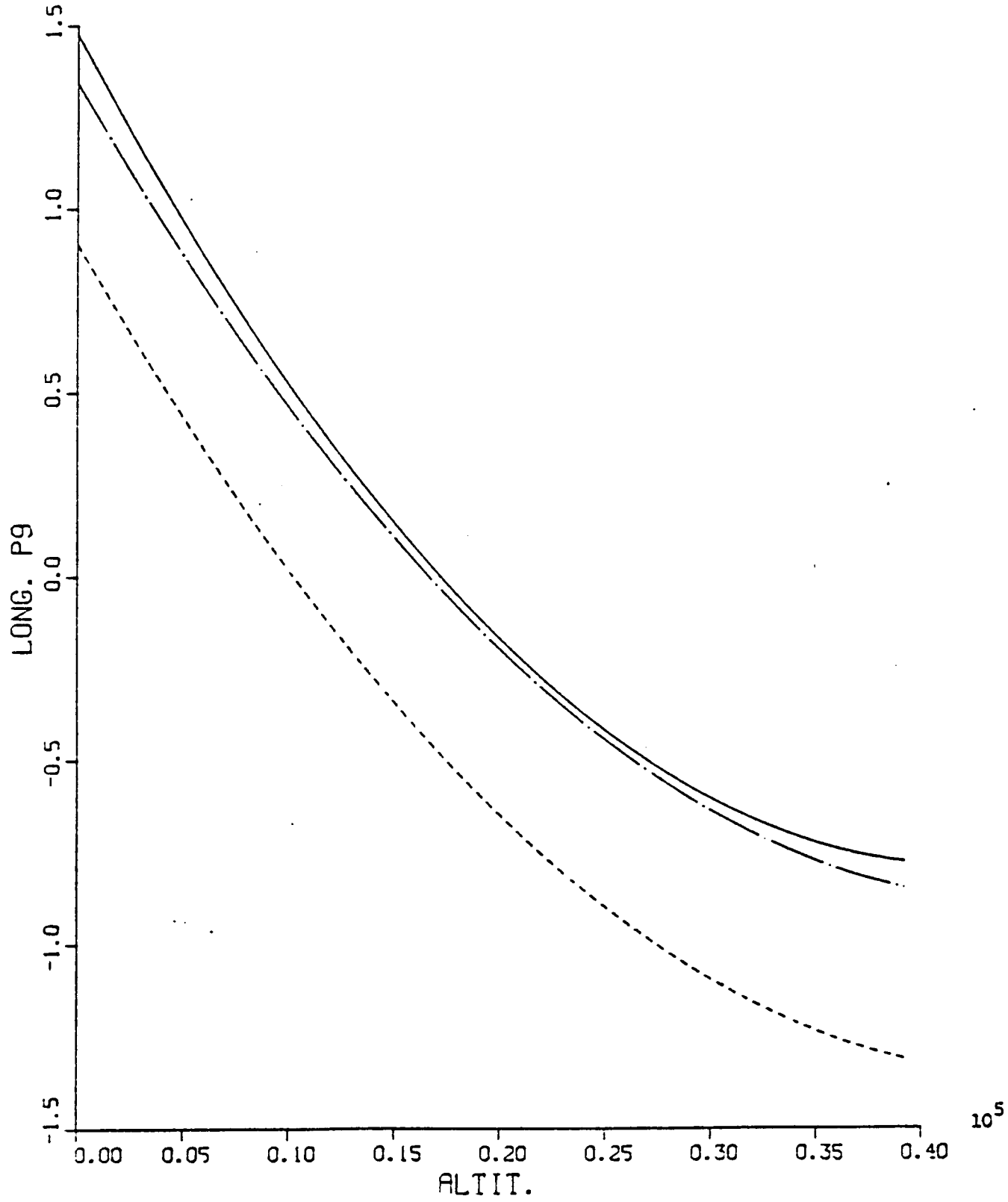

Fig. A.20 LONG. P10 VS. ALTIT. (Newton-Raphson IAS)

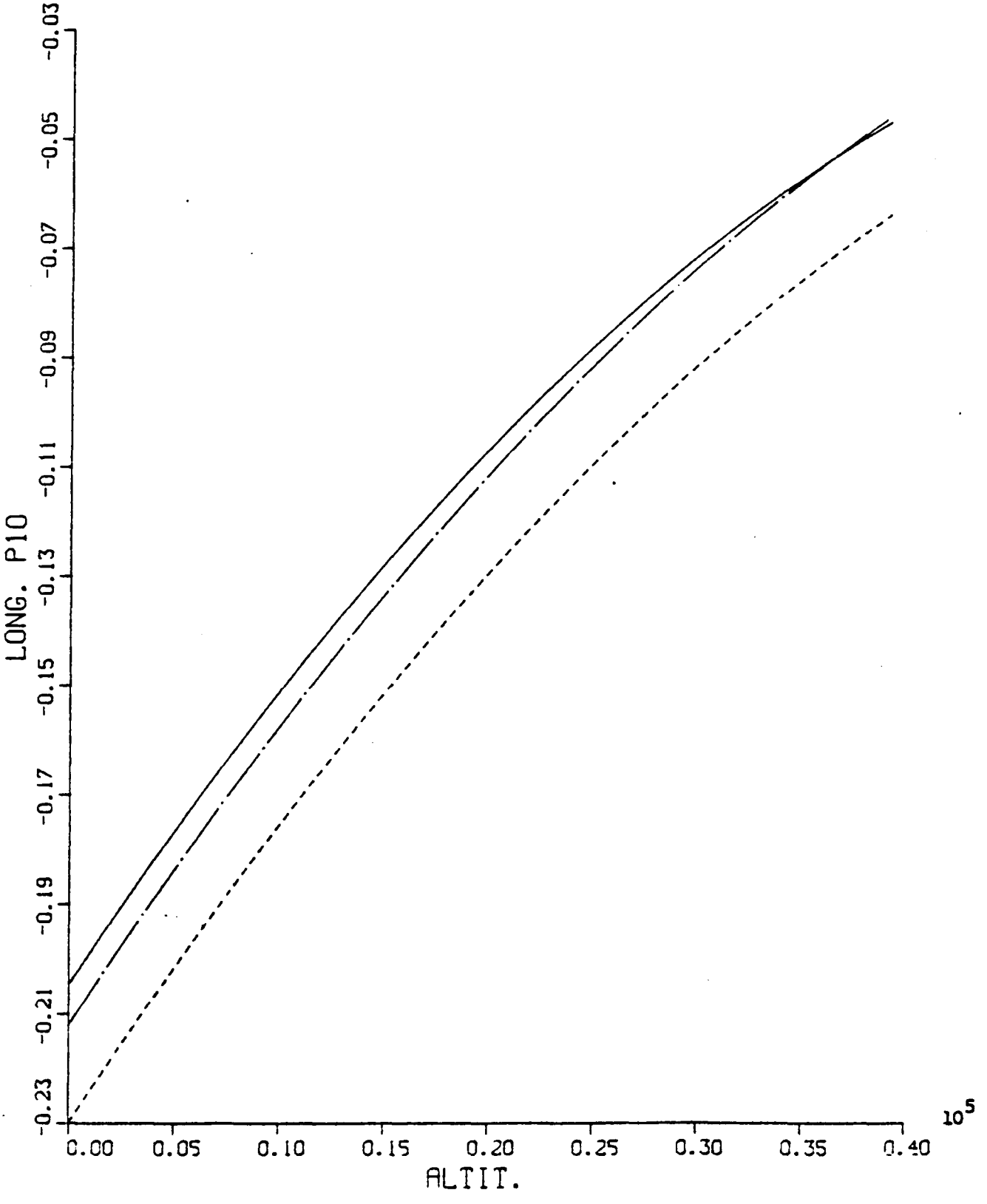

Fig. A.21 LATR. P1 VS. ALTIT. (Liapunov IAS)

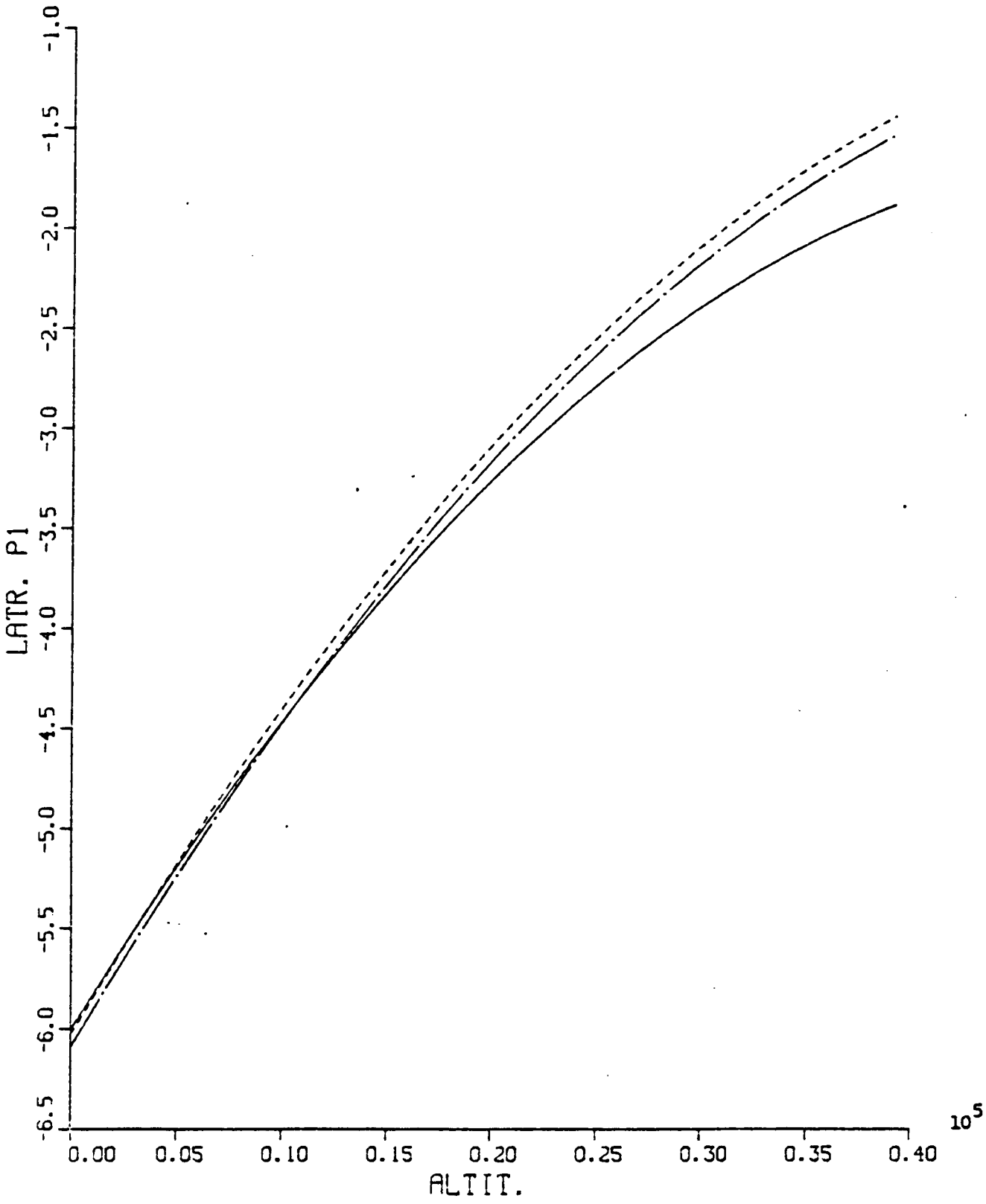

Fig. A.22 LATR. P2 VS. ALTIT. (Liapunov IAS)

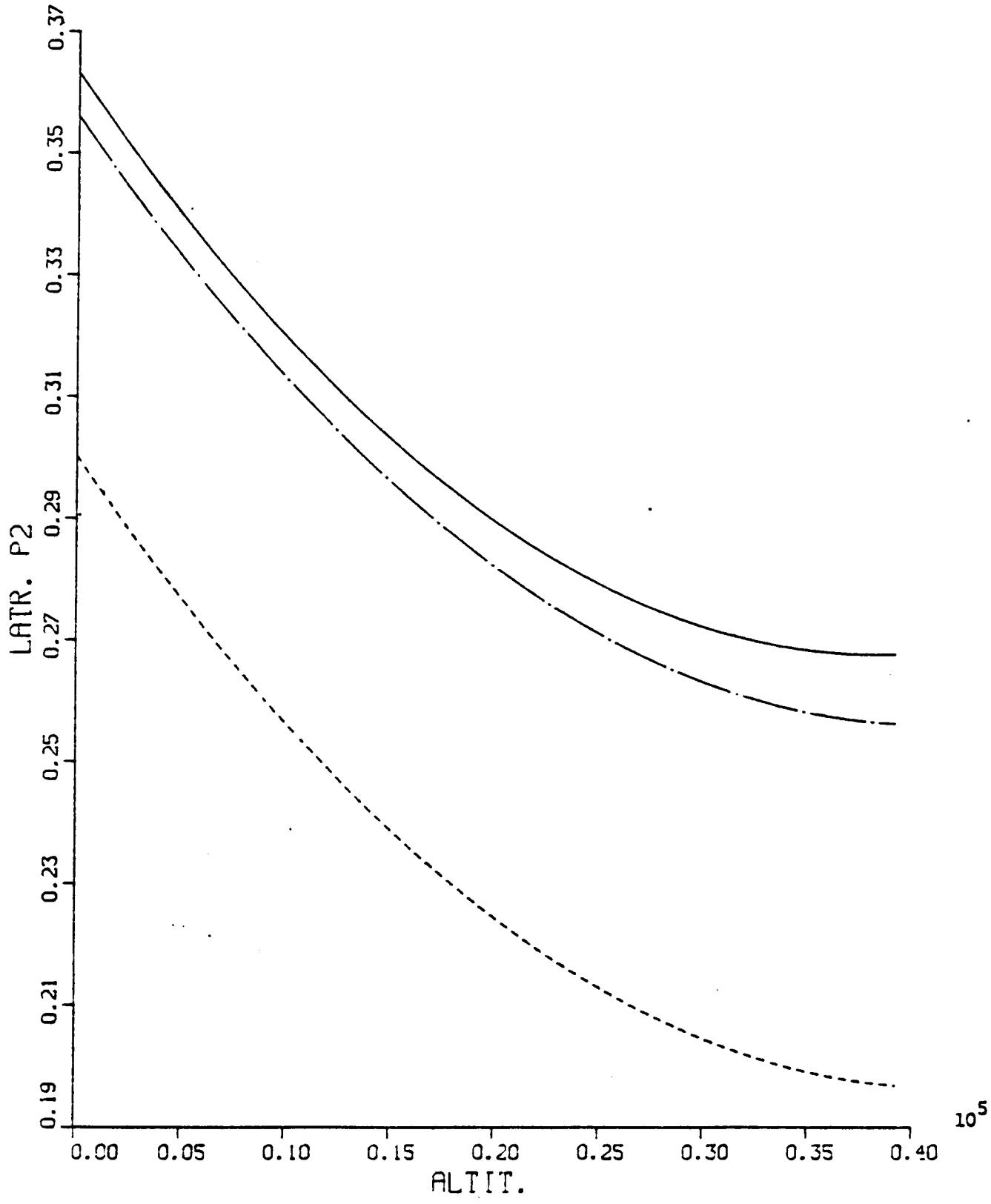

Fig. A.23 LATR. P3 VS. ALTIT. (Liapunov IAS)

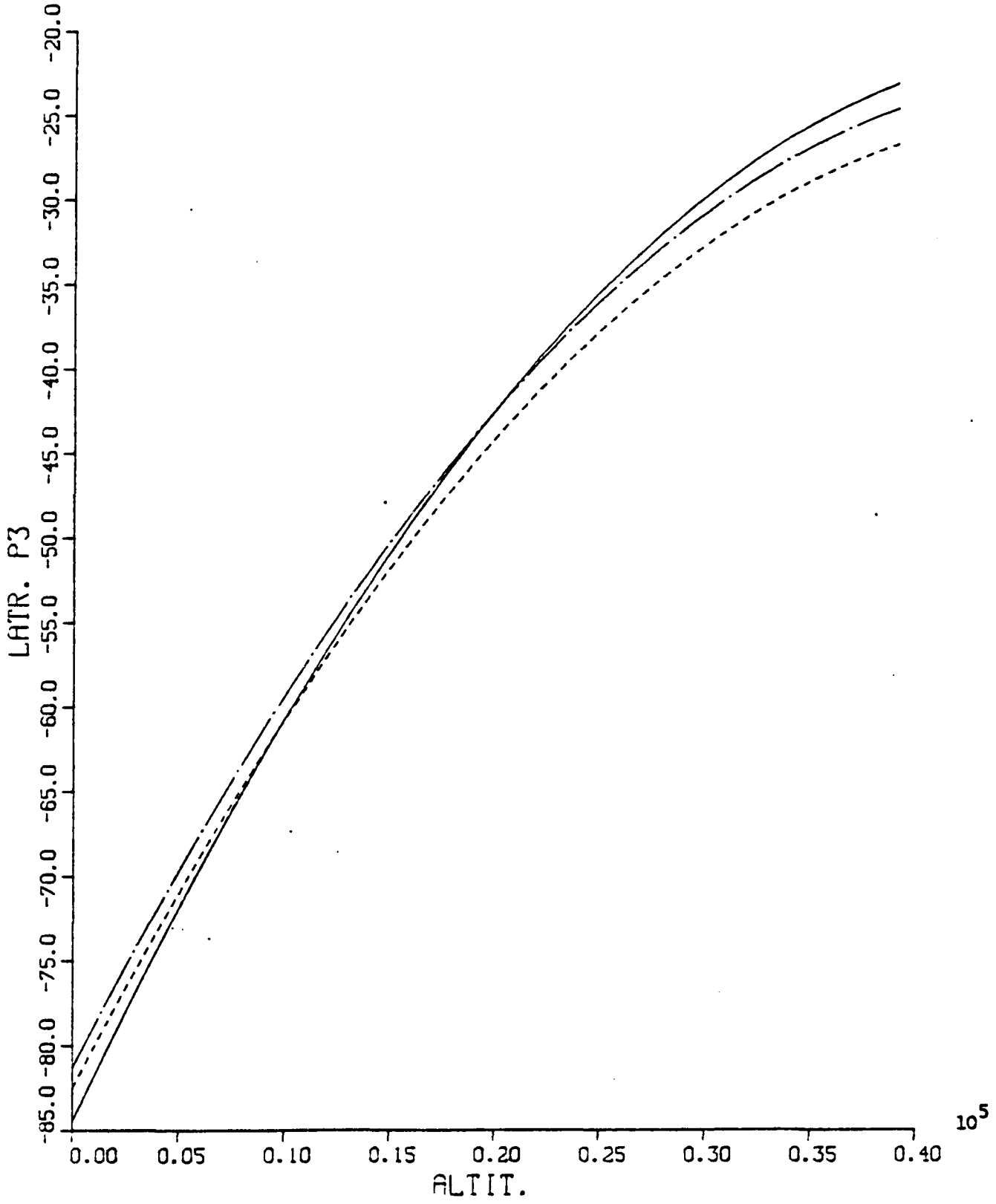

Fig. A.24 LATR. P4 VS. ALTIT. (Liapunov IAS)

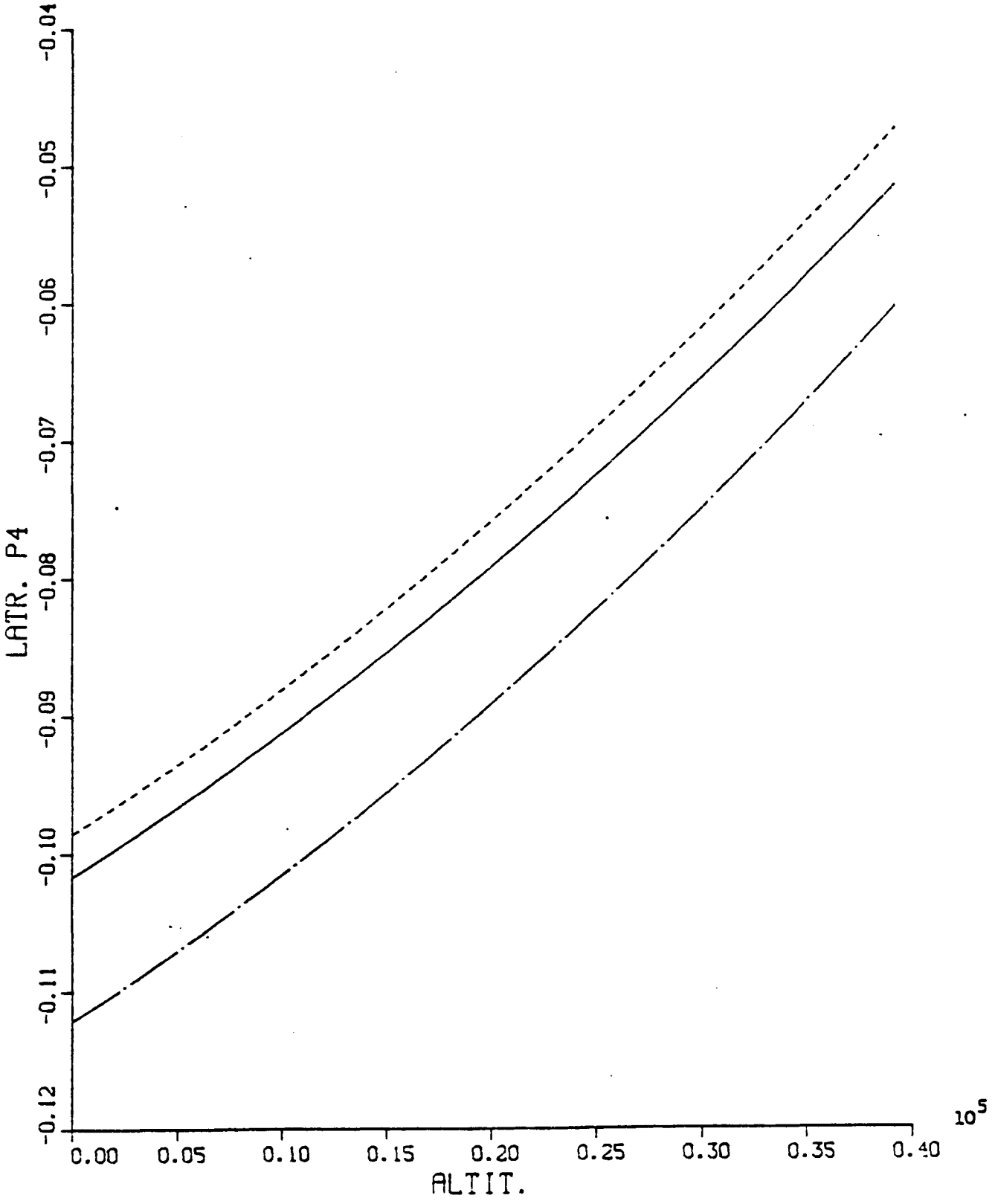

Fig. A.25 LATR. P5 VS. ALTIT. (Liapunov IAS)

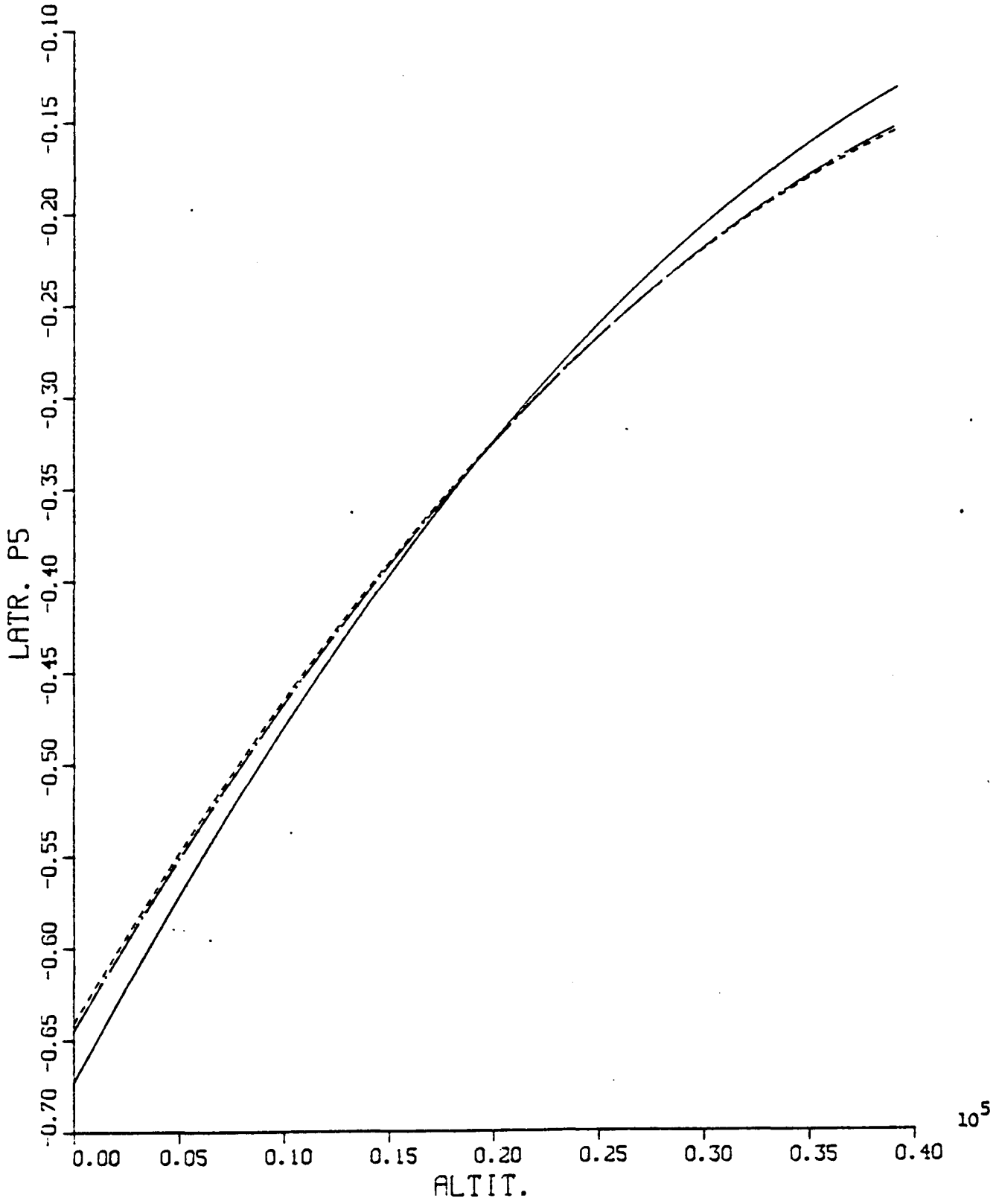

Fig. A.26 LATR. P6 VS. ALTIT. (Liapunov IAS)

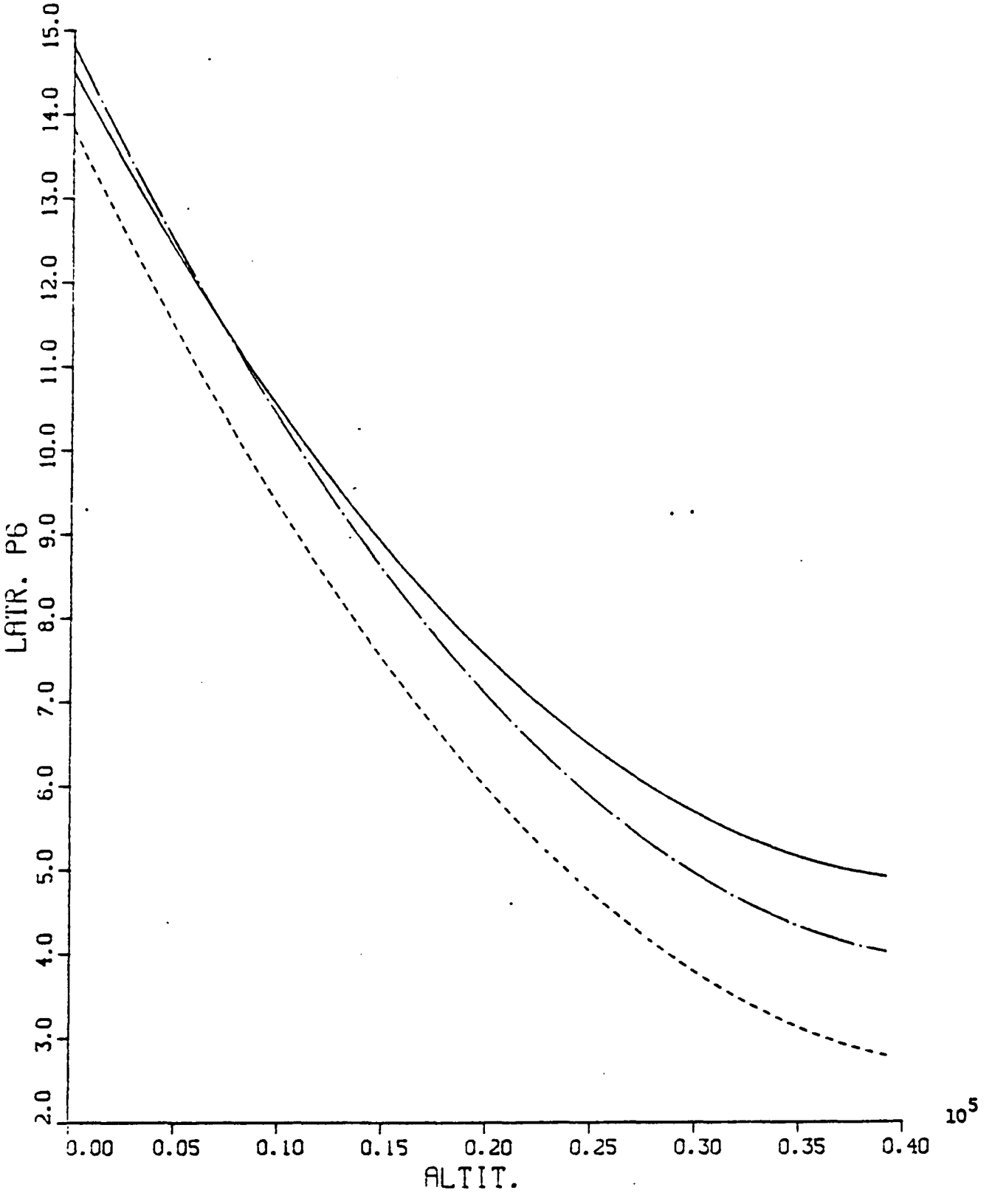

Fig. A.27 LATR. P7 VS. ALTIT. (Liapunov IAS)

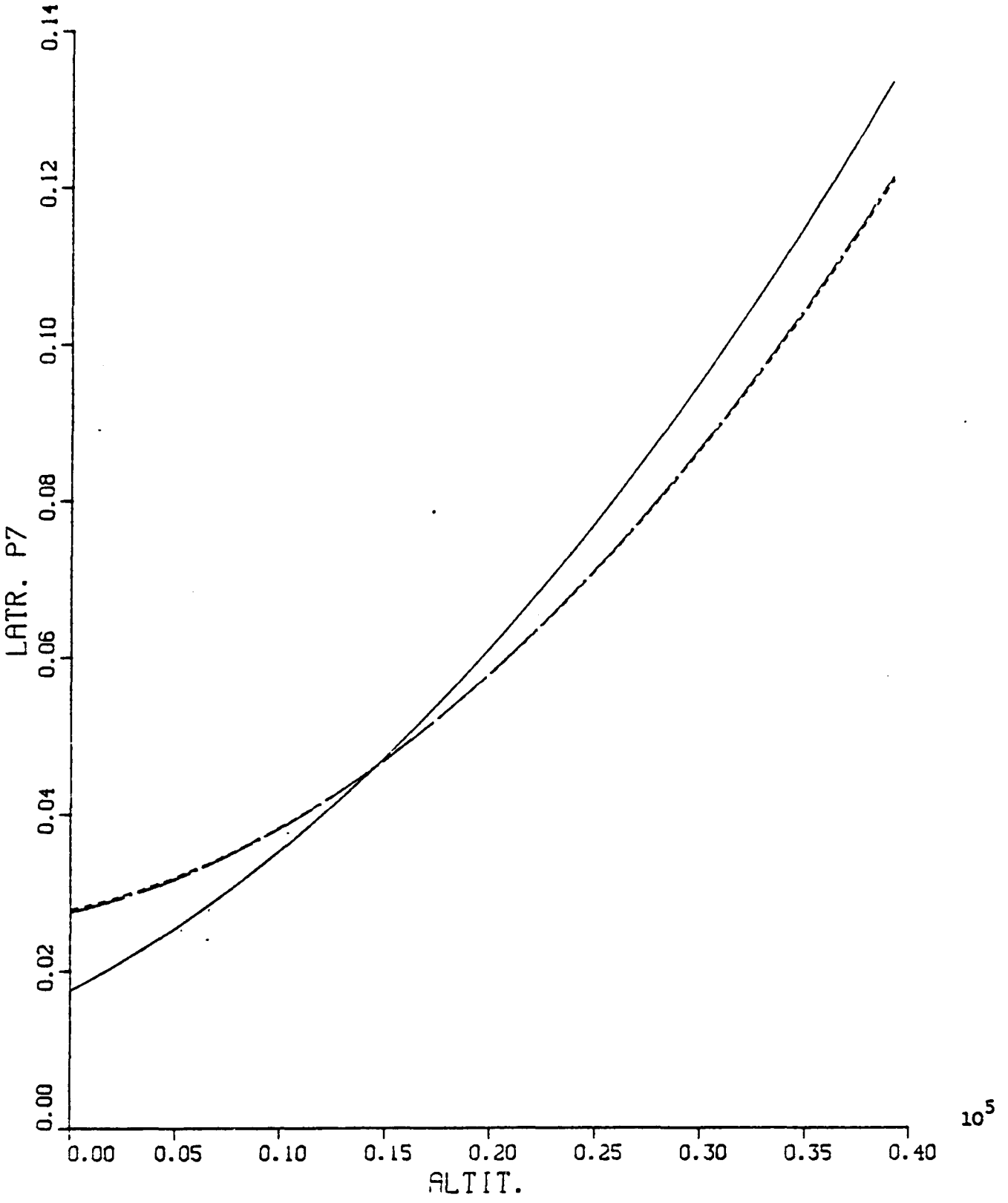

Fig. A.28 LATR. P8 VS. ALTIT. (Liapunov IAS)

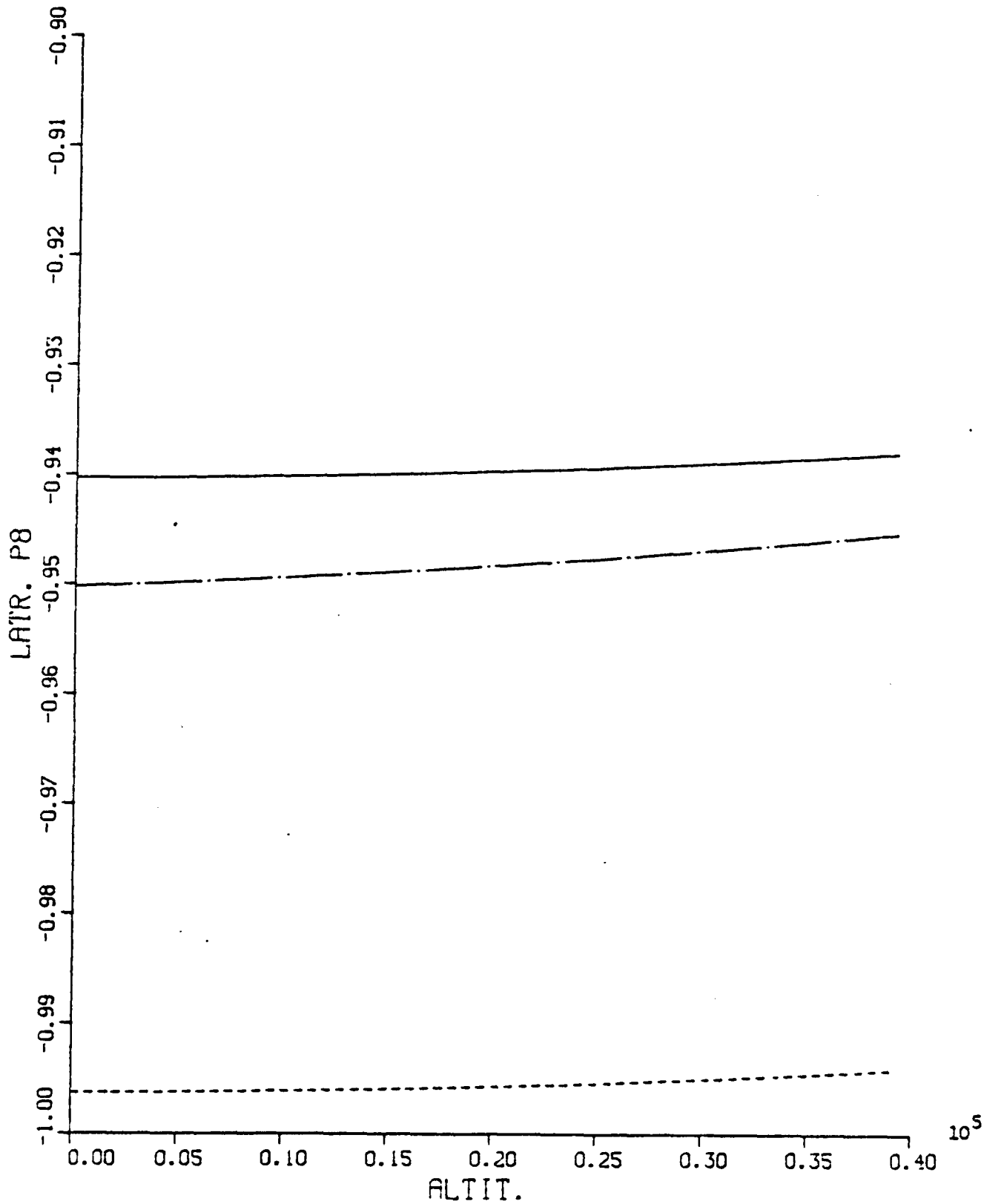

Fig. A.29 LATR. P9 VS. ALTIT. (Liapunov IAS)

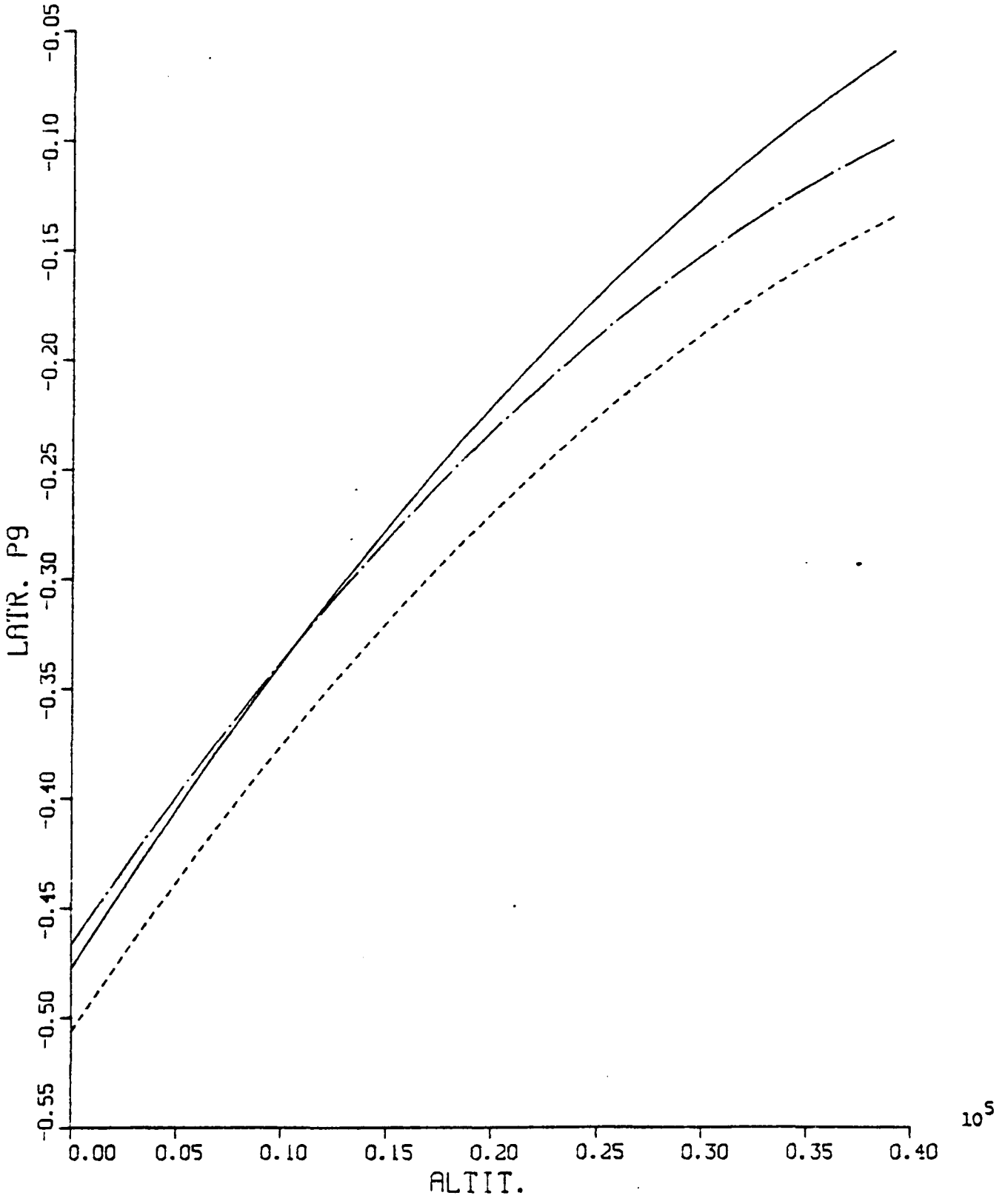

Fig. A.30 LATR. P10 VS. ALTIT. (Liapunov LAS)

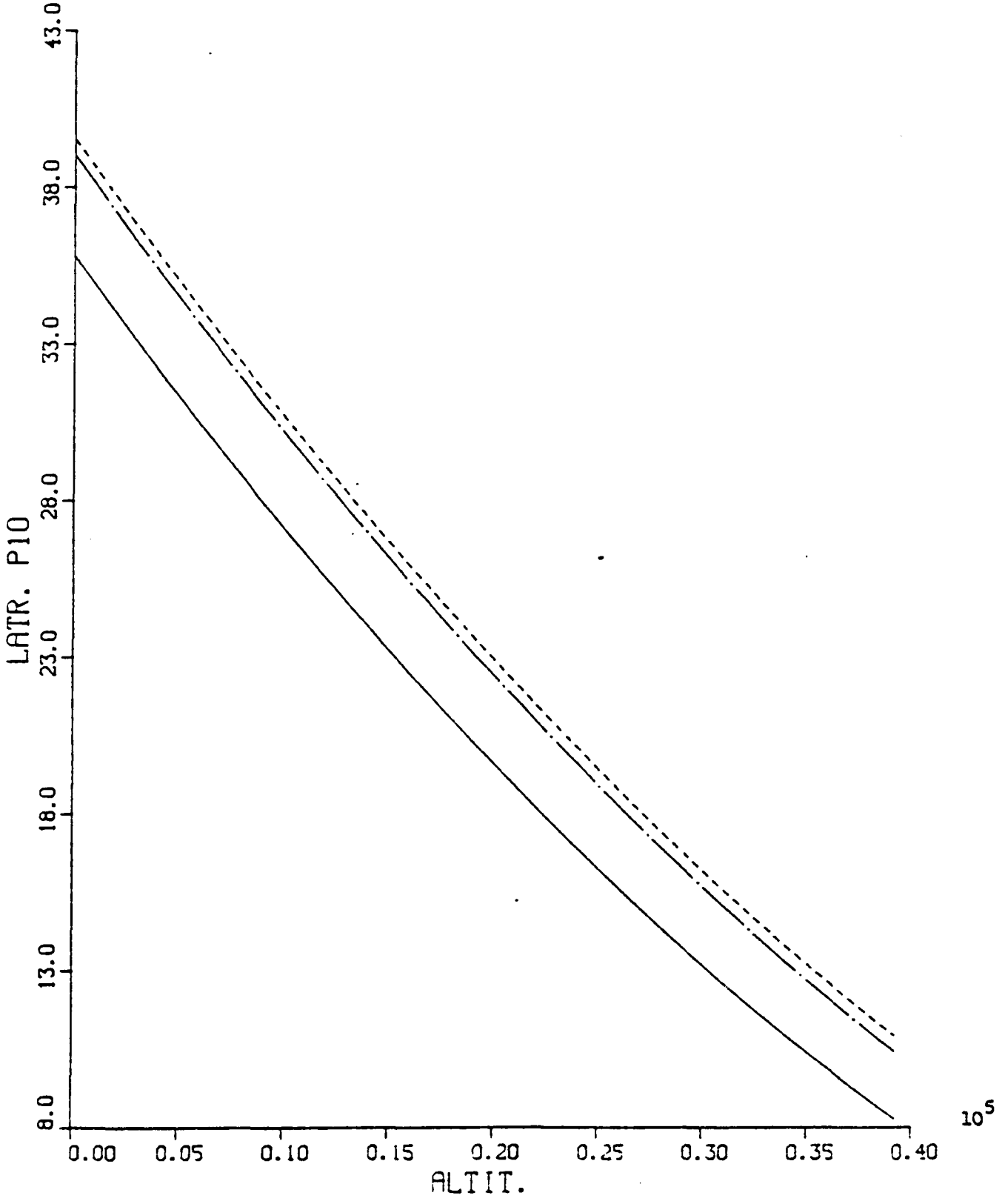

Fig. A.31 LATR. P11 VS. ALTIT. (Liapunov IAS)

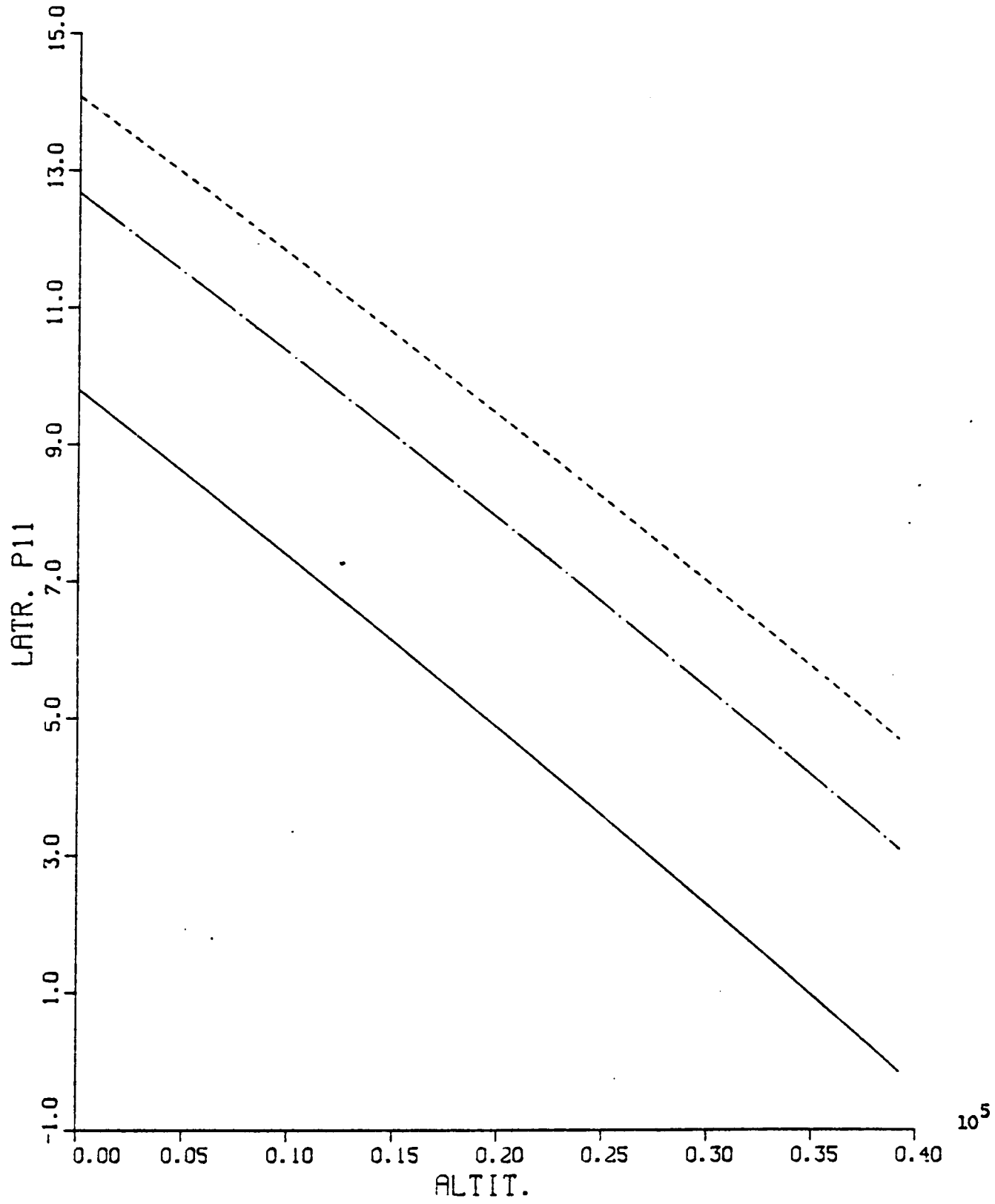

Fig. A.32 LATR. P12 VS. ALTIT. (Liapunov IAS)

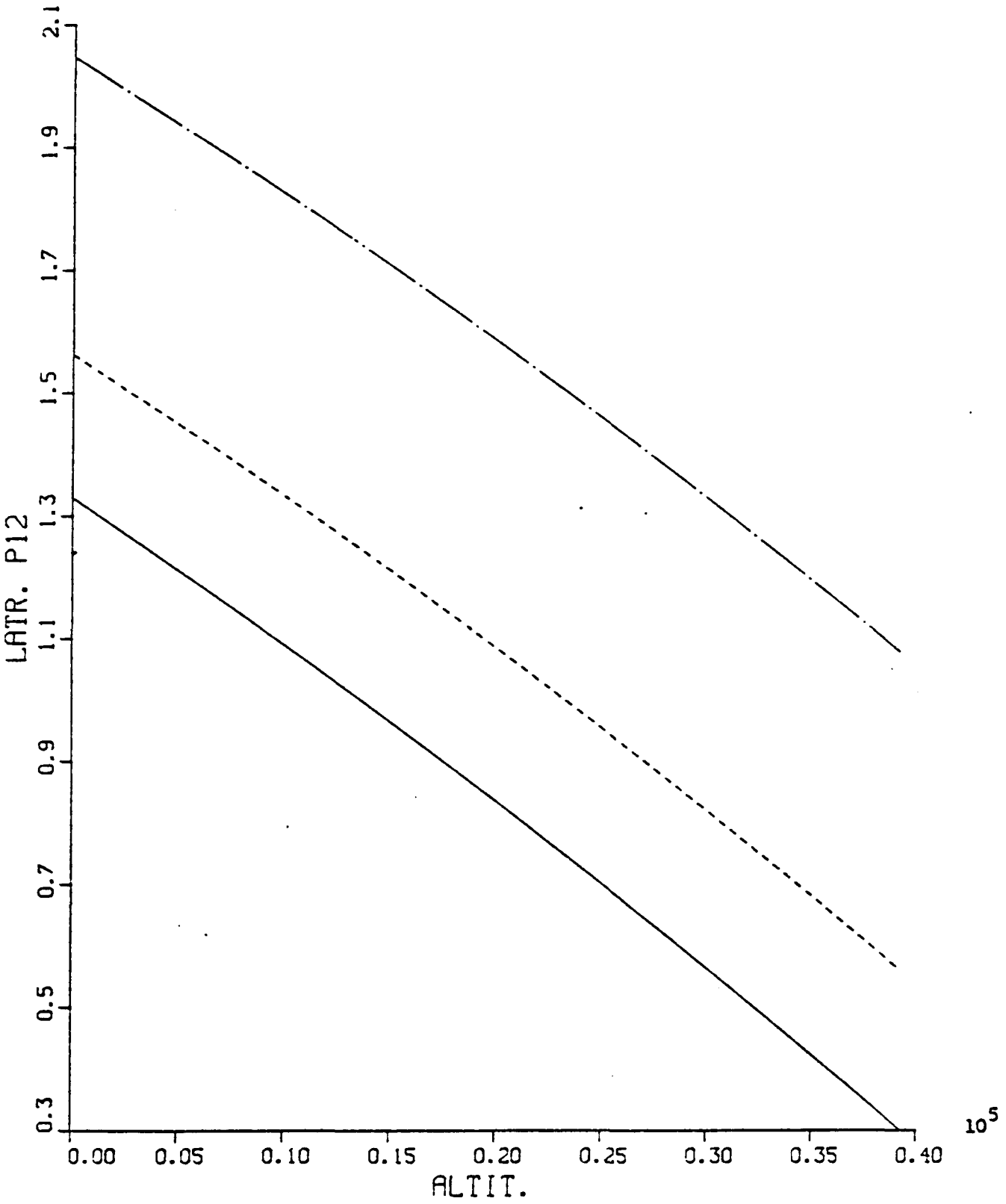

Fig. A.33 LATR. P13 VS. ALTIT. (Liapunov IAS)

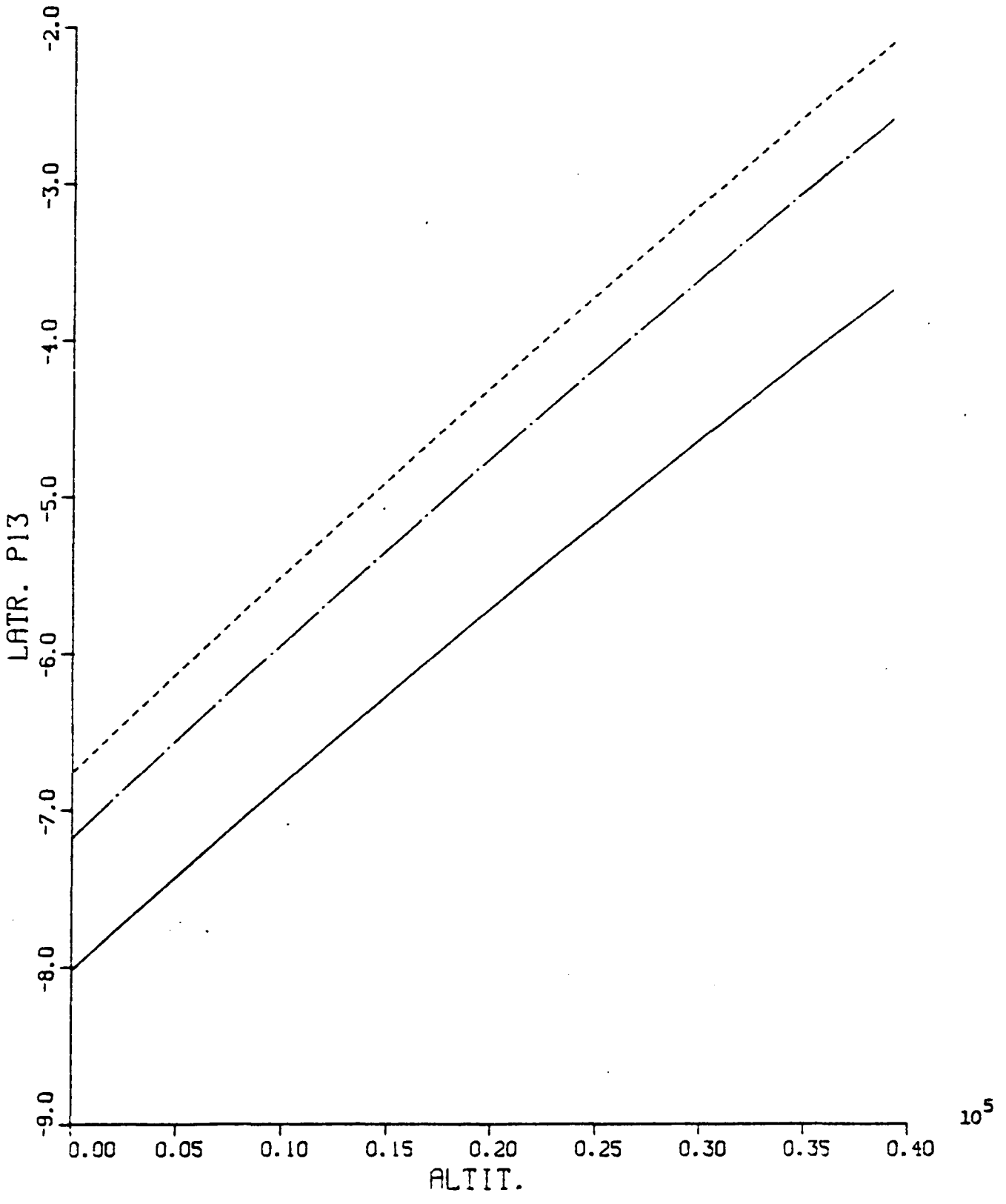

Fig. A.34 LATR. P14 VS. ALTIT. (Liapunov IAS)

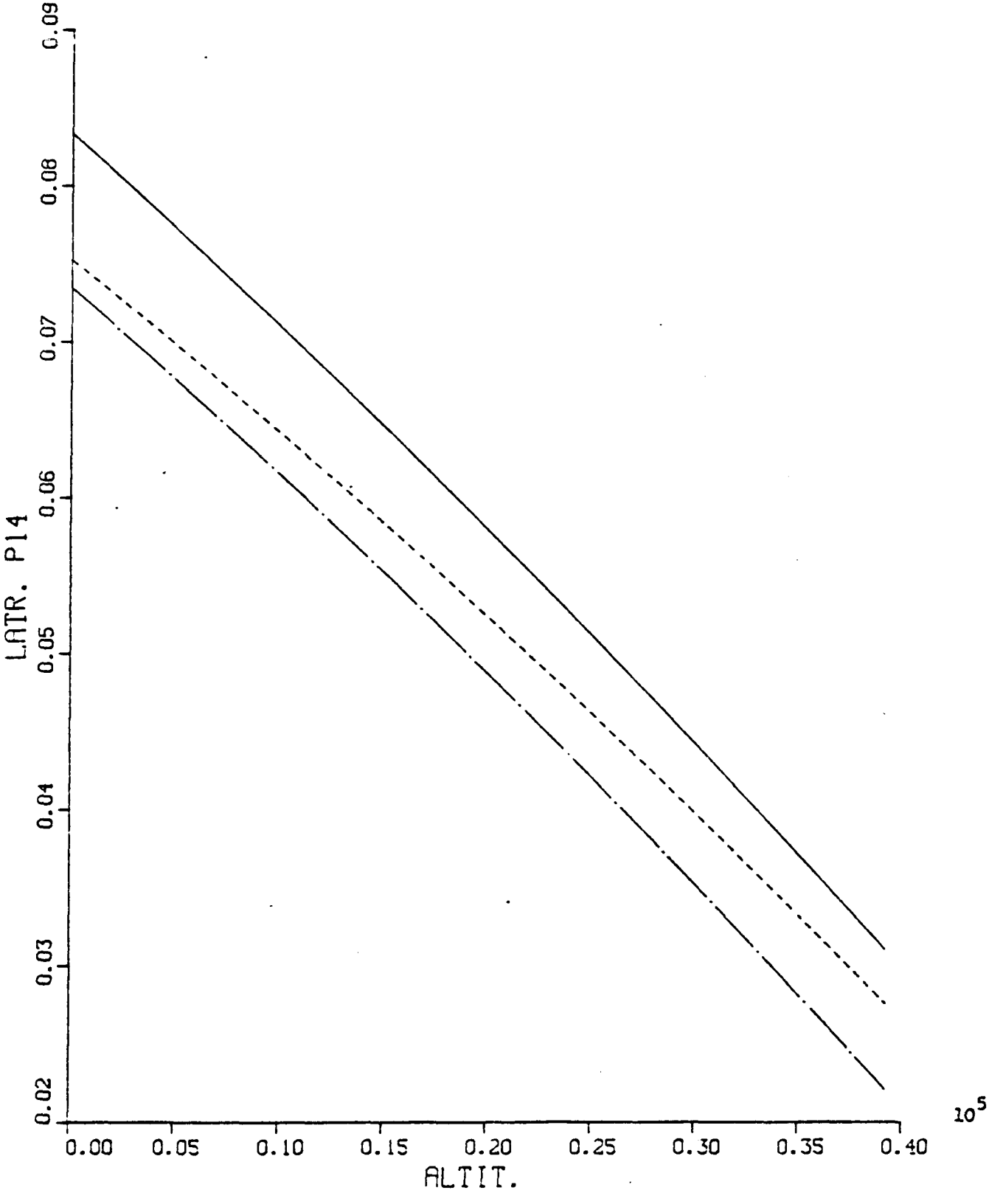

Fig. A.35 LATR. P1 VS. ALTIT. (Newton-Raphson IAS)

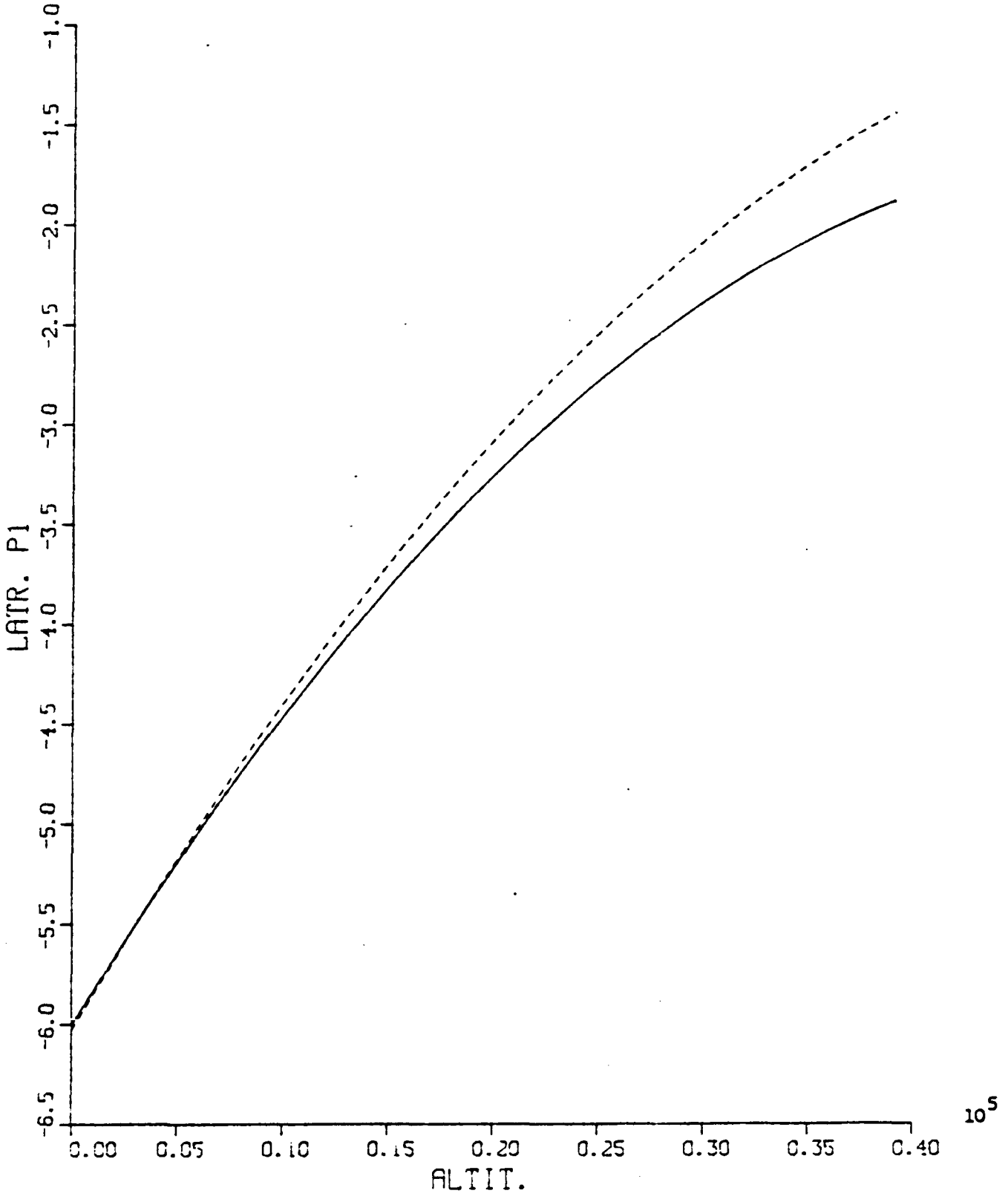

Fig. A.36 LATR. P2 VS. ALTIT. (Newton-Raphson IAS)

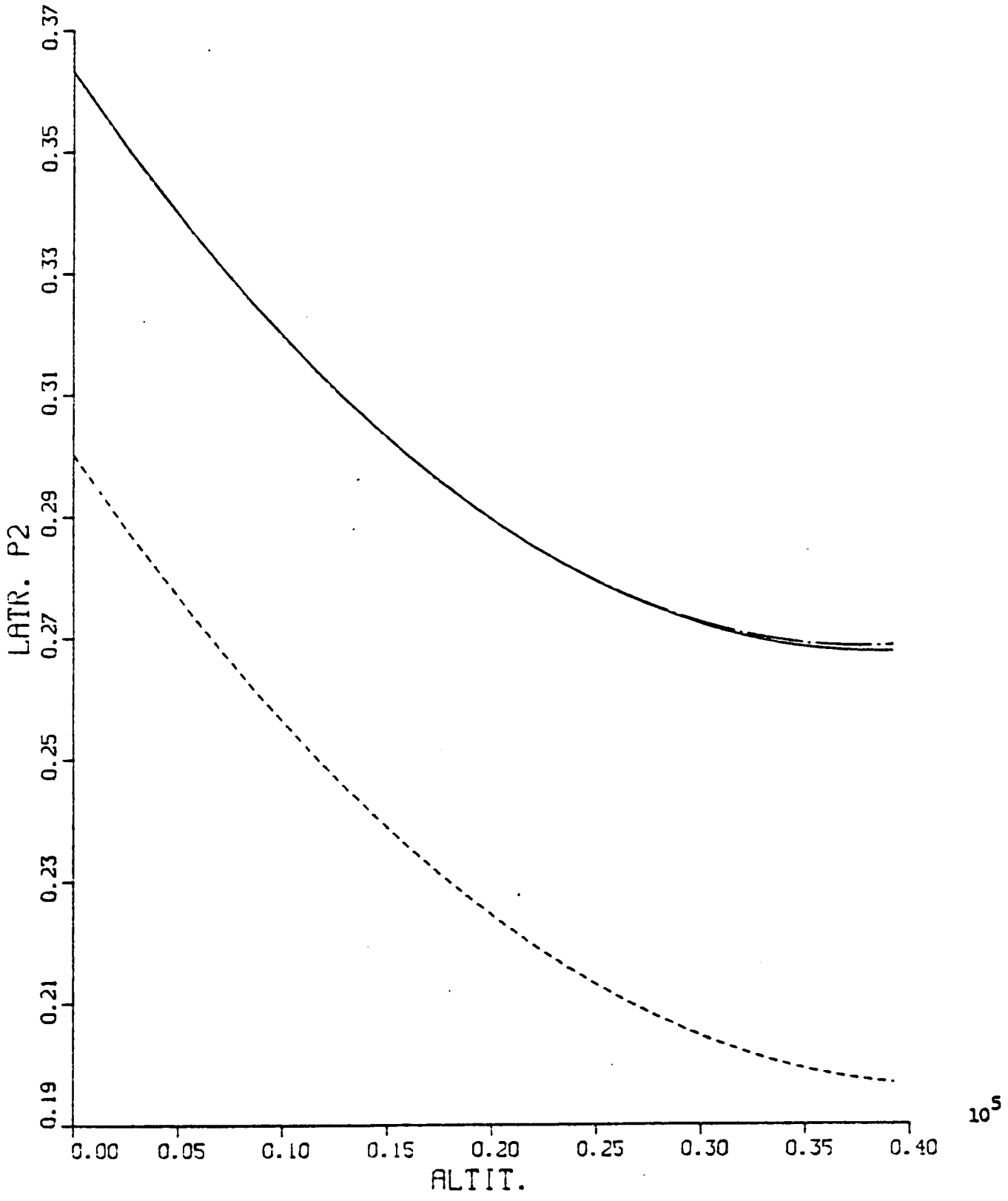

Fig. A.37 LATR. P3 VS. ALTIT. (Newton-Raphson IAS)

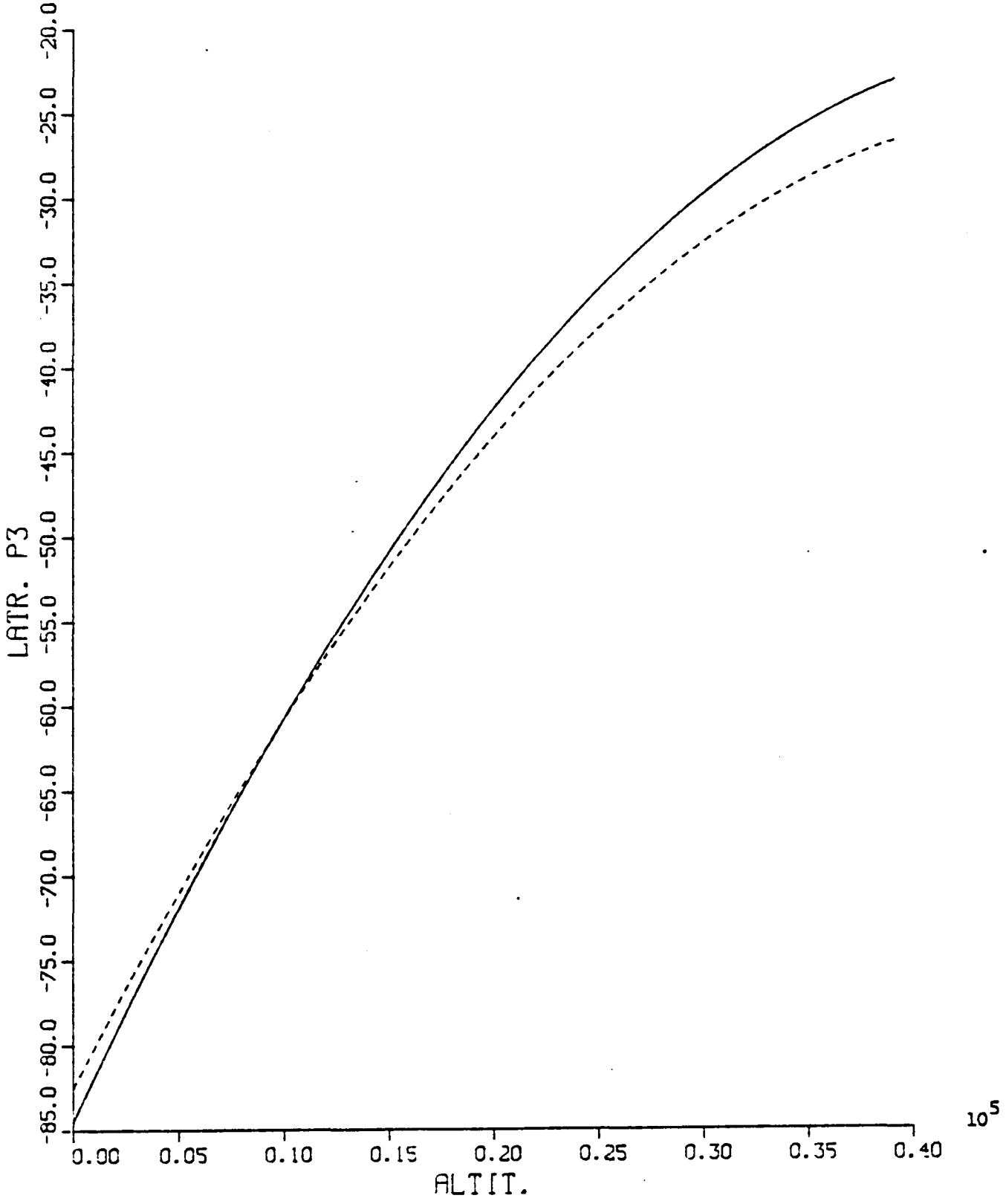

Fig. A.38 LATR. P4 VS. ALTIT. (Newton-Raphson IAS)

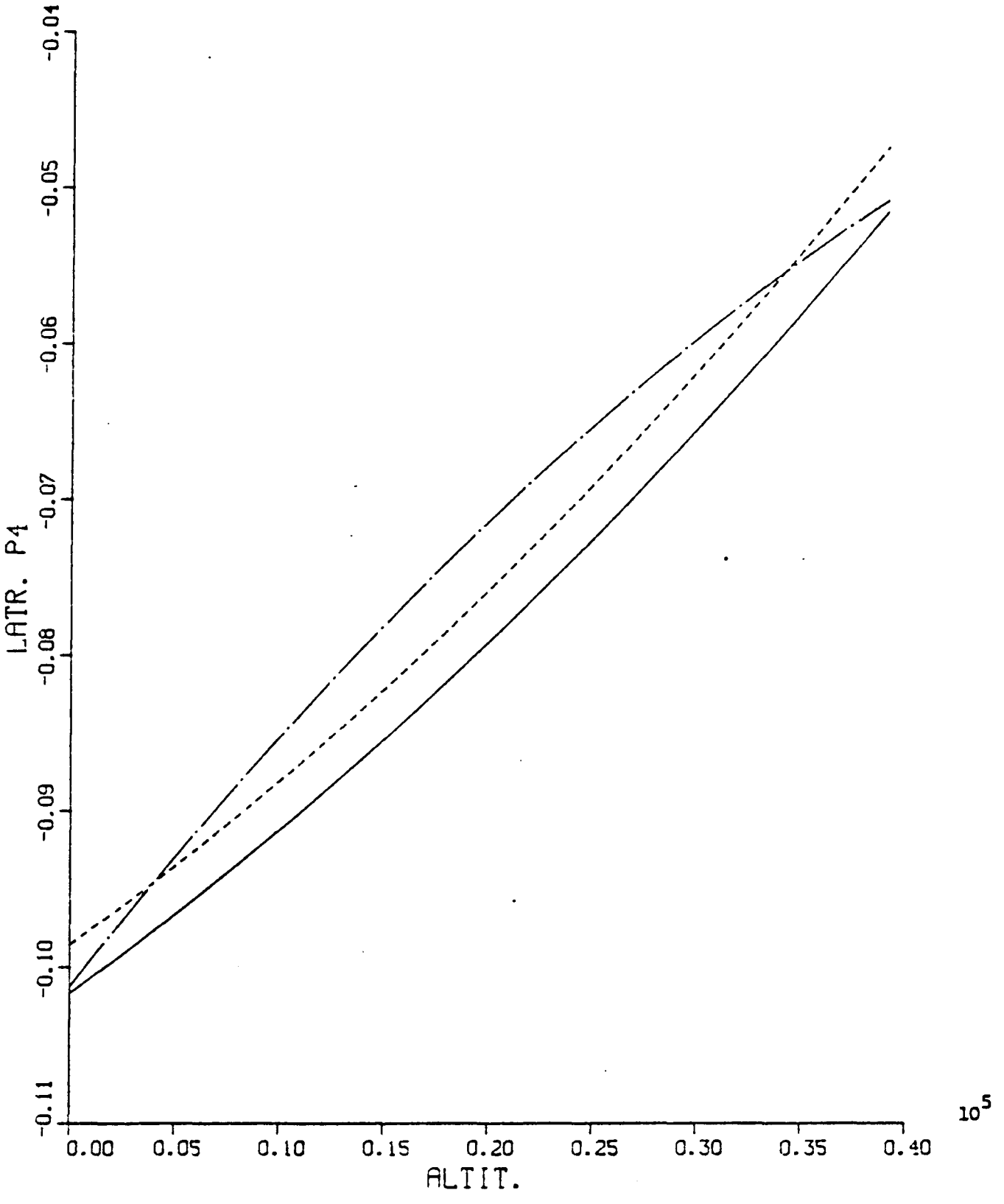

Fig. A.39 LATR. P5 VS. ALTIT. (Newton-Raphson IAS)

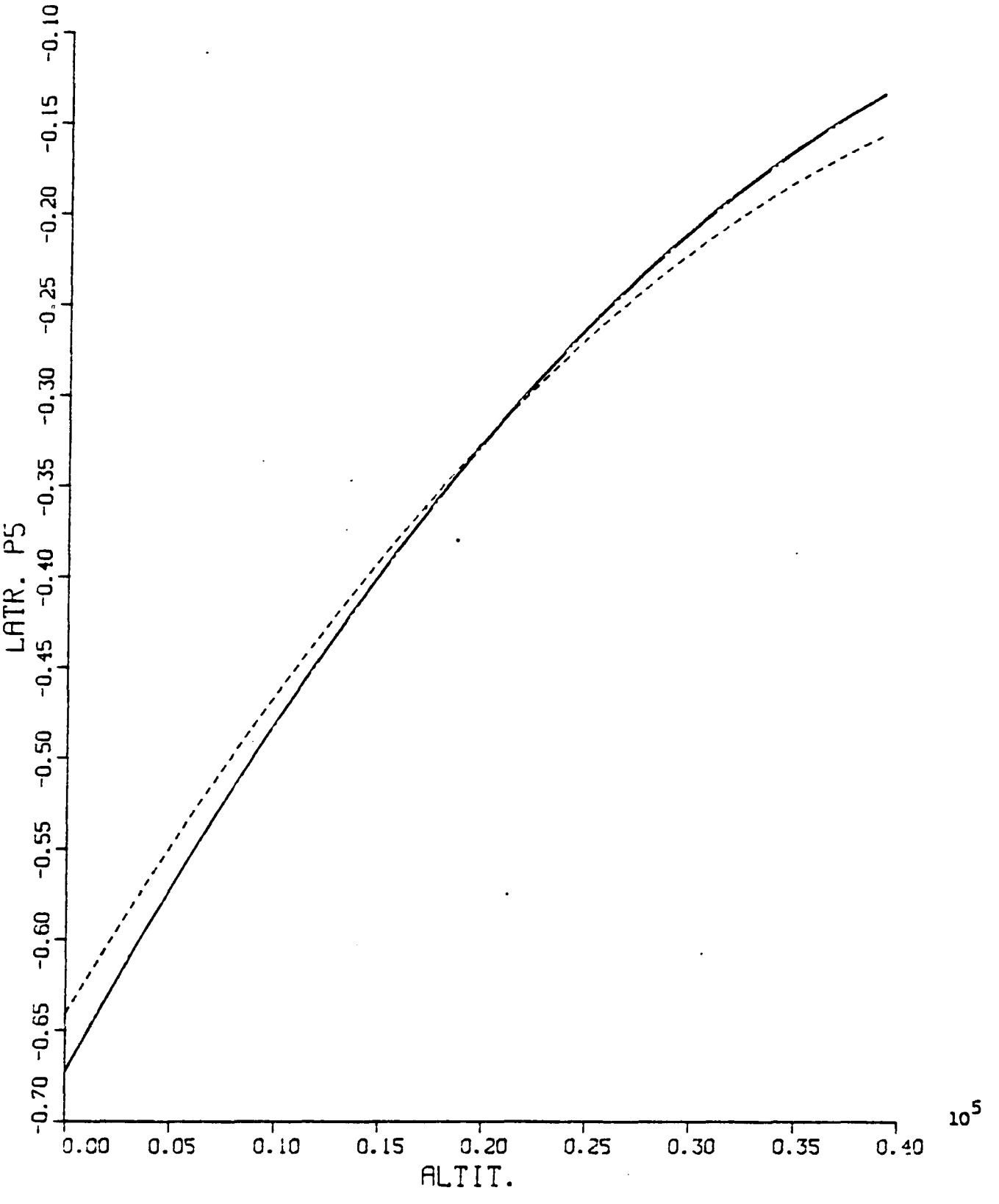

Fig. A.40 LATR. P6 VS. ALTIT. (Newton-Raphson IAS)

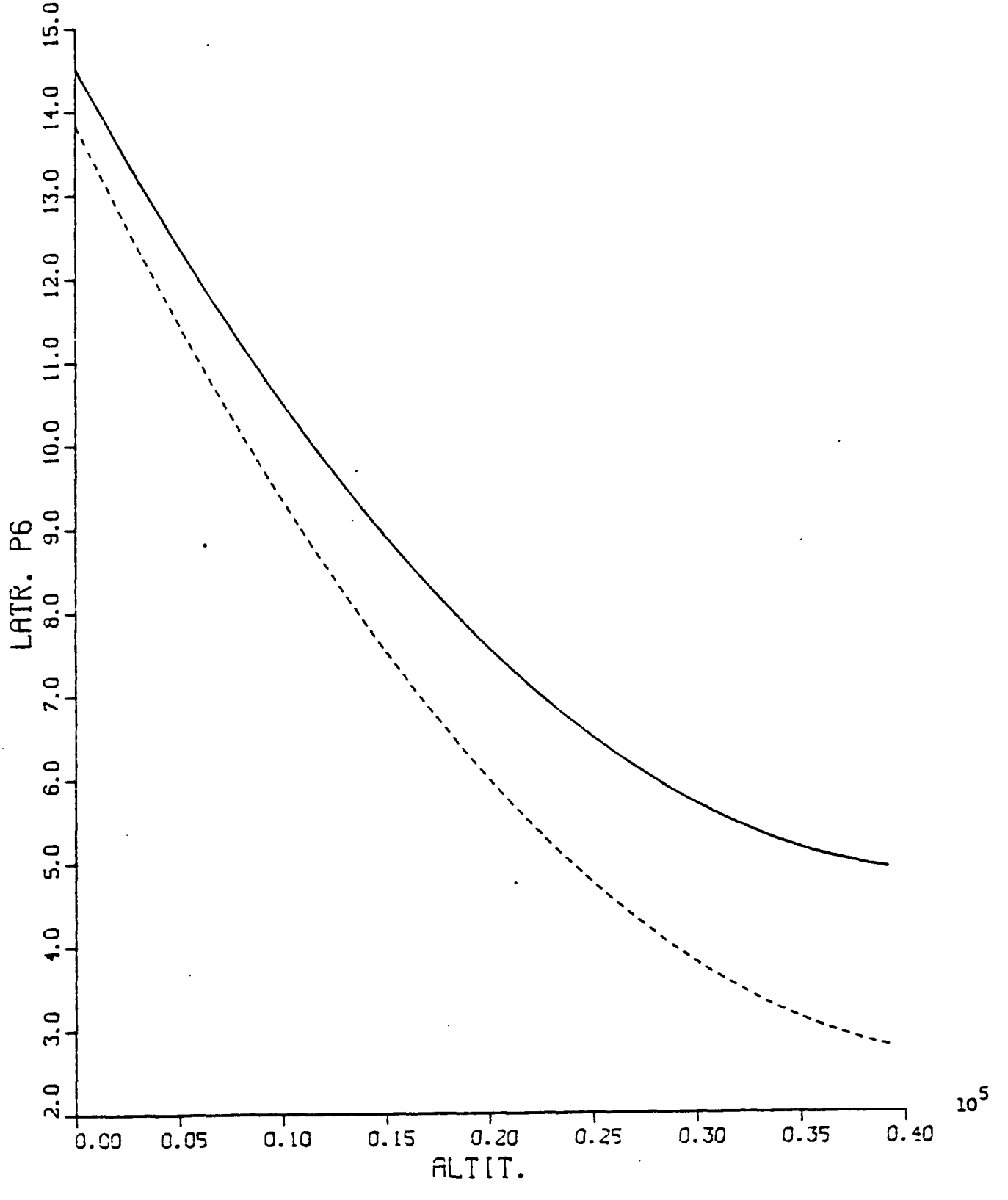

Fig. A.41 LATR. P7 VS. ALTIT. (Newton-Raphson IAS)

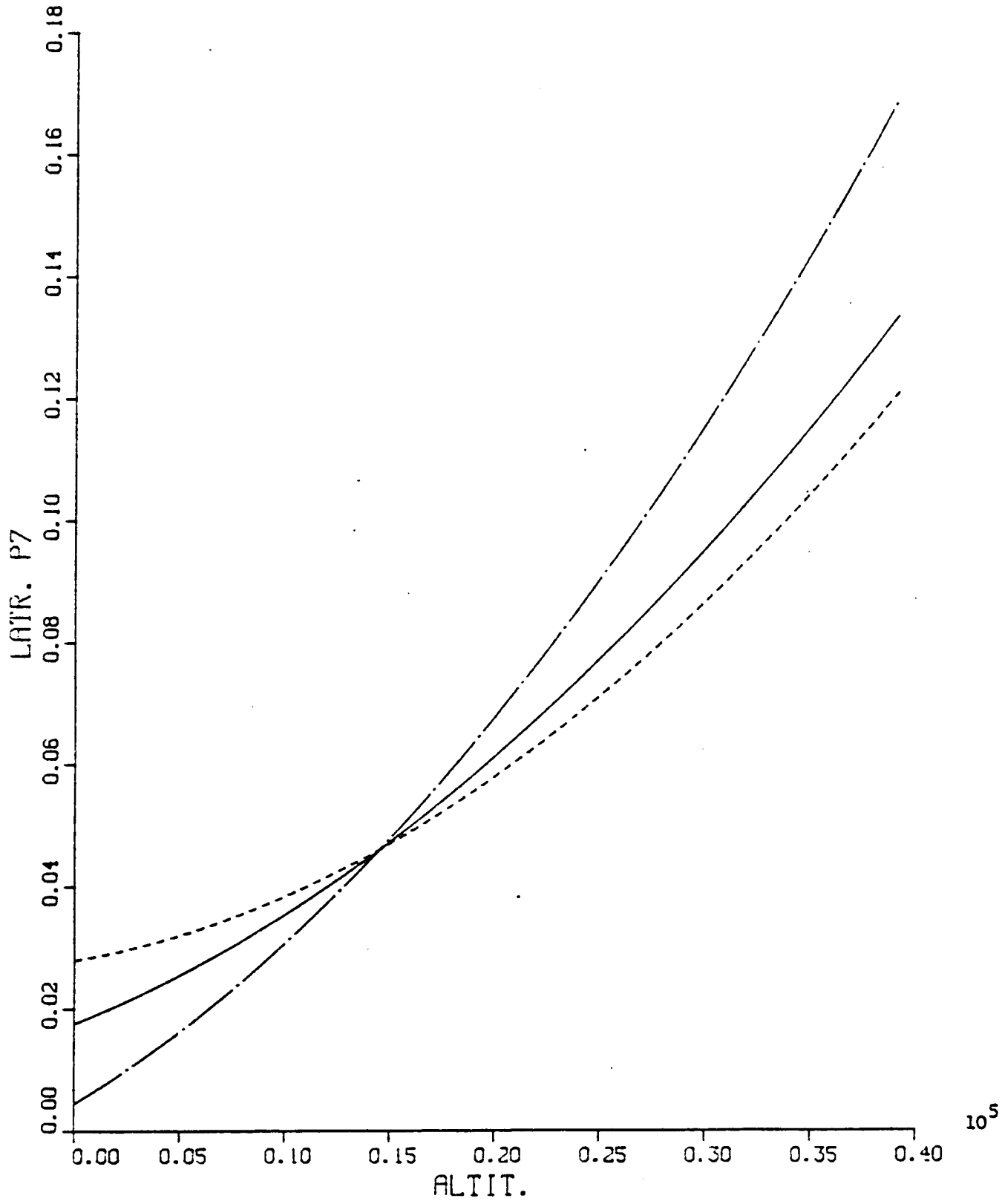

Fig. A.42 LATR. P8 VS. ALTIT. (Newton-Raphson IAS)

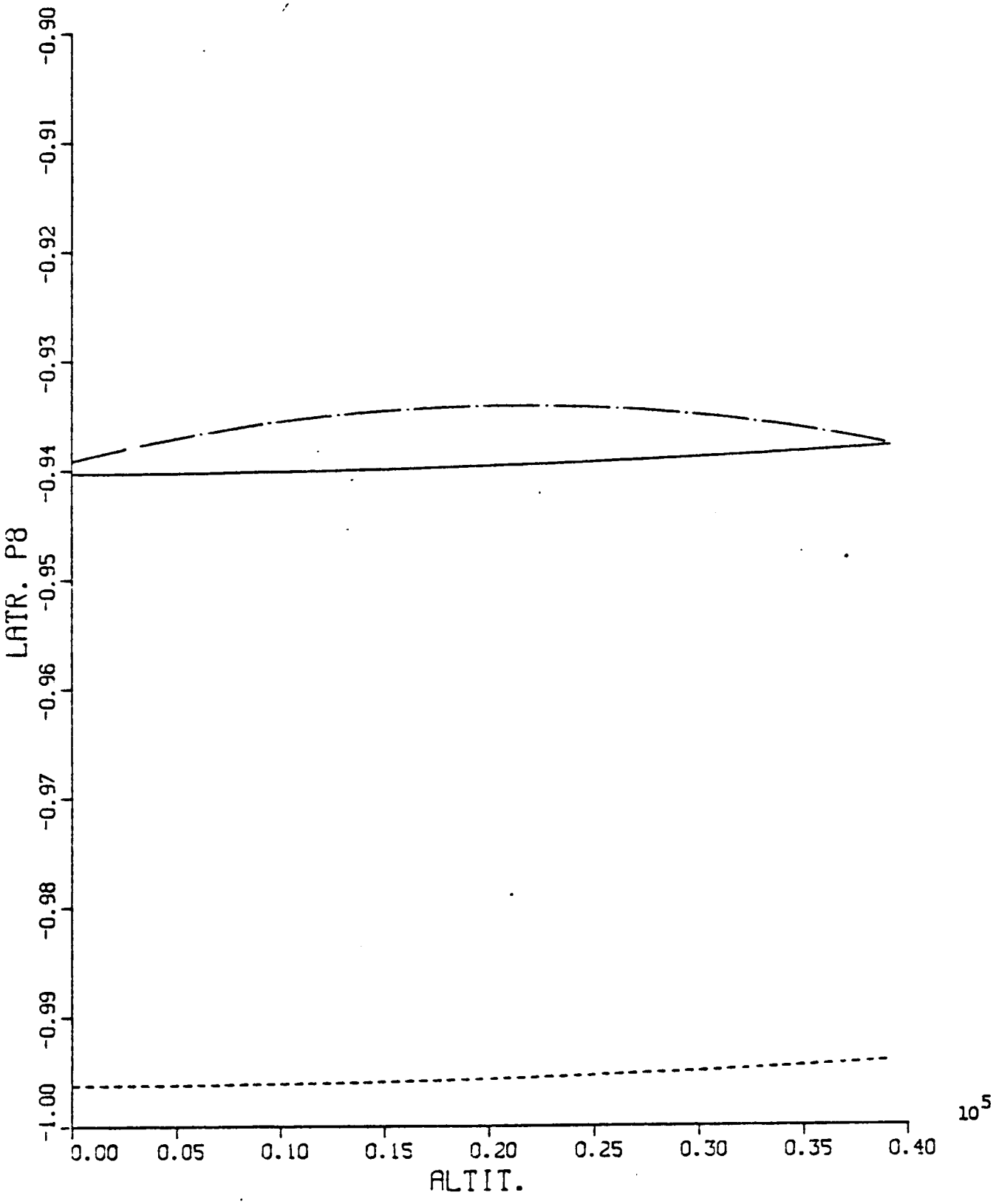

Fig. A.43 LATR. P9 VS. ALTIT. (Newton-Raphson IAS)

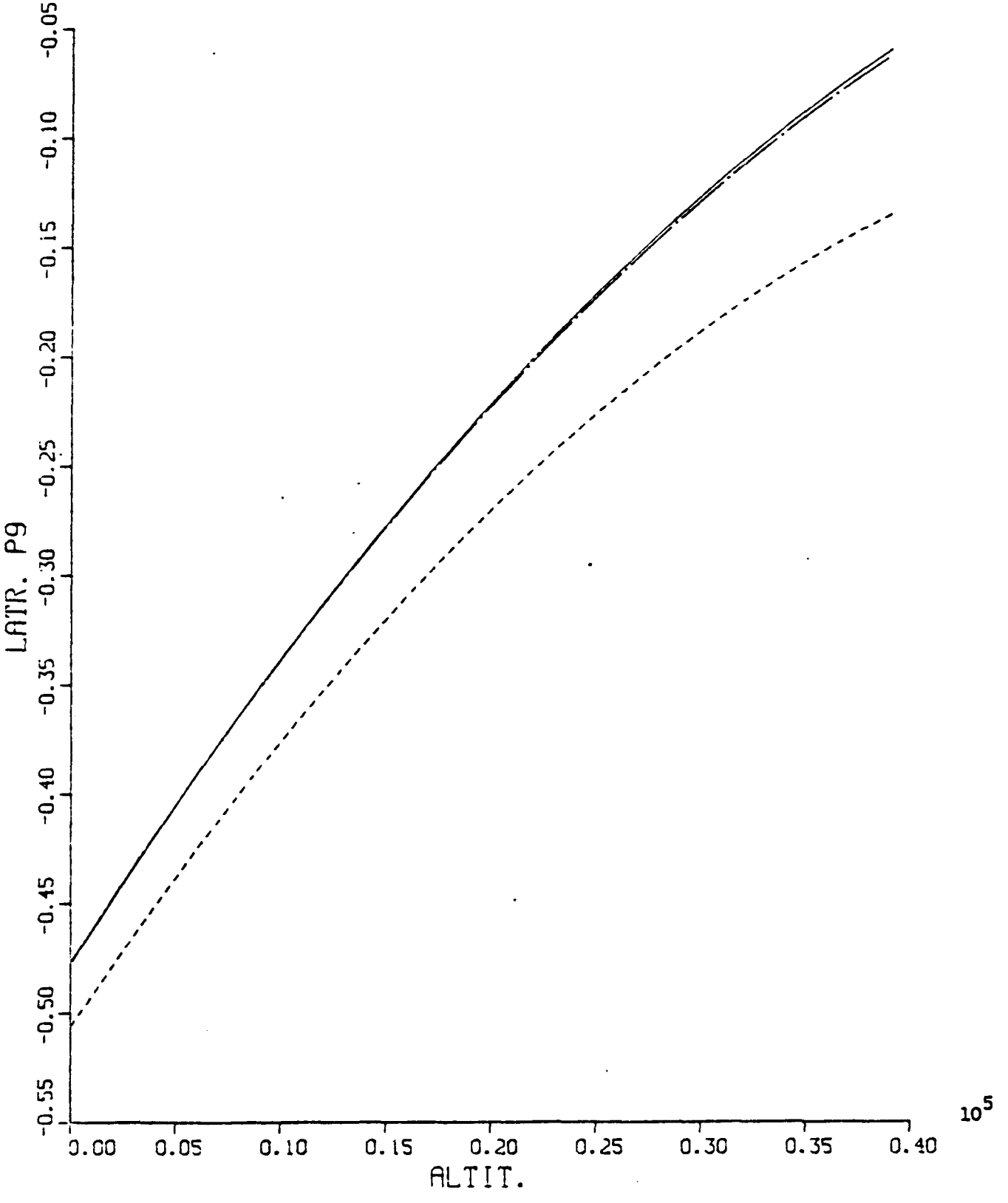

Fig. A.44 LATR. P10 VS. ALTIT. (Newton-Raphson IAS)

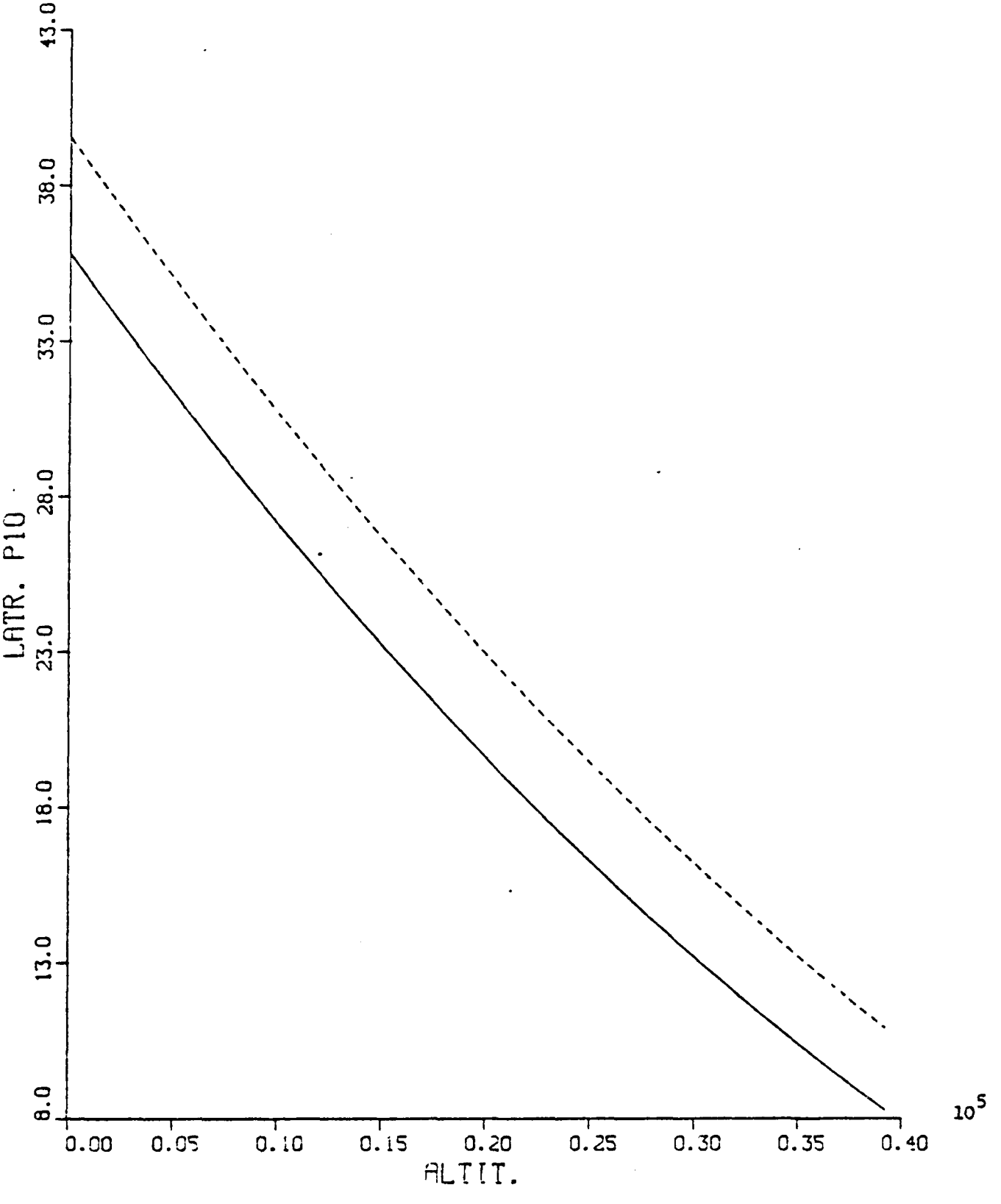

Fig. A.45 LATR. P11 VS. ALTIT. (Newton-Raphson IAS)

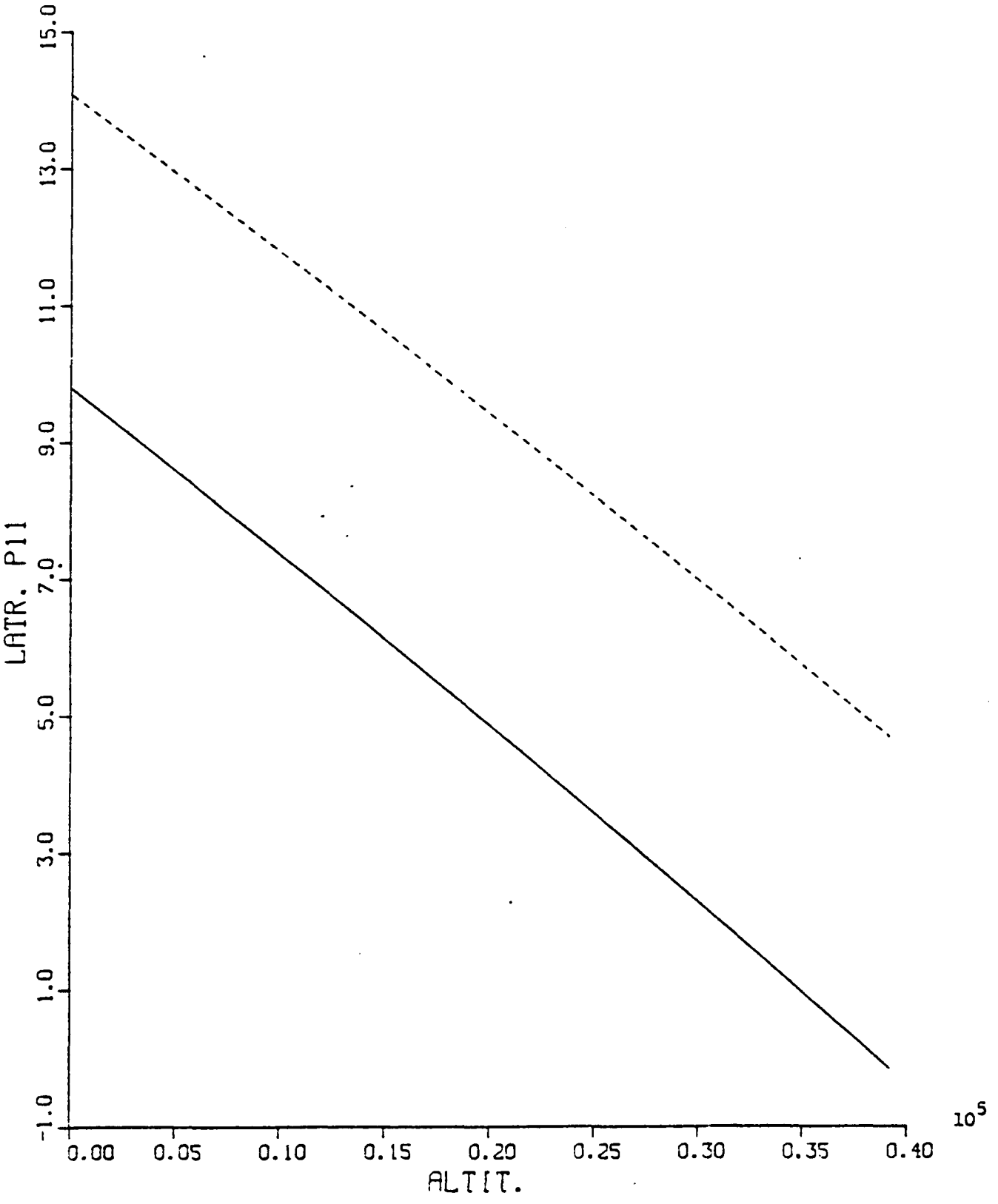

Fig. A.46 LATR. P12 VS. ALTIT. (Newton-Raphson IAS)

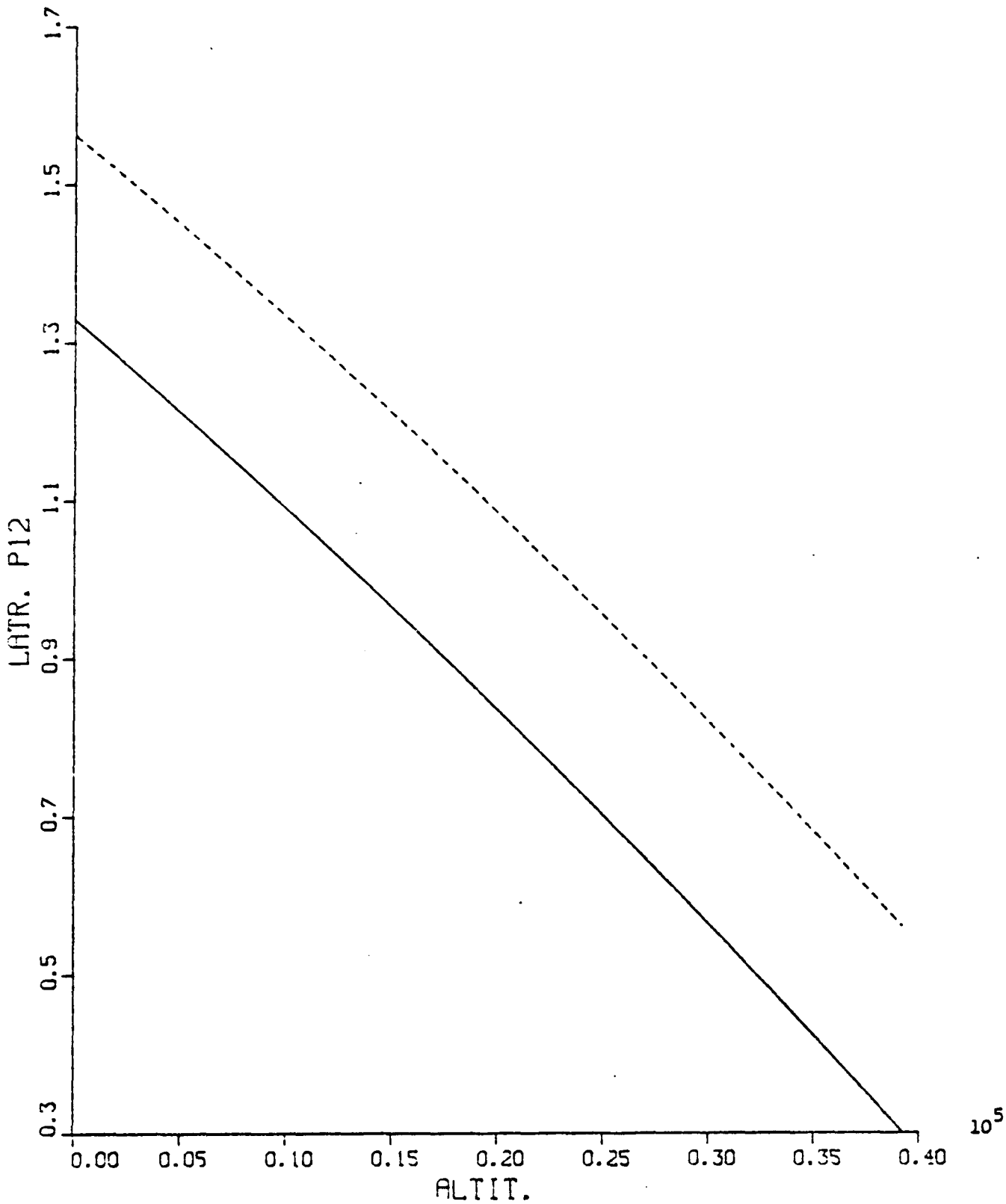

Fig. A.47 LATR. P13 VS. ALTIT. (Newton-Raphson IAS)

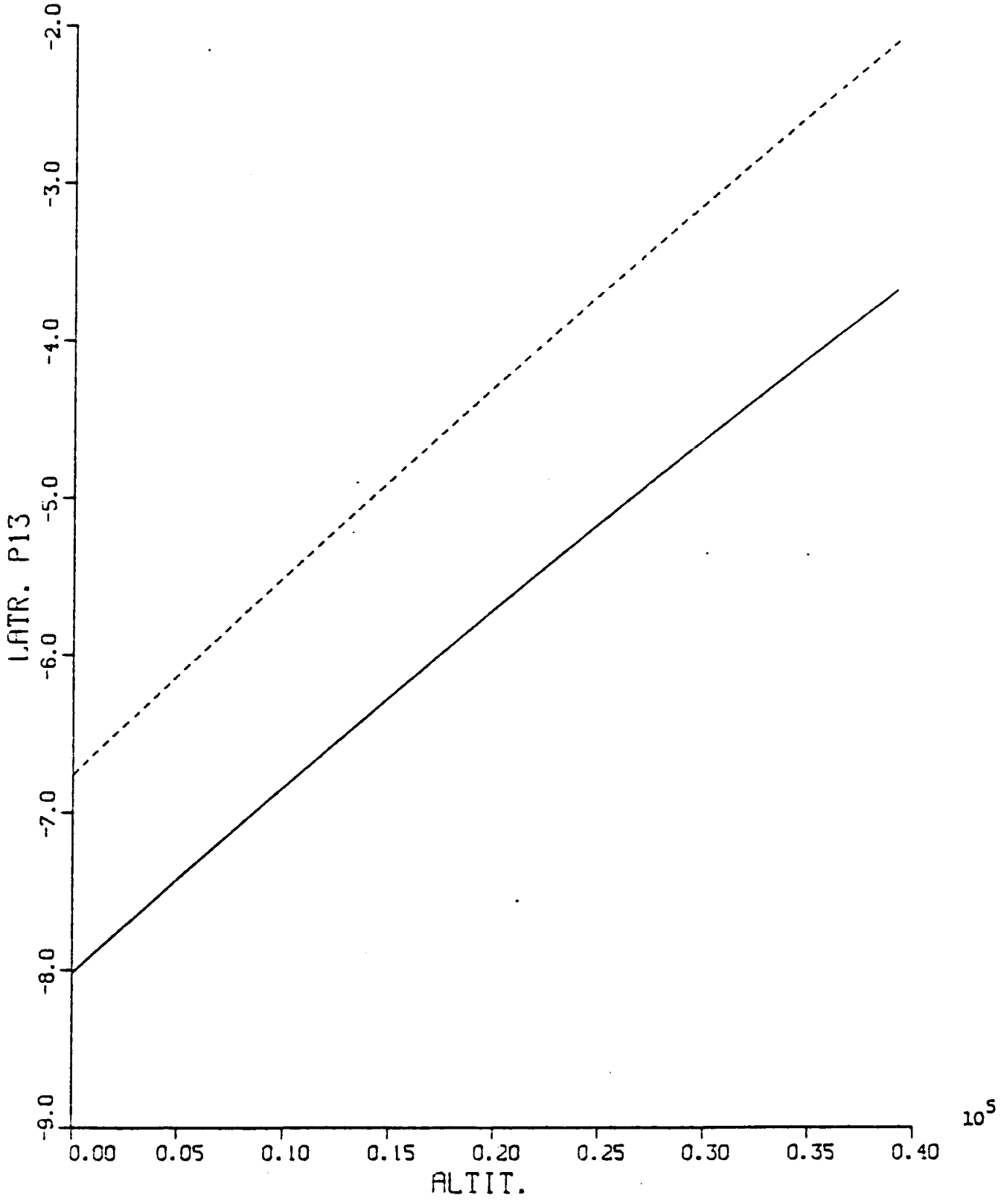

Fig. A.48 LATR. P14 VS. ALTIT. (Newton-Raphson IAS)

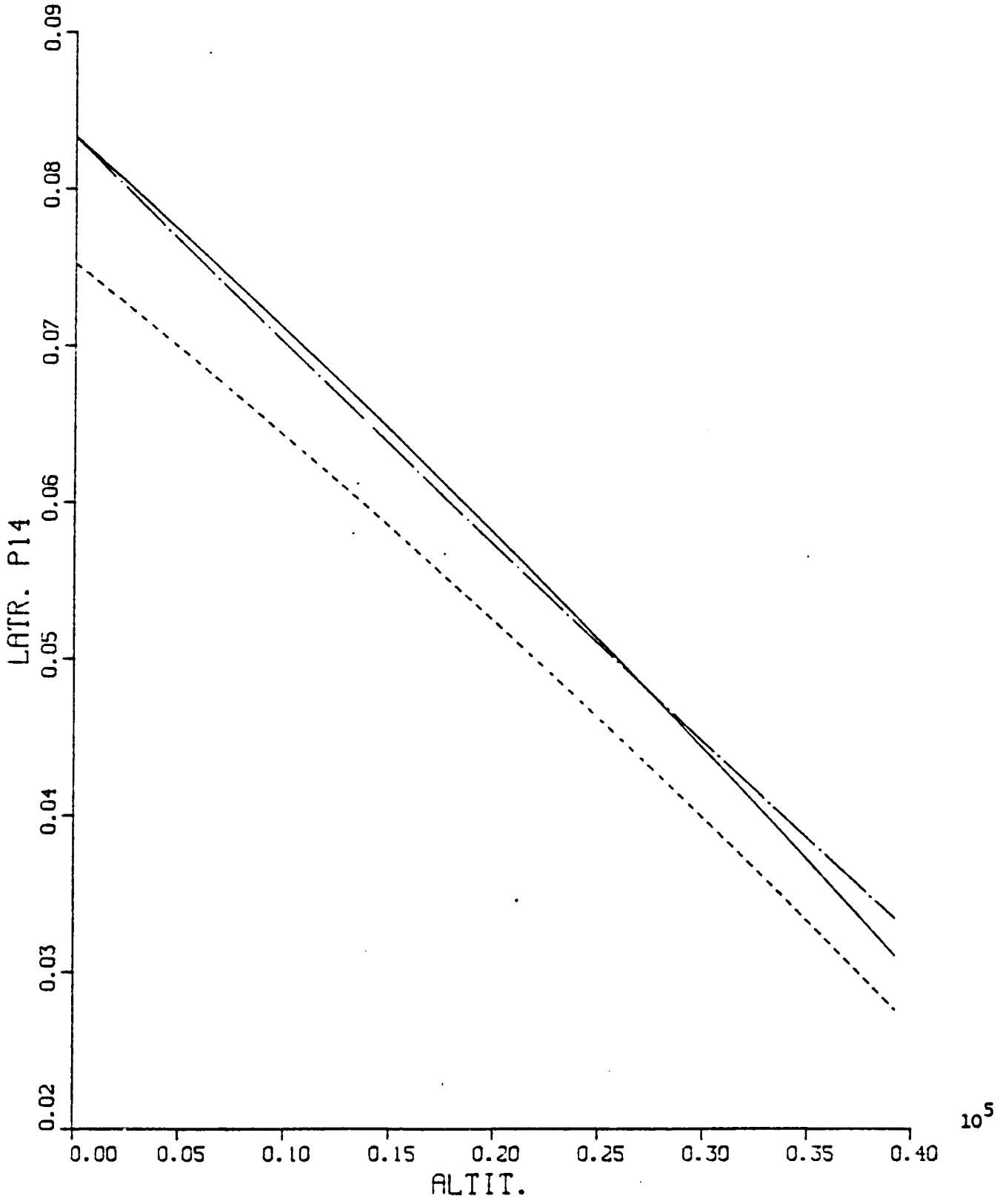

APPENDIX B

A DISCRETE-TIME EVALUATION OF THE TIME RESPONSE OF A CONTINUOUS-TIME SYSTEM (EULER'S METHOD)

Consider the continuous-time linear system represented by the by the vector differential equation of the form

$$\dot{x} = A\,x + B\int_s \tag{B.1}$$

We wish to obtain the time response of the system described by Eq. (B.1) by utilizing a discrete-time approximation. To do so, we divide the time axis into sufficiently small time increments, each of duration T seconds. Then the values of the state variables are evaluated at successive time intervals; that is t = 0, T, 2T, 3T, ..., kT. The definition of a derivative is

$$\dot{x} = \lim_{\Delta t \to 0} \left[x(t + \Delta t) - x(t) \right] / \Delta t \tag{B.2}$$

Since we are interested in the values of the state vector at times that are integer multiples of T, we may substitute in Eq. (B.2) $\Delta t = T$ and $t = kT$. This yields an approximation of the derivative given by

$$\dot{x} = \left\{ x\left[(k+1)\,T\right] - x(kT) \right\} / T \tag{B.3}$$

Substituting Eq. (B.3) into Eq. (B.1) and letting $t = kT$ we obtain

$$\left\{ x\left[(k+1)\,T\right] - x(kT) \right\} T = Ax(kT) + B\int_s (kT) \tag{B.4}$$

Solution of Eq. (B.4) for $x\left[(k+1)\,T\right]$ yields

$$x\left[(k+1)\,T\right] = (T\,A + I)\,x\,(kT) + T\,B\,\mathcal{S}_s\,(kT) \qquad (B.5)$$

Equation (B.5) may be rewritten as a difference equation

$$x\,(k+1) = (T\,A + I)\,x\,(k) + T\,B\,\mathcal{S}_s\,(k) \qquad (B.6)$$

Equation (B.6) is the iterative operation that relates the state vector at the (k + 1)st time instant in terms of the value of x and $\mathcal{S}_s$ at the k-th time instant, and it is used to implement the IAS in real-time.

Due to the real time constraint, our study (Chapter 5) was limited to the first order approximation of the time derivative.

BIBLIOGRAPHY

1. Agrawala, A. K.: "Learning with Probabilistic Teacher", IEEE Transactions on Information Theory, Vol. IT-16, July 1970, pp. 373-379.

2. Alag, G. S. and Kaufman, H.: "Digital Adaptive Model Following Flight Control", AIAA Paper No. 74-886. Presented at the AIAA Mechanics and Control Flight Conference, Anaheim, California, August 5-9, 1974.

3. Astrom, J. J. and Bohlin, T.: "Numerical Identification of Linear Dynamic Systems From Normal Operating Records", Proc. IFAC Symp. Theory of Self-Adaptive Processes, Teddington, 1968.

4. Astrom, K. J. and Eykoff, P.: "System Identification - A Survey", Automatica, Vol. , 1971, pp. 123-162.

5. Athans, M., Castanon, D., Dunn, K-P, Greene, C. S., Lee, W. H., Sandell, N. R. and Willsky, A. S.: "The Stochastic Control of the F-8C Aircraft Using a Multiple Model Adaptive Control (MMAC) Method, Part I: Equilibrium Flight", Report ESL-P-681, September 15, 1976, M.I.T., Cambridge, Massachusetts.

6. Balakrishnan, A. V. and Peterka, V.: "Identification in Automatic Control Systems", Automatica, Vol. 5, 1969, pp. 817-829.

7. Blakelock, J. H.: Automatic Control of Aircraft and Missiles, John Wiley & Sons, 1965.

8. Bohlin, T.: "On the Maximum Likelihood Method of Identification", IBM Journal Research and Development, Vol. 14, No. 1, 1970, pp. 41-51.

9. Butchart, R. L. and Shackcloth, P.: "Synthesis of Model Reference Adaptive Control Systems by Liapunov's Second Method", Proc. 1965 IFAC Symp. Adaptive Control (Teddington, England), ISA, 1966, pp. 145-152.

10. Chien, Y. T. and Fu, K. S.: "A Modified Sequential Recognition Machine Using Time Varying Stopping Boundaries", IEEE Transactions on Information Theory, Vol. IT-12, April 1967, pp. 206-214.

11. Deckert, J. C., Desai, M. N., Deyst, J. J. and Willsky, A. S.: "A Reliable Dual-Redundant Sensor FDI System for the NASA F-8C-DFBW Aircraft", Proceedings of the 1976 IEEE Conference on Decision and Control, December 1-3, 1976, pp. 32-37.

12. Denery, D. G.: "Simplification in the Computation of the Sensitivity Functions for Constant Coefficient Linear System", IEEE Transactions on Automatic Control, Vol. AC-19, August 1971, pp. 348-350.

13. Duffy, J. J. and Franklin, M.: "A Learning Identification Algorithm and its Application to an Environmental System", IEEE Transactions on Systems, Man and Cybernetics, Vol. SMC-5, No. 2, March 1975, pp. 226-240.

14. Edwards, A. W. F.: Likelihood, New York, Cambridge Press, 1972.

15. Elliott, J. R.: "NASA's Advanced Control Law Program For the F-8 Digital Fly-By-Wire Aircraft", Introductory paper for the proposed special issue of the IEEE Transactions on Automatic Control on the F-8 Advanced Control Law Research.

16. Esposito, R.: "On a Relation Between Detection and Estimation in Decision Theory", Information Control, Vol. 12, 1968, pp. 116-120.

17. Etkin, B.: Dynamics of Flight, John Wiley & Sons, Inc. New York, N. Y., 1960.

18. Fu, K. S.: "Learning Control Systems Review and Outlook", IEEE Transactions on Automatic Control, Vol. AC-15, April 1970, pp. 210-221.

19. Fu, K. S. and Chien, Y. T.: "Sequential Recognition Using a Non-parametric Ranking Procedure", IEEE Transactions on Information Theory, Vol. IT-13, July 1967, pp. 484-492.

20. Fu, K. S. and Nikolic, Z. J.: "On Some Reinforcement Techniques and their Relation to the Stochastic Approximation", IEEE Transactions on Automatic Control, Vol. AC-11, October 1966, pp. 756-758.

21. Gera, J.: "Linear Equations of Motion for F-8 DFBW Airplane at Selected Flight Conditions", NASA, Langley Research Center, F-8 Digital Fly-By-Wire Internal Document, Report No. 010-74.

22. Gilbart, J. W., Monopoli, R. V. and Price, C. F.: "Improved Convergence and Increased Flexibility in the Design of Model Reference Adaptive Control Systems", Proc. 9th IEEE Symposium Adaptive Processes Decision and Control, December 1970, pp. IV 3.1-3.10.

23. Goldstein, H.: Classical Mechanics, Addison-Wesley Publishing Co. Inc., Reading, Mass., 1959.

24. Graupe, D.: Identification of Systems, Van Nostrand Reinhold Co. New York, N. Y., 1972.

25. Gupta, N. K. and Mehra, R. K.: "Computational Aspects of Maximum Likelihood Estimation and Reduction in Sensitivity Function Calculation", IEEE Transactions on Automatic Control, Vol. AC-19, December 1974, pp. 774-783.

26. Gura, I. A.: "An Algebraic Solution of the State Estimation Problem", AIAA Journal, Vol. 7, No. 7, July 1969, pp. 1242-1247.

27. Hahn, W.: Theory and Applications of Liapunov's Direct Method, Prentice-Hall, Englewood Cliffs, N. J., 1963.

28. Hamming, R. W.: Numerical Methods for Scientists and Engineers, Mc Graw-Hill, New York, N. Y., 1962.

29. Hang, C. C. and Parks, P. C.: "Comparative Studies of Model-Reference Adaptive Control Systems", IEEE Transactions on Automatic Control, Vol. AC-18, October 1973, pp. 419-428.

30. Hartman, G. and Stein, G.: "Specific Failure Identification Algorithms for the F-8", Proceedings of the 1976 IEEE Conference on Decision and Control, December 1-3, 1976, pp. 29-31.

31. Hildebrand, F. B.: Methods of Applied Mathematics, Prentice Hall, Inc., Englewood Cliffs, N. J., 1952.

32. Ho, Y. C. and Agrawala, A. K.: "On Pattern Classification Algorithms-Introduction and Survey", IEEE Transactions on Automatic Control, Vol. AC-13, December 1968, pp. 676-690.

33. Ho, Y. C. and Lee, R. C. K.: "A Bayesian Approach to Problems in Stochastic Estimation and Control", IEEE Transactions on Automatic Control, Vol. AC-9, October 1964, pp. 333-339.

34. Isaacson, E. and Keller, H. B." "Analysis of Numerical Methods", John Wiley & Sons, New York, N. Y, 1966.

35. Jazwinski, A. H.: "Limit Memory Optimal Filtering", IEEE Trans. on Automatic Control, Vol. AC-13, October 1968, pp. 558-563.

36. Kalman, R. E.: "Liapunov Functions for the Problem of Lure in Automatic Control", Proc. Nat. Acad. Sci. U. S., Vol. 49, February 1963, pp. 201-205.

37. Kalman, R. E. and Bertram, J. E.: "Control System Analysis and Design Via Second Method of Liapunov, Part 1, Continuous Time System", Journal of Basic Engineering, Trans. of the ASME, Vol. 82-D, June 1960, pp. 371-393.

38. Kaufman, H.: "Research in Digital Adaptive Flight Controllers", NASA Contractor Report, CR-2684, May 1976.

39. Kim, C. H. and Lindorff, D. P.: "Input Frequency Requirements for Identification Through Liapunov Methods", Int. Journal Control, Vol. 20, No. 1, 1974, pp. 35-48.

40. Kolk, W. R.: Modern Flight Dynamics, Prentice-Hall, Inc., Englewood Cliffs, N. J., 1961.

41. Lal, M. and Mehrotra, R.: "Design of Model-Reference Adaptive Control Systems for Nonlinear Plants", Int. Journal Control, Vol. 16, No. 5, 1972, pp. 993-996.

42. Landau, I. D.: "A Hyperstability Criterion for Model Reference Adaptive Control Systems", IEEE Transactions on Automatic Control, Vol. AC-14, October 1969, pp. 552-555.

43. Landau, I. D.: "Unbiased Recursive Identification Using Model Reference Adaptive Techniques", IEEE Transactions on Automatic Control, Vol. AC-21, No. 2, April 1976, pp. 194-202.

44. La Salle, J. and Lefschetz, S.: Stability by Liapunov's Direct Method with Applications, Academic Press, New York, N. Y., 1961.

45. Lee, R. C. K.: "Optimal Estimation Identification and Control", M.I.T. Press, Cambridge, Mass., 1964.

46. Lindorff, D. P. and Caroll, R. L.: "Survey of Adaptive Control Using Liapunov Design", Int. Journal Control, Vol. 18, No. 5. 1973, pp. 897-914.

47. Luders, G. and Narendra, K. S.: "Stable Adaptive Schemes for State Estimation and Identification of Linear Systems", IEEE Transactions on Automatic Control, Vol. AC-19, December 1974, pp. 841-847.

48. Luenberger, D. G.: Introduction to Linear and Nonlinear Programming, Addison-Wesley, 1972, Reading, Mass., pp. 1972.

49. Luenberger, D. G.: "Observers for Multivariable Systems", IEEE Transactions on Automatic Control, Vol. AC-11, April 1966, pp. 190-197.

50. McCuskey, S. W.: An Introduction to Advanced Dynamics, Addison-Wesley Publishing Co., Inc., Reading, Mass., 1962.

51. Mehra, R. K.: "Maximum Likelihood Identification of Aircraft Parameters", 1970 Joint Automatic Control Conf., Preprints, Atlanta, Georgia, June 1970.

52. Mekel, R.: "A Class of Liapunov Functions for High Order Nonlinear Control Systems", Proceedings of the First Asilomar Conference on Circuits and Systems, Monterey, Calif., Nov. 1-3, 1967.

53. Mekel, R.: "Nonlinear and Digital Man-Machine Control Systems Modeling", NASA, Langley Research Center, CR-132294, 1972, 106 pages.

54. Mekel, R. and Peruo, P., Jr.: "Design of Controllers for a Class of Nonlinear Control Systems", IEEE Transactions on Automatic Control, Vol. AC-17, April 1972, pp. 206-213.

55. Mekel, R., Montgomery, R. C. and Dunn, H. J.: "An Adaptive Learning Control System for Aircraft", Proceedings of the Eighth Asilomar Conference on Circuits, Systems and Computers, Pacific Grove, Calif., Dec. 3-5, 1974, pp. 562-568.

56. Mekel, R., Montgomery, R. C. and Nachmias, S.: "Learning Control System Studies for the F-8 DFBW Aircraft", Proceedings of the 1976 Conference on Decision and Control, Clearwater, Florida, December 1976.

57. Mekel, R. and Singh, A.: "System Identification Via a Microcomputer", Proceedings of the Twelfth Annual Conference on Manual Control, Urbana-Champaign, Ill., May 25-27, 1976.

58. Mendel, J. M.: "Reinforcement Learning Models and their Application to Control Problems", A Symposium of the AACC Theory Committee, Joint Automatic Control Conference, Ohio State University, 1973.

59. Monopoli, R. V.: "Model Reference Adaptive Control With An Augmented Error Signal", IEEE Transactions on Automatic Control, Vol. AC-19, No. 5, Oct. 1974, pp. 474-484.

60. Monopoli, R. V.: "The Kalman-Yacubovich Lemma in Adaptive Control System Design", IEEE Transactions on Automatic Control, Vol. AC-19 No. 5, October 1973, pp. 527-529.

61. Montgomery, R. C. and Dunn, H. J.: "A Moving-Window Parameter Adaptive Control System for the F-8 DFBW Aircraft", Proceedings of the 1976 Conference on Decision and Control, Clearwater, Florida, December 1976.

62. Montgomery, R. C. and Moul, M. T.: "Analysis of Deep-Stall Characteristics of T-Tailed Aircraft Configurations and Some Recovery Procedures", Journal of Aircraft, Vol. 3, No. 6, Nov. - Dec. 1966, pp. 562-566.

63. Motyka, P. R.: "A Classical Approach to the Design of Model-Following Control Systems", AIAA Paper No. 74-913. AIAA Mechanics and Control of Flight Conference, Anaheim, California, August 5-9, 1974.

64. Narendra, K. S. and Kudva, P.: "Stable Adaptive Schemes for System Identification and Control", Part I & Part II, IEEE Transactions on Systems, Man and Cybernetics, Vol. SMC-4, Nov. 1974, pp. 542-560.

65. Narendra, K. S. and Viswanathan, R.: "A Two Level System for Stochastic Automata for Periodic Random Environments", IEEE Transactions on Systems, Man and Cybernetics, Vol. SMC-2, April 1972, pp. 285-290.

66. Osburn, P. V., Whitaker, H. P. and Keezer, A.: "New Developments in the Design of Adaptive Control System", Institute of Aeronautical Sciences, Paper 61-39, 1961.

67. Parks, P. C.: "Lyapunov Redesign of Model Reference Adaptive Control Systems", IEEE Transactions on Automatic Control, Vol. AC-11, July 1966, pp. 362-367.

68. Raphan, T.: A Parameter Adaptive Approach to Oculomotor System Modeling, Doctoral Dissertation, CUNY, 1976.

69. Sage, A. P.: Optimum Systems Control, Prentice-Hall, Inc., Englewood Cliffs, N. J., 1968.

70. Sage, A. P. and Melsa, J. L.: System Identification, Academic Press, New York, 1971.

71. Saridis, G. N.: "Stochastic Approximation Methods for Identification and Control - A Survey", IEEE Transactions on Automatic Control, Vol. AC-19, December 1974, pp. 798-809.

72. Saridis, G. N., Nikolic, Z. J. and Fu, K. S.: "Stochastic Approximation Algorithms for System Identification, Estimation and Decomposition of Mixtures", IEEE Transactions on Systems Science and Cybernetics, Vol. SSC-5, January 1969, pp. 8-15.

73. Schultz, D. G. and Melsa, J. L.: State Functions and Linear Control Systems, McGraw-Hill Book Co., New York, 1967.

74. Schwartz, R. and Friedland, B.: Linear Systems, McGraw-Hill Book Co., New York, 1965.

75. Shahein, H. I. H., Ghonaimy, M. A. R. and Shen, D. W. D.: "Accelerated Model Reference Adaptation via Liapunov and Steepest Descent Design Techniques", IEEE Transactions on Automatic Control, Vol. AC-17, February 1972.

76. Shapiro, I. J. and Narendra, K. S.: "Use of Stochastic Automata for Parameter Self Optimization with Multimodel Performance Criteria", IEEE Transactions on System Science and Cybernetics, Vol. SMC-5, October 1969, pp. 352-360.

77. Silverman, L. M.: "Transformation of Time-Variable System to Canonical Form", IEEE Transactions on Automatic Control, April 1966, pp. 300-303.

78. Sklansky, J.: "Learning Systems for Automatic Control", IEEE Transactions on Automatic Control, Vol. AC-11, Jan. 1966, pp. 6-19.

79. Smith, F. W.: "Contact Control by Adaptive Pattern Recognition Techniques", Stanford Electronics Laboratory, Stanford University, Stanford, California, Tech. Report 6762-2, April 1964.

80. Stein, G. and Saridis, G. N.: "A Parameter-Adaptive Control Technique", Automatica, Vol. 5, 1969, pp. 731-739.

81. Thau, F. E.: "On Optimum Filtering for a Class of Linear Distributed-Parameter Systems", Proc. Joint Automatic Control Conference, Ann Arbor, Michigan, June 1968, pp. 610-618.

82. Thomson, W. T.: Introduction to Space Dynamics, John Wiley & Sons New York, N. Y., 1963.

83. Tomovic, R.: Sensitivity Analysis of Dynamic Systems, McGraw-Hill, Book Co., 1963.

84. Tsypkin, Ya. Z.: "Automatic Training Systems", Automation and Remote Control, Vol. 4, April 1970, pp. 560-575.

85. Tsypkin, Ya. Z.: "Generalized Learning Algorithms", Automation and Remote Control, Vol. 1, January 1970, pp. 86-92.

86. Tsypkin, Ya. Z.: "On Learning Systems", Automatica, Vol. 8, 1972, pp. 85-91.

87. Tsypkin, Ya. Z.: "Foundations of the Theory of Learning Systems", Academic Press, New York, N. Y., 1973.

88. Udink ten Cate, and Verstoll, N. D. L.: "Improvement of Liapunov Model Reference Adaptive Control Systems in a Noisy Environment", Int. J. Control, Vol. 20, No. 6, 1974, pp. 977-996.

89. Whitaker, H. P., Yarmon, J. and Keezer, A.: "Design of Model Reference Adaptive Control Systems for Aircraft", M.I.T. Instrumentation Lab., Report R-164, September 1958.

90. Wilkie, D. F. and Perkins, W. R.: "Generation of Sensitivity Functions for Linear Systems Using Low-Order Models", IEEE Transactions on Automatic Control, Vol. AC-14, April 1969, pp. 123-130.

91. Winsor, C. A. and Roy, R. J.: "Design of Model Reference Adaptive Control Systems by Liapunov's Second Method", IEEE Transactions on Automatic Control (corresp.), Vol. AC-13, April 1968, p. 204.

92. Wooley, C. T.: "A Real-Time Hybrid Simulation of a Digital Fly-By-Wire Aircraft", 1974 Summer Computer Simulation Conference, Houston, Texas, July 9-11, 1974.

93. Staff of Flight Research Center: "Experience with the X-15 Adaptive Flight Control System", NASA Tech. Note D-6208, March 1971.